



2019

Elucidation of the Molecular Mechanisms of Electrically-Induced Cardioprotection

Anne Elizabeth Roessler

Follow this and additional works at: https://ecommons.luc.edu/luc_diss

 Part of the [Pharmacology Commons](#)

Recommended Citation

Roessler, Anne Elizabeth, "Elucidation of the Molecular Mechanisms of Electrically-Induced Cardioprotection" (2019). *Dissertations*. 3369.

https://ecommons.luc.edu/luc_diss/3369

This Dissertation is brought to you for free and open access by the Theses and Dissertations at Loyola eCommons. It has been accepted for inclusion in Dissertations by an authorized administrator of Loyola eCommons. For more information, please contact ecommons@luc.edu.



This work is licensed under a [Creative Commons Attribution-Noncommercial-No Derivative Works 3.0 License](#).
Copyright © 2019 Anne Elizabeth Roessler

LOYOLA UNIVERSITY CHICAGO

ELUCIDATION OF THE
MOLECULAR MECHANISMS OF
ELECTRICALLY-INDUCED CARDIOPROTECTION

A DISSERTATION SUBMITTED TO
THE FACULTY OF THE GRADUATE SCHOOL
IN CANDIDACY FOR THE DEGREE OF
DOCTOR OF PHILOSOPHY

PROGRAM IN MOLECULAR PHARMACOLOGY AND THERAPEUTICS

BY

ANNE E. ROESSLER

CHICAGO, ILLINOIS

MAY 2019

Copyright by Anne E. Roessler, 2019

All rights reserved.

ACKNOWLEDGEMENTS

This work would not be possible without the extraordinary people in my life who supported me throughout this journey. First and foremost, I would like to thank my family, especially my parents, Ron and Denise Roessler. I am so grateful for your unwavering love, support, and understanding throughout the numerous years of my educational endeavors. To my brilliant sister, Becca Roessler, thank you for teaching me countless life lessons one cannot learn from a textbook, and for the collection of beautiful plants that brightened my desk while I wrote this dissertation. A great debt of gratitude is owed to Dr. Keith Jones for providing me the opportunity to embark on this project and for his mentorship throughout its completion. Thank you to my committee for sharing your feedback, advice, and guidance. This work has been greatly enhanced by your collective scientific expertise and rigor. I'd like to express my deep appreciation to the Pharmacology Department, to Dr. Byron and Dr. Simmons, and to the members of the Jones Lab for creating a supportive and challenging research environment. It has been a pleasure to complete my dissertation work at this institution. I extend a special thank you to my lab mate and friend, Dr. Tom Lynch, whose relentless curiosity and enthusiasm for science has been a great inspiration since the moment I first stepped on Loyola's campus. Lastly, I would like to thank the many friends in my life who have laughed with me, encouraged me, and commiserated with me throughout my PhD. I am so lucky to have such an incredible support system. I could not have done this without you.

For Mom and Dad, Becca, and my grandparents

Words are, of course, the most powerful drug used by mankind.

– Rudyard Kipling

TABLE OF CONTENTS

ACKNOWLEDGEMENTS.....	iii
LIST OF TABLES.....	ix
LIST OF FIGURES.....	x
LIST OF ABBREVIATIONS.....	xii
ABSTRACT.....	xx
CHAPTER I: INTRODUCTION.....	1
CHAPTER II: LITERATURE REVIEW.....	8
The Burden of Cardiovascular Disease.....	8
Cardiovascular Disease and Coronary Artery Disease.....	8
Myocardial Infarction and I/R Injury.....	9
Pathophysiology of MI.....	13
Heart Failure.....	16
Perioperative MI and Points of Intervention.....	17
Cardioprotection Paradigms.....	20
Ischemic Preconditioning.....	20
Perconditioning and Postconditioning.....	23
Remote Ischemic Preconditioning and Clinical Translation Attempts.....	24
Nociceptor-Induced Cardioprotection.....	28
Electrically-Induced Cardioprotection and the Field of Electroceuticals	30
Vagal Nerve Stimulation in Cardioprotection	31
Electrical Stimulation of the Limb and the Humoral Hypothesis.....	34
Electroacupuncture.....	36
Early and Late Phases of Remote Cardioprotection, an Overview and Summary	40
Challenges in Clinical Translation of Ischemic Therapies.....	42
General Rationale for NIC	43
Neural Signaling as a Potential Trigger of NIC.....	44
The Transcription Factors NF- κ B, AP-1, and Cardioprotective Gene Programs in NIC.....	48
The Heat Stress Response, HSF1, and HSP70 as Potential Mediators of NIC	50
Nitric Oxide Synthase 2 and S-Nitrosylation as Potential Mediators of NIC.....	54
Kyphoscoliosis Peptidase as Exemplar of Deep Sequencing Dataset Legacies.....	57
microRNA as Epigenetic Regulators of NIC.....	58
Overall Rationale.....	61
CHAPTER III: HYPOTHESIS AND AIMS.....	62

CHAPTER IV: MATERIALS AND METHODS.....	64
Ethics Statement.....	64
Animal Strains and Numbers	64
Ischemia and Reperfusion Model.....	65
Electrical Stimulation Paradigm.....	66
TTC Staining and Infarct Size Analysis.....	69
Histology and Cell Death Assessment.....	69
RNA Isolation, Reverse Transcription, and Quantitative Real Time PCR Analysis.....	70
Protein Isolation and Western Blot Analysis.....	73
Next-Generation Sequencing of mRNA and microRNA.....	76
DAVID and DIANA Analyses.....	78
Pharmacological and siRNA Inhibition.....	78
Statistical Analyses	80
CHAPTER V: RESULTS.....	82
Electroacupuncture is an Effective Early Phase Cardioprotective Stimulus.....	82
Electrical Stimulation via Cutaneous Patch is Effective as an Early Phase, Late Phase, and Postconditioning Cardioprotective Stimulus.....	84
The Increase in HSP mRNA and Protein is Small and Mostly Insignificant.....	87
Late Phase ES-Induced Cardioprotection Persists in Mice with Genetic and Pharmacological Inhibition of HSP70.1.....	90
Late Phase ES-Induced Cardioprotection Persists in Mice Treated with siRNA Against HSF1...92	
NF- κ B is Involved in Late Phase ES-Induced Cardioprotection.....	94
The Unique Transcriptome of ES-Induced Cardioprotection.....	95
Transcript Levels of NOS2 and KY are Increased after ES-Induced Cardioprotection.....	98
Protein Kinetics of KY and NOS2 after ES-Induced Cardioprotection are Elusive.....	101
Cardioprotection is Abolished in Mice with a Genetic Deletion of NOS2.....	102
Potential c-Jun Activation after ES-Induced Cardioprotection.....	104
NF- κ B Dependent Genes After ES.....	106
The Transcriptome Following IPC Differs from That Following ES.....	111
microRNA is Differentially Expressed after ES.....	113
CHAPTER VI: DISCUSSION.....	117
Establishing Electrically-Induced Cardioprotection.....	117
Electrical Stimulation Reduces Infarct Size in Multiple Models of Cardioprotection.....	117
Hypothesis 1.....	118
Electrical Stimulation Upregulates HSPs.....	118
Genetic and Pharmacological Inhibition of the HSPs.....	118
siRNA Inhibition of HSF1.....	119
Hypothesis 1 Summary.....	120
Hypothesis 2.....	120
Electrically-Induced Cardioprotection is NF- κ B Dependent.....	120

Next-Generation Sequencing in B6/129 Mice.....	121
Validation of Sequencing.....	123
Nitric Oxide Synthase 2 is a Mediator of ES.....	124
The Additional Candidates, KY and c-Jun.....	125
Next-Generation Sequencing in 3M and Nontransgenic Mice.....	127
Sequencing Assay Comparisons.....	128
microRNA Next-Generation Sequencing and Validations.....	130
Hypothesis 2 Summary.....	132
Limitations and Alternatives.....	133
Future Directions.....	134
Clinical Significance.....	137
CHAPTER VII: CONCLUSIONS.....	139
APPENDIX A: mRNA-SEQ DATA, GENES WITH DIFFERENTIAL EXPRESSION BETWEEN ES+/- IN B6/129 MOUSE HEART TISSUE.....	142
APPENDIX B. TRANSCRIPTOMIC ANALYSIS OF GENE ONTOLOGY FOR BIOLOGICAL PROCESSES AND CELLULAR COMPONENTS.....	159
APPENDIX C: mRNA-SEQ DATA, GENES WITH DIFFERENTIAL EXPRESSION BETWEEN ES+/- IN 3M AND NONTRANSGENIC MOUSE HEART TISSUE.....	165
APPENDIX D: miRNA-SEQ DATA, miRs WITH DIFFERENTIAL EXPRESSION BETWEEN ES+/- AND DIANA ANALYSIS OF miRNA KEGG PATHWAYS.....	174
REFERENCE LIST.....	180
VITA.....	228

LIST OF TABLES

Table 1. Mouse Strains.....	65
Table 2. List of Primers.....	72
Table 3. List of Antibodies.....	75
Table 4. Comparison of Strain-Specific Next-Generation Sequencing Results.....	110
Table 5. Comparison of ES and IPC.....	112
Table 6. microRNA Sequencing Results.....	114

LIST OF FIGURES

Figure 1. Ischemia/Reperfusion Injury Schematic.....	12
Figure 2. Heat Shock Protein Schematic.....	51
Figure 3. Rendering of Electrically-Induced Cardioprotection Model.....	67
Figure 4. Cardioprotective Paradigms.....	68
Figure 5. TTC Staining.....	69
Figure 6. Effect of EA on Infarct Size and Apoptosis.....	83
Figure 7. Effect of ES on Infarct Size in Early Phase Cardioprotection.....	84
Figure 8. Effect of ES on Infarct Size and Bcl-2 Expression in Late Phase Cardioprotection.....	86
Figure 9. Effect of ES on Infarct Size in Postconditioning.....	87
Figure 10. Evidence of Autophagosome Accumulation.....	88
Figure 11. Panel of HSP mRNA and Protein Expression Post-EA and Post-ES.....	89
Figure 12. Late Phase ES in Mice with a Genetic Deletion of HSP70.1.....	90
Figure 13. Western Blot of Soluble and Insoluble Beclin with the HSP70 Inhibitor Apoptozole and <i>In Vivo</i> Ability of Apoptozole to Block IPC.....	91
Figure 14. HSF1 siRNA Validation <i>in Vitro</i>	93
Figure 15. Late Phase ES in Mice Post-Pericardial Sac Injection of HSF1 siRNA.....	94
Figure 16. Late Phase ES with Genetic Inhibition of NF- κ B Using 3M Mice.....	95
Figure 17. Selected mRNA Sequencing Results.....	96

Figure 18. DAVID Gene Ontological Analysis of Sequencing Results.....	97
Figure 19. Transcript Validation of Deep Sequencing, NOS2 and KY.....	99
Figure 20. NF- κ B Dependent Genes.....	100
Figure 21. Protein Kinetics of NOS2 and KY.....	102
Figure 22. Late Phase ES With Genetic Inhibition of NOS2.....	103
Figure 23. Transcript Validation of c-Jun, Nuclear Translocation, and Protein Kinetics.....	105
Figure 24. Pharmacological Inhibition of c-Jun Using SP600125 is Unable to Probe Effect.....	106
Figure 25. Schematic of Hypothesis-Driven Sequencing of NF- κ B-Dependent Genes.....	107
Figure 26. Selected Nontransgenic mRNA Sequencing Results.....	108
Figure 27. Sequencing Schematic of ETC Results from Sequencing.....	109
Figure 28. Selected NF- κ B-Dependent mRNA Sequencing Results.....	111
Figure 29. microRNA Sequencing Results.....	115
Figure 30. DIANA Pathway Analysis of microRNA Sequencing Results.....	115
Figure 31. Validation of microRNA Sequencing.....	116
Figure 32. Summary Schematic.....	129

LIST OF ABBREVIATIONS

3'UTR	3' Untranslated Region
3M	Cardiac Specific I κ B α Dominant Negative Mice
α	Alpha
AAALAC	Association for Assessment and Accreditation of Laboratory Animal Care
ACE	Angiotensin Converting Enzyme
AED	Automated External Defibrillator
Akt	Ak (mouse strain) transforming
ANOVA	Analysis of Variance
AP-1	Activator Protein 1
AR	Adrenergic Receptor
ATP	Adenosine Triphosphate
β	Beta
BAX	Bcl-2 Associated X Protein
BCA	Bicinchoninic Acid Assay
Bcl-2	B-Cell CLL/Lymphoma 2
BDNF	Brain Derived Neurotropic Factor
BK2R	Bradykinin Receptor Subtype B2
Ca ²⁺	Calcium

CABG	Coronary Artery Bypass Graft
CAD	Coronary Artery Disease
cDNA	Complementary DNA
cGMP	cyclic guanosine monophosphate
CGRP	calcitonin gene-related peptide
CHAPS	3-[(3-cholamidopropyl)dimethylammonio]-1-propanesulfonate
CIRCUS	Cyclosporine to ImpRove Clinical OUtcome in ST-Elevation Myocardial Infarction patients
CK-MB	Creatine Kinase- Muscle/Brain
COX	Cyclooxygenase
CRSIP-Stent	Cardiac Remote Ischemic Preconditioning in Coronary Stenting
C _t	Cycle Threshold
CVD	Cardiovascular Disease
CYCLE	CYCLOsporinE A in Reperfused Acute Myocardial Infarction
δ	Delta
DAVID	Database for Annotation, Visualization and Integrated Discovery
DMSO	Dimethyl Sulfoxide
DNA	Deoxyribonucleic Acid
ε	Epsilon
EA	Electrical Stimulation via Electroacupuncture Needles
ECG	Electrocardiogram

EF	Ejection Fraction
ERK1/2	Extracellular Regulated Kinase-1 and -2
eNOS	Endothelial Nitric Oxide Synthase
ERICCA	Effect of Remote Ischemic Preconditioning on Clinical Outcomes in Patients Undergoing Coronary Artery Bypass Graft Surgery
ERK	Extracellular Signal-Regulated Kinases
ES	Electrical Stimulation via Cutaneous Patch
ETC	Electron Transport Chain
FAS	First Apoptosis Signal
FDA	Food and Drug Administration
γ	Gamma
GAPDH	Glyceraldehyde 3-Phosphate Dehydrogenase
GC	Guanylyl Cyclase
GO	Gene Ontology
GPCR	G-Protein Coupled Receptor
GSK3	Glycogen Synthase Kinase 3
H ⁺	Hydrogen
HFpEF	Heart Failure with Preserved Ejection Fraction
HFrfEF	Heart Failure with Reduced Ejection Fraction
HO-1	Heme Oxygenase-1
HSF1	Heat Shock Factor 1

HSP	Heat Shock Protein
Hz	Hertz
IACUC	Institutional Animal Care and Use Committee
IgG	Immunoglobulin G
I κ B α	Inhibitor Kappa B Alpha
IL- β	Interleukin Beta
iNOS	Inducible Nitric Oxide Synthase
I.P.	Intraperitoneal
IPC	Ischemic Preconditioning
I/R	Ischemic Reperfusion
I.V.	Intravenous
JAK	Janus Kinase
JNK	c-Jun N-terminal Kinase
JUN	Gene encoding c-Jun
K _{ATP}	Potassium ATP Channel
K _{Ca}	Calcium Activated Potassium Channels
KEGG	Kyoto Encyclopedia of Genes and Genomes
KO	Knockout (Genetic Deletion)
KY	Kyphoscoliosis Peptidase
LAD	Left Anterior Descending Artery
LSD	Least Significant Difference

LTCC	L-Type Calcium Channel
LV	Left Ventricle
MACCE	Major Adverse Cardiac and Cerebrovascular Events
MAPK	Mitogen-Activated Protein Kinases
MI	Myocardial Infarction
miRNA	MicroRNA
mitoK _{ATP}	Mitochondrial Potassium ATP-Dependent K ⁺ Channel
mm	millimeter
Mn-SOD	Manganese Superoxide Dismutase
mPTP	Mitochondrial Permeability Transition Pore
MSC	Mesenchymal Stem Cell
Na ⁺	Sodium
NADPH	Nicotinamide Adenine Dinucleotide Phosphate
NBF	Neutral Buffered Formalin
NE	Norepinephrine
NF-κB	Nuclear Factor Kappa B
NIC	Nociceptor-Induced Conditioning
NIH	National Institute of Health
nNOS	Neuronal Nitric Oxide Synthase
NO	Nitric Oxide
non-STEMI	non-ST-Interval Elevated Myocardial Infarction

nonTG	Nontransgenic
NOS	Nitric Oxide Synthase
PBS	Phosphate Buffered Saline
PCI	Percutaneous Intervention
PCR	Polymerase Chain Reaction
PGI ₂	Prostaglandin I ₂ (Prostacyclin)
PGE ₂	Prostaglandin E ₂
PI3K	Phosphoinositide 3-kinase
PKA	Protein Kinase A
PKB	Protein Kinase B
PKC	Protein Kinase C
PKG	Protein Kinase G
PNS	Parasympathetic Nervous System
PTEN	Phosphatase and Tensin Homolog
qPCR	Quantitative Polymerase Chain Reaction
RIC	Remote Ischemic Conditioning
RICSTEMI	Remote Ischemic Conditioning In ST-Elevation Myocardial Infarction as Adjuvant to Primary Angioplasty
RIN	Ribonucleic Acid Integrity Number
RIPA	Radioimmunoprecipitation Assay
RIPC	Remote Ischemic Preconditioning

RIPHEART	Remote Ischemic Preconditioning for Heart Surgery
RISK	Reperfusion Injury Salvage Kinase
ROS	Reactive Oxygen Species
RPCT	Remote Preconditioning of Trauma
RT-qPCR	Reverse Transcription Quantitative Polymerase Chain Reaction
RYR	Ryanodine Receptor
SAFE	Survivor Activating Factor Enhancement
SDS PAGE	Sodium Dodecyl Sulfate Polyacrylamide Gel Electrophoresis
SEM	Standard Error of the Mean
SERCA	Sarco/endoplasmic Reticulum Calcium Transport ATPase
siRNA	Small Interfering Ribonucleic Acid
SNAP	S-nitroso-N-acetylpenicillamine
SNO	S-Nitrosylation or S-Nitrosothiols
SNS	Sympathetic Nervous System
SPECT	Single-Photon Emission Computerized Tomography
STAT	Signal Transducer and Activator of Transcription Proteins
STEMI	ST-Interval Elevated Myocardial Infarction
TBS-T	Tris-Buffered Saline with Tween
TENS	Transcutaneous Electronic Nerve Stimulation
TNF	Tumor Necrosis Factor
TnI	Troponin I

TRAIL	TNF-Related Apoptosis-Inducing Ligand
TUNEL	Terminal Deoxynucleotidyl Transferase dUTP Nick End Labeling
TTC	Triphenol Tetrazolium Chloride
μl	Microliter
μm	Micrometer
μM	Micromolar
V	Volt
VEGF	Vascular Endothelial Growth Factor
VNS	Vagal Nerve Stimulation

ABSTRACT

Cardiovascular disease is the leading cause of death worldwide. A myocardial infarction (MI), commonly known as a heart attack, is a major event in cardiovascular disease characterized by reduced blood flow to the heart. The ischemia and reperfusion (I/R) injury associated with an MI results in a region of dead tissue in the heart called an infarct, the size of which influences patient prognosis. In the 1980s, it was discovered that short, non-lethal episodes of I/R, termed ischemic preconditioning (IPC), can protect the heart against a subsequent MI. Ischemic preconditioning demonstrated the phenomenon of endogenous cardioprotection. Cardioprotection has great potential to reduce myocardial cell death and improve patient outcomes after MI, and yet most cardioprotective strategies have had limited success in clinical scenarios. Remote nociceptor-induced cardioprotection (NIC) elicits the most powerful reduction of cell death ever reported. Electrical stimulation (ES) administered via cutaneous patches offers a clinically feasible way to induce cardioprotection via NIC.

Our previous work demonstrates that the transcription factor nuclear factor κ -light-chain-enhancer of activated B cells (NF- κ B) regulates many cardioprotective genes in the heart following IPC, including the heat shock proteins (HSPs), which act in concert with each other and their cofactors to assist in protein folding, repair, and degradation following myocardial injury. Little is known about the molecular mechanisms of electrically-induced cardioprotection, which is a barrier to the therapy's optimization and successful translation to the clinic. Based on

our work in IPC, we hypothesized that electrical stimulation of the skin is cardioprotective and requires the synthesis of NF- κ B-dependent distal mediators of cardioprotection.

In the studies herein, a cutaneous, 5-volt electrical stimulus applied to the abdomen reduces infarct size in a mouse surgical model of MI. Genetic blockade of NF- κ B activation demonstrates the requirement of NF- κ B in electrically-induced cardioprotection, yet RT-qPCR revealed small, nonsignificant changes in HSP mRNA and protein. Next-generation sequencing on mRNA and microRNA identified a unique transcriptome associated with electrically-induced cardioprotection that includes both recognized mediators and novel transcripts. Confirmatory studies on select molecular candidates were performed by RT-qPCR and Western blotting, and the functional role of the NF- κ B-dependent gene nitric oxide synthase 2 (NOS2) was demonstrated *in vivo*. Results support that an electrical stimulus is cardioprotective in multiple paradigms of cardioprotection. Cardioprotection occurs without a concurrent increase in HSPs, but NF- κ B and the NF- κ B-dependent gene nitric oxide synthase 2 (NOS2) are required for ES-induced cardioprotection. Electrical stimulation also reduced cardiac levels of miR-10b, a circulating microRNA with no previously known role in cardioprotection. These changes were validated by RT-qPCR.

In conclusion, electrically-induced cardioprotection is a novel and translational strategy to reduce cell death following MI. The molecular mechanisms of ES are cardioprotective via unique transcriptomic changes involving NF- κ B and the NF- κ B-dependent gene NOS2. The effect might be regulated epigenetically by microRNA.

CHAPTER I

INTRODUCTION

Cardiovascular disease (CVD) is the leading cause of death worldwide, claiming the lives of 1 in 3 Americans and accounting for a death every 38 seconds (Benjamin, Virani et al. 2018). Concordant with its prevalence, CVD has an enormous economic burden that is predicted to balloon upwards of \$750 million by 2035. A myocardial infarction (MI), commonly known as a heart attack, is a major cardiovascular event characterized by the reduced blood flow and the deprivation of oxygen and nutrients to the heart. An MI is diagnosed by a clinical evaluation, electrocardiogram (ECG) for the presence or absence of ST-interval elevation (STEMI and non-STEMI, respectively), and elevated troponin (TnI) as a serum biomarker of myocardial cell death. The primary therapeutic goal of timely reperfusion is best achieved with the commencement of emergency revascularization by percutaneous intervention (PCI) and balloon angioplasty with the placement of a metal stent, sometimes drug-eluting, at the site of vascular blockade. PCI must be performed within a narrow time frame from the patient's arrival to the hospital, and if PCI is unavailable, delayed, or if the patient presents too late, fibrinolytic therapy and thrombolysis is initiated instead. Other options, including coronary artery bypass grafting (CABG), are used in certain circumstances, such as if PCI has failed or anatomy is unsuitable for PCI (Wijns, Kolh et al. 2010, Hillis, Smith et al. 2012, Levine, Bates et al. 2016).

Within the cardiomyocytes, the ischemic phase of the injury that occurs during reduced blood flow includes a switch to anaerobic metabolism and reduced ATP levels. This results in

acidosis and H^+ accumulation, Na^+/H^+ exchanger activation, and excess intracellular Na^+ .

Subsequent Na^+/Ca^{2+} exchanger reversal overloads the cell with Ca^{2+} . The Na^+/K^+ -ATP-ase and sarco/endoplasmic reticulum Ca^{2+} -ATPase (SERCA) cannot correct the imbalances in Na^+ and Ca^{2+} due to ATP unavailability. Excess Na^+ leads to cell swelling, and Ca^{2+} overload activates proteases and damages mitochondria. Reperfusion after a period of hypoxia is beneficial and necessary to restore blood flow and normal heart function, but is pathogenic in turn. The reperfusion phase reinstates aerobic metabolism and oxidative phosphorylation, generating a sudden burst of reactive oxygen species (ROS). Reactive oxygen species damage intracellular proteins, and cellular stress responses recruit and activate heat shock proteins (HSPs) to address the accumulation of misfolded proteins. Ultimately the stressors in ischemia and reperfusion (I/R) cumulate in the opening of the mitochondrial permeability transition pore (mPTP), mitochondrial swelling and dysfunction, and cell death. The pathology of MI involves injury from both ischemia and reperfusion in roughly equal parts (Carry, Mrak et al. 1989, Klein, Pich et al. 1989, Gumina, Buerger et al. 1999), resulting in the formation of a region of dead tissue known as an infarct (Yellon and Hausenloy 2007).

The loss of cardiomyocytes in MI can lead to reduced cardiac output that fails to meet the body's perfusion demands, causing local and systemic compensatory responses and eventuating in pathological cardiac remodeling and heart failure (HF). It has long been understood that infarct size is a major predictor of patient progression to HF and death, and as the size of the infarct increases, the likelihood that a patient will experience adverse events like HF and death also increases drastically (Sobel, Bresnahan et al. 1972).

Prompt PCI and timely reperfusion is the preferred intervention for MI. Initial

pharmacological therapies for a patient presenting with MI are morphine or opioids as an analgesic, supplemental oxygen if needed, aspirin or clopidogrel as an antiplatelet agent, and nitrates as vasodilators to reduce preload and pain. Beta blockers, angiotensin converting enzyme (ACE) inhibitors or angiotensin II receptors antagonists, and statins, are routinely prescribed following an MI to reduce oxygen demand, slow the progression of HF, and lower the risk of a subsequent MI or major adverse cardiovascular event. There are no cardioprotective therapies in routine clinical use that directly address cell death and reduce infarct formation independent from restoring blood flow.

In the 1980s, it was discovered that short, sub-lethal bouts of I/R applied to the heart protected against a subsequent ischemic stimulus in a canine model (Murry, Jennings et al. 1986). Termed “ischemic preconditioning (IPC),” this was a critical development in the field because it demonstrated the existence of an endogenous cardioprotective system. Since then, various attempts have been made to harness endogenous cardioprotection and develop novel and translational cardioprotective strategies. These include preconditioning and postconditioning, which intervenes during or after the reperfusion period, and remote preconditioning, which is the phenomenon whereby a stimulus applied at a remote site protects the heart from a subsequent MI (Przyklenk, Bauer et al. 1993, Zhao, Corvera et al. 2003). In the human heart, brief I/R by repeated balloon inflations during PCI can mitigate the extent of injury and improve reperfusion (Laskey 2005, Staat, Rioufol et al. 2005, Ma, Zhang et al. 2006).

There are several issues with IPC of the heart as a clinical strategy, including the risk of plaque rupture, the possibility of a deadly coronary dissection, and extension of surgical time.

Pharmacological means to mimic IPC but avoid the risks of ischemia, like preventing the opening of the mPTP (Cung, Morel et al. 2015), have performed unfavorably in clinical trials. Despite multiple attempts at bringing cardioprotection to the clinic, clinical trials (detailed and critiqued in Chapter II) have been small and poorly designed with mixed results upon progression to phase III (Heusch and Rassaf 2016). Thus, the field of cardioprotection has some potential and there is a need for novel therapeutic strategies.

A breakthrough came from our lab with the discovery that remote cardioprotection could be induced by a surgical incision along the abdomen. This effect was termed “remote preconditioning of trauma (RPCT),” and could be mimicked with a topical application of capsaicin applied along the same site, collectively termed “nociceptor-induced cardioprotection (NIC)” (Ren, Wang et al. 2004, Jones, Fan et al. 2009). The mechanistic effect of NIC for the most part parallels that of IPC, with some exceptions, and molecular studies established the role of protein kinase C (PKC) and bradykinin in the NIC effect (Jones, Fan et al. 2009). Surprisingly, tumor necrosis factor alpha (TNF- α) a molecule involved in wound healing and IPC, is not involved in RPCT (Ren, Wang et al. 2004). Nociceptor-induced cardioprotection was a significant development in the field of cardioprotection because skin stimulation offered the same infarct-sparing benefits as IPC, and the potential to remove the complications and risks associated with IPC is beneficial over ischemic therapies.

Ischemic preconditioning and NIC both invoke an early phase activated within minutes and persisting for hours, and a late phase of signaling from 24 hours post-stimulus that may last for several days. The early phase is characterized by receptor binding events, the activation of signaling cascades, and kinase cascades involving acute phosphorylation or translocation

events. The late phase can be triggered by the early phase and activates the binding of transcription factors and downstream gene regulation. Late phase cardioprotection has a high level of clinical significance in situations where hypoxic injury can be reliably predicted, such as cases of elective PCI and CABG, organ transplantation, and other major cardiac surgeries. Our group and others have published several papers on the acute early phase mechanisms of cardioprotection, but less is known about the late phase of cardioprotection, especially NIC (Ren, Wang et al. 2004, Jones, Fan et al. 2009, Gross, Baker et al. 2011, Gross, Hsu et al. 2013, Chai, Liu et al. 2015). The work herein focuses on the under-explored late phase to address the most translational strategies to elicit long-lasting cardioprotection.

This work uses electrically-based cutaneous therapies, also termed “electroceuticals” to reduce infarct size through NIC. It is the very first characterization of the molecular mechanisms of the late phase of electrically-induced cardioprotection via cutaneous patch on the abdomen (ES). Electroceuticals have been utilized increasingly for a wide range of chronic conditions, including arrhythmia, depression, gout, Parkinson’s and Alzheimer’s Disease (Famm, Litt et al. 2013, Mishra 2017). In the cardiovascular field, pacemakers and automated external defibrillators (AEDs) are the most well-known electroceuticals. Experimental approaches in both rodent and large animal models have demonstrated evidence of reduced ischemic injury after MI with electrically-based therapies, like vagal nerve stimulation (VNS) and spinal cord stimulation, electroacupuncture (EA), and transcutaneous electrical nerve stimulation (TENS) for physical therapy (Calvillo, Vanoli et al. 2011, Shinlapawittayatorn, Chinda et al. 2013, Shinlapawittayatorn, Chinda et al. 2014). We hypothesized that electrically-induced cardioprotection via cutaneous stimulation is also effective as late phase nociceptive stimuli in

reducing infarct size. The aim of this dissertation explored the mechanisms of this effect, and identified and characterized the molecular mediators of electrically-induced cardioprotection.

Most cardioprotective interventions, ischemic or otherwise, activate similar late phase signaling pathways within the cardiomyocyte, but little is known about whether these same mediators are involved in electrically-induced NIC. Our lab and others have demonstrated *in vivo* that the transcription factor nuclear factor κ -light-chain-enhancer of activated B cells (NF- κ B) and its gene program is required for IPC and RPCT (Tranter, Ren et al. 2010, Song, Ye et al. 2016). our lab has shown that downstream of NF- κ B, HSPs and the 70.3 isoform of HSP70 are required for IPC in mouse models (Tranter, Ren et al. 2010, Tranter, Helsley et al. 2011). Other late phase protective proteins include nitric oxide synthases (NOS) acting in coordination with each other and their cofactors to mediate the late phase of cardioprotection (Bolli, Dawn et al. 1998). The complete late phase transcriptome of electrically-induced cardioprotection is underexplored, and it is not known which mediators are functionally involved in cutaneous electrically-induced cardioprotection.

The experiments I performed in this dissertation probed the role of the molecular chaperone HSP70 and other HSPs, the transcription factor NF- κ B, and the enzyme NOS2 in electrically-induced late phase cardioprotection. I identify and characterize the molecular candidates that could be involved in electrically-induced cardioprotection. I utilized both pharmacological and genetic inhibitors with a variety of *in vitro* and *in vivo* models, several mouse strains, multiple molecular biology techniques including reverse transcription-quantitative polymerase chain reaction (RT-qPCR) and Western blots, as well as next-generation sequencing and bioinformatics to identify and validate the mediators of electrically-

induced cardioprotection. I determined that electrically-induced cardioprotection by EA and ES is not associated with HSP70 upregulation, in contrast with IPC. Furthermore, I have concluded that the transcription factor NF- κ B is required for electrically-induced cardioprotection. Deep sequencing identified the transcriptome of electrically-induced cardioprotection, and several unique genes were validated by PCR. The transcript levels of NOS2, c-Jun, and the relatively novel gene kyphoscoliosis peptidase (KY) were reliably increased after ES using both deep sequencing and RT-qPCR. Protein kinetics remain elusive. Electrical stimulation was cardioprotective in wild-type mice, and yet ES was unable to protect mice with a genetic deletion of NOS2. Furthermore, microRNA sequencing identified transcriptomic mediators of cardioprotection that expressed changes after ES, including decreasing the levels of miR-10b and several let-7 family members, which I suggest for follow-up studies.

Based on these data, I conclude that electrical stimulation via skin patches on the abdomen induces a unique cardioprotective transcriptome that does not include a heat shock response but requires NF- κ B and the NF- κ B dependent gene NOS2. The transcriptome is perhaps influenced epigenetically by microRNA.

CHAPTER II

LITERATURE REVIEW

The Burden of Cardiovascular Disease

Cardiovascular Disease and Coronary Artery Disease

Cardiovascular disease is the leading cause of death for both men and women worldwide, and although mortality from CVD has decreased in some high income countries, the absolute number of deaths continues to increase, driven by increased incidences in middle- and low-income countries (Collaborators 2016, Joseph, Leong et al. 2017). Cardiovascular disease affects one in three Americans, leading to a death every 38 seconds, and is associated with an enormous economic burden that is predicted to cost the United States \$750 million by the year 2035 (Benjamin, Virani et al. 2018). Cardiovascular disease is influenced by age, genetics, sex and family history, and comorbid conditions like diabetes and obesity, and is worsened by largely preventable lifestyle choices such as poor diet, low levels of exercise, and smoking. Current therapies include lifestyle changes, surgical and pharmacological interventions, and rehabilitation. Though treatments have come far, there is a continued search to reduce the burden of CVD.

Coronary artery disease (CAD), the most common type of CVD, accounts for 43.8 percent of deaths attributed to CVD (Benjamin, Virani et al. 2018). Coronary artery disease is typically manifested by atherosclerosis and the presence of lipid-rich plaques deposits in the arteries. Microvascular disease, a condition in which the small vessels to the heart are

damaged, can occur without the presence of plaques. Chest pain, or angina, and shortness of breath are common symptoms of CAD that become more severe as the disease worsens. The narrowing vasculature limits blood flow to the heart, and if plaques erode or rupture, the subsequent thrombus or clot formation and patient progression to secondary pathologies like MI and HF can be deadly.

Myocardial Infarction and I/R Injury

An MI is a life-threatening event that occurs when a lipid-laden atherosclerotic plaque in the arteries ruptures or erodes, exposing the circulation to its thrombogenic core and matrix. The event precipitates formation of a thrombus, which can partially or completely block blood flow to the heart through the coronary arteries, most often the left anterior descending. The patient with acute coronary syndrome, a set of symptoms that occur with decreased blood flow to the heart, presents with chest or shoulder pressure and pain (angina), difficulty breathing, dizziness and fatigue, nausea or vomiting, and an impending sense of doom (de Torbal, Boersma et al. 2006).

At the point of first medical contact, an ECG can identify whether an MI is occurring, and if so, differentiate the type. The trace of any non-ST elevated MI will have a ST-interval depression or T-wave inversion, while the more serious ST-elevated MI will have a peaked T-wave and ST-interval elevation. ST-elevated MI is associated with complete occlusion of the artery and a transmural radiating infarction, while non-STEMI is associated with an incomplete occlusion, infarction in the left ventricle in the anterior wall distal to the coronary artery, or ischemia in the left ventricle proximal to the coronary artery. The infarction and death of muscle cells will elevate cardiac enzymes in the blood, and elevated levels of serum TnI and

creatinine kinase-muscle/brain (CK-MB, an enzyme released by injured cardiac cells) can be measured in both STEMI and non-STEMI (Thygesen, Alpert et al. 2012). Unstable angina, a separate subset of acute coronary syndrome, occurs when the buildup of plaques in coronary arteries reduces blood flow to the heart and ischemia to the muscle tissue in absence of a thrombus or infarction. Symptoms of unstable angina are similar to STEMI/non-STEMI, but the condition can be distinguished from STEMI by a normal ECG trace, and troponin levels in the circulation can subclassify non-STEMI from unstable angina and disorders other than acute coronary syndrome.

The initial emergency treatment for patients presenting with coronary artery syndrome is supplemental oxygen in patients with hypoxemia, morphine or opioids as analgesia for severe pain, aspirin as an antiplatelet agent, and sublingual nitroglycerin for relief of ischemic discomfort. An ECG will be obtained and interpreted and blood will be sent for serum cardiac troponin screening. The American Heart Association/ American College of Cardiology guidelines recommends that the ECG is interpreted within 10 minutes of the patient's arrival at the hospital. Upon the diagnosis of MI, rapid reperfusion with primary PCI is the preferred intervention for both STEMI and non-STEMI (Levine, Bates et al. 2016).

Primary PCI is initiated with angioplasty, which is the surgical unblocking of the blood vessel. An interventional cardiologist will use a catheter with a balloon at its end and inflate the balloon at the site of occlusion to compress the plaque and relieve the blockage. A stent, a small meshlike piece of metal, can be placed in the coronary artery to support the vessel and act as a scaffold to hold the vessel open. About 40 percent of patients treated with balloon angioplasty develop later blockages, known as restenosis. Restenosis can be reduced to 30%

with the use of a bare metal stent, and drug-eluting stents can lower the rate of restenosis to less than 10% (Dehmer and Smith 2009).

Rapid assessment, prompt treatment initiation, and quick transport to the hospital are essential components to patient care. Current guidelines recommend PCI as soon as possible, within a goal door-to-balloon time of 90 minutes and no later than 120 minutes after the patient arrives in the emergency department (Levine, Bates et al. 2016). If the hospital does not have the facilities or the expertise to perform PCI, transport to a PCI-capable hospital would take too long, or the patient is delayed seeking treatment, commencement of fibrinolytic (thrombolytic) therapy is recommended. These agents lyse acute blood clots and reestablish blood flow by activating plasminogen to form plasmin, which cleaves fibrin cross-links to break down the thrombus (Amsterdam, Wenger et al. 2014, Levine, Bates et al. 2016). Though PCI has a mortality benefit over thrombolytic therapy, the effectiveness of thrombolysis becomes equivalent to PCI when PCI is delayed an hour or more (Nallamothu and Bates 2003, Joy, Kurian et al. 2016).

In the instance of complete coronary occlusion and reperfusion, the pathology after MI involves two phases, an ischemic phase when the heart is subjected to hypoxic conditions, and a reperfusion phase, when the blood flow is restored (Jennings 2013) (Hausenloy and Yellon 2013). Each phase has its own distinct mechanisms to bring about cardiac injury, detailed in the next section and summarized in Figure 1. This results in the formation of a radiating and transmural infarct. Cardiac cells cannot regenerate at levels sufficient to replace the damaged tissue (Hocht-Zeisberg, Kahnert et al. 2004, Eschenhagen, Bolli et al. 2017), so regions of dead tissue are replaced by fibrosis and the formation of a nonfunctional scar in the heart muscle.

The scar is necessary to prevent cardiac aneurism (Hirai, Fujita et al. 1989), yet the scar is inflexible and limits muscle contraction and relaxation (Tennant and Wiggers 1935, Parmley, Chuck et al. 1973), and thus triggers adaptive responses (Ross and McCullagh 1972, Theroux, Ross et al. 1977, Packer 1992).

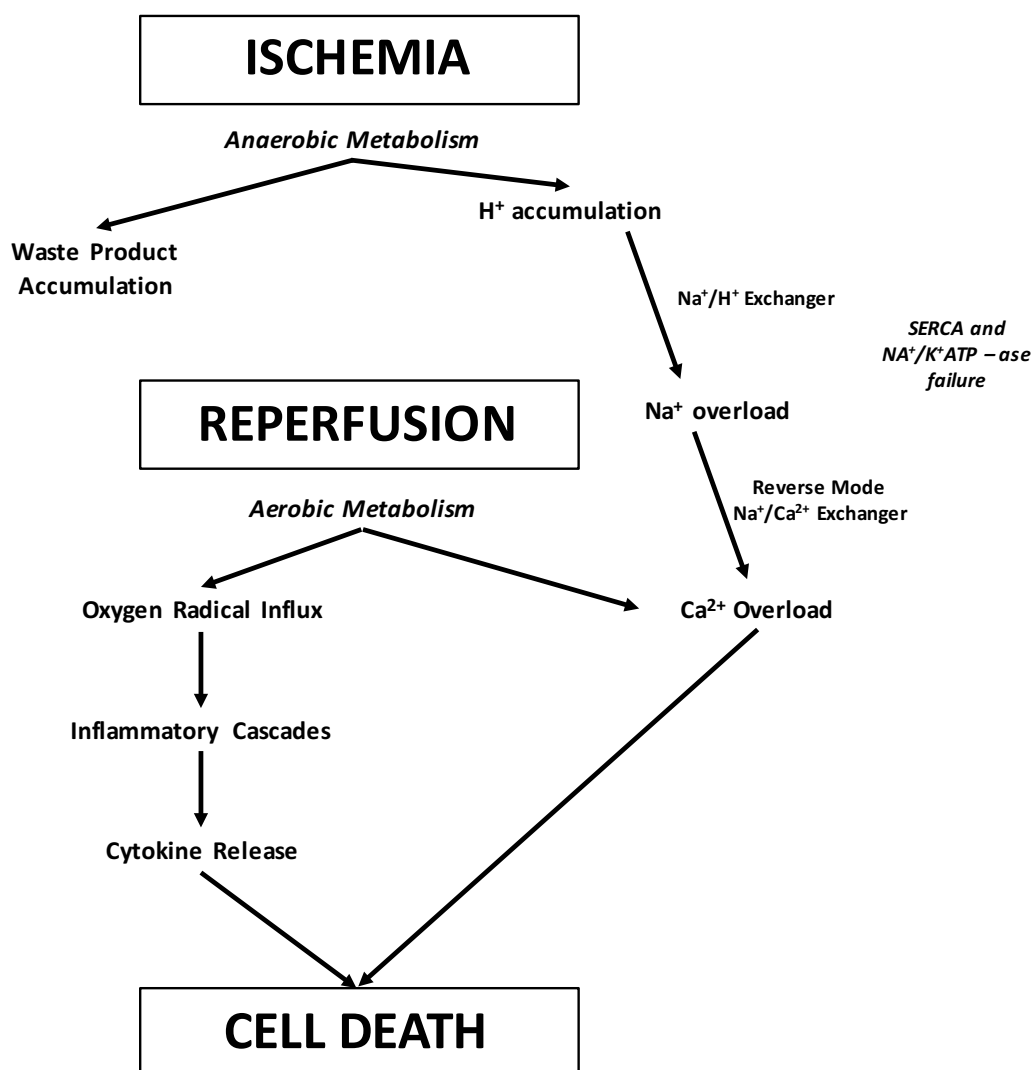


Figure 1. Ischemia/Reperfusion Injury Schematic. The pathophysiology resulting from an MI is due to molecular events in both the ischemic phase and the reperfusion phase. Metabolic fluctuations and altered ion exchange and transport result in intracellular calcium overload and a flush of oxygen radicals, cytokines, and inflammatory mediators. Ultimately, the mitochondrial permeability pore opens and activates inflammatory cascades resulting in cell death. These events lead to death of the myocardium and infarct formation.

The long-term consequence of infarct formation is the heart's impaired ability to meet the perfusion needs of the body, manifested in HF. It has long been known that the final size of the infarct determines patient outcomes and is the best predictor of adverse events such as HF or death (Sobel, Bresnahan et al. 1972).

Pathophysiology of MI

In a normal heart, the contractile filaments in cardiomyocytes depend on ATP production by the mitochondrial electron transport chain (ETC) via oxidative phosphorylation to function. During the ischemic phase of an MI, the heart is subjected to a period of hypoxia which triggers a cascade of intracellular signaling events starting with the cardiomyocyte switch to anaerobic metabolism and glycolysis, which increases the intracellular levels of the byproduct lactate (Kalogeris, Baines et al. 2012). To counteract the resulting decrease in intracellular pH, the Na^+/H^+ exchanger pumps hydrogen ions out of the cardiomyocyte, resulting in increased intracellular sodium levels. This activates the $\text{Na}^+/\text{Ca}^{2+}$ to run in reverse, shunting sodium out of the cell and transferring calcium into the cell. The altered cation exchange ultimately leads to intracellular calcium overload. During reperfusion, blood flow is restored, resulting in an influx of oxygen, as well as the formation of ROS, which can damage DNA, lipids, and proteins. This influx of oxygen restores aerobic metabolism and normalizes intracellular pH, but continues to contribute to altered cation transport and calcium overload. Ultimately, I/R injury results in the opening of the mitochondrial permeability pore and dissipation of the electrochemical protein gradient, mitochondrial swelling and rupture, activation of protease and cytokine signaling and inflammatory cascades, and death of the muscle cell.

The pathophysiology of MI is related to both the duration and extent of ischemia, and paradoxically, reperfusion after a period of oxygen deprivation can partly contribute to the death of cells during MI as well (Jennings, Sommers et al. 1960, Kloner, Ganote et al. 1974, Hachamovitch, Berman et al. 1998, Yellon and Hausenloy 2007). Myocardial reperfusion injury was first proposed in the 1960s with the discovery that the ionic changes initiated during reperfusion could hasten cell death (Jennings, Sommers et al. 1960). In this initial study, morphologic alterations of the myocardium, such as cardiac myocytes swelling, mitochondrial damage, hypercontracture, and loss of myofibrillar organization, were observed upon reperfusion of a canine heart. Cardiac enzyme measurements peak once in ischemia and again in reperfusion, supporting two distinct phases of cell death (Hearse, Humphrey et al. 1973). Reperfusion has its own pathological characteristics that are causal to the restoration of blood flow, including mechanical dysfunction and myocardial “stunning” (Braunwald and Kloner 1982), the no-reflow phenomenon whereby a previously ischemic region resists reperfusion (Kloner, Ganote et al. 1974, Kloner, Ganote et al. 1975), reperfusion arrhythmias (Tennant and Wiggers 1935), and lethal reperfusion injury. Although reperfusion is beneficial in washing out the lactic acid byproducts of metabolism and restoring physiological pH and oxygen levels, the acidosis reversal (Lemasters, Bond et al. 1996), further ion alterations, calcium overload, hypercontracture (Jennings, Sommers et al. 1960), and generation of oxidative stress and free radicals can cause cell death in turn (Zweier 1988). These events, like those in ischemia, culminate on the opening of the mPTP, which can be opposed by a prosurvival reperfusion injury salvage kinase pathway (RISK) involving the activation of phosphatidylinositol-3-OH kinase (PI3K), protein kinase B (PKB/Akt) or extracellular signal regulated kinase (ERK1/2)

(Davidson, Hausenloy et al. 2006).

A large burst of cell death occurs within the first 24 hours after MI (Kajstura, Cheng et al. 1996), and a lower magnitude of cell death can persist for months after MI as remodeling progresses (Sam, Sawyer et al. 2000). The death of cardiomyocytes is due to apoptosis, necrosis, and autophagy, which differ by several features. Apoptotic cell death is characterized by controlled cell shrinkage, nucleic acid condensation, and formation of apoptotic bodies which are phagocytosed by neighboring cells or degraded (Saraste, Pulkki et al. 1997). Apoptosis is mediated by an intrinsic pathway through intracellular signaling and an extrinsic pathway through extracellular stimuli like tumor necrosis factor-alpha-related apoptosis-inducing ligand (TRAIL), first apoptosis signal (FAS), and tumor necrosis factor (TNF) acting on cell surface death receptors. The intrinsic pathway is thought to be more important in the regulation of cardiomyocyte death in MI than the extrinsic pathway (Gomez, Chavanis et al. 2005). In intrinsic apoptosis, the ratio of anti-apoptotic Bcl-2 proteins to pro-apoptotic Bcl-2-associated X-protein (BAX) and BH3-only proteins shifts to favor pro-apoptotic intracellular signaling, eventually resulting in destabilization of the mitochondrial membrane, release of cytochrome c, the formation of an apoptosome, and the activation of caspase 3 and 7 (Maulik, Engelman et al. 1999, Chapman, Magee et al. 2002, Kubasiak, Hernandez et al. 2002). Interventions in experimental models that address intracellular apoptotic signaling, for example, the genetic deletion of BAX, can result in improved function after MI (Hochhauser, Cheporko et al. 2007). Extrinsic apoptotic cell death can also converge on caspase 3 and 7, and caspase inhibition and the amelioration of apoptosis is beneficial in MI (Holly, Drincic et al. 1999, Chandrashekhar, Sen et al. 2004). Necrotic death, once thought to occur due to random

processes, is now known to occur sometimes as a result of its own independent and controlled signaling cascades (Kung, Konstantinidis et al. 2011). Myocardial permeability pore transition appears to be a point of overlap for both necrotic and apoptotic cell death, since pharmacological inhibition of the pore reduced both types of cell death in experimental studies (Bognar, Kalai et al. 2006). Autophagy is characterized by the encapsulation of damaged or degraded proteins in a phagosome and subsequent merging with the lysosome. All types of cell death occur during and after an MI, though the molecular mechanisms are different, which has implications for therapies seeking to target a specific cell death pathway. Necrotic cell death may not be reversible, but therapies targeting necroptosis, apoptosis and autophagy might coax at-risk cardiomyocytes to convert to a pro-survival phenotype.

Heart Failure

Heart failure occurs when the heart is unable to meet the body's perfusion demand to satisfy its metabolic requirements. Ejection fraction (EF), the percentage of blood leaving the heart with each contraction, is important in the further classification of HF. Heart failure with preserved ejection fraction (HFpEF), also known as diastolic HF, occurs when the heart has impaired relaxation driven by stiffness or hypertrophy of the muscle walls and abnormal filling. Heart failure with reduced ejection fraction (HFrEF), also known as systolic HF, is associated with the thinning of the muscle wall, enlarged chambers, and dilation of the organ. An ejection fraction of 40% or less qualifies as HFrEF (Yancy, Jessup et al. 2013). Heart failure of either type can occur on the left side, right side, or both, and can occur secondarily to a variety of pathological insults, including MI.

In the context of MI, the myocyte loss, increased fibrosis, hypertrophy with wall

stiffening and activation of compensatory mechanisms can be adaptive in the short term but evolve into pathological cardiac remodeling under chronic stress and sustained activation. The main consequence of the structural modifications and remodeling is HF. Left ventricular systolic HF is the most common type of HF that develops after MI (Persson, Linder-Klingsell et al. 1995).

A death soon after MI onset can most often be attributed to ventricular fibrillation and cardiac arrest, but HF is a major cause of late morbidity and mortality after MI, and patients that do experience new-onset HF after MI have a significantly higher risk of death during their acute hospitalization (Henkel, Witt et al. 2006, McManus, Chinali et al. 2011, Gerber, Weston et al. 2013, Bhar-Amato, Davies et al. 2017). Potential pharmacological treatments of MI that prevent or treat HF include angiotensin converting enzyme inhibitors, angiotensin receptor antagonists, β -receptor antagonists, diuretics, nitrates, and statins. Since infarct size is a major determinant of left ventricle (LV) dysfunction and HF (Sobel, Bresnahan et al. 1972), therapeutics that reduce cardiovascular damage would likely be more effective than HF symptom treatment. This is supported by evidence from animal models, though no such human therapeutic is available at present.

Perioperative MI and Points of Intervention

The severity and duration of ischemia, time to treatment, and reperfusion strategy contribute to mortality following MI. Time to treatment is currently recommended to be less than 30 minutes (Wang, Nallamothu et al. 2011). Dramatic reductions in treatment delay have driven a reduction in inpatient mortality after acute MI, and yet approximately 25% of MI patients will proceed to develop HF, and 50% of those who develop HF will die within five years (Cahill and Kharbanda 2017, Kochar, Chen et al. 2018). However, cardioprotective therapies to

preserve myocardium could be administered at home, during transport to the hospital, or during PCI, with a massive impact on patient prognosis. Having these therapies available would be needed, and this was the inspiration for the studies we undertook.

Cardioprotection of all types has an early phase that occurs immediately after the initial stimulus and can last for several hours, and a late phase that offers delayed protection and can remain protective for 24-72 hours (Marber, Latchman et al. 1993, Guo, Wu et al. 1998). Though spontaneous MIs are not reliably predictable, there are clinical scenarios beyond acute MI in which one can reasonably expect a risk of hypoxic injury. In such instances, the late phase of cardioprotection would be especially valuable. These situations include: cardiac surgery and CABG surgery, where remote ischemic preconditioning (RIPC) has been shown to reduce signs of myocardial injury clinically (Theroux, Chaitman et al. 2000, Hausenloy, Mwamure et al. 2007, Venugopal, Hausenloy et al. 2009, Li, Luo et al. 2010, Wagner, Piler et al. 2010), elective PCI (Hoole, Heck et al. 2009), or organ transplantation, where situations of I/R adversely affect the organ's lifespan (Selzner, Boehnert et al. 2012). Percutaneous interventions alone are performed on approximately 1 million patients annually in the United States, and perioperative MI occurs in at least 10% of those patients (Prasad, Gersh et al. 2009, Cuculi, Lim et al. 2010, Hanna and Hennebry 2010, Lansky and Stone 2010, Mozaffarian, Benjamin et al. 2015). In such cases, strategies to preserve myocardium can reduce susceptibility to perioperative injury.

Several strategies have been explored to protect the heart and reduce I/R injury in the context of both STEMI and elective surgical procedures. Though advancements in animal studies and small scale clinical trials have indicated some positive outcomes, larger clinical trials

have had mixed results and have received substantive criticism. For example, two major pharmacological studies that employ cyclosporine to inhibit the mPTP in patients with STEMI both failed in large-scale clinical trials, but the follow-up duration was short in one (6 months) and the enrollment criteria was questioned in the other (patients were accepted up to 12 hours after the onset of symptoms) (Cung, Morel et al. 2015, Ottani, Latini et al. 2016). Ischemic preconditioning during surgery failed to improve patient outcomes, though these trials are flawed by the concurrent use of a cardioprotective anesthetic (Hausenloy, Candilio et al. 2015, Meybohm, Bein et al. 2015). The recent Remote Ischemic Conditioning in ST-elevation Myocardial Infarction as Adjuvant to Primary Angioplasty (RIC-STEMI) trial demonstrated reduced infarct size, mortality and hospitalization in STEMI patients treated with RIPC, but there were no differences in serum troponin levels, and deviation from standard statistical analyses, such as the exclusion of patients after randomization, marred the study (Gaspar, Lourenco et al. 2018). Due to the lack of well-designed large, multicenter studies investigating hard clinical endpoints, there is no cardioprotective strategy routinely utilized in the clinic to address myocardial salvage beyond the pharmacomimetic drugs that are already in routine perioperative use for other reasons, like opioids and volatile anesthetics (Heusch 2013, Heusch and Rassaf 2016). A safe and effective infarct-reducing therapy would have monumental benefits for patients.

The focus of the work herein explores therapy of electrically-induced cardioprotection as a bold new strategy to reduce infarct size by harnessing the body's endogenous cardioprotective system for therapeutic benefit. This work is novel because it is translatable, inexpensive, and user-friendly; if successful, electrically-induced cardioprotection carries

massive socioeconomic and clinical implications for the treatment and prevention of CVD.

Understanding the molecular mechanisms on the basic science level, as I have attempted with this dissertation, is critical for refining the stimulus, enhancing its therapeutic benefit, and securing support of its translation into man.

Cardioprotection Paradigms

Ischemic Preconditioning

Several cardioprotective strategies have been evaluated in animal models with potential for translation into man. One of the earliest demonstrations of an intervention with an infarct-sparing effect was performed in a canine model. Ischemic preconditioning was discovered by Murry et al., who demonstrated that when the heart was subjected to brief, sublethal periods of I/R, it was successfully protected from a subsequent ischemic insult (Murry, Jennings et al. 1986). The studies that followed demonstrated that IPC not only reduced infarct size but also successfully reduced arrhythmias and improved cardiac function after MI (Murry, Jennings et al. 1986, Hagar, Hale et al. 1991, Lott, Guo et al. 1996). Since then, IPC has been validated in a variety of animal models (Gill, Kuriakose et al. 2015). The discovery of IPC and its validation was critical to the field of cardioprotection because it demonstrated the existence of an endogenous cardioprotective system that might be harnessed for therapeutic benefit. Early clinical trials of IPC in the human heart by intermittent clamping and unclamping of the aorta were promising, but ultimately deemed unsuitable for large-scale translation because of the invasiveness and time required to complete the procedure (Yellon, Alkhulaifi et al. 1993, Walsh, Tang et al. 2008).

The classical molecular mechanisms of IPC can be organized spatio-temporally into

stimuli/triggers, intracellular *mediators*, and *end effectors*. Multiple G-protein coupled receptors (GPCRs) on the surface of the myocardium confer cardioprotection when activated by autacoids and neurohormones, such as adenosine (A1) (Liu, Thornton et al. 1991, Surendra, Diaz et al. 2013), bradykinin (B2) (Goto, Liu et al. 1995, Schulz, Post et al. 1998, Ersahin, Euler et al. 1999, Schoemaker and van Heijningen 2000), and opioids (Bell, Sack et al. 2000) (Surendra, Diaz et al. 2013). Receptors have an additive effect such that blockade of one increases the cardioprotective threshold of IPC and requires additional cycles of I/R to achieve the same level of protection (Goto, Liu et al. 1995, Yellon and Downey 2003).

Nitric oxide (NO) generated by endothelial nitric oxide synthase (eNOS) can trigger cardioprotection (Bolli, Bhatti et al. 1997, Xuan, Tang et al. 2000, Xuan, Guo et al. 2007). Reactive oxygen species play a dual role in that ROS can be cardioprotective prior to ischemia, but injurious at the time of I/R (Sun, Tang et al. 1996). Proinflammatory cytokines can also confer protection. Antibodies against the TNF- α and IL- β cytokines (Yamashita, Hoshida et al. 2000) and genetic deletion of TNF- α and IL-6 (Dawn, Guo et al. 2004, Dawn, Xuan et al. 2004) have been used to establish the involvement of these proteins in IPC. As initiators, they act upstream of the transcription factors NF- κ B and activator protein 1 (AP-1), and as mediators at the time of I/R, they help initiate wound healing and improve post-MI remodeling (Dawn, Guo et al. 2004, Nian, Lee et al. 2004).

A series of cardioprotective kinase cascades are activated downstream of the cell surface receptors, NO, and cytokines. Blockade of PKC can eliminate protection, and activation of PKC can precondition the heart (Ytrehus, Liu et al. 1994, Mitchell, Meng et al. 1995). Only certain isoforms of PKC appear to play integral roles in cardioprotection: PKC- ε (Gray, Karliner

et al. 1997, Ping, Zhang et al. 1997, Liu, Cohen et al. 1999), PKC- δ (Zhao, Renner et al. 1998), and PKC- α (Wang and Ashraf 1998) in particular are involved in I/R. PKC- δ is considered the injurious isoform and PKC- ϵ is the primary isoform conferring cardioprotection. The intracellular signaling cascades have been simplified into major pathways referring to a group of prosurvival kinases. The RISK pathway includes PKB/Akt and ERK1/2 (Tsang, Hausenloy et al. 2004, Hausenloy, Tsang et al. 2005). The survivor activating factor enhancement pathway (SAFE) triggered by TNF- α consists of JAK/ STAT3 (STAT5 in humans)(Lecour, Suleman et al. 2005, Lacerda, Somers et al. 2009, Lecour 2009, Lecour 2009). The NO/protein kinase G (PKG) pathway is involved as well (Cohen and Downey 2007).

The early phase of IPC is mediated by the ligand-GPCR interactions and activation of preexisting kinases, while the late phase of IPC is conferred by the activation of transcription factors, such as NF- κ B (Tranter, Ren et al. 2010, Wilhide, Tranter et al. 2011) and STAT3 (Lecour 2009). These transcription factors activate cardioprotective gene programs leading to the synthesis of distal mediators. Nitric oxide synthase 2 was the first of these mediators to be identified in that pharmacological inhibition of NOS2 at the time of I/R abrogates IPC (Takano, Manchikalapudi et al. 1998). The production of NO by NOS2 acts on a number of proteins within the cardiomyocyte via S-nitrosylation of cysteine residues of target proteins. This post-translational modification influences their functions, such as inhibiting components of the mitochondrial transport chain to limit reperfusion injury (Jones and Bolli 2006). Next, cyclooxygenase 2 (COX2) was implicated in the late phase of IPC by catalyzing the synthesis of the cardioprotective prostaglandins PGI₂ and PGE₂ (Shinmura, Tang et al. 2000). Nitric oxide synthase 2 can form a complex with and activate COX2 (Shinmura, Xuan et al. 2002, Xuan, Guo

et al. 2003). Heat shock proteins are also induced, and the unfolded protein response salvages damaged proteins during I/R (Marber, Latchman et al. 1993). Free radical scavengers and antioxidants like mitochondrial manganese superoxide dismutase (Mn-SOD) (Hoshida, Yamashita et al. 2002) and heme oxygenase-1 (HO-1) (Jancso, Cserepes et al. 2007) are also active and beneficial in delayed IPC.

Considerable data pinpoints mitochondrial targets as end effectors of cardioprotection. Opening of the ATP-sensitive mitochondrial potassium channel (mitoK_{ATP}) is a major end effector of these signaling cascades, whereby the mechanisms of protection conferred by this event might include maintaining mitochondrial structure, volume, and ATP permeability (Dos Santos, Kowaltowski et al. 2002, Konstantinov, Li et al. 2005). Opening the K_{Ca} channel might also be beneficial in IPC to stem Ca²⁺ influx into the mitochondria (Xu, Liu et al. 2002). Formation of the mPTP is a tipping point for cell death, and cardioprotective therapies link the preservation of myocardium to the prevention of mPTP opening (Hausenloy, Maddock et al. 2002, West, Rokosh et al. 2008). Modulation of ATP is critical for surviving I/R injury, and mitochondrial bioenergetics perturbations that uncouple oxidative phosphorylation and blunt the rate of ATP decline may also be end effectors of IPC signaling cascades (Opie and Sack 2002). Ultimately, these mitochondrial end effectors help the cardiomyocyte avert cell death.

Perconditioning and Postconditioning

Perconditioning therapies intervene in parallel with the ischemic event and prior to reperfusion (Schmidt, Smerup et al. 2007). This later timing makes this therapy more suitable for use in situations of acute MI, ischemic stroke, or major vascular occlusion in unpredictable or nonelective ischemic events and emergency scenarios. The postconditioning variation

intervenes after the ischemic event and at the onset of reperfusion, first demonstrated experimentally in a canine model (Zhao, Corvera et al. 2003), and supported by follow-up studies in several other animal models (Kin, Zhao et al. 2004, Bopassa, Michel et al. 2005, Kin, Zatta et al. 2005, Bopassa, Ferrera et al. 2006) (Tsang, Hausenloy et al. 2004), and some small proof-of-concept studies in clinical trials in patients receiving PCI for acute MI (Staat, Rioufol et al. 2005).

Studies that combine preconditioning, perconditioning, and postconditioning support that these therapies activate similar molecular pathways (Xin, Zhu et al. 2010). Individually, postconditioning and perconditioning are less powerful than preconditioning. However, the additive effect of perconditioning and postconditioning is equivalent to that of preconditioning. Similar patterns were demonstrated on the mechanistic level by probing the activation status of RISK pathway components. Preconditioning in combination with either perconditioning or postconditioning does not confer further benefits in animal studies or clinically, suggesting that the mechanisms are overlapping (Xin, Zhu et al. 2010, Eitel, Stiermaier et al. 2015).

Remote Ischemic Preconditioning and Clinical Translation Attempts

Remote ischemic preconditioning is a phenomenon whereby an ischemic stimulus can be applied to one organ and initiate protection of another. Remote preconditioning can be cardioprotective when a stimulus applied at a remote site incurs protection to the heart. This effect was discovered in 1993 by Przyklenk, who subjected a remote vascular bed of the heart to brief periods of I/R and discovered that this paradigm reduced infarct size in the left ventricle (Przyklenk, Bauer et al. 1993). Since then, it has been discovered that the effect of remote preconditioning can be recapitulated by brief periods of I/R to an organ distant from the heart,

like the kidney or mesentery (Birnbaum, Hale et al. 1997) (Gho, Schoemaker et al. 1996) (Kerendi, Kin et al. 2005). In perhaps the most translatable example of RIPC, it was found that cardioprotection could be achieved by I/R of the hind limb, which was first demonstrated in a porcine model (Kharbanda, Mortensen et al. 2002).

Like IPC, RIPC requires bradykinin (Schoemaker and van Heijningen 2000), adenosine (Ding, Zhang et al. 2001, Liem, Verdouw et al. 2002), opioids (Wong 2012), and PKC activation (Wolfrum, Schneider et al. 2002) to confer cardioprotection. A neurogenic pathway must play a key role in RIPC, as demonstrated by the fact that ganglionic blockade and nerve sectioning reduce the cardioprotection (Gho, Schoemaker et al. 1996, Liem, Verdouw et al. 2002, Wolfrum, Schneider et al. 2002, Loukogeorgakis, Panagiotidou et al. 2005) (Ding, Zhang et al. 2001, Lim, Yellon et al. 2010, Donato, Buchholz et al. 2013). In later paradigms of NIC, the discovery of a circulating, dialyzable mediator that could confer cardioprotection gave rise to the humoral hypothesis of remote cardioprotection (Dickson, Lorbar et al. 1999, Serejo, Rodrigues et al. 2007, Shimizu, Tropak et al. 2009, Redington, Disenhouse et al. 2012, Redington, Disenhouse et al. 2013, Merlocco, Redington et al. 2014).

Attempts to bring cardioprotection to the clinic have had mixed results. Cyclosporine, which increases the threshold for mPTP opening, is one pharmacological mimic of IPC. However, the large-scale phase III Cyclosporine and Prognosis in Acute Myocardial Infarction Patients (CIRCUS) and phase II The CYCLOsporine A in Reperfused Acute Myocardial Infarction (CYCLE) trials demonstrated that a single bolus of intravenous cyclosporine (2.5 mg/kg) before PCI did not improve clinical outcomes or prevent left ventricular remodeling 6 months and 1 year after STEMI (Cung, Morel et al. 2015, Ottani, Latini et al. 2016). In the CIRCUS trial, patients

with reperfusions delayed up to 12 hours from symptoms were accepted into the study. In that window, other pharmacological and potentially cardioprotective interventions could have been administered, and anyway, much of the tissue would have been nonviable after such a prolonged occlusion (Heusch 2015). The CYCLE trial has drawbacks as well, including the selection of endpoints like ST-interval resolution as surrogates of cardioprotection (Chen-Scarabelli and Scarabelli 2016). Overall, both trials are negative on whether cyclosporine is cardioprotective in the clinic.

The first translation of RIPC into humans was a single-blinded, randomized, controlled trial in adults undergoing elective coronary bypass graft surgery (Hausenloy, Mwamure et al. 2007). Patients received three 5-min cycles of I/R induced by repeated inflations of a blood pressure cuff on the arm to 200 mm Hg and intervening 5-minute deflations. Serum troponin was measured 6, 12, 24, and 48 hours after surgery, and a reduced area under the troponin curve in the IPC condition indicated that patients benefitted from the intervention. However, the reduction in troponin release could not be replicated and no clinical outcome benefit at 1 year could be demonstrated in two large, high profile studies that followed: ERICCA (Effect of Remote Ischemic Preconditioning on Clinical Outcomes in CAGB Surgery) and RIPHeart (Remote Ischemic Preconditioning in Heart Surgery) (Hausenloy, Candilio et al. 2015, Meybohm, Bein et al. 2015) . The negative results tempered enthusiasm, but the use of propofol, known to interfere with RIPC, rather than volatile anesthesia is a severe design flaw in both phase III studies (Kottenberg, Thielmann et al. 2012). The Cardiac Remote Ischemic Preconditioning in Coronary Stenting (CRISP-Stent) study, in which RIPC was applied before elective PCI, had more encouraging results. Remote IPC reduced chest discomfort during PCI, attenuated troponin

release, and reduced major cardiac and cerebrovascular events at 6 months (Hoole, Heck et al. 2009). Still, the findings need to be substantiated in larger studies.

A landmark proof-of-concept study was completed on RIPC by blood pressure cuff (four cycles of 5-min inflation and 5-min deflation of a blood-pressure cuff) administered during transport and before reperfusion by PCI. Results demonstrated an improved myocardial salvage index, as estimated by gated single photon emission CT (SPECT) 30 days after primary PCI (Botker, Kharbanda et al. 2010). An echocardiographic sub-study further demonstrated that the most pronounced RIPC-related improvements in LV function occurred in patients with extensive areas at risk (>35% of the LV) and large anterior descending coronary artery infarcts (Munk, Andersen et al. 2010). In a small follow up study (investigated at a median of 3.8 years later) of the initial 2010 cohort, RIPC seemed to improve long-term outcomes defined by significantly fewer major cardiac and cerebrovascular events (MACCE) – a composite of all-cause mortality, MI, readmission for HF, and ischemic stroke/transient ischemic attack (Sloth, Schmidt et al. 2014). Taken together, these studies provide grounds for larger and longer-term investigations of IPC.

On the contrary, the cardioprotective effects of remote postconditioning in STEMI patients have not yet been demonstrated in large-scale clinical trials. In the largest postconditioning study to date, postconditioning (4 cycles of 1-minute reocclusion and 1-minute reperfusion) performed immediately after restoration of coronary flow by PCI was unable to reduce infarct size estimated by cardiac magnetic resonance imaging after 4 months (Limalanathan, Andersen et al. 2014). The effects of postconditioning on secondary endpoints, including markers of necrosis, myocardial salvage, and ejection fraction, as well as adverse

cardiac events during follow-up, were also neutral (Hahn, Song et al. 2013, Limalanathan, Andersen et al. 2014). A study of combined RIPC and postconditioning showed reduced infarct size measured by cardiac magnetic resonance within 3 days after infarction. There was no benefit to postconditioning exclusively. Still, the infarct reduction did not translate to differences in the clinical endpoints of death, re-infarction, and new congestive HF after 6 months (Eitel, Stiermaier et al. 2015).

The recent publication of the RIC-STEMI trial examining the effect of remote ischemic conditioning on long-term clinical outcomes after STEMI supports a long-lasting benefit (Gaspar, Lourenco et al. 2018). Three cycles of intermittent 5 min lower limb ischemia reduced the hard clinical endpoints of cardiac mortality and hospitalization for HF compared with patients who received the standard of care without remote ischemic conditioning. Other measurements, such as in-hospital HF, need for diuretics or inotropes, and echocardiographically documented ejection fraction recovery were also improved in the remote ischemic conditioning group. The study received substantial criticism for the exclusion of a number of patients after randomization (Heusch 2018). Surprisingly, no difference was found in serum troponin I levels between groups, possibly due to patient heterogeneity in the ischemic insult. There was no decrease in all-cause mortality and major adverse cardiac and cerebrovascular events, which remains unexplained. Despite its limitations, this is the largest study to provide evidence for cardioprotection by RIPC, and importantly, using a clinical outcome as the primary endpoint.

Nociceptor-Induced Cardioprotection

Our lab recently established that activation of skin nociceptors is a novel way of

initiating cardioprotection (Ren, Wang et al. 2004, Jones, Fan et al. 2009, Ren, Roessler et al. 2018). In RPCT, a surgical incision applied along the skin of the abdomen reduces the size of the infarct. This effect was mimicked by the application of topical capsaicin. The cardioprotective effects of nociceptor activation by surgical incision or capsaicin application implicate many of the same pathways involved in IPC and RIPC, with several new pathways. Remote preconditioning of trauma requires peripheral nerves and a neural connection to the heart, as in RIPC (Jones, Fan et al. 2009, Gross, Hsu et al. 2013). Specifically, pharmacological applications, nerve transection, and genetic deletion models support that RPCT activates TRPV1 receptors on C-fibers in the peripheral nerves to initiate a reflex in the spinal cord (Tsou, Huang et al. 2004, Jones, Fan et al. 2009). Substance P and calcitonin-gene related peptide (CGRP) released from the sensory nerve endings on the heart facilitate norepinephrine (NE) release from sympathetic cardiac nerves and the activation of adrenergic receptors on the cardiomyocyte, as in IPC (Gao, Fu et al. 2007, Jones, Fan et al. 2009). Like IPC, there is a requirement for bradykinin in NIC (Jones, Fan et al. 2009, Gross, Baker et al. 2011, Gross, Hsu et al. 2013). However, RPCT occurred independently of $\text{TNF-}\alpha$, a major cytokine required for classical IPC (Smith, Suleman et al. 2002, Ren, Wang et al. 2004). Neither opioids or adenosine are required for RPCT by abdominal incision, in contrast to IPC (Ren, Wang et al. 2004, Jones, Fan et al. 2009, Gross, Hsu et al. 2013). Within the cardiomyocyte, PKC is an important mediator in both IPC and RPCT. Our lab and others have shown that RPCT suppresses the injurious PKC- δ isoform and activates the cardioprotective PKC- ϵ isoform (Jones, Fan et al. 2009, Gross, Hsu et al. 2013). PKC- γ , a neuronal isoform, is also activated by surgical incision (Gross, Hsu et al. 2013, Chai, Liu et al. 2015). The signaling cascades in both NIC and IPC terminate on

the mitochondrial K_{ATP} channel as an end-effector (Jones, Fan et al. 2009).

Nociceptor-induced cardioprotection is supported by the observation that chronic pain, such as the chest pain experienced in preinfarction angina, is associated with cardioprotection (Cheng and Chen 2018). When these results are interpreted in the context of all other therapies available, NIC offers an appealing alternative to ischemic-based cardioprotection, which is not feasible or safe for all patients. Since CAD is a major risk factor for MI, non-ischemic strategies are the most appropriate treatment for a wide subset of patients. Thus, NIC is a breakthrough in the field.

Electrically-Induced Cardioprotection and the Field of Electroceuticals

Due to the complications of pharmacological administration and the invasiveness of a surgical incision in bringing about NIC, my dissertation work has focused on eliciting NIC using electricity. “Electroceuticals,” also known as bioelectronics, is a rising field that is gaining attention as a beneficial therapy for a variety of chronic conditions (Famm, Litt et al. 2013, Mishra 2017). In humans, neuromuscular electrical stimulation of the lower extremities at 20-200 Hz for up to an hour was investigated for safety and feasibility. Electrical stimulation implemented 1-5 days postoperatively in a group of patients undergoing major cardiovascular surgery (CABG surgery, valvular surgery, aortic surgery, or combined surgery) was not associated with any changes in heart rate, blood pressure, pacemaker malfunction or arrhythmias (Iwatsu, Yamada et al. 2015). A systemic review of clinical trials with transcutaneous VNS, an exemplar of electronic-based medicine in human subjects, further demonstrates that side effects are mild (local skin irritation, headache, and nasopharyngitis), and only occur in a minority (2.6%) of patients (Redgrave, Day et al. 2018).

In a clinical trial, long term VNS therapy was demonstrated to be safe and tolerable in chronic HF patients. Unfortunately, there was no difference in efficacy endpoint in the VNS group, although quality of life measurements improved. Based on imaging of the heart rate response, investigators suspected that the recruitment of nerve fibers by VNS was substantially lower than what might have been required to evoke an anti-remodeling effect (De Ferrari, Crijns et al. 2011, De Ferrari, Stolen et al. 2017). Vagal nerve stimulation is approved by the FDA for other chronic conditions, such as refractory or drug-resistant epilepsy. Vagal nerve stimulation can reduce seizures up to 28% in the first 3 months, and up to 75% after 10 years (Handforth, DeGiorgio et al. 1998, Elliott, Morsi et al. 2011). After implantation, patients report a short recovery time and improved quality of life (Ryvlin, Gilliam et al. 2014). Alternative indications of neurostimulation, such as spinal cord stimulation to reduce chronic pain, are safe and effective therapies for other patient populations (Deer, Mekhail et al. 2014).

Major industry leaders are also venturing into the electroceuticals market. GlaxoSmithCline, in partnership with Galvani Pharmaceuticals of the Alphabet family of companies, are developing electrically-based devices for heart conditions (Famm, Litt et al. 2013). Surgical and pharmacological approaches remain the standard of care, but electroceuticals present a novel, precise, and personalized approach to managing and preventing CVD, which warrants further investigation from academia and industry alike.

Vagal Nerve Stimulation in Cardioprotection

The vagal nerve is a mediator of the parasympathetic nervous system that acts to reduce the rate and force of contraction of the heart via acetylcholine binding to nicotinic receptors on the ganglion and muscarinic receptors on the cardiomyocyte. It has been

demonstrated that parasympathetic activation through electrical stimulation of the vagus nerve has cardiovascular benefits in disease states. In chronic HF, preclinical studies report the benefits of VNS in reducing inflammation, improving ventricular function, attenuating disease progression and improving overall survival (Morita, Suzuki et al. 2003, Li, Zheng et al. 2004, Zhang, Popovic et al. 2009, De Ferrari, Crijns et al. 2011, Sabbah, Ilsar et al. 2011, Hamann, Ruble et al. 2013, De Ferrari, Stolen et al. 2017). In canine models, continuous low-level electrical vagal stimulation (20 Hz, 100 μ s or 13 Hz, 450 μ s, at one voltage lower than that which slowed the sinus rate) improved atrial fibrillation and arrhythmias (Li, Scherlag et al. 2009, Shen, Shinohara et al. 2011). A flat metal clip attached to the tragus can stimulate the auricular branch of the vagus nerve. This noninvasive, nonsurgical approach improved remodeling and arrhythmia (Wang, Yu et al. 2014, Stavrakis, Humphrey et al. 2015, Wang, Yu et al. 2015).

Specific to MI, Shinlapawittayatorn showed that low level VNS (20 Hz, 500 μ s, 3.5 mA) in swine successfully reduced the size of the infarct, increased ventricular function, and reduced tachycardia and ventricular fibrillation when initiated immediately after the left anterior descending (LAD) artery occlusion (60 minutes) and continued through the end of reperfusion (an additional 120 minutes) (Shinlapawittayatorn, Chinda et al. 2013). As a preconditioning stimulus, VNS (25 Hz, 300 μ s, 10 mA) reduced infarct size and myocardial leukocyte influx when initiated 5 minutes before reperfusion and continued 15 minutes into reperfusion in a swine model (Uitterdijk, Yetgin et al. 2015). In a second study, VNS (20 Hz, 500 μ s, 3.5 mA, in continuously recurring cycles of 21-second on, 30-second off) applied 30 minutes into a 60 minute ischemia and throughout a 120 minute reperfusion was protective, but VNS applied at

the onset of reperfusion was not (Shinlapawittayatorn, Chinda et al. 2014, Uitterdijk, Yetgin et al. 2015). A group performed a time course of VNS (10 Hz, 200 μ s, voltage optimized per subject to obtain a 10% reduction in heart rate) in rodents using 30 minutes of ischemia, followed by 120 minutes of reperfusion. They found that cardioprotection by VNS was greatest when initiated at 15 minutes of ischemia, which they defined as postconditioning, but was also effective at the start of reperfusion and at 30 and 60 minutes of reperfusion. Vagal nerve stimulation reduced both infarct size and cytokine release (Wang, Cheng et al. 2012, Wang, Li et al. 2014). These studies collectively differ in the electrical parameters as well as the timing and duration of the stimulus, but taken together, it appears that VNS can be protective within an optimal window. Electrical stimulation protects against ventricular fibrillation and prevents sudden death after the MI has healed (Vanoli, De Ferrari et al. 1991), and in rats, VNS initiated 1-2 weeks after MI for 2-8 weeks improves left ventricular end diastolic volumes, heart weight, and overall survival, suggesting that in small animal models, VNS can slow the progression to HF after the infarct is consolidated (Li, Zheng et al. 2004, Agarwal, Mokolke et al. 2016). Like many cardioprotective therapies, the mechanistic benefit of VNS in reducing the infarct size may involve the attenuation of mitochondrial dysfunction (Lu, Costantini et al. 2013) and prevention of mPTP opening (Katare, Ando et al. 2009), as well as reduced inflammatory responses (Calvillo, Vanoli et al. 2011, Kawaguchi, Takahashi et al. 2011) with measurable decreases in free radicals, interleukin 17A (Yi, Zhang et al. 2016), interstitial NE release (Tsutsumi, Ide et al. 2008), and interstitial myoglobin release (Kawada, Yamazaki et al. 2008).

The vagus nerve is known to be activated by RIPC as well. In a rabbit model of RIPC by hindlimb ischemia, vagal nerve sectioning, spinal cord sectioning at T9-T10, and atropine

administration each abolished cardioprotection. Vagal stimulation at 100 μ s and 10 Hz (the intensity adjusted for each animal to obtain a heart rate reduction between 10 and 20%) mimicked the infarct-sparing and left ventricular functioning improvements of RIPC (Donato, Buchholz et al. 2013). In another study, the protective effects of RIPC by limb ischemic was abolished by silencing the dorsal motor nucleus of the vagus or systemic muscarinic receptor blockade with atropine. Optogenetic activation of the dorsal vagal motor neurons also was found to reduce infarct size (Mastitskaya, Marina et al. 2012). In combination, VNS and remote preconditioning provide stronger infarct size reduction and myocardial inflammatory cytokine decline than either therapy alone. However, the interaction is not thought to be additive or synergistic because the infarct size reduction is less than the sum of individual therapies. The authors proposed that the suppression of inflammation is a shared cardioprotective mechanism between the two treatments (Wang, Liu et al. 2015).

Vagal stimulation has major drawbacks that hinder its translation. An implanted device is invasive and not practical in an emergency situation. Occasionally patients experience complications, such as device malfunction, mechanical problems and lead migration, nerve injury or persistent pain at the site of implantation, or infection. Complications should be minimized with improved practitioner training and improved devices, but when malfunctions do occur, they can potentially be life threatening and require removal of the device.

Electrical Stimulation of the Limb and the Humoral Hypothesis

It has been demonstrated in a series of studies that electrical stimulation of the limbs is an effective cardioprotective stimulus. Blood drawn from rabbits and humans treated with limb TENS (500 μ s pulse width, 3.1 Hz, 2–3 mA, 4 cycles of 5 minutes of stimulation followed by 5

minutes of rest) was cardioprotective in a mouse Langendorff heart ischemia model (Merlocco, Redington et al. 2014). Transcutaneous electrical nerve stimulation reduced the size of the infarct and improved functional recovery. The effect was blocked by pretreating the heart with naloxone, an opioid antagonist. The same group demonstrated that dialysate from the blood of rabbits treated with capsaicin (5 ml of 0.1% capsaicin topical analgesic cream instead of TENS applied to a 15 cm by 4 cm rectangle of shaved abdomen), remote ischemic cardioprotection, or femoral nerve stimulation (500 μ s pulse width, 3.1 Hz, 0.5–1.0 mA, four cycles each followed by a 5-minute rest period) reduced the size of the infarct and improved cardiac performance (Redington, Disenhouse et al. 2012, Redington, Disenhouse et al. 2013). The effect was blocked when the rabbits were pretreated with topical dimethyl sulfoxide (DMSO) or the NO donor S-Nitroso-N-acetyl-DL-penicillamine (SNAP). Both studies introduce the possibility that a dialyzable humoral factor in the serum initiates cardioprotection from a remote site. The studies both indicate that intact sensory nerve innervation of the remote limb or organ is required for the effect. The identity of a humoral factor remains undetermined, though recent data in RIPPC implicated microRNAs (Li, Rohailla et al. 2014). A study that systemically isolated individual branches of the vagus nerve by subdiaphragmatic vagotomy demonstrated that electrical stimulation of the posterior gastric vagal branch reduced the extent of myocardial ischaemia/reperfusion injury in rats (Mastitskaya, Basalay et al. 2016). This study provides further evidence that the remote preconditioning stimulus is not entirely humoral.

The exact effects of femoral nerve stimulation depend on the electrical parameters and duration of the stimulus. Five minutes of high frequency electrical stimulation (10 V, 100 Hz, 1 ms) but not low frequency electrical stimulation (10 V, 10 Hz, 1 ms) reduced infarct size in rats

(Dong, Liu et al. 2004). The effect was blocked by i.v. naloxone and i.v. glibenclamide, suggesting involvement of opioid receptors and K_{ATP} channels (Dong, Liu et al. 2004). A longer duration of remote electrical stimulation of medial nerves (2/15 Hz, alternatively, 1–2 mA, 400 μ sec for 30 minutes) reduced the infarct size in rat model of MI. Cardioprotection was blocked by α and β adrenergic receptor antagonists and by antagonists against the κ opioid receptor and δ opioid receptor subtypes, supporting the role of both catecholamines and opioids in electrically-induced cardioprotection. The levels of phosphorylated Akt, phosphorylated glycogen synthase kinase 3 (GSK3) and phosphorylated PKC- ϵ were increased in heart tissue after electrical stimulation, which was reduced with the κ/δ opioid antagonists (Tsai, Huang et al. 2015).

Electroacupuncture

Electroacupuncture is emerging as a more clinically translatable strategy to bring about RPCT and NIC. Electroacupuncture delivers an electrical current to the nerves and underlying muscles through a small needle, typically 7 mm long and 0.16 mm in diameter, inserted several mm into the subcutis at relatively specific regions of the body (Wu, Sheen et al. 2002, Na, Jahng et al. 2009, Li, Luo et al. 2012). In our own studies applying EA to a nerve field, we do not puncture the underlying muscles with the needle. Electroacupuncture is different than traditional acupuncture in that it includes the application of electricity. Though parameters vary among individual investigators, EA for cardioprotection is generally performed at the Neiguan acupoint located on the forelimbs at low frequencies (20 Hz or less) for brief time periods (30 minutes or less). In some cases, EA is repeated consecutively for several days before I/R, but a single session can be cardioprotective. Needles without electricity or applied to nonacupoints,

such as the junction between the tail and buttock, are not cardioprotective and are used as controls.

In rodent, porcine (Wang, Xiao et al. 2003), and rabbit models of MI, EA reduces the infarct size, improves cardiac function and microcirculation (Cao, Liu et al. 1998), and enhances anti-apoptotic signaling pathways (Fang, Zhou et al. 2002, Tsou, Huang et al. 2004, Lu, Huang et al. 2016). The combination of EA and mesenchymal stem cell (MSC) treatment extended the survival of MSCs and upregulated protective gene expression in ischemic heart tissue (Zhang, Jia et al. 2013). Electroacupuncture also slows the progression to chronic HF (Ma, Cui et al. 2014) and reduces tachycardia and hypotension associated with coronary artery occlusion (Wu, Cao et al. 2015). Clinically, EA prior to PCI in humans reduced post-PCI myocardial injury measured by cardiac troponin release, reduced MACCE and improved cardiac function at a 2-year follow-up (Wang, Liang et al. 2015). Electroacupuncture also reduced complications after heart valve replacement with cardiopulmonary bypass (Yang, Yang et al. 2010, Zhang, Yu et al. 2017). The studies above were all conducted at forearm acupoints.

The mechanisms of cardioprotection afforded by EA are unclear and may depend on the specific nerves and/or underlying muscles being stimulated and the parameters of stimulation, but similar to RIPC, it is understood that cardioprotection invokes an intact peripheral nervous system, bradykinin, adenosine, and opioids, and intracellular mediators including PKC (Tsou, Huang et al. 2004). In the heart, EA upregulates expression of the adenosine receptor (Lu, Tang et al. 2018) and activates vascular endothelial growth factor (VEGF)-induced angiogenesis (Fu, He et al. 2014). Electroacupuncture also increases the expression of myocardial opioid receptors (Li, Zhong et al. 2011), and the cardioprotective effect is abolished by naloxone (Tsou,

Huang et al. 2004, Zhou, Ko et al. 2012), severing of the vagal nerve (Tsou, Huang et al. 2004), and the nonspecific PKC inhibitor chelerythrine (Zhou, Ko et al. 2012). Our previous studies of EA as a NIC stimulus applied at the abdominal nerve field (cutaneous nerves only) demonstrated the requirement for an intact peripheral nervous system, bradykinin 2 receptor (BK2R) activity and activation of PKC, specifically, PKC- α (Ren, Roessler et al. 2018). In addition to GPCR-related pathways, EA normalizes the changes in sodium and potassium channel expression, current, and ion exchange that occurs during MI (Dong, Li et al. 2014, Wang, Wang et al. 2014, Bian, Tian et al. 2016).

Catecholamine modulation is involved in EA-induced cardioprotection, though the effect is less straightforward and depends on the timing and duration of intervention. Daily, 30-minute EA sessions (5 mA, 20 Hz) for 3 consecutive days before MI reduces infarct size in a rat model, but the cardioprotection is abolished by propranolol administration before each EA session (Gao, Fu et al. 2006). Electroacupuncture alone downregulates β -adrenergic receptor (β -AR) expression in the cardiomyocyte after 3 consecutive days of stimulation (Gao, Fu et al. 2006, Gao, Fu et al. 2007). This suggests that repetitive EA activation of the sympathetic nervous system spurs downregulation of β -AR in the heart, subsequently protecting the cardiomyocytes against sympathetic overload in MI. The antiarrhythmic effect of repeated EA might also be due to the suppression of β -AR signaling through adenylyl cyclase, protein kinase A (PKA), and the L-type calcium channel (LTCC) (Gao, Zhang et al. 2008). Conversely, one session of EA initiated at the onset of LAD occlusion (Neiguan-Jianshi acupoints, 2 Hz, 30 minutes) decreased interstitial NE concentration and reduced infarct size after MI in a rabbit model, which was blocked by pretreatment with naloxone and chelerythrine (Zhou, Ko et al.

2012).

In addition to the infarct-sparing effect, EA reduces inflammation, edema of an injected irritant, and the expression of inflammatory mediators $\text{TNF-}\alpha$, $\text{IL1-}\beta$, $\text{NF-}\kappa\text{B}$, and IL-8 after MI (Zhang, Lao et al. 2005, Wang, Yuan et al. 2018). EA suppresses the release of HMGB1 protein, believed to exacerbate inflammation and injury after MI (Zhang, Yong et al. 2015), as well as serum markers of tissue damage such as CGRP and creatine kinase (Zhu, Zhang et al. 2007). In mice, a humoral mediator was reported to be released by EA at the Neiguan point, which can confer cardioprotection to a naïve heart (Redington, Disenhouse et al. 2012, Redington, Disenhouse et al. 2013). This mediator's exact identity is unknown, but miR-214 is implicated in the context of RIPC (Li, Rohailla et al. 2014). Electroacupuncture at the Neiguan point (4/20 Hz, 0.5 ms, 1 mA) promoted miR-214 upregulation in heart tissue (Liu, Tian et al. 2014).

The role of HSPs and NOS2, both known cardioprotective mediators in late phase IPC, has not been thoroughly investigated after EA. One study observed increased mRNA levels of HSP70 in pig myocardium after EA treatment (Wang, Xiao et al. 2003). In rat cardiac tissue sections, upregulation of NOS activity after 30 minutes of EA (2/15 Hz and 1-3 mA increased gradually) has also been observed by NADPH-diaphorase staining (Wang, Chen et al. 2008). Neither study assayed the functional involvement of either protein. The role of HSPs and NOS2 in electrically-induced cardioprotection is a gap in knowledge and a major focus of this dissertation.

It is clear that EA is effective and beneficial in animal models and well tolerated in the clinic, but there are major discrepancies in the design of EA studies. First, EA is mostly initiated by the Neiguan acupoint at the wrist for the examination of its effect on MI, which is difficult

to achieve in animal models. The stimulus varies in each study depending on the chosen electrical parameters (repetitive vs. one-time, high vs low frequency), duration of administration, and initiation prior to MI. The exact depth of the needles and precise location of the acupoints is unclear and likely inconsistent between investigators and species. Without a consistent rodent paradigm, few studies using EA have utilized the extensive genetically modified mouse toolkit available to researchers, thus the functional involvement of the molecular mediators using mouse models is desperately needed. Furthermore, few have attempted complete pathway-based analysis in animal studies to summarize the complete transcriptome.

Early and Late Phases of Remote Cardioprotection, an Overview and Summary

As detailed in the paragraphs above, the mechanisms of the early phase of cardioprotection are attributed to the activation of GPCRs like opioids, adenosine (not necessary in RPCT by skin incision, but implicated in EA and limb stimulation), bradykinin, and catecholamines. The early phase of cardioprotection is most relevant in patients undergoing acute STEMI, such as those in the ambulance en route to the hospital prior to intervention and stenting. Though the early phase is well-studied by our group and others, this leads to questions of whether late phase cardioprotection is mediated by the activation of transcription factors and induction of cardioprotective gene programs.

The late phase is triggered by signaling activities that occur in the early phase. Protein kinase C (activation of the ϵ or α isoform and suppression of the δ isoform), the RISK pathway, the SAFE pathway, and the NO/PKG pathways bridge the early phase to the late phase of cardioprotection. The late phase of cardioprotection primarily engages transcription factors like

NF- κ B and AP-1 binding to promoters of genes and downstream protein induction such as HSPs. This late phase has a delayed onset 12 hours after the cardioprotective event and can last for days (Marber, Latchman et al. 1993, Guo, Wu et al. 1998). Although one cannot predict the onset of an MI, and therefore preconditioning is said to have little clinical relevance, the late phase of cardioprotection is, in fact, highly clinically relevant in situations where an infarct can be reliably predicted, or at least has a high probability of occurring as a complication to be avoided. In elective stenting, CABG surgery, organ transplant, where a donor organ could undergo preconditioning to improve graft function and survival, or other major cardiac surgeries, the late phase of cardioprotection might be induced in an outpatient setting as an adjunct to any standard pre-surgical recommendations.

Cardioprotection of all types activate common mediators in both the early and late phases, with some exceptions, like RPCT's independence of adenosine and TNF- α . Unfortunately, ischemic conditioning studies of all types have major drawbacks that challenge their effective translation. Any prolongation of operative time increases the risk of adverse outcomes and patient discomfort, and IPC and RIPC are particularly unsuitable for atherosclerotic patients at risk of unstable plaque rupture and carry the potential of vessel dissection. Ischemic interventions are considered invasive when they require access to the coronary artery, and alternative remote ischemic interventions via blood pressure cuff have had limited success in large-scale clinical trials. As an alternative, electrically-based therapies like EA and VNS are safe perioperationally, but little is known about their efficacy in STEMI in humans. Therefore, lower-risk alternatives to cardioprotection continue to be investigated.

Challenges in Clinical Translation of Ischemic Therapies

There are inherent technical limitations in utilizing the second window of protection. In animal models, the intervention is initiated at a defined timepoint prior to the ischemic event, while in the clinic, the exact timing of the onset of an MI is impossible to predict. Clinical trials have attempted to translate cardioprotection to clinical scenarios where there is a predictable risk of hypoxic injury, with limited success. The ERICCA trial and the RIPHeart trial showed little benefit of IPC in CABG surgery and other heart surgeries, respectively, while the CRISP-STENT study showed improved outcomes after IPC in the context of elective PCI. Perconditioning during MI may be beneficial in humans, though perhaps only in certain patient populations, such as those with STEMI and large risk regions (Botker, Kharbanda et al. 2010, Munk, Andersen et al. 2010, Sloth, Schmidt et al. 2014, Gaspar, Lourenco et al. 2018). Several of these studies have design flaws, like complications with anesthetics, and none were powered to assess the effect on clinical endpoints like mortality. Most were single center, un-blinded studies, and many utilize surrogate endpoints like serum biomarkers for cardiac injury. There are few rigorous and long-term clinical studies that measure clinical outcomes. Optimal dosing, timing, and duration of the cardioprotective effect in humans remains unknown. Overall, the clinical translation of ischemic conditioning has been disappointing.

Ischemic conditioning via blood pressure cuff has several issues as a clinical therapy. Not every patient can receive a standard size blood pressure cuff, especially those at risk of plaque disruption or dissection of the vasculature, the elderly or weak, and the obese. A non-ischemic, electrically-based therapy offers an alternative to IPC. Electrically-based cardioprotection has been investigated in animal models of VNS, EA, and limb nerve stimulation, and as a mimic of

RPCT by surgical incision and topical capsaicin applied at an abdominal nerve field, collectively considered NIC. Insight into the mechanisms of NIC has been established by our group and others, but little is known about the late phase of NIC. A clear mechanistic understanding, followed by optimization of the dosing, timing, intensity, and duration of stimulation are key to defining the second window of protection for clinical use. Further, mechanistic understanding can justify the application of NIC to other fields. Hypoxic cell death that culminates in the opening of the mitochondrial permeability pore is a common end effectors in the programmed cell death associated with both MI and cerebrovascular stroke, and preventing it could be beneficial to both patient populations (Mattson and Kroemer 2003). Nociceptor-induced cardioprotection that recruits a nerve field on the abdomen is the most clinically translatable form of electrically-induced cardioprotection available and the reason we undertook the studies herein.

General Rationale for NIC

Electrically-induced cardioprotection offers benefits over IPC, but there are several barriers to its clinical translation. Namely, basic scientists are still uncovering the molecular mechanisms of late phase electrically-induced cardioprotection. Though a complete elucidation of the complex processes mediating cardioprotection is not necessary for FDA approval, a clear and thorough mechanistic understanding of how a therapeutic works may help enhance its efficacy, optimize the therapy, provide insight into adverse effects, and increase the likelihood for successful therapeutics development and application.

In previous studies on ischemic cardioprotection, large-scale studies via microarray and next-generation sequencing have surveyed transcriptomic changes associated with

cardioprotection (Onody, Zvara et al. 2003, Konstantinov, Arab et al. 2005, Tranter, Ren et al. 2010, Wilhide, Tranter et al. 2011, Pavo, Lukovic et al. 2017, Luther, Haar et al. 2018). On the basis of these assays, we were able to query the known components of late phase cardioprotective stimuli. We know that cardioprotection generally fits within an established framework: protection is initiated via the activation of neurobiology to the heart and/or initiators of cardioprotection, intracellular mediators, and end effectors. Building on this framework, we focused upon common players in different paradigms of late phase cardioprotection to guide the present studies. In the sections to follow, I will review the known mechanisms related to NIC and form the theory that activation of the nerves and PKC leads to the activation of NF- κ B and induction of downstream cardioprotective gene programs that include NOS2.

Neural Signaling as a Potential Trigger of NIC

The neurobiology of NIC involves the peripheral nervous system. The peripheral nervous system in humans is divided into the sympathetic (SNS) and parasympathetic (PNS) branches. Sympathetic responses result in global enhancement of the pumping function of the heart. In MI, acute sympathetic activation is a compensatory mechanism that preserves homeostasis and low levels may be cardioprotective (Bankwala, Hale et al. 1994), but chronic activation is deleterious (Triposkiadis, Karayannis et al. 2009). The parasympathetic branch of the nervous system is mediated through activation of the vagus nerve and acts to calm the heart in stressful scenarios. In RIPC, there are requirements for neural innervation demonstrated by ganglionic blockade and nerve sectioning, the nature of which could be sympathetic or parasympathetic (Gho, Schoemaker et al. 1996, Liem, Verdouw et al. 2002, Wolfrum, Schneider et al. 2002,

Loukogeorgakis, Panagiotidou et al. 2005) (Ding, Zhang et al. 2001, Lim, Yellon et al. 2010, Donato, Buchholz et al. 2013). Pharmacological studies targeting individual components of the SNS or PNS have paradoxically implicated both branches in many methods of inducing cardioprotection. The SNS is involved in various forms of preconditioning via norepinephrine/epinephrine release and binding to cardiomyocyte and α and β adrenergic receptors (ARs) (Bankwala, Hale et al. 1994, Lameris, de Zeeuw et al. 2000, Frances, Nazeyrollas et al. 2003, Minatoguchi, Uno et al. 2003, Shaffer, McCraty et al. 2014). Cardioprotection by spinal cord stimulation or EA is eliminated with prazosin (an α_1 -AR antagonist), blunted by timolol (a β -AR antagonist), or reduced by propranolol (a nonselective β -antagonist), and RPCT is abolished by β -AR blockade and ganglionic blockade (Gao, Fu et al. 2006, Southerland, Milhorn et al. 2007, Jones, Fan et al. 2009). Though β -receptors make up the majority of cardiac ARs, α_1 -ARs account for approximately 10% of cardiac ARs and are known to be cardioprotective when activated (O'Connell, Jensen et al. 2014). *In vivo*, constitutively active α_1A -AR and cardiac α_1A -AR overexpression is cardioprotective, and pharmacological α_1AR blockade abrogates IPC (Zhao, Park et al. 2012) (Rorabaugh, Ross et al. 2005, Kudej, Shen et al. 2006). The SNS-to-AR signaling pathways are relevant to both early and late phase, though the downstream effectors following AR activation beyond IPC have not yet been established in the context of ES.

Importantly, β -blocker therapy is recommended for some classes of patients at risk of STEMI, and so the question arises whether the therapeutic effect of NIC would persist in this population. In a *post-hoc* analysis of patients with STEMI, the infarct sparing effects of arm pressure cuff treatment were enjoyed by β -blocker medication users and drug-free patients

alike. This effect was supported in a cohort of elective CABG patients that received ischemic conditioning by repetitive blood pressure cuff inflation/deflation, where RIPC reduced post-operative markers of injury that was not influenced by the patient's medication status (Kleinbongard, Neuhauser et al. 2016). However, data from a meta-analysis confirmed cardioprotection conferred by RIPC in adult cardiac surgery, but suggested that the effect may be attenuated when combined with β -blockers (Zhou, Liu et al. 2013). Clinically, β -blockers reduced perioperative infarct in patients receiving elective PCI in the absence of any additional cardioprotective intervention (Ibanez, Macaya et al. 2013). Clinical responses appear to be influenced by the type of insult to the heart itself, as well as the timing, methodology, and type of cardioprotective intervention.

Studies supporting SNS involvement do not necessarily exclude the role of the PNS in cardioprotection (Basalay, Davidson et al. 2018). It has repeatedly been demonstrated that VNS has an infarct sparing effect when applied as a preconditioning, perconditioning, or postconditioning stimulus in experimental models (Katare, Ando et al. 2009, Katare, Ando et al. 2010, Calvillo, Vanoli et al. 2011, Shinlapawittayatorn, Chinda et al. 2013, Shinlapawittayatorn, Chinda et al. 2014, Buchholz, Kelly et al. 2018). Furthermore, a clinical study demonstrated that transcutaneous stimulation of the vagal nerve in patients with acute STEMI reduced arrhythmia and serum markers of cardiomyocyte injury and inflammation, though this result could be mechanistically different and related to heart rate reduction, which is not seen in non-vagal electrically-induced cardioprotection (Heusch 2017, Yu, Huang et al. 2017). Though it is clear that cardioprotection can be evoked by the vagus nerve, there is an ongoing debate on whether the activity of one vagal nerve alone is sufficient to mediate cardioprotection (Basalay,

Barsukevich et al. 2013).

A number of researchers have debated sympathetic versus parasympathetic involvement in cardioprotection (Gourine and Gourine 2014). Considering the complex interactions between the two systems, it is likely that therapeutic modulation of one affects the other. On the molecular level, many signaling mediators are common to both pathways, such as the sensory C-fibers and K_{ATP} channels that characterize RPCT (Jones, Fan et al. 2009). Furthermore, in a discussion of the neurobiology of NIC, one cannot ignore the evidence pointing to the involvement of a humoral mediator that can be dialyzed from the effluent of a protected heart and transfer that cardioprotection to a naïve heart (Redington, Disenhouse et al. 2012, Redington, Disenhouse et al. 2013, Merlocco, Redington et al. 2014, Mastitskaya, Basalay et al. 2016, Maciel, de Oliveira et al. 2017, Heinen, Behmenburg et al. 2018). Clinicians and scientists alike are increasingly recognizing the value of neuroscience-based cardiovascular therapeutics for CVD despite not entirely understanding the complexity of the system (Shivkumar, Ajjola et al. 2016).

Following the recruitment of a neural signaling pathway and receptor-ligand interactions, kinase cascades that include PKC are activated within the cardiomyocyte in both IPC and NIC by surgical incision (Tsuchida, Liu et al. 1994, Mitchell, Meng et al. 1995, Node, Kitakaze et al. 1997, Meng, Shames et al. 1999, Jones, Fan et al. 2009). Chelerythrine (a PKC inhibitor) partially blocked the cardioprotective effects of EA and RPCT, so PKC seems to be consistently required (Jones, Fan et al. 2009, Zhou, Ko et al. 2012). It is thought that PKC is the bridge from the neural pathways terminating on GPCRs in early signaling to downstream gene transcription and the late phase of cardioprotection. There is little known about non-

cardiomyocyte cells in the heart, such as fibroblasts and vascular cells, but these cells could play a role in cardioprotection as well. In IPC, NO generated from eNOS in endothelial cells activates PKC in the heart to confer cardioprotection (Bolli, Dawn et al. 1998, Lochner, Marais et al. 2000, Xuan, Tang et al. 2000, Lochner, Marais et al. 2002, Xuan, Guo et al. 2007). In NIC, the responses of these non-myocyte cell types are unknown.

The Transcription Factors NF- κ B, AP-1, and Cardioprotective Gene Programs in NIC

The late phase of cardioprotection is initiated within 12 hours and persists for several days. Due to its persistence, late phase cardioprotection is believed to be mediated by transcription factors and the *de novo* synthesis of downstream mediators of cardioprotection (Rizvi, Tang et al. 1999). The NF- κ B transcription factor is a dimer of its five subunits: p50, p52, c-Rel, RelA and RelB. The NF- κ B dimers are located in the cytoplasm in an inactive form by associating with I κ B α inhibitor proteins. In response to a wide array of stimuli including hypoxia, lipopolysaccharide, ultraviolet radiation, and kinases like MAPK and PKC, I κ B α is rapidly phosphorylated on serine residues 32 and 36, ubiquitinated, and degraded by the proteasome. The freed NF- κ B dimer translocates to the nucleus where it can modulate specific gene expression by binding to its response elements within enhancers or promoters.

In the context of preconditioning, NF- κ B activation is required for the late phase of cardioprotection (Xuan, Tang et al. 1999) via binding to promoter regions of cardioprotective genes within the cardiomyocytes, including NOS2 (Bolli 2001, Morris, Lutz et al. 2003). Remote preconditioning by hind limb ischemia induces NF- κ B-dependent NOS2 mRNA, and both the increase in NOS2 mRNA and the protection is blocked in mice with a genetic deletion of the p105 subunit of NF- κ B (Li, Labruto et al. 2004). In the 3M mouse (Tg(Myh6-NF-

κ BIA*S32A*S36A*Y42F)), the 2 serine residues and an additional, lesser-known residue is mutated in I κ B α rendering it a dominant negative and unable to be phosphorylated and degraded in a cardiocyte-specific manner (Brown, McGuinness et al. 2005). Using this 3M model, it was demonstrated that late phase IPC and RPCT requires NF- κ B, and in late IPC, HSP70.3 is NF- κ B-regulated (Jones, Brown et al. 2003, Tranter, Ren et al. 2010, Song, Ye et al. 2015).

In addition to its role in cardioprotection, NF- κ B has paradoxical role in cardiac injury associated with MI. The transcription factor is rapidly activated after MI *in vivo* and in isolated hearts, but inhibition by an NF- κ B decoy oligomer led to reduced infarct size, possibly via inducing pro-inflammatory mediators like cytokines and chemokines (Chandrasekar and Freeman 1997, Morishita, Sugimoto et al. 1997, Li, Browder et al. 1999). There appears to be a dual role for NF- κ B in MI, both in pathology and cardioprotection on the basis that various stimuli activate distinct gene expression programs (Jones, Brown et al. 2005, Tranter, Ren et al. 2010, Wilhide, Tranter et al. 2011).

The transcription factor AP-1 complex is a dimer of Jun (c-Jun, JunB, and JunD) and Fos (c-Fos, FosB, Fra1, and Fra2) family members, of which c-Fos and c-Jun are the principle components. Both c-Jun and c-Fos are immediate early genes quickly induced in response to I/R injury (Kingma 1999). C-Jun N-terminal kinase (JNK) phosphorylation and activation of c-Jun protects against cell death from I/R injury in cardiomyocytes *in vitro* and *in vivo* using genetically modified mice (Bishopric, Andreka et al. 2001, Dougherty, Kubasiak et al. 2002, Sadoshima, Montagne et al. 2002, Kaiser, Liang et al. 2005, Tran, Andreka et al. 2007). C-Jun also promotes adaptive heart growth by hypertrophy (Windak, Muller et al. 2013). There is

some crosstalk between the NF- κ B and AP-1 signaling pathways. Both transcription factors can be activated simultaneously in tissue I/R and angina, and NF- κ B and AP-1 cooperate in targeting some of the same inflammatory genes; though they are primarily regulated by different mechanisms, it has been proposed that NF- κ B can influence c-Jun and AP-1 activation (Zwacka, Zhang et al. 1998, Valen, Hansson et al. 2000, Tang, Minemoto et al. 2001, Papa, Zazzeroni et al. 2004). The role of c-Jun and AP-1 in electrically-induced cardioprotection is unknown.

The Heat Stress Response, HSF1, and HSP70 as Potential Mediators of NIC

Heat shock factor 1 (HSF1) is a key transcription factor involved in the cell's response to environmental challenges, such as thermal stressors that cause misfolding of proteins. Heat shock factor 1 exists as a monomer in the cytoplasm bound to HSP90, and when triggered by high temperatures, HSP90 binds to misfolded proteins and releases HSF1 in an ATP-dependent step which can be disrupted pharmacologically (Conde, Belak et al. 2009). Heat shock factor 1 transiently enters the nucleus and forms homotrimers, where it binds to the heat shock response elements and upregulates the molecular chaperone HSP70 and a number of other HSPs (Ankar and Sistonen 2007). Mice with cardiac overexpression of HSF1 recover faster, have smaller infarcts, and reduced apoptotic cell death compared to wild-type mice after MI, and HSF1 overexpression in cultured cardiomyocytes improves cell viability following simulated I/R injury *in vitro* (Zou, Zhu et al. 2003, Date, Mochizuki et al. 2005). The increase in HSF1 after whole body hypothermia and subsequent protection against I/R injury is abolished with siRNA against HSF1 (Yin, Xi et al. 2005).

There are six families of HSPs that are sorted based on their size. Heat shock factor 1 upregulates several protective genes, including HSP70 (Zou, Zhu et al. 2003, Date, Mochizuki et

al. 2005). Heat shock protein 70 protects cells from elevated temperatures by binding to thermally denatured, unfolded proteins and preventing their misfolding and aggregation (Figure 2) (Lepore, Knight et al. 2001). Co-chaperones such as HSP40 bind to substrates the ATP-binding domain of HSP70 to enhance its functions (Summers, Douglas et al. 2009). Heat shock factor 1 and the HSPs it targets have been recognized for their role in human disease and their modulation in response to a variety of stressors, including oxidative stress and I/R injury (Nishizawa, Nakai et al. 1996, Nishizawa, Nakai et al. 1999, Tanonaka, Toga et al. 2003).

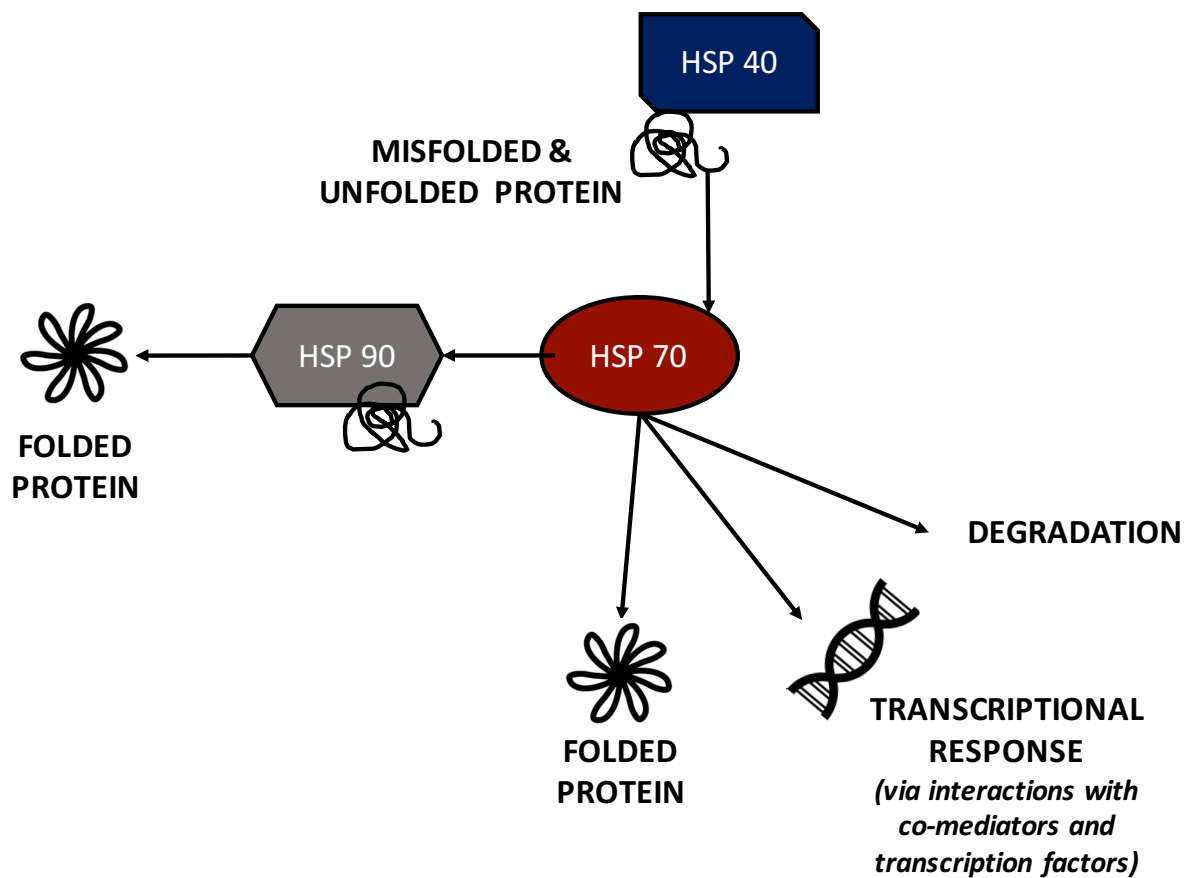


Figure 2. Heat Shock Protein Schematic. Heat shock proteins, including HSP70, HSP90, and HSP40 act in concert with each other and their co-factors to assist in protein repair and degradation following MI.

Multiple studies have demonstrated the important of HSP70 in cardioprotection.

Overexpression of HSP70 in rodent models increases the resistance of the heart to ischemic injury, improves post-ischemic myocardial recovery, and prevents myocardial dysfunction after I/R injury (Marber, Mestril et al. 1995, Plumier, Ross et al. 1995) (Plumier, Ross et al. 1995) (Troost, Omens et al. 1998). Heat shock protein 70 has long been known to be induced in I/R injury, following other immediate early genes like c-Fos and c-Jun (Kingma 1999), and is thought to be an end effector of cardioprotection (Guisasola, Desco Mdel et al. 2006) and therapeutic target for I/R injury (Song, Zhong et al. 2018).

Our work shows a role for NF- κ B in HSP70 transcription, which accounts for about $\frac{1}{2}$ of the transcriptional increase (Tranter, Ren et al. 2010). In heat stress, HSP70 in the myocardium is increased as rapidly as 30 minutes after initiation and continues to increase at 3, 6, and 24 hours. The quick rise in HSP70 does not necessarily correlate to the cardioprotection of heat stress, which occurs 24 hours later (Cornelussen, Garnier et al. 1998). Heat shock protein 70 upregulation by transfection is beneficial in improving post-ischemic recovery of left ventricular mechanical function after I/R (Jayakumar, Suzuki et al. 2000, Jayakumar, Suzuki et al. 2001). Heat shock protein 70 assists in refolding misfolded proteins, and the HSP70 substrates in the context of protection are located at multiple sites in the heart that regulate processes like calcium overload, since blockade of HSP70 with an antisense oligonucleotide impaired the improvement in calcium homeostasis conferred by pharmacological cardioprotection (Liu, Kam et al. 2004, Liu, Kam et al. 2006). Perhaps the most intriguing parallel to nociception and ischemia is the observation that patients with unstable angina, a nociceptive stimulus, have increased myocardial HSP70 and nuclear translocation of NF- κ B in biopsies taken from the right atrium, an effect not found in patients without symptoms (Valen, Hansson et al. 2000). The

transcription factors AP-1 and NF- κ B are each thought to be modulated by HSPs themselves (Carter 1997, Guzhova, Darieva et al. 1997).

In IPC, targeted microarray identified HSPs as one of the most significant groups of NF- κ B dependent genes after IPC. Late IPC is lost in mice with genetic deletions of both HSP70.1 and HSP70.3, though IPC was preserved in HSP70.1 KO, indicating that it is the HSP70.3 isoform that is important to cardioprotection (Tranter, Ren et al. 2010, Tranter, Helsley et al. 2011, Kraynik, Gabanic et al. 2015). The post-transcriptional regulation of HSP70.3 is important in the context of IPC, where an ischemic or heat shock stimulus induces alternative polyadenylation of HSP70.3 and the accumulation of HSP70.3 with a shortened 3' UTR. The shortened 3' UTR is missing a microRNA binding site, allowing for enhanced polyribosome loading, reduced microRNA suppression, and a more robust increase in protein expression (Tranter, Ren et al. 2010, Tranter, Helsley et al. 2011, Kraynik, Gabanic et al. 2015). In the context of permanent coronary occlusion, microarray analysis identified 16 genes that were differentially expressed and NF- κ B dependent, but knockout (KO) of HSP70.1 contributes to cardioprotection, thus HSP70 might have an antithetical role in myocardial injury and protection (Wilhide, Tranter et al. 2011).

Experimental evidence links HSP70, microRNA, and exosomes. Ischemic preconditioning increased miR-1, miR-21, and miR-24 in mouse cardiac tissue; when these microRNAs were isolated and injected into the left ventricle of a naïve mouse, transcript levels of eNOS, HSF1, and HSP70 increased in the heart and infarct size was reduced post-I/R (Yin, Salloum et al. 2009). Serum exosomes possess surface HSP70 and conferred cardioprotection *ex vivo*, *in vivo*, and *in vitro*, but an antibody against the HSP70 surface antigen prevented cardioprotection

(Vicencio, Yellon et al. 2015).

Due to the neural nature of NIC, evidence suggests that catecholamine signaling invoked by nociceptor activation of the SNS might modulate HSP70 expression and function. In rats, NE treatment (3.1 $\mu\text{mol/kg}$, i.p.) is shown to improve post-ischemic recovery of heart function and upregulate cardiac protein levels of HSP72 24 hours post-treatment, while prazosin eliminates both the cardioprotection and the NE-induced increase in cardiac HSP70 (Meng, Brown et al. 1996). A conflicting study shows that the α and β receptors on the myocardium are required for heat stress-induced cardioprotection, but the heat stress-induced HSP70 upregulation occurs despite α or β blockade (Joyeux, Godin-Ribuot et al. 1998). In heat stress, the increase in HSP persists despite pharmacological inhibition of NOS2, indicating that NOS2 activation is not required for HSP induction in these studies (Arnaud, Laubriet et al. 2001).

Studies on the heat shock response in cardioprotection using animal models establishes that heat shock-induced cardioprotection is dependent on strain, temperature, time after stress, and subject size (Patel, Hsu et al. 2001). Some small HSPs, such as HSP20 and HSP22, have also been shown to be beneficial in cardioprotection *in vivo*, *in vitro*, and *ex vivo*. Cardiac-specific overexpression of HSP20, for example, exhibit improved contraction and reduced infarct size after I/R (Fan, Ren et al. 2005), though these small HSPs were not investigated in the current dissertation.

Nitric Oxide Synthase 2 and S-Nitrosylation as Potential Mediators of NIC

There are three isoforms of nitric oxide synthase: NOS1 (neuronal NOS, nNOS), NOS2 (inducible NOS, iNOS), and NOS3 (endothelial NOS, eNOS) (Alderton, Cooper et al. 2001)(Wang and Marsden 1995). All isoforms are found in the mammalian heart. The genes for NOS1 and

NOS3 are constitutively active and regulated by intracellular calcium concentrations and calmodulin; NOS2 is calcium-independent and induced by stress and inflammatory stimuli. All isoforms lead to the generation of NO which exerts a variety of physiological and pathological responses in the cell, but compared with NOS1 and NOS3, NOS2 has the strongest NO generating potential (Griffith and Stuehr 1995).

An enormous number of studies have established the beneficial role of NOS and NO in cardioprotection in IPC (Guo, Jones et al. 1999, Wang, Guo et al. 2002, Bencsik, Kupai et al. 2010), postconditioning (Zhao, Wang et al. 2010, Wang, Li et al. 2015), and RIPC (Li, Labruto et al. 2004). Cardiac NOS activation is biphasic, whereby early cardioprotection activates vascular eNOS, which initiates NOS2 transcription via PKC- ϵ and NF- κ B in cardiocytes (Bolli, Dawn et al. 1998). The transcription of NOS2 mRNA peaks at 3 hours after the last cycle of IPC and remains elevated for 24 hours (Wang, Guo et al. 2002). Protein expression of NOS2 is increased 24 hours after IPC, and immunohistochemistry and in situ hybridization determined cardiac myocytes to be the main source of NOS2 upregulation (Wang, Guo et al. 2002). Overwhelming evidence suggests that NOS2 and NO biosynthesis is responsible for the late phase of cardioprotection when triggered by ischemic, pharmacological, or exercise stimuli (Bolli 2001, Lin, Steenbergen et al. 2009). Furthermore, extensive *in vivo* studies with the gene transfer of NOS2 demonstrates that gene therapy provides long-lasting cardioprotection without functional deficits (Bolli 2001, Li, Guo et al. 2003, Li, Guo et al. 2006, Li, Guo et al. 2007, Li, Guo et al. 2009, Li, Guo et al. 2011, Li, Guo et al. 2011).

There are two major effects downstream of NO in the cell. Nitric oxide binds to soluble guanylyl cyclase (GC) and accelerates the conversion of GTP to cyclic guanosine

monophosphate (cGMP) to activate PKG and open the mitochondrial K_{ATP} channel. It is now clear that NO exerts its influence in the cardiomyocyte by a second function. Nitric oxide can S-nitrosylate key proteins in the cardiomyocytes at cysteine residues to generate S-nitrosothiol (SNO) groups; substrates of particular physiological importance include SERCA, the LTCC, components of the ETC, and ryanodine receptors (RyRs) (Xu, Eu et al. 1998, Lima, Forrester et al. 2010, Murphy, Kohr et al. 2014). This post-translational modification is generally inhibitory by changing the function, activity, and localization of these targets. S-nitrosylation is a major effector of NO activity in vascular and cardiac cells (Murphy, Kohr et al. 2014). In cardioprotection, the antiapoptotic effect of NOS2 involves the production of NO and the S-nitrosylation of proteins like pro-apoptotic effector caspase 3, which inhibits its activity (Hoffmann, Haendeler et al. 2001, Maejima, Adachi et al. 2005).

In the mouse heart, 116 endogenously SNO proteins are expressed, and when treated with an endogenous SNO agent, 951 potential SNO sites were identified (Kohr, 2011). Although NOS2 does not appear to be localized in a specific cellular compartment and S-nitrosylation has numerous targets in the cardiomyocyte, the cardioprotective effects appear to culminate on the mitochondria (Ziolo and Bers 2003, Prime, Blaikie et al. 2009). A membrane fraction of heart tissue immediately following IPC identified several S-nitrosylated proteins involved in regulation of mitochondrial energetics and calcium transport (Sun, Morgan et al. 2007). Mitochondrial preparations have surveyed the increased S-nitrosylation of mitochondrial proteins after ischemic postconditioning, pharmacological postconditioning, and treatment with endogenous nitrosylation agents (Penna, Perrelli et al. 2013) (Murray, Kane et al. 2011). In IPC, over 31 differentially S-nitrosylated proteins have been identified post-IPC (Kohr, Sun et al.

2011). Mitochondrial targeting of S-nitrosylation appears to protect against I/R injury by inhibiting complex I (Leist, Single et al. 1999) and preventing mitochondrial transition (West, Rokosh et al. 2008). S-nitrosylation shields components of the ETC from reperfusion injury. Although reperfusion restores O₂ levels after ischemia, a surge of ROS can react with the respiratory chain complexes in their reduced state, an adverse event that would otherwise contribute to protein dysfunction.

Kyphoscoliosis Peptidase as Exemplar of Deep Sequencing Dataset Legacies

It is likely that multiple cardioprotective proteins are induced by novel and non-ischemic stimuli, like NIC, that haven't been fully explored. In my dissertation, the contractile protein kyphoscoliosis peptidase (encoded by the *KY* gene) emerged from the sequencing data sets and became a curious candidate for neuromuscular junction preservation in situations of stress. The kyphoscoliosis mouse model arose out of a spontaneous mutation in the BDL strain, resulting in kyphoscoliosis, muscle atrophy, and intervertebral disc degeneration (Mason and Palfrey 1984, Bridges, Coulton et al. 1992).

Subsequent studies determined that the KY protein was only expressed in skeletal and cardiac muscle (Blanco, Coulton et al. 2001). It is found in the Z-band complex interacting with contractile proteins like filament C and myosin binding protein C under normal conditions, where it acts to degrade filament C and is involved in structural support (Baker, Riley et al. 2010). The gene is homologous to the human KY gene (Skynner, Gangadharan et al. 1995). In the clinic, mutations in KY are associated with neuromuscular disorders, myopathies, and paraplegia (Hedberg-Oldfors, Darin et al. 2016, Straussberg, Schottmann et al. 2016).

The mixed myopathies-neurologic features that are presented with disruption of KY

suggest the gene's involvement the nerve-heart connection. Interestingly, this mRNA has never been investigated in the context of cardioprotection. However, we do see significant changes in the mRNA level from our sequencing data, which appears to be specific to the stimulus. The inclusion of KY in this dissertation is put forward with the understanding that many proteins like KY could be buried in extensive data sets that would require coordinated bioinformatics mining to reveal.

microRNA as Epigenetic Regulators of NIC

At this point, the signaling cascades involved in cardioprotection are complex, and the exact choreography of the molecular events is not entirely defined. In recent years, microRNA (miRNAs or miRs) have been presented as nodes in complex signaling networks, including that of cardioprotection, which can regulate the signaling networks in very precise ways with robust consequences. microRNAs are a class of nucleotides approximately 19-25 base pairs in length. They can arise from introns or exons regions in the genome as pri-miRs, which are then cleaved and processed by the enzymes drosha and dicer into the final mature molecules. When processed, mature microRNA can act as pivotal regulators of signaling nodes that can degrade or inhibit their target transcripts with high specificity. MicroRNAs have important roles in both normal physiology and disease states, including myocardial I/R injury and cardioprotection.

Most focused microRNA studies, ours included, are initiated with a microarray or an RNA sequencing dataset, followed by functional screening and sorting. Validation by PCR and mechanistic support *in vivo* and *in vitro* further edits lists of microRNA into functional mediators. MicroRNA can be pursued as both biomarkers and therapeutic targets (Ong, Katwadi et al. 2018). There are several microRNA that have been identified in sequencing

assays and implicated in cardioprotective signaling (Varga, Zvara et al. 2014) (Salloum, Yin et al. 2010). These species function as cardioprotective miRs that are increased by preconditioning stimuli, and when transfected into cardiomyocytes show cytoprotective effects, most often by downregulating apoptotic and inflammatory end effectors (Varga, Zvara et al. 2014). Other species of microRNA are injurious and inhibition is beneficial, for example, let-7 and miR-476-5p antagonization is cardioprotective, (Pan, Guo et al. 2012, Li, Ren et al. 2016), and in a porcine model, regional miR-92 inhibition correlated with improved function and decreased cell death and leukocyte influx after MI (Hinkel, Penzkofer et al. 2013). The correct combination of microRNAs is particularly powerful in a fine-tuned cardioprotective response.

It has been suggested that the humoral effect of IPC is mediated by circulating microRNA in serum exosomes, supported by evidence that perfusates from an IPC heart confer protection to a naïve heart, which is lost when the perfusates are depleted of exosomes (Giricz, Varga et al. 2014). A distinct compartment of protective microRNA have been identified in exosomes and extracellular vesicles, especially secreted from specific cell-types such as cardiac-derived progenitor cells or stem cells, and there is great interest in how these vesicles can improve function and scar size following myocardial injuries (Barile, Milano et al. 2017, Barile, Moccetti et al. 2017). MiR-21 exists in high abundance in exosomes, as well as miR-146, and both can produce cardioprotection (Ibrahim, Cheng et al. 2014, Barile, Moccetti et al. 2017, Wang, Jiang et al. 2017, Luther, Haar et al. 2018). Exosomes can also be loaded with microRNA before delivery to bring about cardioprotection, as was demonstrated with miR-181b, introducing the concept that exosomes could be the infrastructure of a cell-free therapeutic (de Couto, Gallet et al. 2017).

Studies have found specific microRNA associated with the protective effects of remote preconditioning. Remote preconditioning increases miR-144, which may be a circulating effector (Li, Rohailla et al. 2014). Intravenous infusion of miR-144 reduces LV remodeling after MI in a mouse model (Li, Cai et al. 2018), while mice with a genetic deletion of miR-144 have worse outcomes after MI (He, Wang et al. 2018). Precursors of miR-144 are enriched in plasma exosomes by RIPC, and systemic treatment of the microRNA can induce early and late cardioprotection with improved function and reduced infarct size, indicating that miR-144 could be released systemically in RIPC (Li, Rohailla et al. 2014). MiR-21 is another established cardioprotective microRNA in remote ischemic pre- and postconditioning. Following the stimulus, miR-21 is upregulated and required for protection, possibly by targeting the Akt/PTEN pathway (Yin, Wang et al. 2008, Tu, Wan et al. 2013). *In vivo* and *in vitro* studies identify an extensive and expanding list of additional microRNAs that could have a role in heat shock, hypoxia, preconditioning, remote preconditioning, and cardioprotection, including: miR-1, miR-24, miR-126, miR-133, miR-150, miR-206, miR-214, miR-221, and miR-532 (Chen, Zhou et al. 2016, Zhou, Chen et al. 2016, Bayoumi, Teoh et al. 2017) (Yin, Wang et al. 2008, Slagsvold, Rognmo et al. 2014, Tang, Wang et al. 2015). (Shi, Chen et al. 2013, Brandenburger, Grievink et al. 2014, Pan, Han et al. 2018). Others, including miR-29b, 133a, and 146b, fulfill the requirements to be potentially causal mediators of protection, though confirmatory studies are sparse (Baars, Skyschally et al. 2014). Pharmacologically-induced protection modulates its own set of microRNA, depending on the drug. Nitrite administration during reperfusion, for example, is cardioprotective in MI through maintenance of baseline expression levels of a handful of microRNAs that would otherwise be upregulated in I/R (Hendgen-Cotta, Messiha et

al. 2017).

Our own group has shown that IPC regulates HSP70 gene products through post-transcriptional modifications involving microRNA binding to the 3'UTR and suppression of translation (Tranter, Helsley et al. 2011). Recent research in our lab demonstrated that exosomes are cardioprotective in vivo against I/R injury, but that effect is lost in exosomes without miR-21 (Luther, Haar et al. 2018). Electroacupuncture upregulates miR-214 in rats, and transfection of the mimic protects cells in vitro from simulated I/R (Liu, Tian et al. 2014). The exact microRNA that are induced in other types of NIC have not been studied, and their targets remain a mystery.

Overall Rationale

In summary, nociceptor induction of neural signaling and activation of PKC on the first day of NIC could lead to NF- κ B-dependent gene induction invoking the heat shock response and NOS2 upregulation on the second day. As discussed in the above sections, each of these mediators has a distinct, recognized cardioprotective role in IPC and RIPC, but little is known about whether these same pathways are involved in the late phase of NIC. Large-scale, transcriptomic studies can be used as a comprehensive strategy to survey the late phase of NIC, and individual genes can be examined to determine their functional involvement in NIC.

CHAPTER III

HYPOTHESIS AND AIMS

Preliminary studies demonstrated that electrically-induced cardioprotection via cutaneous patches or needles was effective as an NIC stimulus and reduced infarct size *in vivo* after MI. A dose curve in mice revealed that a 5 V, 4 Hz, 100 μ second pulse duration, 15-minute stimulus was the most effective in reducing I/R injury after an MI consisting of a 45-minute ischemia and 24-hour reperfusion. Though the role of several individual genes has been established in the late phase of IPC, little is known about the transcriptomic changes associated with the late phase of cardioprotection after electrically-induced NIC. Therefore, I identified the novel transcriptomic changes associated with electrically-induced cardioprotection in my dissertation. My central hypothesis was that late phase of electrically-induced NIC is by the *de novo* synthesis of NF- κ B dependent distal mediators of cardioprotection. This hypothesis was tested in two specific aims.

In Specific Aim 1, I clarified the role of HSPs in electrically-induced cardioprotection. I hypothesized that a transcriptional increase in HSPs would follow cutaneous, electrically-induced cardioprotection applied at the abdomen, similar to IPC. To test this aim, I performed RT-qPCR reactions and Western blotting to address the mRNA and protein changes of a panel of HSPs in LV tissue after electrical stimulation. Genetic inhibition via transgenic/KO mice and siRNA was employed to probe the functional role of HSP70 in electrically-induced cardioprotection.

In Specific Aim 2, I identified the transcriptome of electrically-induced cardioprotection. Next-generation sequencing was performed to identify the differentially expressed mRNA and microRNA in the heart after electrically-induced NIC induction. I hypothesized that the transcription of NF- κ B-dependent mediators was required for late phase electrically-induced cardioprotection. Bioinformatics analyses using DAVID and DIANA softwares assigned a standardized vocabulary to the gene and microRNA lists and sorted candidates into cellular components, biological processes, and signaling pathways to clarify potential mediators of cardioprotection. Candidates were selected based on high fold changes and previously known roles in cardioprotection, validated by RT-qPCR, and investigated by Western blotting. Functional validation was performed using a combination of pharmacological and genetic inhibition. Further, I identified and validated differentially expressed microRNA that might influence the transcriptome after electrically-induced NIC induction.

In this document, I present the data that addresses these specific aims and the conclusions made based on the results. The dissertation supports that ES is cardioprotective via NF- κ B and NOS2.

CHAPTER IV

MATERIALS AND METHODS

Ethics Statement

Animal protocols were performed at Loyola University Chicago, an Association for Assessment and Accreditation of Laboratory Animal Care (AAALAC) certified facility, with Institutional Animal Care and Use Committee (IACUC) approval. Animals were housed at Loyola's on-site vivarium with *ad libitum* access to food, water, and a trained veterinary staff. All efforts were made to minimize animal numbers and suffering. All procedures were carried out by skilled staff that were qualified to accomplish the techniques successfully and humanely.

Animal Strains and Numbers

Equal numbers of male and female mice between 12 and 16 weeks old were utilized for these studies. Depending on the strain, mice were bred in-house in Loyola's on-site vivarium or purchased from Jackson labs at 10-11 weeks old and allowed to acclimatize for 7 days or more post-arrival prior to any procedures (Table 1). The cardiomyocyte-specific dominant negative I κ B α (3M) mice were developed in our lab and have been previously characterized (Brown, McGuinness et al. 2005). Breeding of 3M mice was done by selecting a transgenic mother from the colony and purchasing a new nontransgenic father of the appropriate strain (C57, JAX) each generation. The controls for 3M mice were nontransgenic littermates. For breeding the B6/129 mice, we purchased two new parents to cross C57BL/6J females (B6) and 129S1/SvImJ males (129S) to breed F1 hybrids. The F2 hybrids were the offspring of an F1 X F1 mating.

Strain	Catalogue Number
C57BL/6J (C57)	000664 (Jackson)
B6129SF1/J and B6129SF2/J (B6/129)	101043 and 101045 (Jackson) and bred in-house
B6.129P2-Nos2tm1Lau/J (NOS2 KO)	002609 (Jackson)
HSP70.1 KO	Bred in-house
3M	Bred in-house

Table 1. Mouse Strains. Depending on the strain, subjects in this study were bred on-site in Loyola's on-site vivarium or purchased from Jackson labs at 10-11 weeks old and allowed to acclimatize for 7 days or more post-arrival prior to any procedure.

The HSP70.1 and NOS2 KO mice were previously characterized and are on the C57BL/6J strain (Laubach, Shesely et al. 1995, Shim, Kim et al. 2002). In all of our breeding, we follow Jackson Lab protocols to avoid inbreeding our mice (Behringer, Gertsenstein et al.). All studies utilized B6/129 F2 unless otherwise specified.

Mice were maintained per the NIH guidelines in the Guide for the Care and Use of Laboratory Animals (2010). Physiological inclusion parameters were set to between 20-35g body weight. Subjects were excluded from the study if evidence of scratching or biting in the abdominal area was observed to avoid complications from nonelectrical nociception, scarring or scabbing that might interfere with the application of NIC in the same region.

Ischemia and Reperfusion Model

Throughout this work we utilized an *in vivo* model of MI and I/R injury via LAD coronary artery occlusion as detailed previously (Ren, Wang et al. 2004, Jones, Fan et al. 2009). In brief, mice were anesthetized with sodium pentobarbital (90 mg/kg) intraperitoneal (i.p.) and intubated and ventilated with room air supplemented with oxygen at a rate of 100 ± 5 /min using a miniventilator. Access to the LV was gained via lateral thoracotomy at the fourth

intercostal space to expose the heart. A loop occluder was placed around the LAD coronary artery 2-4 mm from the tip of the left auricle and ligated with a suture stabilized against a short piece of flexible silicon tubing for a 45-minute ischemic period that was confirmed by ST-elevation, widening of the QRS complex, and T-wave inversion typical of MI on the ECG trace. Blanching of the heart tissue by visual inspection was employed as a secondary measure of MI confirmation. Animal temperature was maintained at 33.5-36.5 °C via rectal probe thermometer and thermos-controlled heating pad throughout the experiment. Mice were excluded from the experiment if the ST interval did not change, if the change was inconsistent throughout ischemia, or if the ST-elevation was not reversed with reperfusion. We also excluded mice that recovered overnight in colder room conditions (sometimes unavoidable due to room issues) after pentobarbital anesthesia, as we found that hypothermic mice were cardioprotected by cold exposure. For molecular studies, the heart was dissected from the specimen, rinsed of blood in ice-cold phosphate buffered saline (PBS), and the right ventricle and LV separated. The anterior wall of the LV was further sectioned into aliquots, and when possible, approximate regions of the LV were kept consistent within studies for each subject. These zones encompassed both the ischemic and border zones in infarcted tissue, as was the case for the few studies where we collected protein post-I/R. All tissue was collected rapidly and flash frozen in liquid N₂ immediately after being harvested.

Electrical Stimulation Paradigm

Electrical stimulation via EA needles or electrical stimulation via cutaneous patches (ES) was completed as described previously in nociceptor-induced cardioprotection (Figure 3) (Jones, Fan et al. 2009). To deliver the EA stimulus, auricular needles 0.18 mm x 7 mm

(Sinic Avenue) were placed in a line cutaneously on the abdomen via a shaved patch on the trunk, halfway between the zyphoid process and the pubis, as detailed previously (Ren, Roessler et al. 2018). Our stimulus was not the same as traditional EA, which places the needles into deep tissue at traditionally recognized acupoints. Acupoints are mapped to certain meridians based on traditional Chinese medicinal theory or patient reported sensations when stimulated by either mechanical or electrical stimuli (Kaptchuk 2002). In

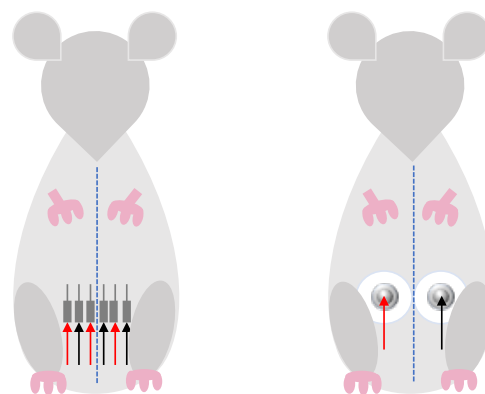


Figure 3. Rendering of Electrically-Induced Cardioprotection Model. Electroacupuncture with needles (EA, left) or electrical stimulation with cutaneous patches (ES, right) was applied halfway between the zyphoid and pubis on an anesthetized mouse.

contrast, we placed the needles in the skin to stimulate the skin and associated nociceptors and did not penetrate underlying tissues. Our rationale was based on evidence that RPCT is abolished by cutaneous sensory nerve blockade (Jones, Fan et al. 2009). To deliver ES via patch, two modified neonatal electrodes were constructed from neonatal electrodes (Cardinal, catalogue #31439725) modified by trimming the foam padding and leaving a small circle of adhesive around the electrode. The patches were placed on a shaved area of the mouse abdomen, halfway between the zyphoid and pubis. The electrodes were stabilized by surgical tape to maintain contact with the abdomen. The application is similar to the TENS devices routinely used in physical therapy and investigated in large animal models (Merlocco, Redington et al. 2014). As an alternative, we considered delivering electricity through microneedle arrays, which are being optimized for vaccine delivery, for deeper penetration into the skin (Kim, Park et al. 2012). Each electrode was coupled to an FDA approved electrical signal

generator (AWQ 104L digital acupunctoscope), which applies the electrical current to the trunk of the abdomen. The parameters of the stimulus were: 15 minutes of stimulation at 100 μ sec, 4 Hz, and 2.5-7.5 V as an early phase, late phase, or postconditioning stimulus.

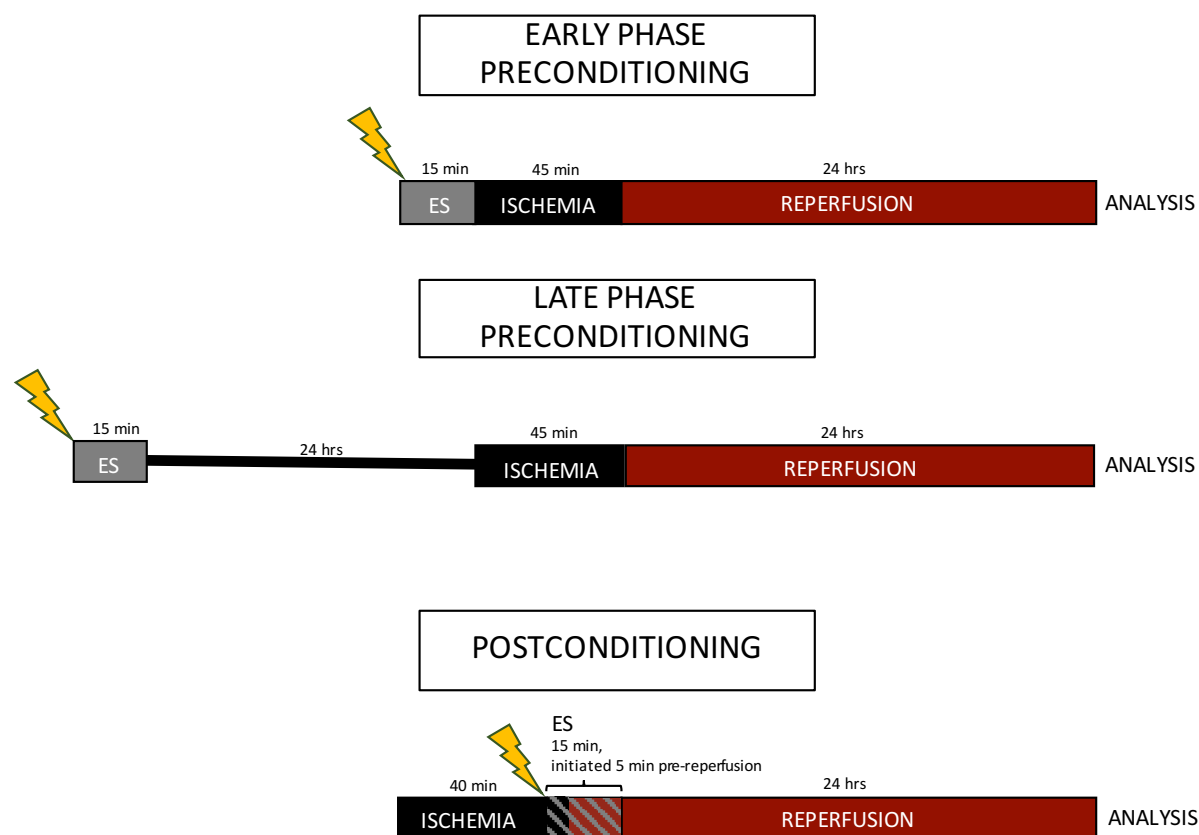


Figure 4. Cardioprotective Paradigms. In our models of electrically-induced cardioprotection, mice received electrical stimulation immediately before I/R for early phase studies, 24 hours before I/R for late phase studies, and 5 minutes before reperfusion.

Since 5 V elicited the most robust cardioprotective response as a preconditioning stimulus, this voltage was chosen for all follow-up evaluations of the molecular mechanisms in multiple paradigms (Figure 4). For all early phase preconditioning experiments, mice received electrical stimulation immediately prior to I/R. For late phase preconditioning experiments, mice received electrical stimulation 24 hours prior to I/R. Mice with IPC received open-chest surgery, occluder placement, and six 4-minute coronary occlusions interspersed with 4 minutes

of reperfusion. For all postconditioning experiments, mice received electrical stimulation initiated 5 minutes prior to the onset of reperfusion. For all studies, control-operated mice underwent the identical preparation and needle or patch placement but received no electrical signal.

TTC Staining and Infarct Size Analysis

After 24 hours of reperfusion, animals were sacrificed by sodium pentobarbital overdose and perfused transaortically with 1% triphenyltetrazolium chloride (TTC) in phosphate PBS (pH 7.4, warmed to 37 °C) at a pressure of 60 mmHg (~3 ml over 3 min). The area not at risk was differentiated by 5% phthalo blue dye diluted in PBS. Triphenyltetrazolium chloride is a redox-sensing dye that is metabolized to a brick red color by living cells while dead cells remain a pale pink or white. The tissue was frozen, sectioned into 4-5 1 mm sections, weighed and photographed. Infarct size was determined by digitally tracing the total area, area at risk, LV cavity area, and area not at risk using the NIH software ImageJ (Figure 5). The infarct size was calculated as a percent area at risk as previously described (Fishbein, Meerbaum et al. 1981).

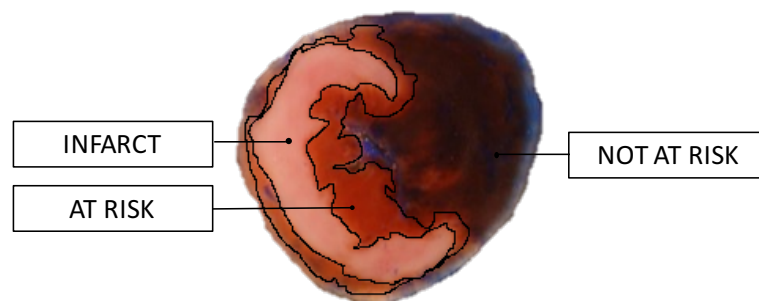


Figure 5. TTC Staining. Infarcted area (pale pink), area at risk (brick red), and area not at risk (deep blue) were delineated with phthalo blue dye and the redox sensor TTC.

Histology and Cell Death Assessment

For the histological assessment of cell death, mice were transcardially perfused with

saline followed by 10% neutral buffered saline (NBF) 3 hours after the onset of reperfusion. Tissues were fixed in a volume of 1:10-1:15 10 % NBF for 24-72 hours at room temperature, then paraffin embedded and processed by the Purdue Histology Core for the apoptotic marker Bcl-2 (Abcam, ab182858) with a hematoxylin counterstain or the apoptotic cell death marker TUNEL (Abcam, ab206386) with a Fast Green counterstain. In both TUNEL and Bcl-2 quantifications, NIH ImageJ software was employed, and the thresholds were kept the same for all images within each analysis. Bcl-2 positive regions (color threshold set between 190-255) were calculated as a percent total area (color threshold set between 110-255). All TUNEL positive nuclei were counted in three separate visual fields within the infarcted region and averaged to quantify cell death for that section. For TUNEL quantifications, total TUNEL negative nuclei were counted within the visual field by setting thresholds for size (20-50), roundness (0.5-1.0) and color (hue between 90-200). All TUNEL positive nuclei were counted manually within the visual field. The TUNEL positive nuclei were calculated as a percentage of total nuclei (the sum of TUNEL positive and negative nuclei). We counted approximately 122 total nuclei on average per section and less than 45 TUNEL positive nuclei per slice.

RNA Isolation, Reverse Transcription, and Quantitative Real Time PCR Analysis

For mRNA and microRNA isolation from animal tissues, tissue was weighed and Qiazol (Qiagen) was added at 1 mL/ 100 mg tissue, then homogenized with a pestle in a microcentrifuge tube. After a 5-minute incubation at room temperature, 0.27 μ L chloroform was added per 1 μ L Qiazol lysis reagent, then the sample was shaken vigorously for 15 seconds. After incubating at room temperature for 2-3 minutes, the samples were centrifuged at 12,000 X G for 15 minutes at 4°C, and the upper aqueous phase was transferred to a new tube.

Glycogen (RNase free, Glycoblue, Ambion) was added as a carrier to the aqueous phase before adding 0.67 μ L 100% isopropanol per 1 μ L Qiazol used in homogenization. Samples were incubated at room temperature for 10 minutes, centrifuged at 12,000 X G at 4 °C for 10 minutes, and the supernatant was carefully aspirated and discarded. The pellet containing RNA was washed with 1.33 μ L 75 % ethanol per 1 μ L Qiazol lysis reagent, vortexed to mix, centrifuged at 7,500 X G for 5 min at 4 °C, and air dried. The RNA was re-dissolved in 30 μ L of RNase-free water and incubated in a heat block at 55-60 °C for 10-15 minutes. The RNA concentration and purity was measured by nanodrop and 260/280 ratios greater than 1.8 were selected for follow-up experiments. RNA was stored at -80 °C. All steps not performed at room temperature were carried out on ice.

For reverse transcription polymerase chain reaction (RT-PCR) of mRNA extracted from tissue samples, water, 2X RT buffer, 20X RT enzyme mix, and 200 ng of isolated RNA were prepared in a reaction mix (Applied Biosystems). The RNA was placed in a thermal cycler under the following conditions: 1 hour at 37 °C, 5 minutes at 95 °C, and held at 4 °C. The cDNA was diluted in 180 μ L RNase free water and stored at -20 °C for the long term or at 4 °C for up to 24 hours.

For real time quantitative PCR (qPCR) of mRNA extracted from tissue samples, primers for the genes of interest were designed using the NIH Primer Blast software and ordered from Integrated DNA Technologies (IDT), with the exception of HSP90, which was ordered from Qiagen, and NOS2, which was based on a template from previous studies (Table 2) (Cummings and Tarleton 2004). New primers were validated in-house. Following a temperature gradient, products of the reaction were run on a gel to assess an annealing temperature that produced a

single final product. A reaction mix containing 2X SYBR green master mix (Applied Biosystems), sense and antisense primers, RNase-free water and template cDNA was prepared in a volume of 20 μ L. Polymerase chain reaction was performed for 40 cycles under the following conditions: 15 minutes at 95 °C, denatured for 15 seconds at 95 °C, annealed for 30 seconds at the temperature optimized for each primer between 55 °C-60 °C, and extended for 30 seconds at 70 °C, followed by a melt curve.

Target	S: 5'-3'	AS: 5'-3'	Annealing Temperature (°C)
<i>HSP70.1</i>	GAAGACATATAGTCTAGCTGCCAGT	CCAAGACGTTTGTTTAAGACACTTT	55
<i>HSP70.3</i>	GGCCAGGGCTGGATTACT	GCAACCACCATGCAAGATTA	55
<i>hmrDNAJa1</i>	GGTGAAGGAGACCAAGAACCAGGA	TTGACAATCTGACCTGGATGAGAGG	55
<i>hmrDNAJb1</i>	ATGTTTGCTGAGTTCTTCGGTGGC	CCGCTGTAGATCTCTTCAAGGGAGAC	55
<i>KY</i>	TCATCGAGGATCACTTCCCAG	CCGGCTCTCGATGGTGATT	55
<i>NOS2</i>	CAGCTGGGCTGTACAAACCTT	CATTGGAAGTGAAGCGGTTCG	61
<i>JUN</i>	TTGTTACAGAAGCGGGGACG	GAGGGCATCGTCGTAGAAGG	61
<i>GAPDH</i>	ACCACAGTCCATGCCATCAC	TCCACCACCCTGTTGCTGTA	55
<i>hmr18s</i>	AGTCCCTGCCCTTTGTACACA	CCGAGGGCCTCACTAAACC	55

Table 2. List of Primers. Sense and antisense sequences of primers used in PCR studies were developed using NIH Primer Blast software and ordered from Integrated DNA Technologies.

All reactions were performed in triplicate and normalized to 18s using the $2^{(-\Delta\Delta CT)}$ method (Livak and Schmittgen 2001). In brief, the average cycle threshold (C_T) values of the replicates were calculated for the housekeeping gene and the gene of interest for each sample. The differences between a sample's gene of interest and the housekeeping gene were calculated (ΔC_T) and transformed to $2^{-\Delta CT}$. The control average $2^{-\Delta CT}$ was calculated for the control condition, and every sample's $2^{-\Delta CT}$ was divided by the control average $2^{-\Delta CT}$ to calculate

the $2^{(-\Delta\Delta CT)}$ value for that sample. Fold change was calculated by averaging the $2^{(-\Delta\Delta CT)}$ values for experimental and control conditions, which sets the experimental value to 1 (Livak and Schmittgen 2001).

For RT-PCR of microRNA from tissue RNA samples, nucleic acid mix, 5X HiFlex buffer, and MiScript reverse transcriptase enzyme (Qiagen) were added to RNase free water and 100ng of microRNA samples in a reaction mix in a volume of 20 μ L and placed in the thermocycler for cDNA synthesis according to the following conditions: 1 hour at 37 °C, 5 minutes at 95 °C, and held at 4 °C. For real time quantitative PCR of cDNA made from microRNA from tissue RNA samples, 10X miScript primer assay specific to the primer of interest (ordered from Qiagen), 10X miScript universal primer, RNase-free water, SYBR green, and RT product were combined in a reaction mix (Qiagen). The PCR was performed for 40 cycles under the following conditions: 15 minutes at 95°C, denatured for 15 seconds at 94 °C, annealed for 30 seconds at 55 °C, and extended for 30 seconds at 70 °C, followed by a melt curve. The reactions were run in triplicate and normalized to U6 using the $2^{(-\Delta\Delta CT)}$ method as in the above paragraph.

Protein Isolation and Western Blot Analysis

Tissues were weighed and rapidly homogenized with a hand-held motorized pestle. Total protein was isolated from LV heart tissue using 3 mL/mg complete radioimmunoprecipitation assay lysis buffer (RIPA) with 10% protease inhibitor cocktail, 10 % Na_3VO_4 , and 10 % PMSF per manufacturer's recommendations (Santa Cruz Biotechnology, #sc-24948A). Lysates were incubated on ice for 30-60 minutes, spun at 10,000 X G at 4 °C for 15 minutes to pellet debris, and the supernatant was collected and stored at -80 °C or processed immediately. In experiments in which the nuclear and cytoplasmic fractions were separated,

tissues were homogenized in 10 μ L/mL solution A (10 mM HEPES, 1.5 mM $MgCl_2$, 10 mM KCl, and 0.1 % Triton X), incubated on ice for 10 minutes, and spun at 5,000 X G at 4 °C for 10 minutes. The supernatant cytoplasmic fraction was collected, and the pellet was dissolved in 5 μ L/mL solution B (20 mM HEPES, 10 % glycerol, 1.5 mM $MgCl_2$, 0.6 M KCl, and, 0.2 mM EDTA), incubated on ice for 40 minutes with occasional vortexing, centrifuged at 10,000 X G at 4 °C for 15 minutes, and supernatant collected as the membrane or nuclear fraction. In experiments that separated soluble and insoluble fractions, tissue was homogenized in complete RIPA and centrifuged at 12,000 X G at 4 °C to separate the soluble protein fraction in supernatant. The insoluble fraction was washed and solubilized in urea buffer (50 mM Tris HCl, pH 7.5, 4 M urea, 1 M thiourea, 0.4 % CHAPS detergent, 20 mM spermine, 20 mM dithiothreitol) (de Marqui, Vidotto et al. 2006).

Total protein level was quantified using bicinchoninic (BCA) protein assay (Pierce). Cells were diluted 1:4, tissues were diluted 1:10, and standards were diluted 125-2000 μ g/mL in RIPA, plus a RIPA negative control, in volumes of 20 μ L. Samples were plated in triplicate and 200 μ L BCA working reagent was added to each well, incubated at 37 °C for 30 minutes, cooled to room temperature for 30 minutes, and read at an absorbance of 562 nm by a Cytation 3 imaging machine.

For gel electrophoresis and Western blots, a maximum of 50 μ g protein was loaded into each well of an 8-12 % gel, depending on the size of the protein of interest. Electrophoresis was carried out at 70 V for 15 minutes, then 140 V for 60 minutes, and transfer to a nitrocellulose membrane was done at 160 mA for 2 hours or 40 mA overnight at 4 °C. Membranes were blocked for 1 hour at room temperature or overnight at 4 °C with 5 % (w/v) nonfat dry milk in

tris-buffered saline with tween (TBS-T) and probed with primary antibodies for proteins of interest followed by the appropriate horseradish peroxidase-conjugated secondary antibodies against mouse (1:2000; 7076, Cell Signaling Technology, Danvers, MA) and rabbit IgG (1:2000; 7074, Cell Signaling Technology) (Table 3).

Target	Company	Catalogue Number	Dilution	Validation
HSP70 (W27)	Santa Cruz	SC-24	1:1000	Western blotting and flow cytometry of heat shocked cells as positive control (by company)
HSP70	Cell Signaling	4872S	1:1000	Western blotting of cell lysates and IHC of cancer tissues as positive control (by company)
HSP90	Thermo-Fisher	PA3-013	1:2000	Western blotting of purified, recombinant HSP90 (by company)
HSP40 (DNAJB1)	Thermo-Fisher (Origene)	TA502194	1:1000	Western blotting of cell lysates of transfected HEK293 cells overexpressing HSP40 (by company)
HSP40 (DNAJA1)	Thermo-Fisher	ms-225-p0 / MA5-12748	1:2000	Western blotting of siRNA mediated knockdown of HSP40 in HeLa cells (by company)
KY	Invitrogen	PA5-23914	1:1000	Western blotting of mouse liver tissue lysates as positive control (by company)
JUN (60A8)	Cell Signaling	9165	1:1000	Western blotting of neuroblastoma cell lysates and IHC of cancer tissues as positive control (by company)
NOS2 (EPR16635)	Abcam	178945	1:1000	Western blotting of tissue lysates from mice with a genetic deletion of NOS2 (in-house)
LC3	Novus Biologicals	NB100-2220	1:1000	Western blotting of cell lysates from an LC3 knockout HeLa cell line (by company)
HSF1 (E4)	Santa Cruz	SC-17757	1:500	Western blotting of HSF1 siRNA transfected HeLa cells (by company)
Actin	Thermo-Fisher	MA5-15739	1:2000	Western blotting reveals a single clear line at predicted molecular weight (in-house)
GAPDH	Thermo-Fisher	MA5-15738	1:2000	Western blotting reveals a single clear line at predicted molecular weight (in-house)
Anti-rabbit	Cell Signaling	7074S	1:5000	Secondary antibody alone produces no non-specific binding in the Western blotting application (in-house)
Anti-mouse	Cell Signaling	7076S	1:2000	Secondary antibody alone produces no non-specific binding in the Western blotting application (in-house)

Table 3. List of Antibodies. Relevant information on the antibodies utilized in these studies.

Blots were developed using SuperSignal West Dura Extended Duration Substrate (catalogue #34075, Thermo Fisher Scientific) blotting detection reagents, and signal density was measured and calculated with ImageJ and normalized to actin, GAPDH, or total protein using the NIH software ImageJ. For some blots, membranes were incubated in stripping buffer and reprobed or cut and probed separately to investigate multiple proteins of interest.

Next-Generation Sequencing of mRNA and microRNA

Next-generation sequencing was performed on: 1. mRNA from ES+ or ES- B6/129 mice (N=2-3) or 2. mRNA from 3M or nontransgenic mice treated with ES+ or ES- (N=4) or 3. microRNA from ES+ or ES- B6/129 mice (N=3). In all next-generation sequencing studies, the ischemic areas of the LVs were dissected 3 hours after stimulation. Library preparation and sequencing were completed by the University of Chicago Functional Genomics Facility. Analysis, quality control of raw sequencing data, and differential expression were completed by Michael Zilliox and Gina Kuffel at the Loyola Genomics Facility.

Quality control. Total RNA were isolated and purity was determined by nanodrop for 260/280 absorbance ratios. Ratios over 1.8 were submitted for sequencing. The total RNA in each sample was quantified using the Qubit 2.0 Fluorometer (Invitrogen) and quality was measured using the RNA6000 Nano chip on the Agilent 2100 Bioanalyzer (Agilent Technologies). Samples with an RNA integrity number (RIN) greater than 7 were used for sequencing.

mRNA library preparation and sequencing. Using the Illumina TruSeq Stranded mRNA Library Prep kit, the mRNA in the total RNA was converted into a library of template molecules of known strand origin. Specifically, mRNA molecules were isolated using poly-T oligo attached magnetic beads. The resulting mRNA were fragmented and reverse transcribed using random primers. The cDNA product was then amplified, incorporating sequencing adapters and barcodes to create a final double-stranded cDNA library ready for sequencing. The samples were sequenced on the Illumina HiSeq platform rendering 50 base pair single-end reads.

mRNA data analysis. Cutadapt v.1.11 (Martin 2011) was used to remove adapter sequences and to trim low quality sequencing reads. The resulting reads were mapped to the Ensembl mouse genome assembly GRCm38 using the splicing aware aligner, Tophat2 v. 2.0.13. (Kim, Pertea et al. 2013). Raw counts were generated using the Python package HTSeq v. 0.6.1p1. (Anders, Pyl et al. 2015). R Studio and R v3.5.1 were used for further analysis. DESeq2 (version 1.22.1 and earlier) (Love, Huber et al. 2014, Love, Anders et al. 2017) was used to determine differential expression between sample groups. Wald tests were used for significance testing (Chen, Liu et al. 2011).

miRNA library preparation and sequencing. cDNA libraries were generated using the TruSeq Small RNA library prep kit (Illumina). Specifically, adapters were ligated using the 5' phosphate and 3' hydroxyl group common to most mature miRNAs as a result of the cellular pathways used to create them. After adapter ligation, samples were reverse transcribed and amplified. Finally, the libraries were size selected using a 6 % polyacrylamide gel and concentrated using an ethanol precipitation. Purified libraries were normalized and pooled to create a double stranded cDNA library ready for sequencing. The samples were sequenced on the Illumina MiSeq to render 50 base pair single end reads.

miRNA data analysis. Adapter sequences were removed and low quality reads were trimmed from raw sequencing reads using Cutadapt (v.1.11) (Martin 2011). The resulting reads were mapped to the most recent release of the mouse genome from Ensembl, GRCm38 using Bowtie2 (v. 2.2.1) (Langmead and Salzberg 2012). An annotation file from miRBase release 21, describing miRNA coordinates, and the sequence alignment mappings were used as input for the Python package HTSeq (v. 0.6.1p1) (Griffiths-Jones, Saini et al. 2008, Anders, Pyl et al. 2015)

to generate a table of raw counts of miRNAs observed in the alignments. Further analysis was conducted using R v3.5.1 and R studio. DESeq2 (v. 1.22.1 and earlier) (Love, Huber et al. 2014, Love, Anders et al. 2017) was used to determine differential expression between sample groups using the raw count table as input. Wald tests were conducted to determine significance (Chen, Liu et al. 2011).

DAVID and DIANA Analyses

The Database for Annotation, Visualization and Integrated Discovery (DAVID) bioinformatics database was utilized to characterize the biological processes, cellular components, and signaling pathways of the sequencing dataset to assign biological meaning to the data (Huang da, Sherman et al. 2009, Huang da, Sherman et al. 2009). The software calculates the enrichment score, which ranks overall importance of gene groups. A gene ontology (GO) enrichment score of ≥ 1.3 was used as criteria of inclusion for biological process, and we present the entire list for cellular component. The enrichment score ranks overall importance of gene groups. It is recommended that enrichment scores of 1.3 should be given the most attention, but groups with lower score could potentially be interesting and could be considered for exploration (Huang da, Sherman et al. 2009). DIANA and the mirPath V3 software was utilized to determined GO analysis and Kyoto Encyclopedia of Genes and Genomes (KEGG) pathway analysis of the microRNA dataset (Vlachos, Zagganas et al. 2015).

Pharmacological and siRNA Inhibition

Four pairs of single stranded DNA oligonucleotides targeting heat shock factor 1 (HSF1) were synthesized to block the HSF1 cDNA sequence (accession #XM_128055), as evaluated in Yin, 2005 (Yin, Xi et al. 2005). In those studies, i.p. injection of siRNA against the same

sequences blocked the induction of HSP mRNA and protein levels *in vivo* by whole body hyperthermia. The silencing effect of the siRNA against HSF1 was associated with the reduction of late phase (48 hour) heat-shock-induced cardioprotection.

The oligonucleotides were designed and synthesized by IDT with or without modifications to protect against endonucleases and enhance cellular uptake: 2'-*O*-methyl-modified oligonucleotides, phosphorothioate linkage, and a cholesterol addition, as done in Wang, 2012 (Wang, Zhu et al. 2012). Their group designed antagomirs, which are engineered oligonucleotides designed to silence endogenous microRNAs, specifically against miR-144 and miR-451. These were deployed by three consecutive daily tail vein injections (3 × 40 mg/kg body weight) to downregulate the expression of each respective microRNA in the heart, and knockdown of miR-451 significantly impaired IPC and enhanced oxidative stress.

The 4 sequences were pooled and delivered locally in *In Vivo* Transfection Reagent (Altogen, Catalog #5030) to the hearts of anesthetized mice via pericardial sac injection with a Hamilton syringe, 22.5 µg siRNA in transfection reagent in PBS, 24 hours before ES±, based on standards found in the literature. The transfection reagent alone in a comparable volume was selected as the control. Mice were repositioned periodically during recovery to ensure complete dispersal of the solution in the pericardial sac. The specificity of the sequences was investigated *in vitro*. The pooled oligos or a nontargeting control sequence was applied to mouse 3T3 fibroblast cells with Lipofectamine 2000 (Thermo Fisher, catalogue #11668027) in a dose curve ranging from 0-200 pmol/well as instructed by the manufacturer's protocol. Cells were maintained in a 37 °C incubator and split 1:10 regularly prior to experiments.

In our use of *in vivo* pharmacological inhibitors, the drug, dose, and timing was selected

based upon the drug's use in the literature with *ex vivo* validations when possible. Apoptozole, an ATP-ase inhibitor of HSP70, was employed at a dose of 10 mg/kg dose i.p. administered 1 hour prior to I/R in order to examine HSPs in the late phase of cardioprotection (Baek, Zhang et al. 2015, Ko, Kim et al. 2015). SP600125, a reversible, selective, ATP-competitive inhibitor of JNK, was employed to inhibit c-Jun activation and translocation. This inhibitor is reported to markedly enhance apoptosis and infarct size when administered at a dose of 30 mg/kg i.p. during brief periods of ischemia, effectively reducing the protective effect of JNK (Wei, Wang et al. 2011). We used a dose of 30 mg/kg dissolved in 8 % DMSO in corn oil, administered i.p. 15 minutes prior to the initiation of ES+ or ES- in mice that subsequently received I/R. Control groups received the same volume of the vehicle.

Statistical Analyses

Power analysis, both *a priori* and *post-hoc*, were performed to assess effect size, assure that sample sizes were sufficient and the effect was real based on the power achieved, and predict sample size based on pilot studies. The criteria used to determine acceptable power were 80% power at an $\alpha=0.05$. Student's t-tests were performed when datasets included two groups, and a 1-way ANOVA with Dunnett's *post-hoc* test of multiple mean comparisons was performed when datasets were more than two groups. When two or more groups were assessed on two or more independent variables, 2-way ANOVA with Bonferroni (most commonly used), Sidak's (more power), or Tukey (when comparing all group means) *post-hoc* tests were performed for multiple comparisons. Statistics were performed and graphs generated in Matlab Prism, and group data is reported as mean \pm standard error of the mean (SEM). Histology experiments were quantified, but statistics were not performed due to low

sample numbers (N=2-3), and are presented for qualitative assessments only. Alpha is set at 0.05 unless otherwise specified, as in next-generation sequencing tables where $P \leq 0.1$ is the default cut-off (Love, Anders et al. 2017). To this end, we only show sequencing data at $P \leq 0.05$ within the text, but complete tables of mRNA, microRNA, and 3M comparisons up to $P \leq 0.10$ can be found in the appendices. The 4X4 and 3X3 alternative analyses presented in the Appendix are limited to data in which $P \leq 0.05$ was achieved since we did not pursue these datasets further. Since only one microRNA was significant at $P \leq 0.10$ after adjustments for multiple comparisons, we conservatively expanded this list to include microRNAs differentially expressed up to $P \leq 0.05$ *without multiple adjustments* for pathway analysis studies, and present differentially expressed microRNAs up to $P \leq 0.10$ *without multiple adjustments* in the Appendix.

CHAPTER V

RESULTS

Electroacupuncture is an Effective Early Phase Cardioprotective Stimulus

To determine whether electrical stimulation via EA needles was effective as a cardioprotective stimulus that mimics the effects of NIC and RPCT, B6/129 mice were treated with electrical stimulation via EA needles (5 V, 4 Hz, 100 μ seconds, 15 minutes) immediately before I/R in a preconditioning paradigm (Figure 4). Electroacupuncture applied via needles into the skin of the abdomen significantly ($P \leq 0.05$) reduced the infarct size calculated as a percentage of the area at risk in EA-treated mice (Figure 6A). There was no significant difference in the area at risk as a percent of total area (Figure 6B). We processed the infarcted region of the left ventricle anterior walls collected from EA-treated mice for TUNEL staining, a nuclear marker of cell death, to determine whether this reduction in infarct size was due to decreased apoptosis. Qualitative assessment of the TUNEL stained heart tissue found that EA reduces the TUNEL positive nuclei compared to TUNEL negative nuclei, which was quantified in the small group of heart tissues that were processed, but statistics were not performed due to low sample numbers (N=2-3) (Figure 6C-D). Together, these data demonstrate that electroacupuncture applied at the same region as RPCT reduces infarct size to the same degree as RPCT, offering an alternative to surgically or chemically-induced NIC.

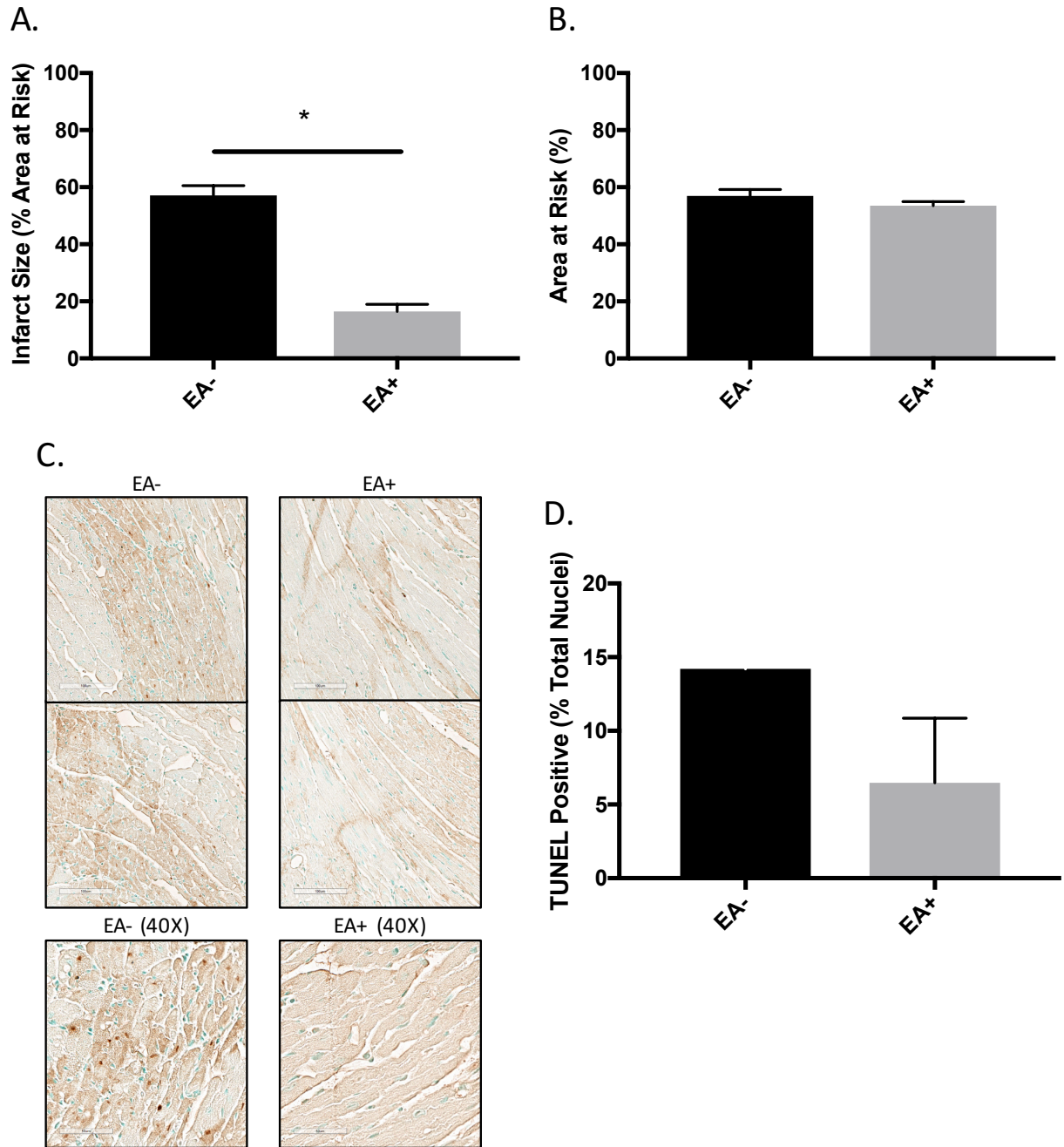


Figure 6. Effect of EA on Infarct Size and Apoptosis. Quantifications of infarct parameters in hearts from B6/129 mice treated with EA immediately prior to I/R. Figure 6A portrays the infarct size as a percent area at risk, and the area at risk is also shown as a percent of total area (B) (N=6 for all groups). Representative images (C) and semi-quantitative measurements (D) of TUNEL positive cells in the infarct zone of the left ventricle of EA-treated mice collected 6 hours after ischemia and processed for apoptotic cell death by TUNEL staining (N=2,3). * $P \leq 0.05$. Mean \pm SEM. An unpaired, 2-tailed Student's t-test revealed a significant effect of EA on infarct size [$t(10)=9.626$, $P < 0.0001$] and no difference in area at risk [$t(10)=1.278$, $P = 0.2301$]

Electrical Stimulation via Cutaneous Patch is Effective as an Early Phase, Late Phase, and Postconditioning Cardioprotective Stimulus

Electrically-induced cardioprotection via EA reduced infarct size as a mimic of NIC and RPCT. Therefore, to improve the translation of electrically-induced cardioprotection, I investigated the effectiveness of electrical stimulation via cutaneous skin patches. To test the hypothesis that there would be a difference between the ES+ group and a control ES- group, ES+ was applied at different voltages in the early-phase paradigm. It was revealed that electrical stimulation delivered via cutaneous patch achieved reduction of the infarct size at 5 V as an early phase stimulus. Therefore, 5 V was maintained consistently as the cardioprotective stimulus in all subsequent ES studies (100 μ seconds, 4 Hz, and 5 V, 15 minutes, Figure 7A). There were no differences in area at risk in this study (Figure 7B).

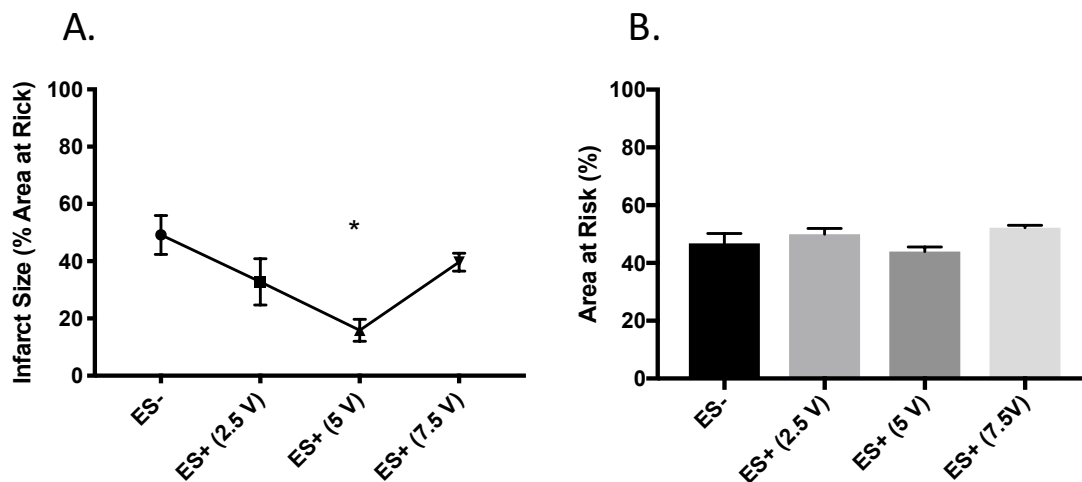


Figure 7. Effect of ES on Infarct Size in Early Phase Cardioprotection. Quantifications of infarcted hearts from B6/129 mice treated with electrical stimulation via cutaneous patch immediately prior to I/R portray the infarct size as a percent area at risk (A) and area at risk as a percent of total area (B) with increasing voltage of ES (N=10, 5, 7, 4 for 0, 2.5, 5, and 7.5 V, respectively). A one-way ANOVA revealed a significant effect of ES treatment [$F(3, 22) = 5.506$, $P=0.0056$]. Dunnett's *post-hoc* test for multiple comparisons performed for each group against ES- showed a lower infarct size in 5 V ES treated mice. * $P \leq 0.05$ compared to ES-, mean \pm SEM. There was no difference in area at risk [$F(3, 22)=1.217$, $P=0.3269$].

Electrically-induced cardioprotection via cutaneous patch also reduced the size of the infarct in a late phase paradigm, when 5 V of electrical stimulation was applied via patches 24 hours prior to MI (Figure 8A-B). To gain further insights into the possible mechanisms of this late phase of cardioprotection, I investigated Bcl-2 expression as a marker of cardiac injury that is found concomitantly with MI (Hockenbery, Zutter et al. 1991).

Bcl-2 has low expression in non-infarcted myocardial tissue and is induced in cardiomyocytes in the areas surrounding the infarction after the onset of ischemic injury (Hockenbery, Zutter et al. 1991). Qualitative immunohistological assessments of Bcl-2 proteins in the anterior wall of infarcted hearts demonstrated lower levels of the Bcl-2 positive regions in the ES+ groups compared to the ES- groups, which was quantified in the small group of heart tissues that were processed (Figure 8C-E). The effect size was not large and the difference was not statistically significant. Power was 0.10 for these data. To achieve significance ($\alpha=0.05$) at a power level of 0.80, a sample size of over 50 additional animals is projected based on this pilot study. Electrically-induced cardioprotection via cutaneous patch is effective in the postconditioning paradigm where ES applied 5 minutes prior to the start of reperfusion reduces the size of the infarct (Figure 9). In the clinic, this time point would coincide with the placement of a stent in the cardiac catheterization laboratory. The ES- infarcts are noticeably smaller in these studies compared to previous studies, possibly due to complications with the *in vivo* model, discussed later in this document. Together, these data demonstrate that electrical stimulation applied at the same region as RPCT effectively reduces the infarct, perhaps as a mimic of NIC.

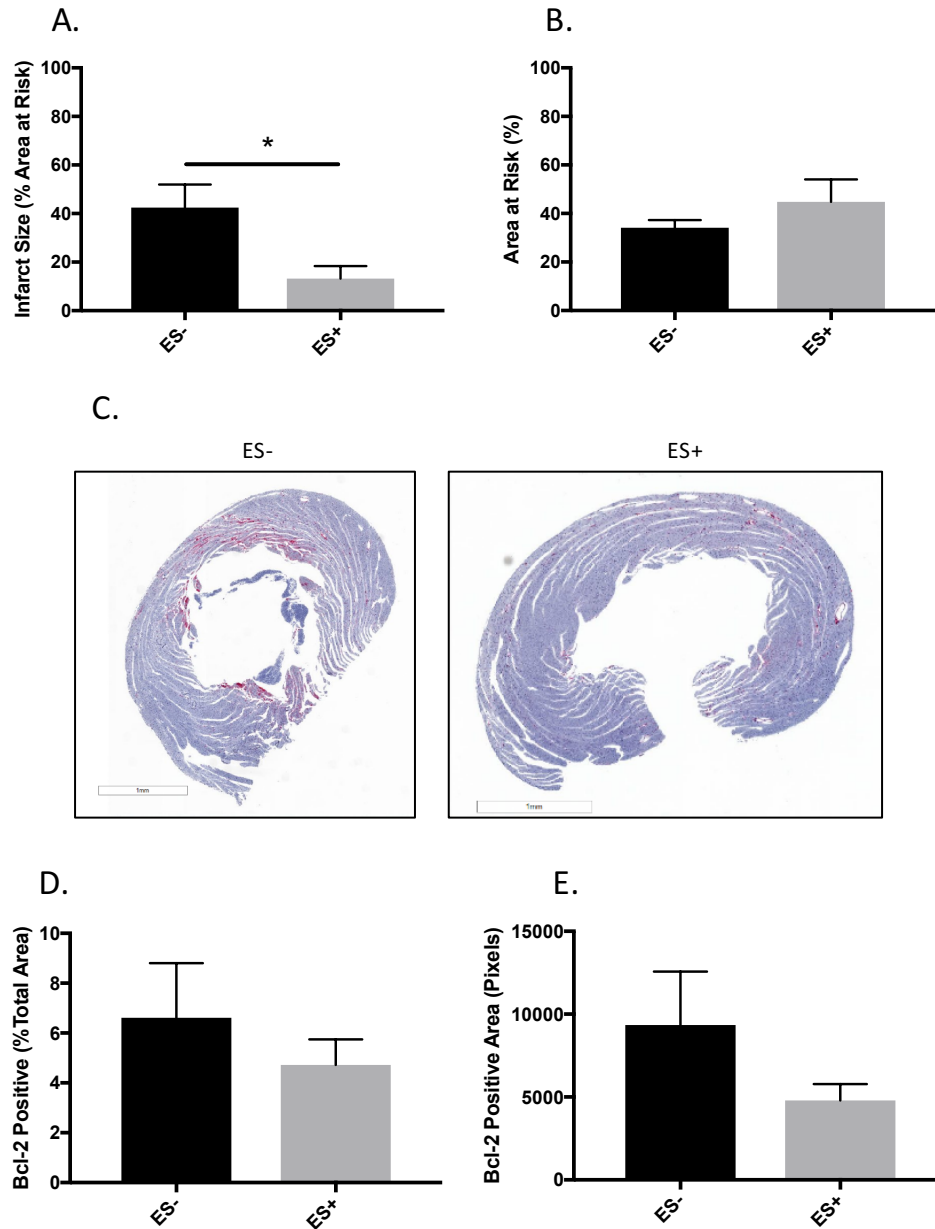


Figure 8. Effect of ES on Infarct Size and Bcl-2 Expression in Late Phase Cardioprotection.

Quantifications of infarct size from B6/129 mice treated with electrical stimulation 24 hours prior to I/R. Infarct size is shown as a percent of area at risk (A) and area at risk as a percent of total area (B) (N=4,5 for ES- and ES+, respectively). An unpaired, 2-tailed Student's t-test revealed a significant effect of ES on infarct size [$t(7)=2.867$, $P<0.0241$] and no difference in area at risk [$t(7)=1.118$, $P=0.3004$]. * $P\leq 0.05$. Mean \pm SEM. Representative images (C) and quantifications (D-E) of infarcted zones of the left ventricle of ES-treated mice collected 6 hours after ischemia and processed for apoptotic cell death by Bcl-2 staining (N=4 for all groups). An unpaired, 2-tailed Student's t-test revealed no significant differences between Bcl-2 positive area as a % total area (D) [$t(6)=0.7796$, $P=0.4652$] or as Bcl-2 positive area (E) [$t(6)=1.351$, $P=0.2254$].

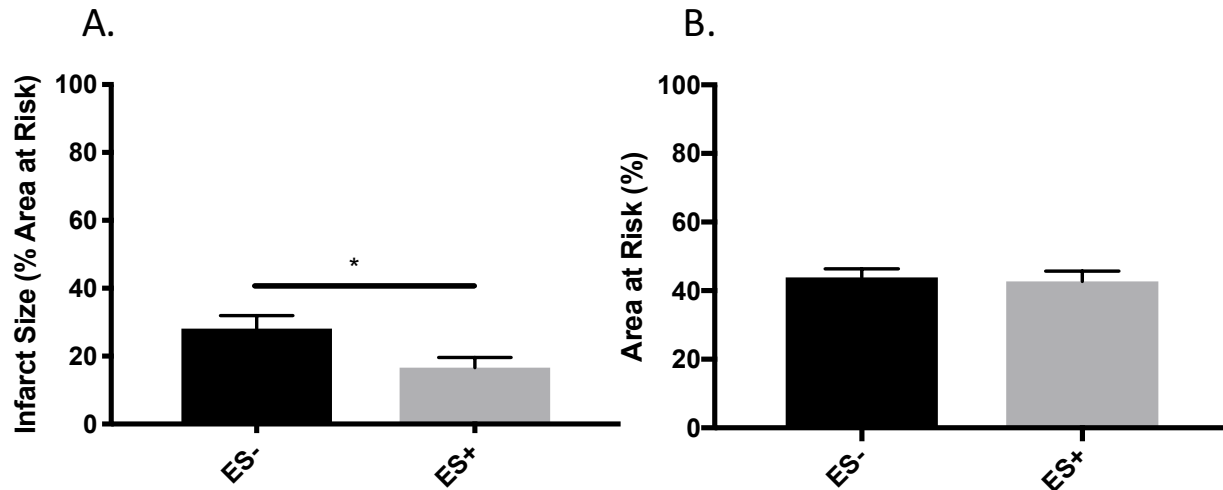


Figure 9. Effect of ES on Infarct Size in Postconditioning. Quantifications of infarct size in B6/129 mice treated with electrical stimulation 5 minutes before the start of reperfusion portray the infarct size as a percent area at risk (A) and area at risk as a percent of total area (B) (N=14 for all groups). An unpaired, 2-tailed Student's t-test revealed a significant effect of ES+ on infarct size [$t(26)=2.384$, $P=0.0247$] and no difference in area at risk [$t(26)=0.3064$, $P=0.7617$]. * $P\leq 0.05$. Mean \pm SEM.

Electroacupuncture and electrical stimulation via cutaneous patch are effective in multiple paradigms of cardioprotection: early phase preconditioning, late phase preconditioning, and postconditioning. The reduction in infarct size corresponds to a nonsignificant trend towards decreased Bcl-2 expression and decreased TUNEL positive nuclei in late-phase preconditioning. Neither electrical stimulation or EA was associated with arrhythmias or heart rate changes during stimulation or I/R.

The Increase in HSP mRNA and Protein is Small and Mostly Insignificant

Heat shock proteins play a critical role in IPC in that they act as molecular chaperones that mediate protein folding, degradation, and repair. However, it is unclear if HSPs are involved in electrically-induced cardioprotection. The heat shock response is tightly linked to autophagy in cellular stress and injury (Dokladny, Myers et al. 2015). A panel of HSP transcripts

and expression levels was investigated following EA or ES, including HSP70, HSP90, and HSP40.

In a preliminary study to investigate autophagy as part of the aberrant protein folding response in I/R, LC3BII levels were measured as a marker of autophagosome formation. There was no difference observed in LC3BII protein levels following EA (Figure 10). A power analysis revealed that this study achieved a power of 0.31 with its effect size and variability.

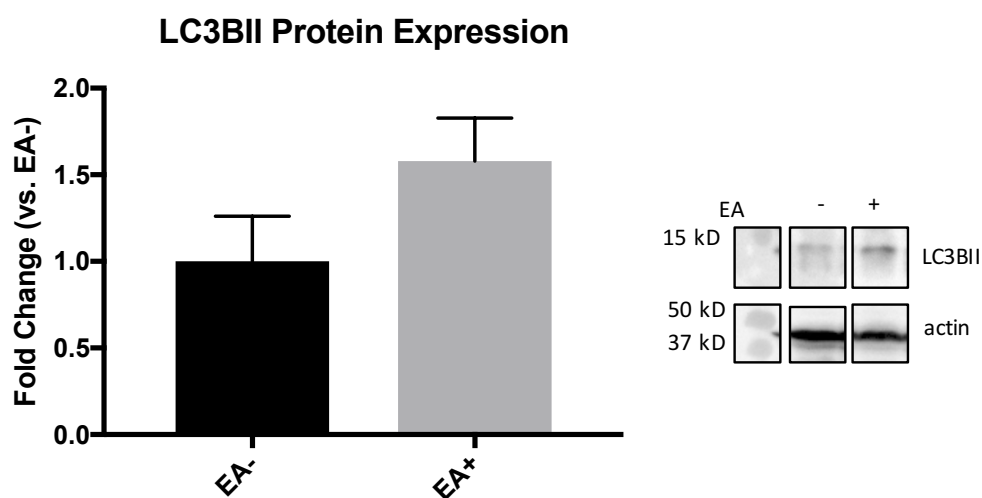


Figure 10. Evidence of Autophagosome Accumulation. Six hours following EA, anterior walls of the LVs of B6/129 mice were collected and processed by Western blotting for LC3B fold change compared to actin. An unpaired, 2-tailed Student's t-test showed no difference between groups [$t(10)=1.611$, $P=0.1383$] ($N=6$ for all groups). Mean \pm SEM.

Instead of further pursuing this, we decided to instead clarify the role of HSPs in the cardioprotective effect of electrically-induced cardioprotection. Quantitative real-time PCR was performed on cDNA from hearts of mice treated with EA, ES, or the control for each respective condition and normalized to 18s (Figure 11 A-B). Western blotting was performed on cardiac protein collected from mice 6 hours and 12 hours post-EA or ES (Figure 11 C-F).

Electroacupuncture increased the transcript levels of DNAJA1 and DNAJB1 (encoding HSP40 isoforms) and HSP90, but changes in HSP70.3 and HSP70.1 were not significant.

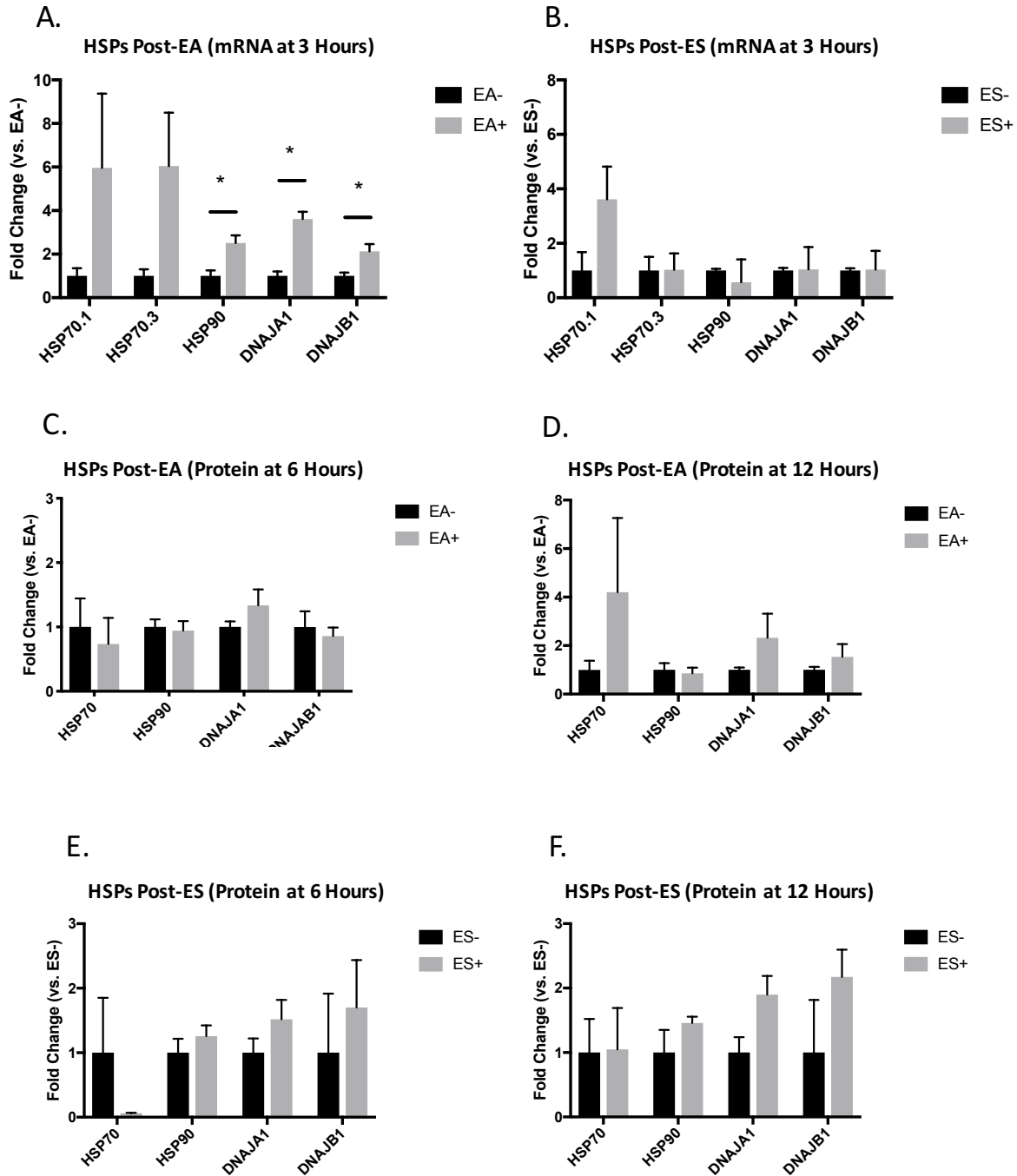


Figure 11. Panel of HSP mRNA and Protein Expression Post-EA and Post-ES. Analysis of RT-qPCR and Western blots of HSP transcripts and proteins harvested from the anterior walls of the LVs 3 (A, B), 6 (C, E), and 12 (D, F) hours after EA+ or EA- (A, C, D) or ES+ or ES- (B, E, F) in B6/129 mice. N=5 (A), N=6 (C), and N=4 (B, D, E, F). Mean \pm SEM. Unpaired, 2-tailed Student's t-tests revealed significant increases post-EA in mRNA transcripts of DNAJA1 [$t(8)=6.711$, $P=0.00015$], DNAJB1 [$t(8)=3.103$, $P=0.0146$], and HSP90 [$t(8)=3.524$, $P=0.0077$], $*P\leq 0.05$. There were no changes in any other transcripts in EA or ES on the mRNA and protein level.

The increase in protein levels of the corresponding transcripts was not significant at either 6 hours or 12 hours after EA stimulation. Taken together, these data support the hypothesis that HSP synthesis is not triggered by EA and ES and is unlikely to play a critical role in their cardioprotective effects.

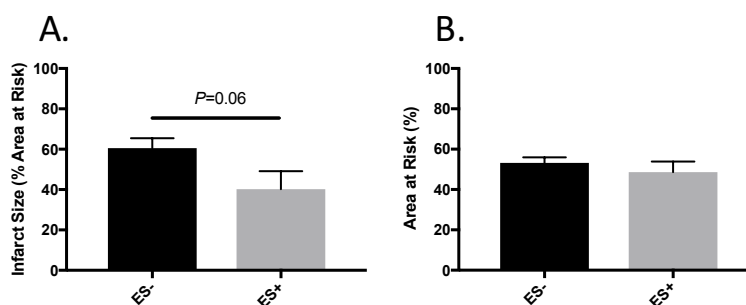


Figure 12. Late phase ES in Mice with a Genetic Deletion of HSP70.1. Quantifications of infarct size (A) and area at risk as a percent total area (B) from HSP70.1 KO mice treated with electrical stimulation via cutaneous patch 24 hours prior to I/R (N=6 and 4 for ES- and ES+, respectively). Mean \pm SEM. An unpaired, two-tailed Student's t-test revealed no significance differences between ES- and ES+ groups [$t(8)=2.202$, $P=0.0588$] and no significant difference between area at risk [$t(8)=0.8521$, $P=0.4189$].

Late Phase ES-Induced Cardioprotection Persists in Mice with Genetic and Pharmacological

Inhibition of HSP70.1

Infarct size was determined in hearts of HSP70.1 KO mice treated with ES+ or ES- 24 hours prior to MI in a small pilot study (Figure 12). Though this data is underpowered and not significant (power analysis suggests 10 mice per group to achieve significance at $\alpha=0.05$), it would not be surprising if cardioprotection persisted with HSP70.1 deletion, since it is the HSP70.3 isoform that mediates IPC. Based on our previous data that HSP70.3 is required for IPC (Tranter, Ren et al. 2010), we sought to obtain this double KO in these studies to determine functional involvement of HSP70.3 by using mice with genetic deletion of both isoforms of HSP70 (HSP70.1 and HSP70.3). However, these mice were unavailable, and we could not

employ this approach. Since we could not compare the two KOs, we did not complete this study by adding to the N.

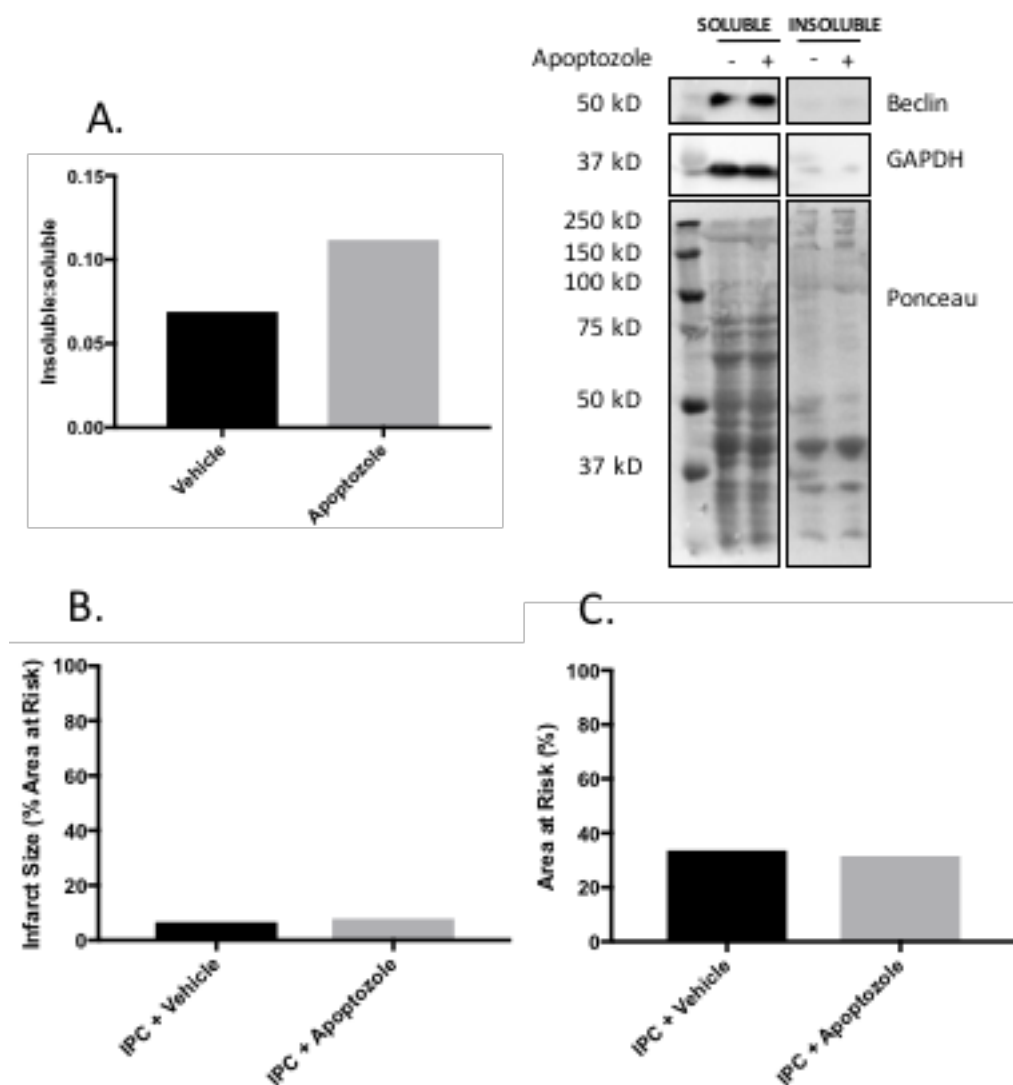


Figure 13. Western Blot of Soluble and Insoluble Beclin with the HSP70 Inhibitor Apoptozole and *In Vivo* Ability of Apoptozole to Block IPC. Western blots of soluble and insoluble fractions of protein collected from the anterior wall of a test heart LV after apoptozole i.p. injection and probed for beclin (A, N=1). Quantifications of infarcts from mice treated with apoptozole and IPC as mean infarct size (B) and mean area at risk as a percent of total area (C) (N=2 hearts per group).

We next attempted to employ the allosteric HSP70 inhibitor apoptozole. Apoptozole is reported to displace HSP70 from its substrates, resulting in aggregation of the substrates in an

insoluble fraction of an isolated protein preparation (Budina-Kolomets, Balaburski et al. 2014).

We attempted to measure the HSP70 substrate beclin in the soluble and insoluble protein fractions to validate that the drug was indeed inhibiting HSP70 as reported. We were unsatisfied with the result in a test heart, so we investigated whether apoptozole could successfully block IPC as a second measure of validating the drug's action. However, in our hands, it appeared that infarct size was not different in the pilot study of the two mice with a 10 mg/kg dose of apoptozole i.p. administered 1 hour prior to I/R (Figure 13). These studies attempting to investigate HSP70 isoforms were not pursued further in light of no positive data for heat shock response involvement.

Late Phase ES-Induced Cardioprotection Persists in Mice Treated with siRNA Against HSF1

Due to the lack of pharmacological tools available to probe the role of HSP70 in ES-induced cardioprotection, we sought to determine whether a general heat shock effect was functionally involved in electrically-induced cardioprotection. A pool of 4 siRNA targeting HSF1 was designed and a dose curve of the 4 pooled siRNA was evaluated in NIH 3T3 cells. Protein levels of HSF1 were determined 48 hours after transfection (Figure 14). Protein levels of HSF1 were reduced to 78% of control levels at the maximum concentration evaluated (Figure 14). For our *in vivo* experiment, we used a local (pericardial sac) injection of the same pooled siRNA oligonucleotide sequences, and siRNAs were further modified with cholesterol to enhance uptake and protections against endonucleases.

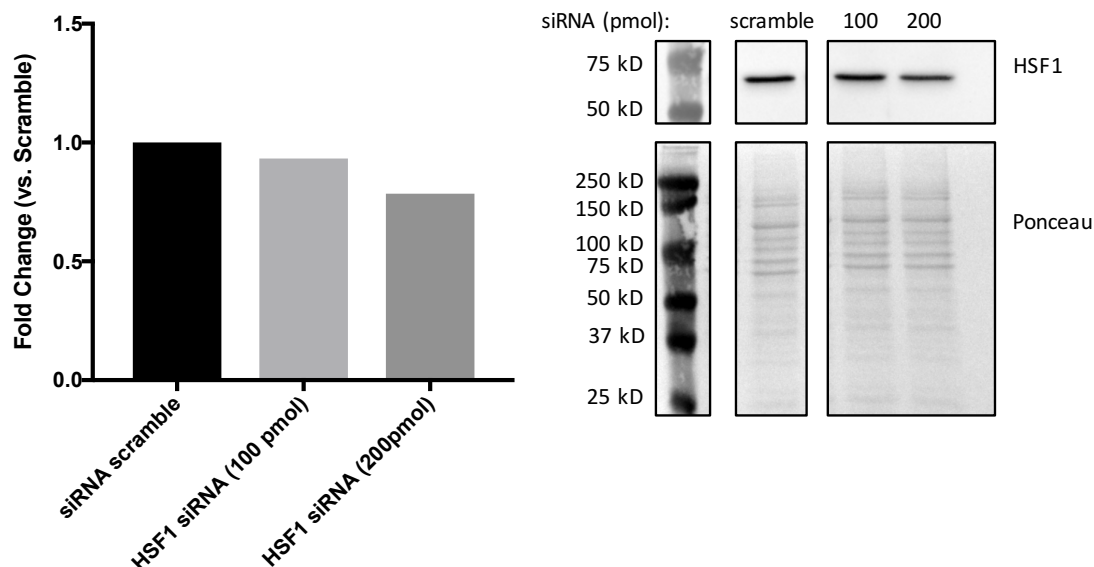


Figure 14: HSF1 siRNA Validation *in Vitro*. Quantification of Western blots of lysates collected from 3T3 cells transfected with a pool of siRNA targeting HSF1. N=1.

To deplete hearts of HSF1 *in vivo*, 1.25 μ g of pooled, modified siRNA in 40 μ L of *In Vivo*

Transfection Reagent was injected into the pericardial sac 24 hours prior to ES+ or ES- (Figure 15). A two-way ANOVA revealed no differences between groups in a pilot study (N=4).

However, there were significantly different areas at risk between groups, possibly due to sampling error and the small number of animals employed. Overall, despite repeated attempts, the pharmacological and siRNA tools available were ultimately deemed unsuitable to test our hypothesis within the limits of our resources – apoptozole did not shift beclin into the insoluble fraction or abolish IPC, so we were unable to validate that it targeted HSP70; HSF1 showed a small reduction in HSF1 *in vitro*, and there were small infarcts and no differences between groups in the *in vivo* study. Since the results of this pilot study with a low N were inconclusive, these studies were not further pursued.

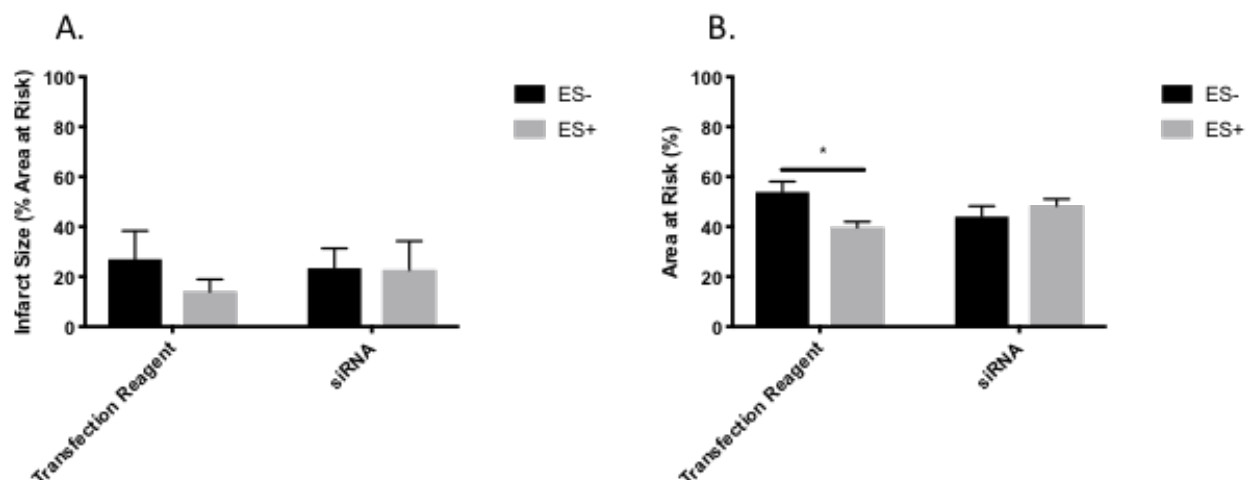


Figure 15. Late Phase ES in Mice Post-Pericardial Sac Injection of HSF1 siRNA. Infarct analysis of mice treated with HSF1 siRNA via pericardial sac injection 48 hours prior to I/R and ES+ or ES- and 24 hours prior to I/R, calculated as infarct size as a percent area at risk (A) and area at risk as a percent of the heart (B) (N=4, all groups). Mean ± SEM. There were no significant differences in the infarct area as a % area at risk. However, a 2-way ANOVA with Sidak's multiple comparisons on the area at risk revealed an interaction between siRNA and ES [$F(1, 12)=7.378$, $P=0.0187$]. *Post-hoc* analysis determined that for mice treated with the transfection reagent alone, the area at risk was smaller in the ES+ treated mice compared to the ES- mice.

NF- κ B is Involved in Late Phase ES-Induced Cardioprotection

Based on our negative findings investigating the heat shock response in ES-induced cardioprotection, we focused on the transcription factor NF- κ B and its transcriptional program in ES-induced cardioprotection. It is well-established that NF- κ B is required for IPC, so I investigated whether NF- κ B was also involved in ES-induced cardioprotection. I employed previously characterized NF- κ B dominant negative (3M) mice and assessed infarct size in ES+ versus ES- animals (Figure 16). Nontransgenic ES+ mice had smaller infarcts compared to nontransgenic ES- mice ($P \leq 0.05$), but the effect is prevented in 3M mice ($P > 0.05$), and as such indicates the involvement of NF- κ B in ES-induced cardioprotection. Areas at risk were not significantly different between groups. Data support that NF- κ B activity is required for ES-induced cardioprotection.

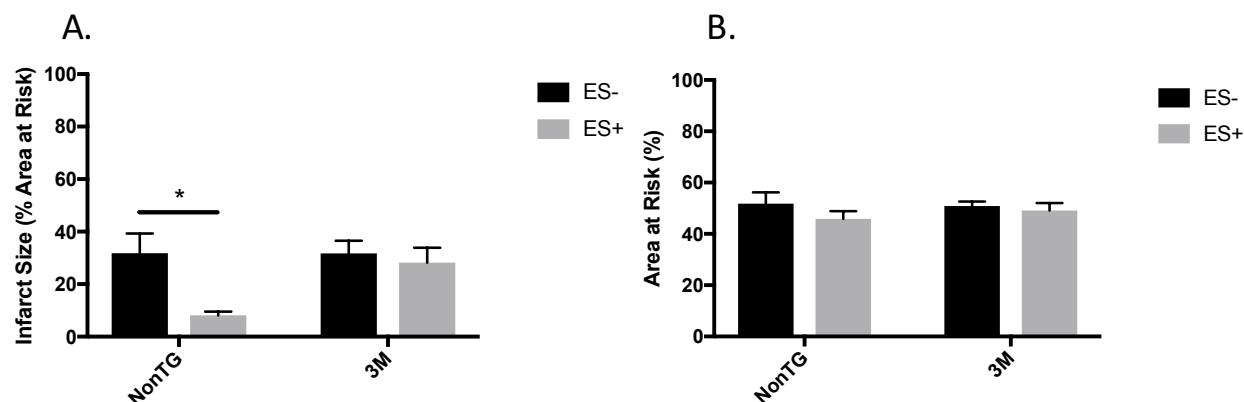


Figure 16. Late Phase ES with Genetic Inhibition of NF- κ B Using 3M Mice. Infarct analysis of 3M and nontransgenic (NonTG) mice treated with ES+ or ES- in the late phase paradigm. Calculated as infarct size as a percent area at risk (A) and area at risk as a percent of total area (B). Mean \pm SEM. N=10, 9, 16, 15 in NonTG ES-, NonTG ES+, 3M ES- and 3M ES+, respectively. A 2-way ANOVA revealed a significant main effect for ES [F (1, 46) = 5.666, P = 0.0215], and Bonferroni *post-hoc* test of multiple comparisons revealed that infarct size was lower in the NonTG mice treated with ES+ compared to the NonTG ES- mice, * P ≤ 0.05. There is no difference in infarct size between the 3M mice treated with ES- and ES- (P > 0.99).

The Unique Transcriptome of ES-Induced Cardioprotection

Based on the fact that the transcription factor NF- κ B was required for ES-induced cardioprotection, we proposed that gene expression would also be required for ES-induced cardioprotection. Next-generation sequencing was performed to assess the transcriptome of ES-induced cardioprotection. A comparison of 2 ES- and 3 ES+ animals (2X3) yielded the greatest number of differentially expressed genes for subsequent investigation. Our rationale for selecting this design was based on narrowing the samples to those that clustered together by Euclidean distance, while evaluating the widest number of differentially expressed genes for follow up. The number of samples selected for RNA-sequencing was a trade-off between cost and precision. The RNA Society Recommends at least 6 biological replicates (Schurch, Schofield et al. 2016). We chose to submit 4 samples per group to be processed, using the sequencing as a screen to identify possible targets for follow up with PCR validation. Alternative analyses

including up to 4 samples per group (4X4 and 3X3) are included in Appendix A.

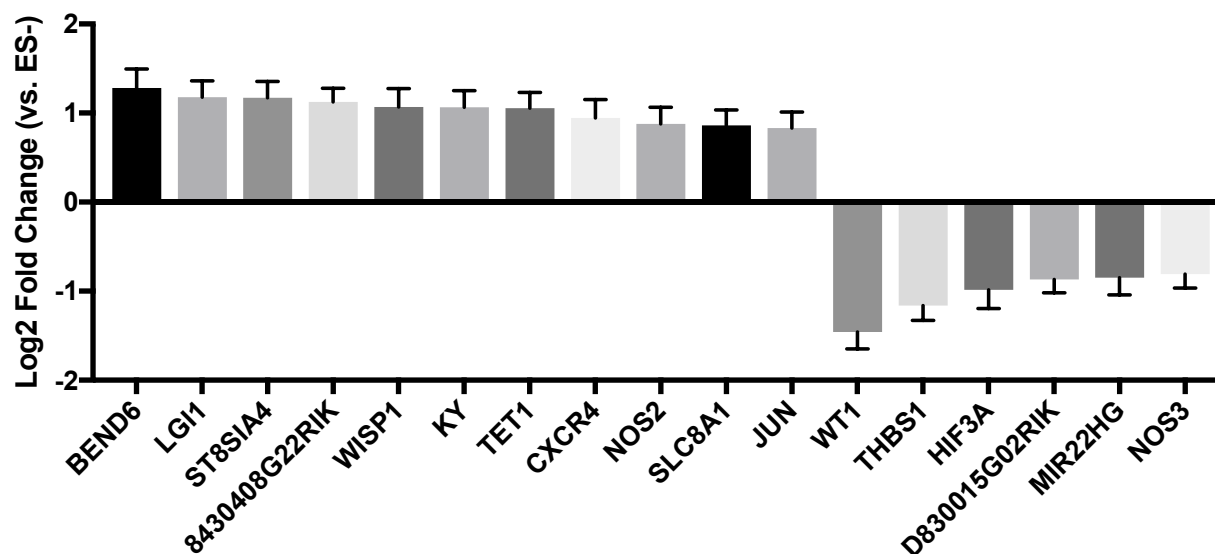
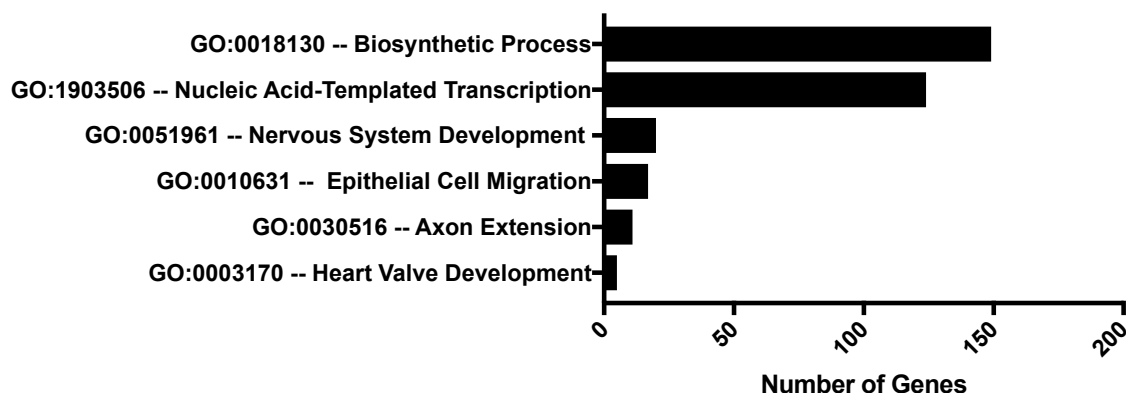


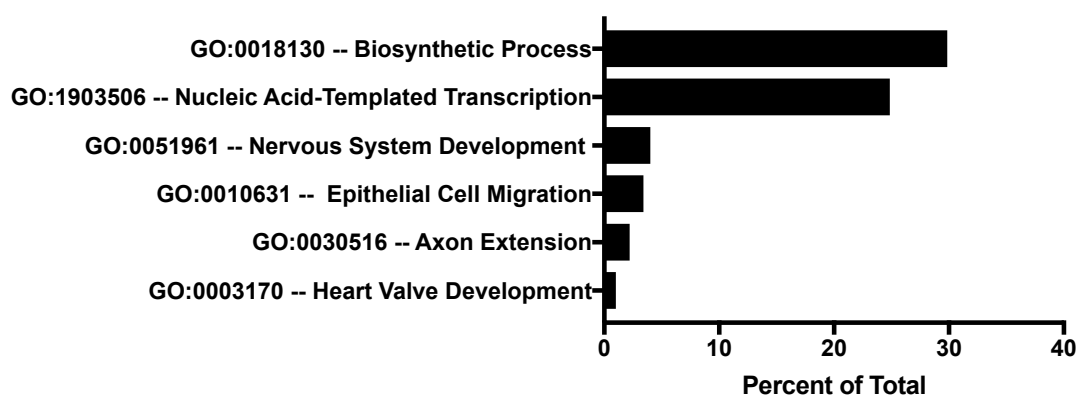
Figure 17. Selected mRNA Sequencing Results. Sequencing of LV mRNA from mice treated with ES+ or ES- (N=3,2 respectively) revealed that a total of 269 genes were significantly upregulated and 255 genes were significantly downregulated post-ES with an adjusted $P \leq 0.10$ relative to ES- (limited selection shown due to space). Log2 Fold Change \pm SEM.

A total of 524 genes were differentially expressed after ES, including 269 upregulated and 255 downregulated genes (Figure 17 and Appendix A). We observed that the average level of up or down regulation was much smaller than that of IPC. For comparison, taking the average *fold changes* of the top 20 genes in each assay, we found an average 1.5-fold change for the top 20 genes in ES, and an average 3.6-fold change for the top 20 genes after IPC calculated from previous work in our lab (Luther 2016). Our group and other's previously published studies on IPC indicate that HSP70.1 was a top upregulated gene after IPC, increasing 8.53-fold by microarray, 45-fold by RT-qPCR, and 690.7-fold by mRNA sequencing (Marber, Latchman et al. 1993, Tranter, Ren et al. 2010, Luther 2016).

A.



B.



C.

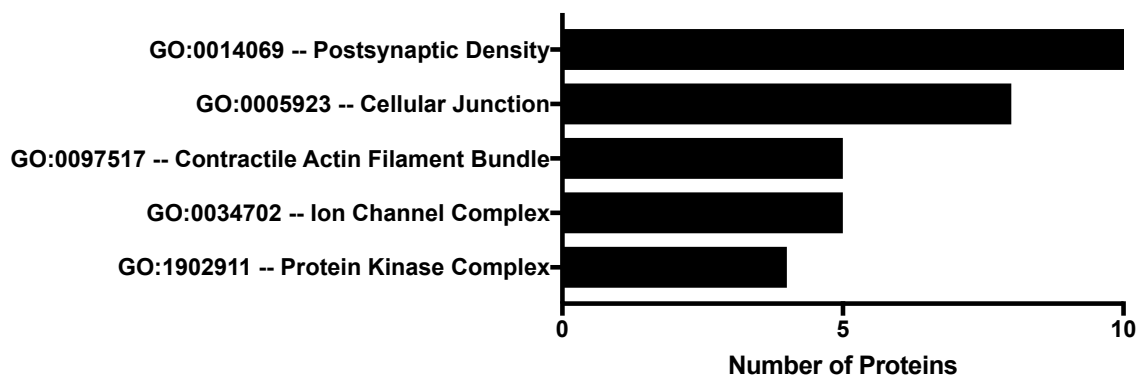


Figure 18. DAVID Gene Ontological Analysis of Sequencing Results. Functional annotation via DAVID software resulted in a significant enrichment for GO terms grouped into biological processes (A-B) and cellular components (C). A selection here is shown for space. A GO enrichment score of ≥ 1.3 was used as a cut-off for biological process groupings of gene ontologies (Huang da, Sherman et al. 2009). The complete list is shown in Appendix B.

Using the software DAVID, I assigned GO terms to the differentially expressed genes, which sorts the list into a standardized vocabulary related to known structure/function (Figure 18 and Appendix B) (Huang da, Sherman et al. 2009, Huang da, Sherman et al. 2009). The DAVID software calculates enrichment scores to measure the association between genes and the assigned GO term. The differentially expressed genes were sorted into biological process and cellular component categories.

Among the GO terms selected by the software, biosynthetic process, nucleic-acid templated transcription, nervous system development, epithelial cell migration, axon extension and heart valve development were major groupings within biological processes. These genes sorted into cellular components that associated with GO terms for post-synaptic density, cellular junctions, contractile actin filament bundles, ion channel complex, and protein kinase complex, among others. Though conclusions are somewhat subjective, the GO terms suggest that there is a nerve-heart interaction with gene induction occurring in the effect. As a precedent, a similar approach of a gene list associated with IPC by microarray identified angiogenesis, programmed cell death and heat shock response associated groupings of gene ontologies (Tranter, Ren et al. 2010).

Transcript Levels of NOS2 and KY are Increased after ES-Induced Cardioprotection

From the deep sequencing data, we discovered that the mRNA levels of the cardioprotective and neuroprotective gene *NOS2* were increased (1.84-fold change) in the hearts of mice treated with ES. *NOS2* is upregulated 2.5-3-fold after IPC, is required for IPC and is transcribed by NF- κ B (Bolli 2001, Morris, Lutz et al. 2003, Li, Labruto et al. 2004). Thus, we selected *NOS2* for follow-up. We also recognized the novel and clinically important gene *KY*

was differentially expressed (fold change of 2.09) in our deep sequencing data set, though little is known about the role of KY in cardioprotection.

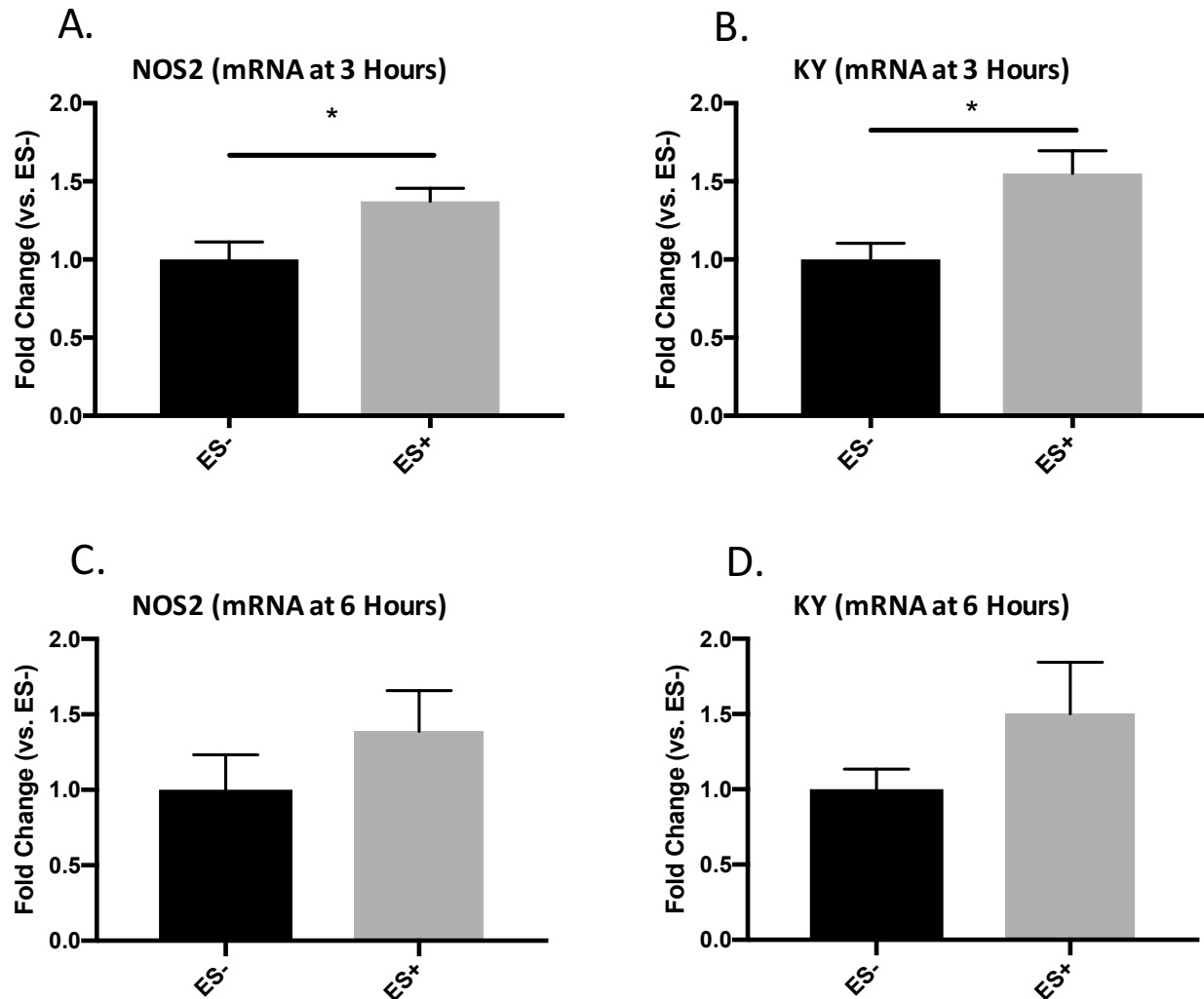


Figure 19. Transcript Validation of Deep Sequencing, NOS2 and KY. Quantifications of RT-qPCR of NOS2 (A, C) and KY (B, D) transcripts harvested from the LV anterior walls 3 hours (A-B) or 6 hours (C-D) after ES+ or ES- in B6/129 mice. Mean \pm SEM. An unpaired, 2-tailed Student's t-test revealed a significant increase in the fold change of mRNA in mice treated with ES+ for both the NOS2 [$t(14)=2.661$, $P=0.0186$] and KY [$t(14)=3.09$, $P=0.008$] transcripts at 3 hours. Differences at 6 hours were not significant. $N=8$ in both groups (3 hours) and $N=5$ ES-, 4 ES+ (6 hours). * $P\leq 0.05$.

To validate the deep sequencing results and determine whether transcript levels of genes of interest were increased following ES compared to the mice that did not receive electrical stimulation, I performed RT-qPCR analysis using primers designed to target the NOS2

and KY transcripts (Figure 19) and 18s as a control (normalized data, see Methods). Levels of KY and NOS2 transcripts were increased in mouse LV tissue 3 hours after ES. The 6 hour experiments achieved less than 30% power each with the sample size employed. The fold changes of the transcripts were similar in size and magnitude to the fold changes detected post-ES by mRNA sequencing, indicating the validity of the deep sequencing and supporting the induction of these genes as candidate mediators of electrically-induced cardioprotection. Though NOS2 is reported to be an NF- κ B dependent-gene, there is nothing in the literature that links KY to NF- κ B.

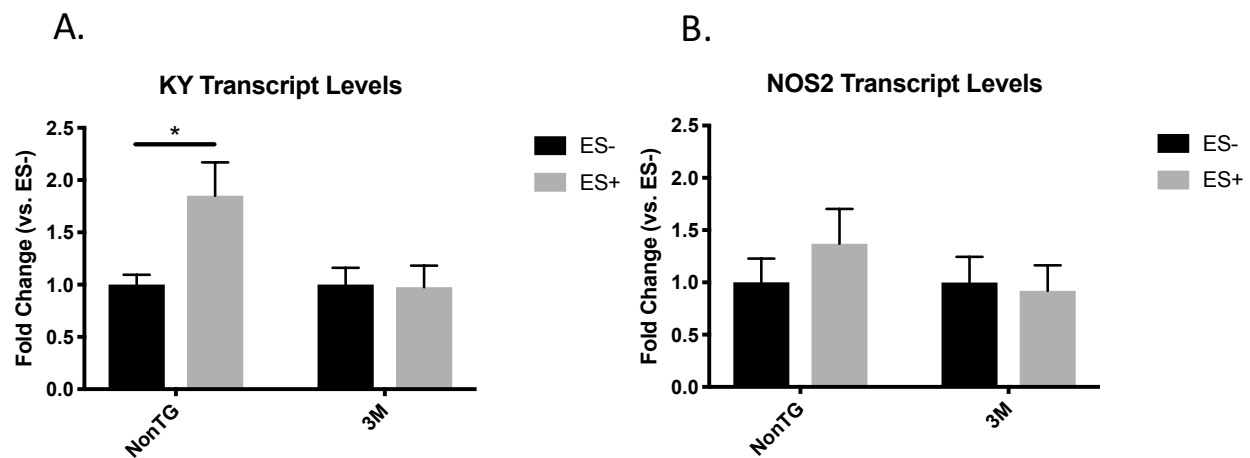


Figure 20. NF- κ B Dependent Genes. Quantifications of RT-qPCR of KY (A) and NOS2 (B) transcripts harvested from the LV anterior walls 3 hours after ES+ or ES- in 3M and NonTG littermates. A two-way ANOVA was used to assess the effect of ES and 3M status on transcript level fold change. There was no interaction for KY [$F(1, 12)=4.287$, $P=0.0606$] or NOS2 [$F(1,12)=0.7222$, $P=0.4121$], but a main effect of ES on fold change was followed up with Sidak's multiple comparison's *post-hoc* test. Infarct size was reduced in the non-TG mice treated with ES+ ($P=0.0291$) for the KY transcript only. Mean \pm SEM. N=4 for all groups. * $P\leq 0.05$.

Therefore, I investigated whether the ES-induced upregulation of KY is NF- κ B dependent. An RT-qPCR was performed on cDNA from the anterior walls of the LVs of 3M or nontransgenic mice treated with ES+ or ES-, and fold change was calculated (Figure 20). The

transcript of KY was upregulated in nontransgenic mice after ES (1.8-fold change compared to ES-, N=4, $*P \leq 0.05$). That induction was blocked in 3M mice with NF- κ B blockade in cardiomyocytes (0.98-fold change compared to ES-, N=4, $P > 0.05$). Thus, the KY transcript is NF- κ B -dependent and must either be in the cardiomyocyte or dependent upon a cardiomyocyte factor, since the 3M blockade is effective only in cardiomyocytes (Brown, McGuinness et al. 2005). We also investigated transcripts of NOS2, but there was no difference in transcript level among groups. For NOS2, the effect size and sample size were small in this pilot study (N= 4, observed power=0.12 for the interaction effect), making the NF- κ B effect difficult to discern with the time and resources available.

Protein Kinetics of KY and NOS2 after ES-Induced Cardioprotection are Elusive

To determine whether the protein levels of NOS2 and KY were increased after ES, I performed gel electrophoresis and Western blot analysis to assess protein levels of NOS2 and KY at 18 hours and 24 hours after electrical stimulation (Figure 21). After IPC, the level of NOS2 has been shown to increase 2-3-fold at 24h post-reperfusion (Wang, Guo et al. 2002). The mice treated with ES were expected to have increased levels of NOS2 and KY protein at these time points to coincide with late phase cardioprotection. Western blot analysis did not detect changes in protein levels of NOS2 and KY at either time point. We investigated whether ES may have a “priming effect,” such that increased levels of mRNA transcripts may have required a subsequent ischemic stimulus for translation (Luther 2016). However, we still saw no significant differences in protein levels for NOS2 and HSP70 6 hours after I/R ($P > 0.05$) in the late phase paradigm (Figure 21, E and F).

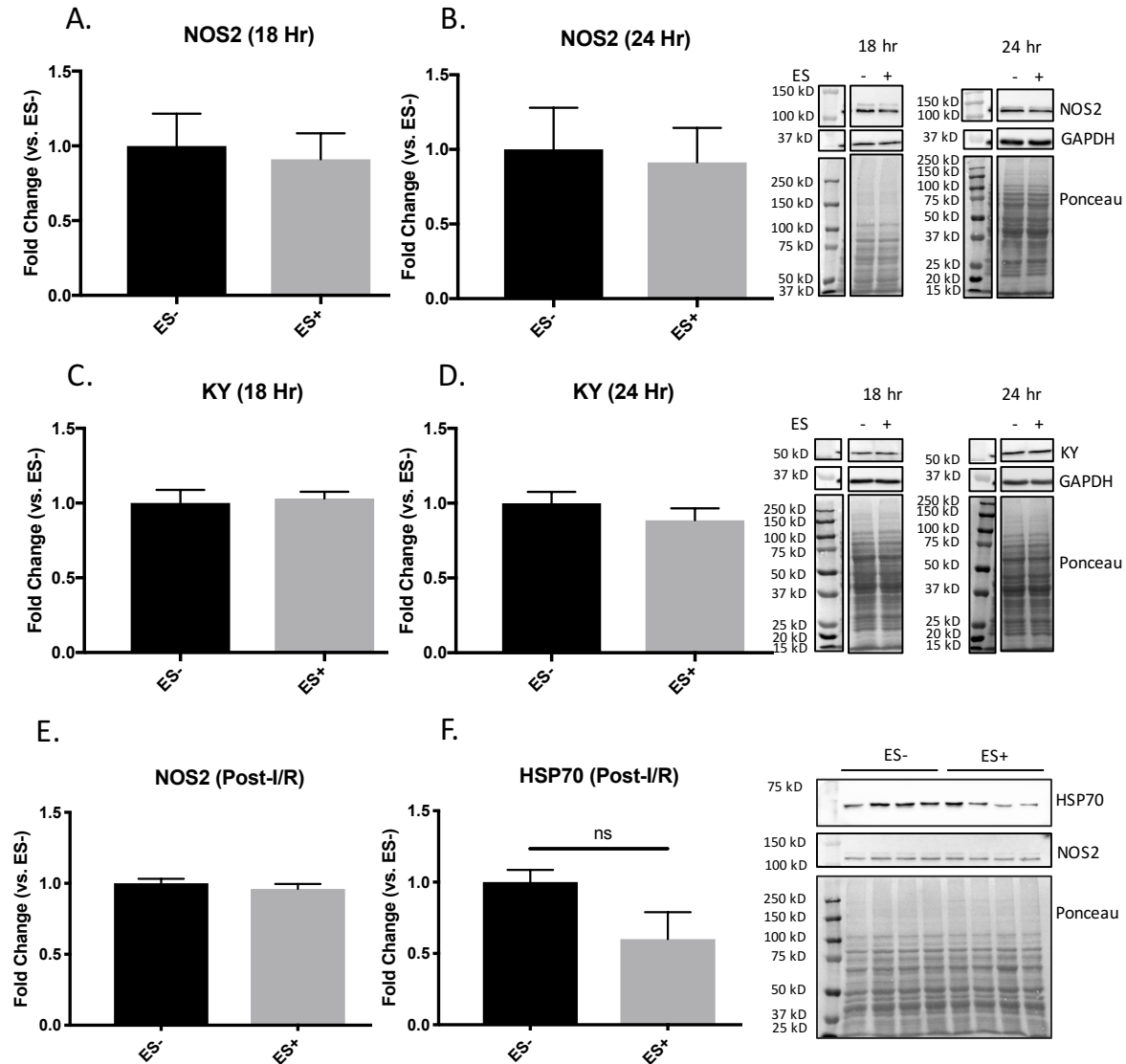


Figure 21. Protein Kinetics of NOS2 and KY. Quantifications of NOS2 (A-B) and KY (C-D) proteins harvested from the anterior walls of the LVs 18 (A, C) and 24 (B, D) hours after ES+ or ES- in B6/129 mice. Values are mean \pm SEM. An unpaired, two-tailed Student's t-test revealed no differences. N=8 (all groups, 18 hour), N=7,8 (ES- and ES+, respectively, 24 hour), and N=4 (all groups, Post-I/R). Tests were repeated with 2 technical replicates. We designed these experiments powered with a 0.8 probability of finding a significant difference ($P \leq 0.05$) if one exists in the population. We failed to find an effect of ES on protein levels at these time points.

Cardioprotection is Abolished in Mice with a Genetic Deletion of NOS2

After evidence supported that NOS2 mRNA levels were increased following ES but protein levels were not, I investigated the functional involvement of NOS2 in ES-induced

cardioprotection by assessing infarct size in mice with a genetic deletion of NOS2 (Figure 22).

We compared these data to both B6/129 and C57 control mice. No significant difference in area at risk was detected after ES+ or ES- in NOS2 KO mice.

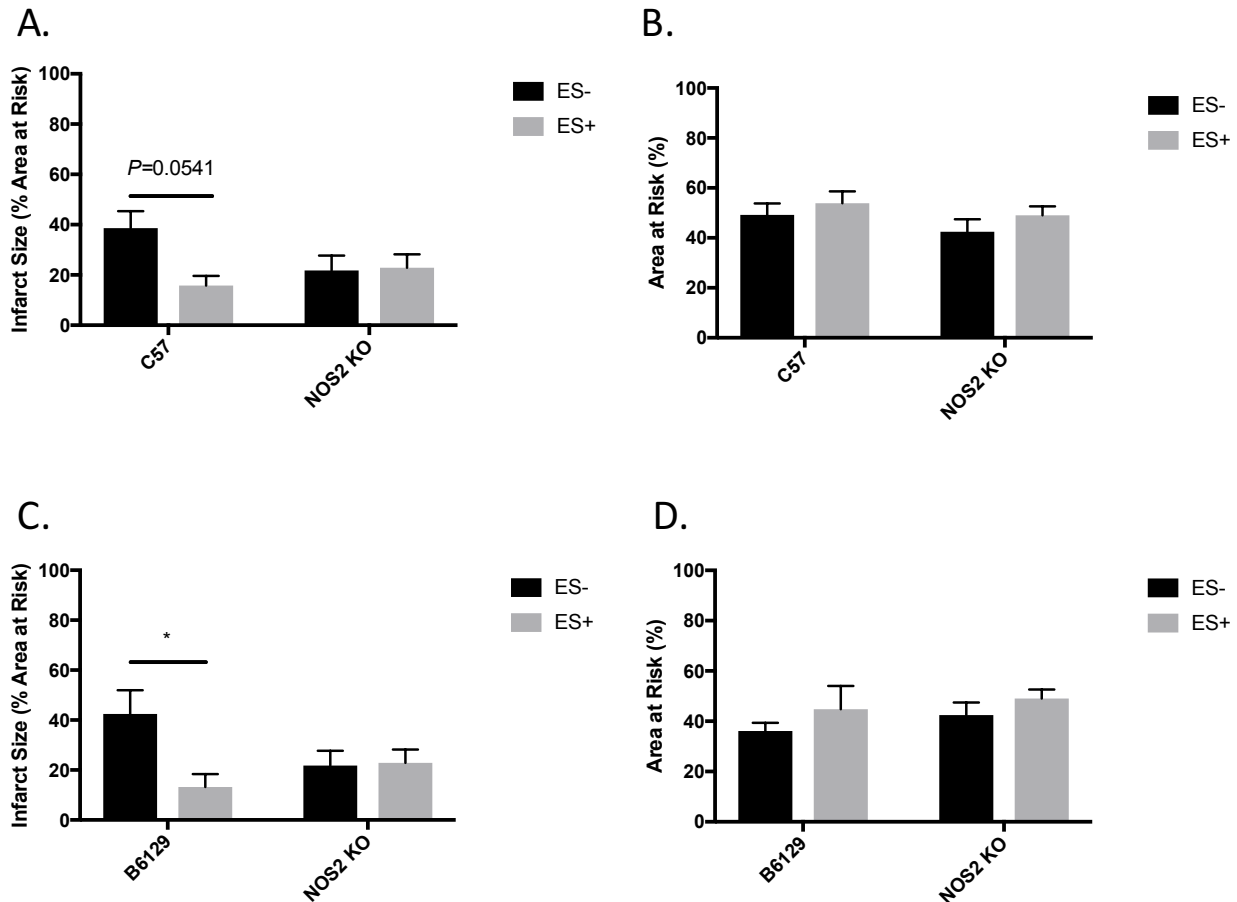


Figure 22. Late Phase ES in Mice with a Genetic Deletion of NOS2. Quantifications of infarct size (A, C) and area at risk (B,D) from NOS2 KO mice treated with ES via cutaneous patch 24 hours prior to I/R. Tests were run with both C57 controls (A-B, N=5, 6, 8, 12) and B6/129 controls (C-D, N=4, 5, 8, 12). * $P \leq 0.05$ compared to ES-. A two-way ANOVA was used to assess the effect of ES and KO status on infarct size. There was no significant interaction for the C57 mice [$F(1, 27)=3.839$, $P=0.0605$], and the effect of ES was followed up with Bonferroni's multiple comparisons *post-hoc* test ($P=0.0541$). There was a significant interaction for ES in the B6/129 mice [$F(1,25)=4.796$, $P=0.0381$, and a Bonferroni multiple comparisons *post-hoc* test revealed that ES+ reduced the infarct size in B6/129 control mice $P=0.0342$ Mean \pm SEM. The C57 studies appear to be underpowered (power=0.472 for the interaction effect).

There was no significant difference in the normalized infarct size in hearts of NOS2 KO mice

treated with ES+ vs. ES- ($P>0.05$, Figure 22), despite a borderline significant or significant decrease in infarct size with ES in control C57 and B6/129 mice ($P\leq 0.05$). These data demonstrate that NOS2 is required for the late phase of electrically-induced cardioprotection.

Potential c-Jun Activation after ES-Induced Cardioprotection

In addition to *NOS2* and *KY*, we recognized that *JUN* (encoding c-Jun) was differentially expressed (1.78-fold change) in the deep sequencing data set, and decided to follow up on this gene because of its involvement in IPC (Brand, Sharma et al. 1992, Li, Ping et al. 2000).

Generally, c-Jun is thought of as an immediate early gene and a marker of neuronal activation when rapidly expressed in neurons following stimulation. However, c-Jun can also dimerize with c-Fos to form the transcription factor AP-1, which can coordinate with NF- κ B to upregulate target genes, including its own (Angel, Hattori et al. 1988). The role of c-Jun in the cardioprotective effects of ES has not so far been examined. To further validate the deep sequencing results, PCR was performed using primers designed to target the c-Jun transcript (Figure 23 A-B). Levels of c-Jun transcripts were significantly increased in mouse LV anterior wall tissue 6 hours after ES.

To determine whether c-Jun was activated and translocated into the nucleus and whether protein levels of c-Jun were increased after ES, nuclear and cytoplasmic fractions were extracted 30 minutes after ES+ or ES- to assess translocation, and total protein was extracted from mouse left ventricle 18 hours and 24 hours after ES+ or ES- to assess c-Jun expression (Figure 23 C-E, N=4). Based on this pilot study, a power analysis predicted that over N=20 would be needed to achieve significance ($P\leq 0.05$) at a 0.80 power level with this effect size.

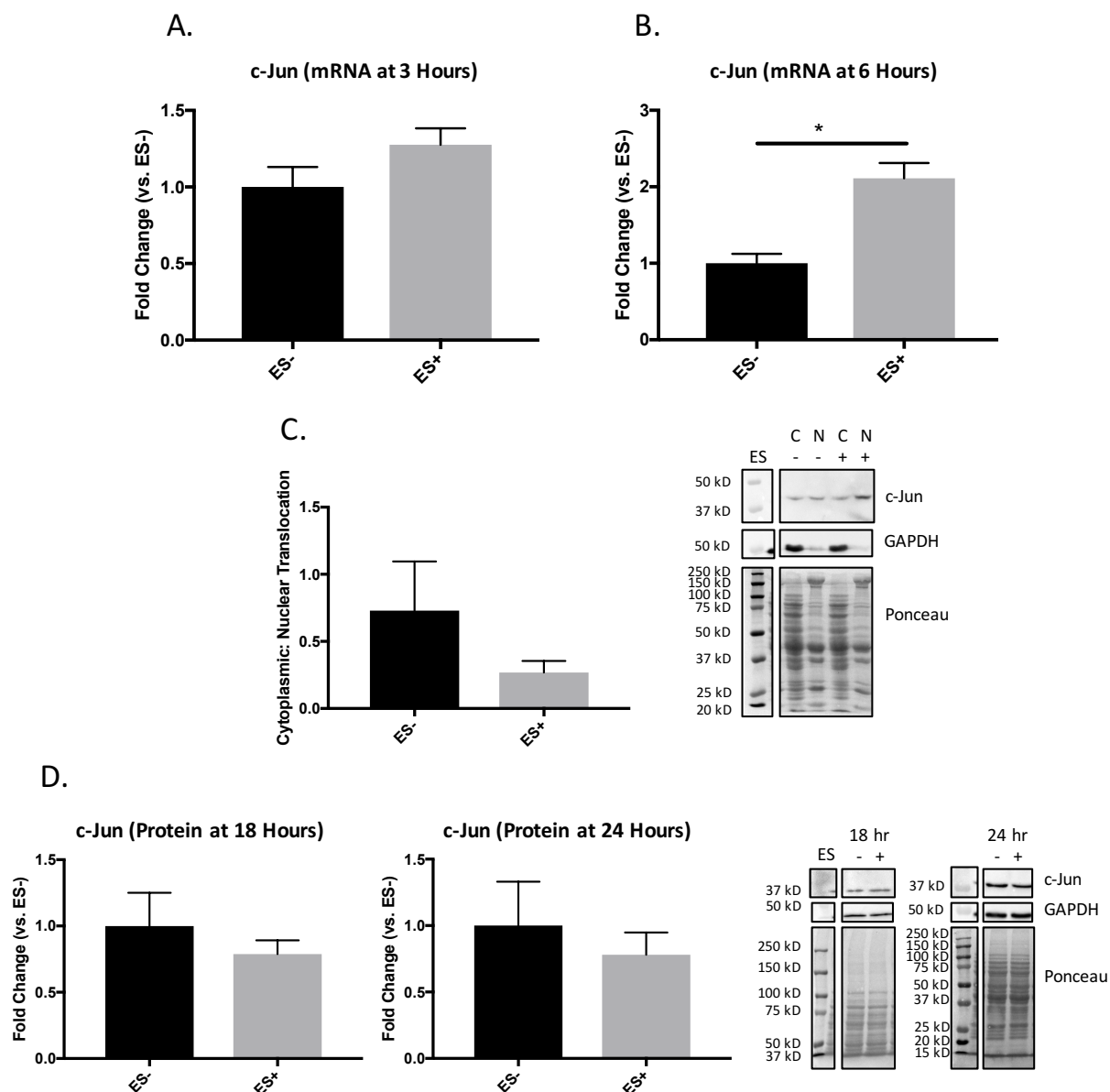


Figure 23. Transcript Validation of c-Jun, Nuclear Translocation, and Protein Kinetics. Analysis of RT-qPCRs of c-Jun transcripts harvested from the anterior walls of LVs 3 hours (A, N=8, both groups) and 6 hours (B, N=5, 4 for ES-, ES+, respectively) after ES- or ES+ in B6/129 mice. Western blot of protein lysates from cytoplasmic and nuclear fractions of mouse hearts collected 30 minutes post-ES (C), N=4, both groups. Western blot of c-Jun protein lysates collected 18 hours (N=8, 7 for ES-, ES+, respectively) and 24 hours (N=7, 8 for ES-, ES+, respectively) post-ES- or ES+ (D), mean \pm SEM. An unpaired, two-tailed Student's t-test revealed an increase in c-Jun transcript levels at 6 hours post-ES [$t(7)=4.948$, $P=0.0017$]. * $P \leq 0.05$.

To determine whether c-Jun might also be functionally involved in ES-induced cardioprotection, SP600125, a pharmacological inhibitor of JNK, was employed *in vivo* at a dose

reported to block JNK in the heart, 30 mg/kg i.p., to inhibit the activation of c-Jun (Figure 24) (Wei, Wang et al. 2011). There was a significant reduction of infarct size between ES- mice treated with vehicle and SP600125. This result was not entirely unexpected, since JNK inhibition is known to be both injurious and cardioprotective after I/R injury. We concluded that JNK inhibition is protective on its own against I/R. As such, this small molecule inhibitor is not an appropriate tool to probe the role of c-Jun in ES-induced cardioprotection. Mice with a genetic deletion of c-Jun or JNK are not available.

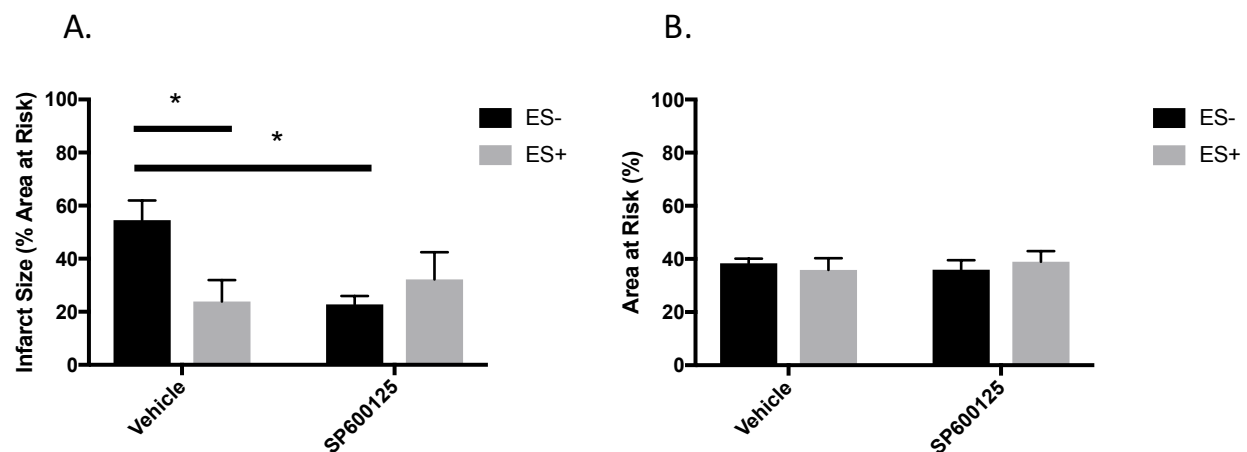


Figure 24. Pharmacological Inhibition of c-Jun Using SP600125 is Unable to Probe Effect. Mice were treated with SP600125 or vehicle at 30 mg/kg ip 30 minutes prior to I/R. Infarct size (A) and area at risk (B) were calculated. N=5 (vehicle ES-, vehicle ES+, SP600125 ES-) and 4 (SP600125 ES+). A two-way ANOVA revealed an interaction between ES treatment and SP600125 treatment [$F(1, 15)=7.343$, $P=0.0161$] on infarct size. Tukey's *post-hoc* analysis revealed significant reduction in infarct size in mice treated with ES+ compared to ES- in the vehicle condition ($P=0.0384$), as well as a reduction in infarct size in mice treated with SP600125 in the absence of ES ($P=0.031$). * $P\leq 0.05$. There were no significant differences in area at risk.

NF- κ B Dependent Genes After ES

We performed next-generation sequencing of mRNA harvested from nontransgenic mice 3 hours after treatment with ES+ to further our previous work that established a profile of genes that were differentially expressed (Figure 25).

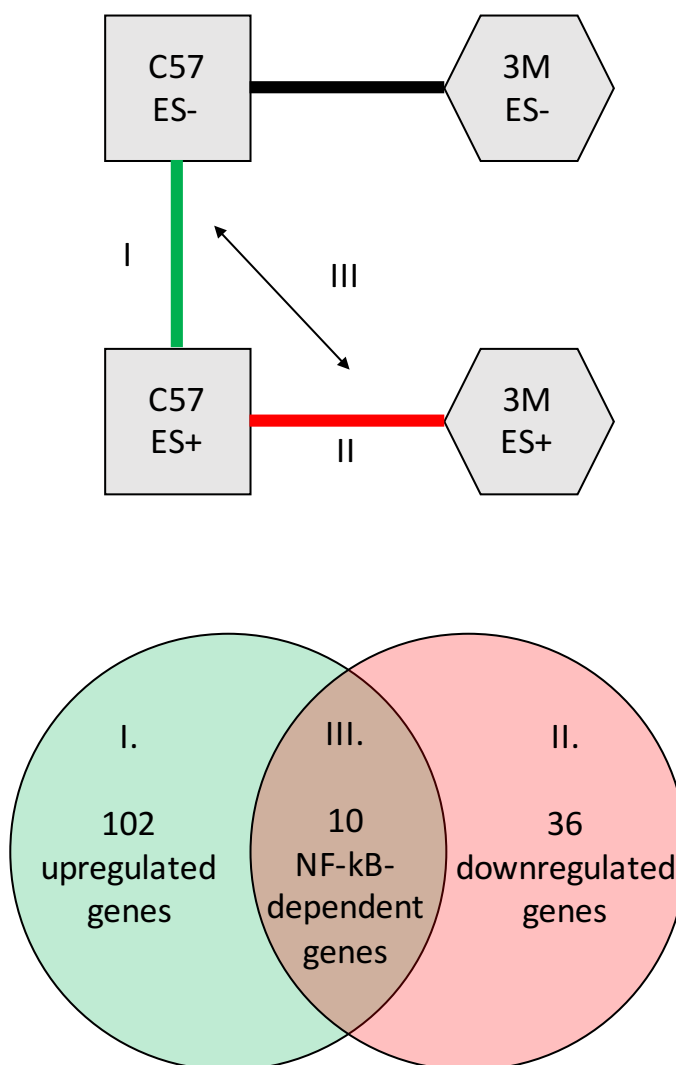


Figure 25. Schematic of Hypothesis-Driven Sequencing of NF-κB-Dependent Genes. Two different next-generation sequencing comparisons were made as represented by the colored lines in Figure 25A. Comparison I, green, is nontransgenic C57 ES- vs. nontransgenic C57 ES+. Comparison II, red, is nontransgenic C57 ES+ vs 3M ES+, and comparison III identifies genes that are common between I and II. The Venn diagram in Figure 25B represents the number of significantly dysregulated genes between C57 ES- and C57 ES+ mice (green circle) and C57 ES+ and 3M ES+ mice (red circle). The 10 genes represented by the overlap (comparison III) are genes whose expression post-ES requires NF-κB. N=4, all groups.

As before, mRNA was collected 3 hours after ES+. A total of 152 genes were differentially expressed in the nontransgenic mice, with 112 upregulated and 40 downregulated genes after ES+ (Appendix C). A selection of genes that are significant ($P \leq 0.05$) and showed a high fold change (>1.2 or <-0.8 -fold change) and a high base mean (the mean of the normalized counts

for all samples (>100)), are presented in Figure 26, while the entire table is included in Appendix C (up to $P < 0.10$).

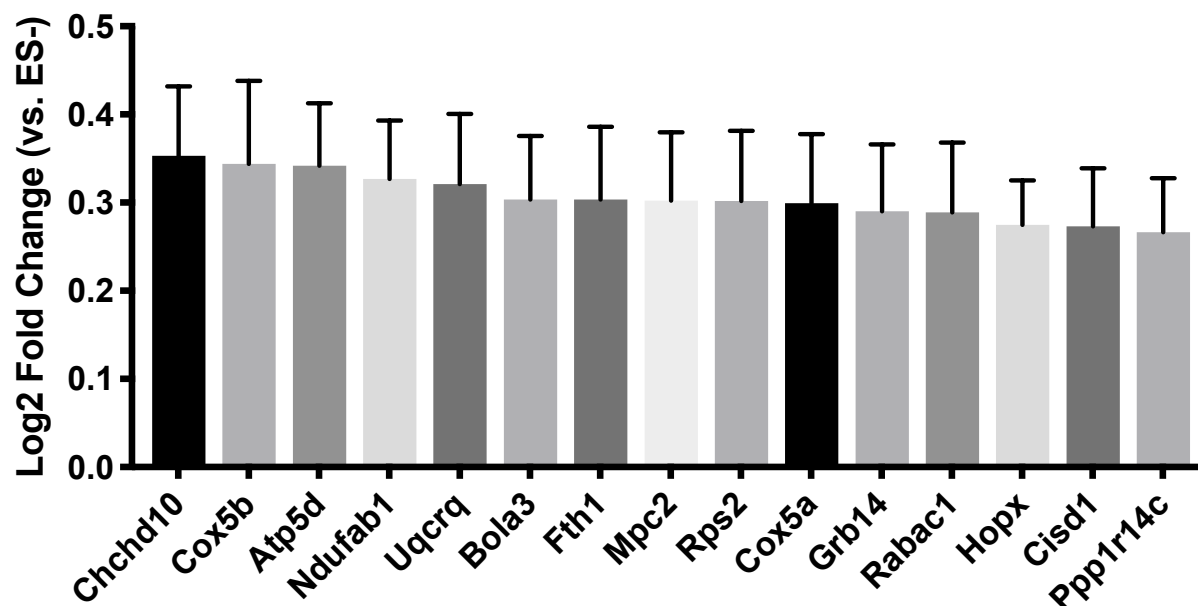


Figure 26. Selected Nontransgenic mRNA Sequencing Results. Sequencing of LV mRNA from mice treated with ES+ revealed that a total of 152 total genes were differentially expressed after ES in the nontransgenic mice, with 112 upregulated and 40 downregulated genes after ES+ with an adjusted $P \leq 0.10$ included in the table in Appendix C ($N=4$, both groups). Selection shown here due to space; all shown here have $P \leq 0.05$ relative to ES-. Log2 Fold Change \pm SEM.

Many of the top upregulated genes in this experiment are involved in oxidative phosphorylation and the mitochondrial respiratory chain, including NADH dehydrogenase/complex I (Ndufb8 and Ndufv2), ubiquinol-cytochrome c reductase/complex III (Uqcc2 and Uqcrcq), cytochrome c oxidase/complex IV (Coa6, Cox5a, and Cox5b), and ATP synthase/complex V (Atp5g3, Atp5d, Atp5c1) (Figure 27). In MI, there is a global metabolic shift from oxidative phosphorylation to glycolysis during hypoxia, and ultimately the mitochondrial permeability pore transition and cell death. Findings that ES+ enhanced transcription of these mitochondrial proteins prior to I/R suggests that these proteins might help prevent cell death.

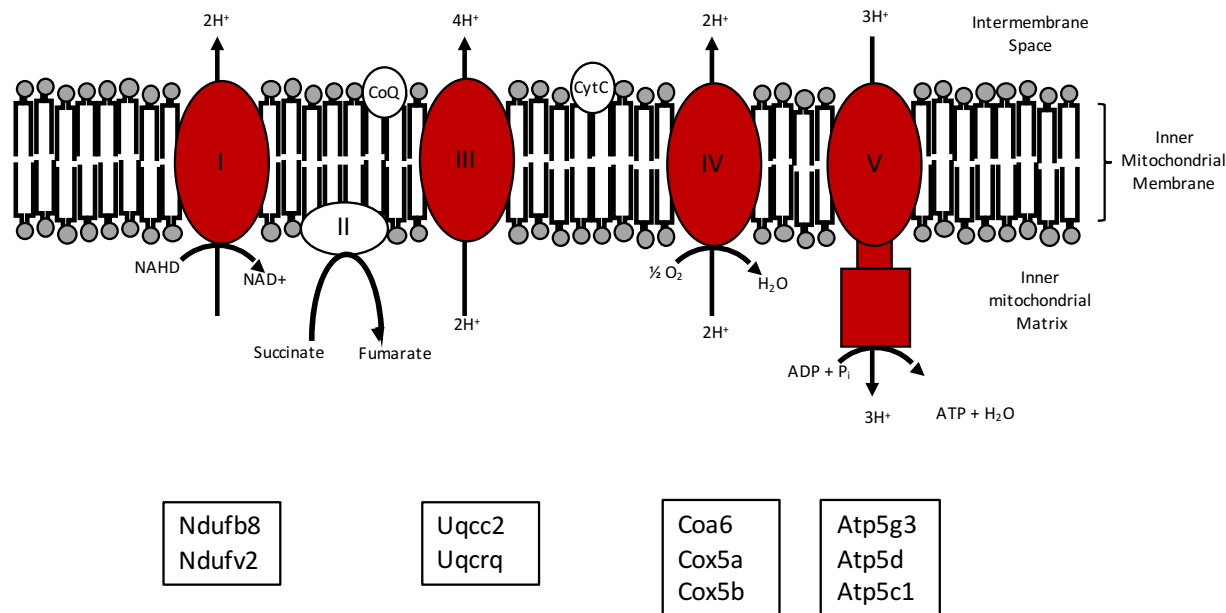


Figure 27. Sequencing Schematic of ETC Results from Sequencing. Many of the top upregulated genes in this sequencing experiment are involved in oxidative phosphorylation and the mitochondrial respiratory chain, including NADH dehydrogenase/ complex I (Ndufb8 and Ndufv2), and ubiquinol-cytochrome c reductase/ complex III (Uqcc2 and Uqcrq), cytochrome c oxidase/ complex IV (Coa6, Cox5a, and Cox5b, and ATP synthase/ complex V (Atp5g3, Atp5d, Atp5c1).

A comparison of differentially expressed genes revealed by our first next-generation sequencing experiment in B6/129 mice and the second sequencing experiment with nontransgenic mice on a C57 background offered little agreement on the identity of differentially expressed genes or the magnitude and direction of changes (Table 4). Though we expected that these gene lists would be similar, a comparison of the fold changes detected in both assays revealed only 6 genes in common. *NOS2*, *KY*, and *JUN* (encoding c-Jun), which were upregulated in B6/129 mice, were not upregulated in the C57 background mice. The discrepancy may be due to the low magnitude change overall or strain-specificity (Guo, Flaherty et al. 2012).

Next-generation sequencing identified the genes in the setting of ES that were changed

between the 3M and nontransgenic mice (Appendix C). A comparison of the genes whose post-ES upregulation was blocked by the inhibition of NF- κ B revealed 10 genes that were NF- κ B dependent in ES (Figure 28). This reveals the genes which are no longer upregulated in the absence of NF- κ B. Three of the 10 were annotated “Rik” genes from the Riken mouse genome encyclopedia project with no canonical name (Hayashizaki 2003). The list also included the transcription factors NR2F6 and Nkx2-5, the gene-coding proteins Tsc22d4 and Hopx, the cell cycle protein Gadd45gip1 and mitochondrial protein chchd10. The notion that these genes may play a role in cardioprotection is novel and provides a potential avenue for exploration.

Gene	C57 Fold Change	B6/129 Fold Change
<i>Irx3</i>	1.26	1.50
<i>Prob1</i>	1.24	1.45
<i>2310002L09Rik</i>	1.21	0.73
<i>mt-Nd1</i>	1.19	0.78
<i>Ggta1</i>	0.79	1.66
<i>Vwa3a</i>	0.79	0.63

Table 4. Comparison of Strain-Specific Next-Generation Sequencing Results. Next-generation sequencing was performed on mRNA collected from B6/129 and nontransgenic (C57 background) mouse hearts following treatment with or without ES. Fold change was calculated between ES- and ES+ conditions. This table compares the results between the two independent sequencing studies for genes that were revealed to be changed post-ES+ in C57 mice (the 3M nontransgenic littermates) and B6/129 mice. Few genes agree in magnitude or direction of expression.

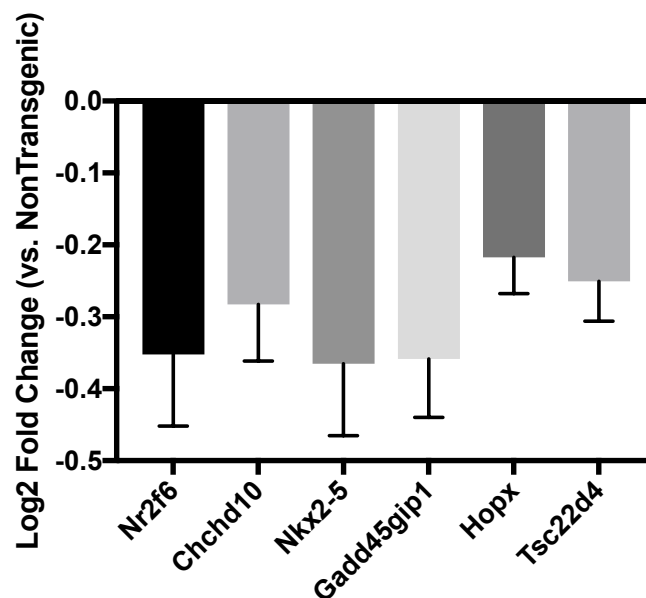


Figure 28. Selected NF- κ B-Dependent mRNA Sequencing Results. Sequencing of LV mRNA from mice treated with ES+ revealed that a total of 72 total genes were differentially expressed in the 3M mice compared to the nontransgenic mice, with 26 upregulated and 46 downregulated genes after ES+ with a $P \leq 0.10$ (complete list in Appendix C; N=4, both groups). These differentially expressed genes were cross-referenced against those genes that were differentially expressed after ES+ in nontransgenic mice to reveal the NF- κ B-dependent genes. These genes obtained from sequencing were considered candidates for validation and follow-up studies, and a selection is presented here (Rik genes excluded due to space). Log2 Fold Change \pm SEM, all shown here are $P \leq 0.10$.

The Transcriptome Following IPC Differs from That Following ES

Previous work in our lab has established a profile of genes differentially expressed after IPC by next-generation sequencing and bioinformatics analysis of the mRNA of IPC and control heart tissues collected 3 hours after IPC in a pilot study (N=2) (Luther 2016). Table 5 is a comparison of the fold changes detected after IPC (fold change IPC) and the fold changes detected after ES (fold change ES), presenting genes differentially expressed in both assays (Luther 2016). The major HSPs differentially expressed after IPC by next-generation sequencing in this dataset included *HSPA1B*/HSP70.1 (690-fold change), *HSPA1B*/HSP70.3 (541.6-fold change) *HSP90AA1*/HSP90 (9.1-fold change), and *DNAJA1*/HSP40 (7.1-fold change).

Gene Symbol	Gene Name	Fold Change (IPC)	Fold Change (ES)
<i>Akap12</i>	A kinase (PRKA) anchor protein (gravin) 12	3.07	0.60
<i>Arid5b</i>	AT rich interactive domain 5B (MRF1-like)	2.58	1.44
<i>Ccdc14</i>	coiled-coil domain containing 14	0.43	1.52
<i>Egr1</i>	early growth response 1	2.43	0.61
<i>Fam110b</i>	family with sequence similarity 110, member B	2.61	1.54
<i>Hif3a</i>	hypoxia inducible factor 3, alpha subunit	0.43	0.51
<i>Icosl</i>	icos ligand	2.33	0.73
<i>Kdm6b</i>	KDM1 lysine (K)-specific demethylase 6B	1.84	0.66
<i>Klf6</i>	Kruppel-like factor 6	1.94	1.62
<i>KY</i>	kyphoscoliosis peptidase	0.42	2.09
<i>Litaf</i>	LPS-induced TN factor	2.11	0.59
<i>Maff</i>	v-maf musculoaponeurotic fibrosarcoma oncogene family, protein F (avian)	3.01	0.55
<i>Nt5e</i>	5' nucleotidase, ecto	2.55	0.63
<i>Ppara</i>	peroxisome proliferator activated receptor alpha	0.57	1.39
<i>Ppp1r18</i>	protein phosphatase 1, regulatory subunit 18	2.14	0.65
<i>Rassf1</i>	Ras association (RalGDS/AF-6) domain family member 1	2.39	0.61
<i>Sat1</i>	spermidine/spermine N1-acetyl transferase 1	1.93	0.70
<i>Socs3</i>	suppressor of cytokine signaling 3	2.33	0.61
<i>Thbs1</i>	thrombospondin 1	10.13	0.45
<i>Zfp420</i>	zinc finger protein 420	0.47	1.77
<i>Zfp948</i>	zinc finger protein 948	2.75	0.67

Table 5. Comparison of ES and IPC. Next-generation sequencing was performed on mRNA collected from B6/129 mouse hearts following treatment with ES- or ES+ (N=4, both groups) and data was compared to historic data performed on mRNA collected from mouse hearts following treatment with IPC (N=2, both groups). Fold change was calculated compared to ES- or IPC-. Few genes agree in magnitude or direction of expression.

These HSPs were not detected in the post-ES next-generation sequencing data set. In

general, the two datasets do not agree with fold change magnitude or direction, indicating that the molecular mechanisms of these mediators might be substantially different between stimuli. *HIF3α* is among those genes that agree in both assays. Neither *NOS2* and *JUN* (encoding c-Jun) are not found in the list of genes differentially expressed after IPC in this sequencing assay.

microRNA is Differentially Expressed after ES

Considering the widely recognized understanding that microRNAs can function as regulatory nodes in diverse signaling networks, I identified the microRNA that were changed following ES. To this end, total microRNA was extracted from the left ventricles of B6/129 mice treated with ES+ or ES- (N=3/group). The profile of microRNAs in Table 6 and Figure 29 (and Appendix D) reveals the differential expression following electrical stimulation. Only one microRNA (miR-10b-5p) was significantly changed ($P \leq 0.10$) after performing the statistical analysis corrected for multiple comparisons. Little is known about miR-10b-5p in the context of cardioprotection, but elevated levels of circulating miR-10b-5p are found in hypertrophic cardiomyopathy patients with myocardial fibrosis, possibly caused by its upregulation in stressed myocardium or endothelial cells (McCall, Kent et al. 2011, Fang, Ellims et al. 2015). Furthermore, the role of miR-10b-5p and its targets, including brain derived neurotropic factor (BDNF), a secreted protein that contributes to nervous system survival, and α -synuclein, have been explored in the neuroscience space as a diagnostic tool for early stage Parkinson's disease and Huntington's Disease pathogenicity (Muller 2014, Hoss, Labadorf et al. 2015, Dos Santos, Barreto-Sanz et al. 2018).

For exploratory pathway analysis, this list was expanded to include the 13 microRNA that were highly significant *without* correcting for multiple comparisons (up to $P \leq 0.05$). These

13 microRNA differentially expressed post-ES+ are presented in Table 6 and Figure 29 (up to $P \leq 0.05$; up to $P \leq 0.10$ are included in Appendix D).

microRNA	Base Mean	Log ₂ Fold Change	Fold Change	SE	p-value	p-adj
mmu-miR-10b-5p	1007.14	-1.11	0.46	0.24	0.00	0.00
mmu-let-7b-5p	2496.04	-0.79	0.58	0.23	0.00	0.16
mmu-let-7c-5p	10023.39	-0.66	0.63	0.22	0.00	0.69
mmu-miR-379-5p	80.36	-0.58	0.67	0.28	0.04	0.98
mmu-miR-10a-5p	1517.10	-0.57	0.68	0.24	0.02	0.98
mmu-miR-218-5p	90.81	-0.56	0.68	0.27	0.04	0.98
mmu-miR-423-5p	195.49	-0.54	0.69	0.25	0.03	0.98
mmu-let-7e-5p	612.65	-0.52	0.70	0.23	0.02	0.98
mmu-let-7a-5p	13927.07	-0.46	0.73	0.22	0.04	0.98
mmu-miR-28a-5p	310.58	-0.45	0.73	0.21	0.04	0.98
mmu-miR-378c	538.08	0.48	1.39	0.24	0.05	0.98
mmu-miR-1291	13.42	0.60	1.51	0.30	0.05	0.98
mmu-miR-6236	5.95	0.72	1.65	0.28	0.01	0.98

Table 6. microRNA Sequencing Results. Next-generation sequencing was performed on microRNA collected from B6/129 mouse hearts following treatment with ES+ or ES- (N=3, both groups). $P \leq 0.05$ shown here. Appendix D contains the complete table up to $P \leq 0.10$ (no multiple adjustments).

All 13 microRNAs were sorted by GO term and KEGG pathways using the miRBase software (Figure 30, complete list in Appendix D). It was discovered that these genes clustered into endocytosis, neurotrophin signaling pathway, axon guidance, HIF-1 signaling, cell cycle, and NF- κ B signaling pathways. The list of microRNAs sorted into GO term categories for response to stress, cell cycle, cell death, endosome, and growth.

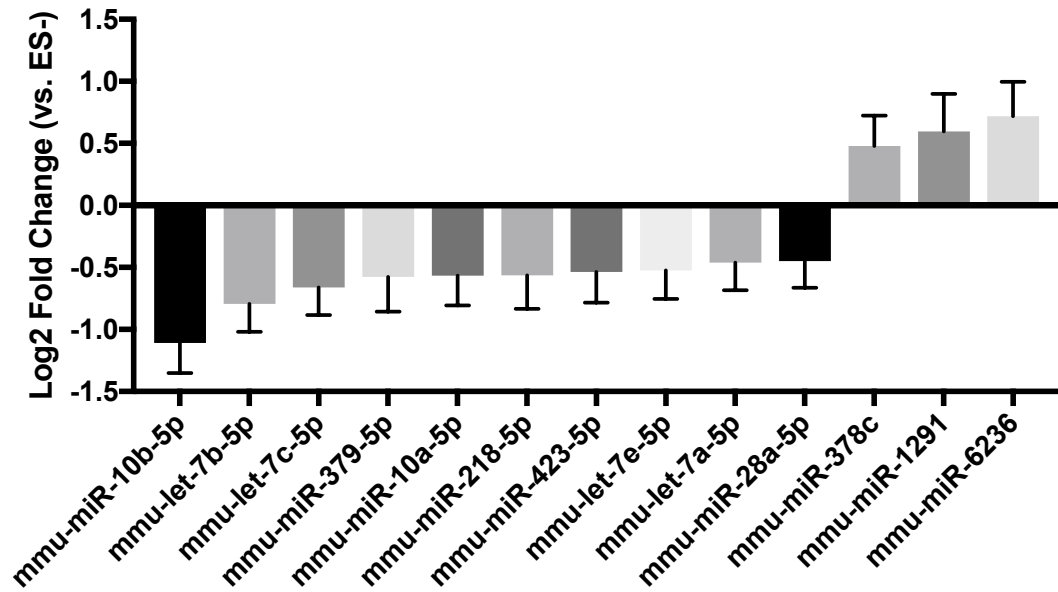


Figure 29. microRNA Sequencing Results. Sequencing of LV microRNA from mice treated with ES+ or ES- (N=3) revealed that a total of 13 total microRNA were differentially expressed in the ES+ mice compared to the ES- mice, with 3 upregulated and 10 downregulated microRNA after ES+ with $P \leq 0.05$ (not adjusted for multiple comparisons), shown here. Log2 Fold Change \pm SEM.

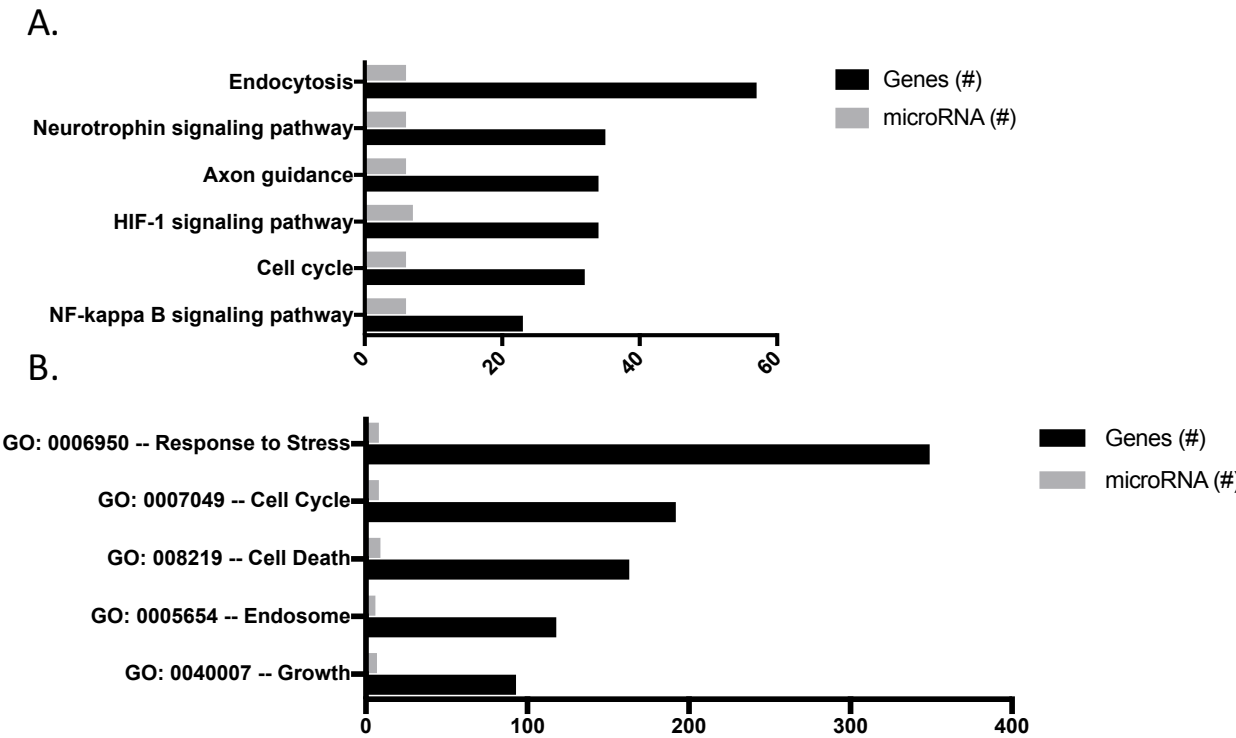


Figure 30. DIANA Pathway Analysis of microRNA Sequencing Results. Functional annotation via DIANA miR-base software resulted in a significant enrichment for KEGG pathways (A) and GO terms (B), $P \leq 0.05$. Selection shown here, complete list in Appendix D.

RT-qPCR supported a significant decrease in miR-10b-5p transcripts 3 hours after ES, though the decrease in let-7b and let-7c could not be confirmed (Figure 31). These results indicate that miR-10b-5p may regulate the transcriptome of electrically-induced cardioprotection. DIANA-microT-CDS software predicts that miR-423-5p binds NOS2 3'UTR, but this interaction has yet to be validated experimentally (Reczko, Maragkakis et al. 2012, Paraskevopoulou, Georgakilas et al. 2013).

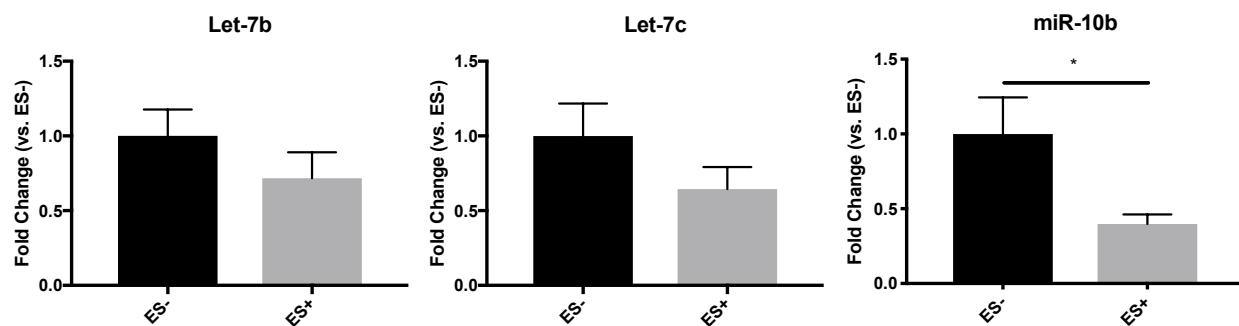


Figure 31. Validation of microRNA Sequencing. Analysis of RT-qPCR of let-7b (N=11,12 for ES-, ES+, respectively), let-7c (N=11, both groups), and miR-10b (N=15,14 for ES-, ES+, respectively) after ES. * $P \leq 0.05$. An unpaired, two-tailed Student's t-test was performed to analyze fold change in ES- vs. ES+. Only miR-10b fold change was reduced in ES+ compared to ES- conditions [$t(27)=2.297$, $P=0.0296$]. Mean \pm SEM. * $P \leq 0.05$.

CHAPTER VI

DISCUSSION

Establishing Electrically-Induced Cardioprotection

Electrical Stimulation Reduces Infarct Size in Multiple Models of Cardioprotection

The data in this work support my central hypothesis that electrically-based cutaneous stimuli applied to a particular region of the anterior abdomen are cardioprotective. The results of my experiments support that electrically-induced cardioprotection via EA needles and cutaneous patches significantly reduces infarct size and cell death in a mouse model of MI as an early phase preconditioning, late phase preconditioning, and per/postconditioning stimulus. This effect may be another example of NIC achieved by surgical incision or the topical application of capsaicin applied along the same region, and it is novel by its use of electricity via cutaneous patch at the abdominal region (Ren, Wang et al. 2004, Jones, Fan et al. 2009, Ren, Roessler et al. 2018). We used equal numbers of both male and female mice in ES- and ES+ groups. Although studies were not powered to compare the effect of sex, we did look for sex-related differences in mean and variance. If found, we would have increased the N to sufficiently power the comparison. This meets the NIH standards for inclusion of sex as a source of biological variation. In general, the parameters used agree with those investigated in the EA field, generally performed at the Neiguan acupoint at low frequencies (20Hz or less) for brief time periods (30 minutes or less).

Hypothesis 1

Electrical Stimulation Upregulates HSPs

Transcripts of several cardioprotective HSPs are increased with electrical stimulation, but the increases were small and mostly insignificant. This is different from the robust induction of HSPs after IPC, which is reported to be over 25-fold expression for mRNA levels measured by RT-qPCR and over an 8-fold change by microarray, 3.5 hours after IPC, and approximately 2.5-fold by Western blot 24 hours after IPC (Marber, Latchman et al. 1993, Hampton, Shimamoto et al. 2003, Tranter, Ren et al. 2010). Further, the protein levels of these transcripts are not elevated at the time points investigated after electrical stimulation, despite several technical replicates. These results do not support the hypothesis that transcriptional increases of HSPs are associated with electrically-induced cardioprotection, in contrast to IPC. We did not investigate the small HSPs, like HSP20, in the panel of HSPs probed, though several of these are important in cardioprotection (Fan, Ren et al. 2005). Protein and mRNA increases may occur outside the range of time points investigated, which remains unknown.

Genetic and Pharmacological Inhibition of the HSPs

We began an investigation of the different isoforms of HSP70 to determine if there was a functional role for either HSP70.1 or HSP70.3. We utilized mice with a genetic deletion of HSP70.1, and though this data is underpowered and not significant (Chapter 5, Figure 12), it would not be surprising if cardioprotection persisted with HSP70.1 deletion, as it is understood that the HSP70.3 isoform is required for the cardioprotective effect of IPC (Tranter, Ren et al. 2010). In previous studies, mice with a genetic deletion of both HSP70.1 and HSP70.3 could be utilized to clarify which isoform(s) of HSP70 are involved in the cardioprotective effect. In the

absence of an available double KO, the HSP70.1 data alone would not have been sufficient to test our hypothesis. As an alternative, we considered employing the HSP70 inhibitor apoptozole at a dose used commonly in the literature to block HSP70 (Baek, Zhang et al. 2015, Ko, Kim et al. 2015). A second HSP70 inhibitor, pifithrin, is commonly used *in vivo*, but we did not employ it based upon reports that the drug itself is cardioprotective against MI (Yuan, Lei et al. 2011). There was no precedent for how apoptozole performs in the heart and cardioprotection. In-house assays were employed to validate HSP70 inhibition by apoptozole (Chapter 5, Figure 13) (Budina-Kolomets, Balaburski et al. 2014). *In vivo*, apoptozole is unable to block IPC (which required HSP70) in a pilot study, and we decided not to pursue this pharmacological tool for our purpose of probing the cardioprotective effects of HSP70.

siRNA Inhibition of HSF1

A third strategy to inhibit the heat shock response was employed using siRNA against HSF1. Heat shock factor 1 is the major transcription factor that induces the heat shock response by binding to heat shock response elements within the promoters of HSP genes. We used a previously validated pool of four siRNA against HSF1, which blocked the effects of whole body hyperthermic preconditioning (Yin, Xi et al. 2005). Initial *in vitro* attempts to validate this siRNA resulted in a 22% reduction of HSF1 protein at the highest siRNA concentration recommended in the manufacturer's protocol. For HSF1 siRNA *in vivo*, we modified the siRNA to protect against endonuclease degradation and enhance cellular uptake based upon previous literature that employed the use of these modifications *in vivo* to target RNAs in the heart in the context of IPC (Wang, Zhu et al. 2012, Zheng, Yu et al. 2016). We delivered the pool of siRNAs as a local injection in the pericardial sac of the heart. In a small pilot study with a limited number of

animals, the result was not conclusive since treatments with the transfection reagent alone appeared to be cardioprotective. We did not test the modified material *in vitro* due to its cost. We also were not able to determine if the siRNA blocked HSPs *in vivo* since TTC staining cannot be performed in the same tissue used for protein lysate collection and Western blotting. An assay of efficacy is needed, such as Western blot, PCR, or *in situ* immunohistochemistry to confirm that the synthesized siRNA appropriately diminished the endogenous HSF1 and HSPs in the area of interest. We thought to pursue these validation steps, but there were no resources to continue the project to the scope required. Genetic deletion of HSF1 is not an option, as mice deficient of HSF1 are not viable.

Hypothesis 1 Summary

Electrically-induced cardioprotection can be administered via EA needles and cutaneous patches, effectively reducing infarct size in a mouse model of MI. However, this reduction in infarct size is not associated with an increase in HSP mRNA and protein expression. After exhausting options for evaluating the heat shock response within our resources, the question of whether the heat shock response is functionally required in electrically-induced cardioprotection remains open. The siRNA inhibition approach could probably be refined to obtain these results, but with the time and resources available to us, and in light of the negative results with mRNA and protein expression, we did not pursue this.

Hypothesis 2

Electrically-Induced Cardioprotection is NF- κ B Dependent

Ischemic preconditioning is NF- κ B -dependent and requires NF- κ B -dependent gene programs (Xuan, Tang et al. 1999, Tranter, Ren et al. 2010). Considering this, I used previously

characterized cardiomyocyte-specific dominant negative I κ B α (3M) mice to probe the role of NF- κ B in late phase electrically-induced cardioprotection. Results indicate that mice with the 3M mutation do not show electrically-induced cardioprotection, indicating that the transcription factor NF- κ B in the cardiomyocyte is required for electrically-induced cardioprotection. These findings helped us to direct and interpret subsequent next-generation sequencing studies. In previous studies, we determined the NF- κ B-dependent gene programs in IPC by identifying the transcriptome in wild-type and 3M mice by microarray and comparing the gene lists (Tranter, Ren et al. 2010). We employed a similar approach herein with complementary next-generation sequencing studies after ES, first sequencing B6/129 mice and validating the genes by PCR, and subsequently sequencing the 3M strain and nontransgenic controls and comparing the gene lists (Figure 25).

Next-Generation Sequencing in B6/129 Mice

This is the first study of its kind to perform deep-sequencing of the LV and identify the complete transcriptome of electrically-induced cardioprotection via cutaneous patch on the abdomen. We performed next-generation sequencing with multiple analyses of the data after removing and including subjects that did not cluster with others by Euclidian distances, excluding the possibility of batch effects. The 2X3 analysis gave us the widest selection of differentially expressed genes for follow-up studies. A total of 524 genes were differentially expressed after electrically-induced cardioprotection, including *NOS2*, *JUN* (encoding c-Jun) and *KY*. The top two significant ($P \leq 0.05$) genes with the greatest differential expression in our next-generation sequencing experiments, Gm6472 (8.6-fold change, 5.9×10^{-47}) and Gm6969 (4.9-fold change 7.9×10^{-23}), were mapped to predicted pseudogenes and are nonfunctional as identified

by the Mouse Genome Informatics Database, which is the central repository for gene nomenclature in the mouse (Bult, Krupke et al. 2015, Finger, Smith et al. 2017, Smith, Blake et al. 2018). To confirm their status as pseudogenes, these genes were searched in NCBI and PubMed for any publications on their functional involvement in physiological processes, of which there were none. To assign biological meaning to this large list of genes, we utilized DAVID enrichment analysis software. These genes grouped into gene ontology pathways including “biosynthetic process,” “nucleic acid templated transcription,” “nervous system development,” “epithelial cell migration” and “axon extension” (Chapter 5, Figure 18, and Appendix B). They grouped into cellular components for post-synaptic density, cellular junction, contractile actin filament, ion channel complex, and protein kinase complex (Chapter 5, Figure 18, and Appendix B). Together, these groupings suggest that electrically-induced cardioprotection might have an action at the intersection of the nervous system and cardiovascular system. No enrichment software available is considered perfectly suitable for all analysis scenarios, and many very good alternatives exist, such as PANTHER, which is part of the Gene Ontology Phylogenetic Annotation Project (Mi, Muruganujan et al. 2013, Mi, Huang et al. 2017). The DAVID software used for these analyses is advantageous for its experimentally-validated grouping assignments and was utilized to compare these results to what was done previously for IPC (Tipney and Hunter 2010). Gene ontology terms associated with IPC included “angiogenesis,” “programmed cell death,” and “heat shock response” categories. Gene ontology terms in these categories are not found in the set of GO terms associated with electrically-induced cardioprotection.

Validation of Sequencing

From the top 40 upregulated genes on this list, I identified several genes for follow-up validation: nitric oxide synthase 2 (*NOS2*), kyphoscoliosis peptidase (*KY*), and the Jun proto-oncogene (*JUN*, encoding c-Jun). Criteria for selection was that the genes were among the top 40 differentially expressed (above 1.7-fold change), significantly so ($P \leq 0.05$), and associated with cardiovascular disease, cardioprotection, or neuroprotection based on a literature review in PubMed. *NOS2* is an NF- κ B dependent gene that is required for the late phase of IPC and known to be both neuroprotective and cardioprotective. C-Jun dimerizes with c-Fos to form the transcription factor AP-1, which also has a known role in cardioprotection, but can also be used as an early marker of neuronal activation. Kyphoscoliosis peptidase is a little-studied but clinically-important regulator of proteins associated with the contractile filaments in the heart, providing neuromuscular junction stability in the healthy heart and leading to muscular dystrophy when mutated. Validation of upregulated mRNA levels of *NOS2*, *KY*, and c-Jun after ES by PCR supports the sequencing data (Chapter 5, Figures 19 and 23).

A gene's mRNA levels do not consistently predict protein levels due to factors like protein stability, decay and degradation, a reality that holds true in this study. We investigated *NOS2*, *KY*, and c-Jun protein level at multiple time points and were unable to detect any significant changes (Chapter 5, Figure 21A-D). We also investigated whether I/R is required for protein expression post-ES. However, we did not find evidence of protein upregulation in this "priming" scenario (Chapter 5, Figure 21E-F). Furthermore, we considered whether a noncoding RNA identified within the *NOS2* transcript might have a cardioprotective function independently of *NOS2* protein expression. This remains to be determined. This study probed

proteins under the influence of a systemic neural signal with translation rates that are unknown and not a constant for all transcripts. Our inability to detect protein increase at 18 or 24 hours and 6 hours post-I/R does not disprove our hypothesis that these are mediators of cardioprotection, rather, they could still be part of a specific and coordinated response to stress, and the cell may induce expression or release inhibition of their expression in a tightly regulated and energy-efficient process.

Nitric Oxide Synthase 2 is a Mediator of ES

Nitric oxide synthase 2, an NF- κ B -dependent gene, was identified as a potential mediator of cardioprotection and was pursued for functional validation. The promoter of murine NOS2 contains the NF- κ B binding site, and NF- κ B -dependent transcription occurs in neurons (Arias-Salvatierra, Silbergeld et al. 2011), microglia (Guo and Bhat 2006), and macrophages (Xie, Kashiwabara et al. 1994, Hughes, Srinivasan et al. 2008). Cardiac myocytes are the main source of NOS2 induction after IPC (Wang, Guo et al. 2002). Using mice with a genetic deletion of NOS2, we identified that this protein is required for electrically-induced cardioprotection. Since we were unable to detect the increase in NOS2 protein and could not establish NOS2 dependence on cardiomyocyte NF- κ B, we cannot rule out the possibility that NOS2 is being expressed in a different cell type, like neurons; thus NOS2 would escape cardiomyocyte NF- κ B blockade. It would be challenging to detect the protein, since neural cells make up a very small part of the myocardium. Cardiomyocytes constitute 30-40% of all cells in the adult mammalian heart, which is about 70-85% of the heart's mass because of their large volume, while fibroblasts, endothelial cells, and smooth muscle cells are the next most abundant non-cardiomyocyte cells in the heart (Nag 1980, Banerjee, Fuseler et al. 2007, Pinto,

Illykh et al. 2016). A small number of neurons concentrate in cardiac ganglia and branch throughout the heart (Ursell and Mayes 1995, Rysevaite, Saburkina et al. 2011). Indeed, multiple isoforms of NOS in different cell types are involved in IPC. In IPC, eNOS in epithelial cells generates NO, which activates PKC and NF- κ B in cardiomyocytes to trigger the late phase of cardioprotection (Bolli, Dawn et al. 1998, Lochner, Marais et al. 2000, Xuan, Tang et al. 2000, Lochner, Marais et al. 2002, Xuan, Guo et al. 2007). These results conflict with a group in China that was unable to establish the role of NOS2 in remote preconditioning of trauma by surgical incision (Song, Ye et al. 2016). Our own result was employed with great scientific rigor and repeated multiple times utilizing infarct studies to corroborate sequencing and PCR findings.

Downstream of NOS2, NO acts as a major signaling molecule in many different cell types and tissues, including neurons, through two main pathways. In the classic pathway, NO can stimulate guanlyl cyclase to produce cGMP and activate protein kinase G. Alternatively, NO can S-nitrosylate proteins by attaching an NO moiety to a nucleophilic protein sulfhydryl group, a post-translational activity that modifies protein activity and function. S-nitrosylation seems to be important to cardioprotection by preventing components of the ETC from the damage of ROS during reperfusion, among numerous other actions in a number of other proteins (Sun and Murphy 2010). Measuring the levels of NO and SNO modifications on key proteins after electrically-induced cardioprotection is discussed as a possible future direction.

The Additional Candidates, KY and c-Jun

The possibility that KY and c-Jun were also involved in electrically-induced cardioprotection was explored after validation. Kyphoscoliosis peptidase is clinically important, cardiac-specific, and interacts with critical components of the contractile filament, but its role in

cardioprotection is unknown. In a small set of mice, the significant increase in KY mRNA after ES is abolished in the 3M mice. This indicates that KY levels are dependent on cardiomyocyte NF- κ B, meaning that it is either in the cardiomyocyte or dependent on a cardiomyocyte NF- κ B-dependent factor. There is a predicted NF- κ B binding site in the KY sequence, but its experimental validation remains to be determined (Chen, Huang et al. 1998). There are no known pharmacological inhibitors of KY, and the severe motor defects of the KY mutant mouse model makes it unsuitable for evaluation in cardioprotection (Dickinson and Meikle 1973, Bridges, Coulton et al. 1992, Blanco, Coulton et al. 2001). Kyphoscoliosis peptidase might be considered an exemplar of the many novel and understudied genes within this data set that do not have an assigned role in cardioprotection.

Differential expression of c-Jun was observed in the sequencing data and corroborated by PCR. Known as an immediate early gene that upregulates itself in a feed-forward loop (Angel, Hattori et al. 1988), we were uncertain if c-Jun had a functional role in ES-induced cardioprotection. Disagreement persists on whether c-Jun/JNK is cardioprotective, because sustained inhibition or activation can be both proapoptotic and antiapoptotic (Bishopric, Andreka et al. 2001, Dougherty, Kubasiak et al. 2002, Sadoshima, Montagne et al. 2002, Kaiser, Liang et al. 2005, Tran, Andreka et al. 2007). We utilized the JNK inhibitor SP600125 based on its selectivity and 3-4 hour half-life *in vivo*, reasoning that the drug would be present throughout the duration of ES and immediately afterwards, but fully metabolized by day 2 (Bennett, Sasaki et al. 2001). Our pilot study demonstrates that SP600125 alone is cardioprotective. Reports using SP600125 in the heart shown that JNK inhibition is conditionally protective and beneficial against extended ischemia but injurious against acute ischemia (Wei,

Wang et al. 2011). Reports in other tissues have also shown that SP600125 reduced I/R injury in the brain, lungs, kidney and liver (Marderstein, Bucher et al. 2003, Ishii, Suzuki et al. 2004, Gao, Signore et al. 2005, Wang, Ji et al. 2007). Unfortunately, our result meant that we could not utilize SP600125 to evaluate the effects of c-Jun in electrically-induced cardioprotection.

Transcription factors, including c-Jun, generally reside in the cytoplasm and translocate to the nucleus when activated to exert control over cellular genes. C-Jun was not translocated into the nucleus in a small set of animals after ES, so there is no evidence at this point that it is acting as a transcription factor after ES.

Next-Generation Sequencing in 3M and Nontransgenic Mice

We repeated our sequencing data with the 3M mice and nontransgenic littermates to discover additional NF- κ B-dependent candidate genes involved in cardioprotection. As was done by Tranter, Ren et al. (2010), our strategy was to make comparisons between the overlap of genes upregulated after ES-induced cardioprotection in the 3M and nontransgenic mice to delineate genes that were NF- κ B-dependent in the context of ES (Chapter 5, Figure 25). In this approach, the genes that were upregulated in the nontransgenic ES+ condition (compared to the nontransgenic ES-) were cross-referenced to the genes that were downregulated in the ES+ 3M condition (compared to the nontransgenic ES+ condition). This strategy does not account for genes that are upregulated in nontransgenic ES+ (compared to nontransgenic ES-), but do not change in 3M ES+ mice compared to 3M ES- mice, which is a caveat. The response to electrically-induced cardioprotection is remarkably strain-specific based on the limited agreement between the nontransgenic mice raised on the C57 background and the B6/129 mice. Rodents do have strain-specific cardiovascular responses in response to various stimuli,

which provides some explanation for this result (Patel, Hsu et al. 2001, Berthonneche, Peter et al. 2009). We cannot fully clarify why NOS2, which was investigated in the previous data set, was not differentially expressed in the sequencing of nontransgenic (C57) mice. One rationalization is that the small induction of genes by ES-induced cardioprotection (approximately 1.5-fold induction on average for the top 20 genes) is milder compared to the robust induction of genes by IPC (approximately 3.6-fold induction on average for the top 20 genes), making changes much more difficult to detect in studies with limited numbers of animals.

In the nontransgenic sequencing set, many of these differentially expressed genes were components of the ETC. Mitochondria are essential for maintaining energy homeostasis in cardiomyocytes. Pharmacological blockade of electron transport can reduce injury during ischemia, but the consequences of ETC upregulation prior to I/R is unclear (Chen, Camara et al. 2007). The components of the transport chain do have complex interactions with reactive oxygen species ROS, HSPs, and NO under normal and stressful scenarios. Previous studies have shown that heat shock regulates respiration via NO. In H9C2 cells, NOS forms a complex with HSP90 and NO competitively binds to the complexes of the respiratory chain to downregulate O₂ consumption throughout ischemia (Ilangovan, Osinbowale et al. 2004). In our paradigm, endogenous HSPs might stabilize ES-upregulated NOS2, acting in concert to shield components of the ETC from reperfusion damage, preserving metabolism and preventing permeability pore transition and mitochondrial bursting (Figure 32).

Sequencing Assay Comparisons

A comparison of genes differentially expressed in IPC vs ES-induced cardioprotection by

next-generation sequencing suggests somewhat different transcriptomes between stimuli.

Kyphoscoliosis peptidase is downregulated after IPC but upregulated after ES. It is unclear why NOS2 is not differentially expressed after IPC in that sequencing dataset; it was in the C57 strain and known to be upregulated at the same time point (3 hours) post-IPC in other reports (Wang, Guo et al. 2002).

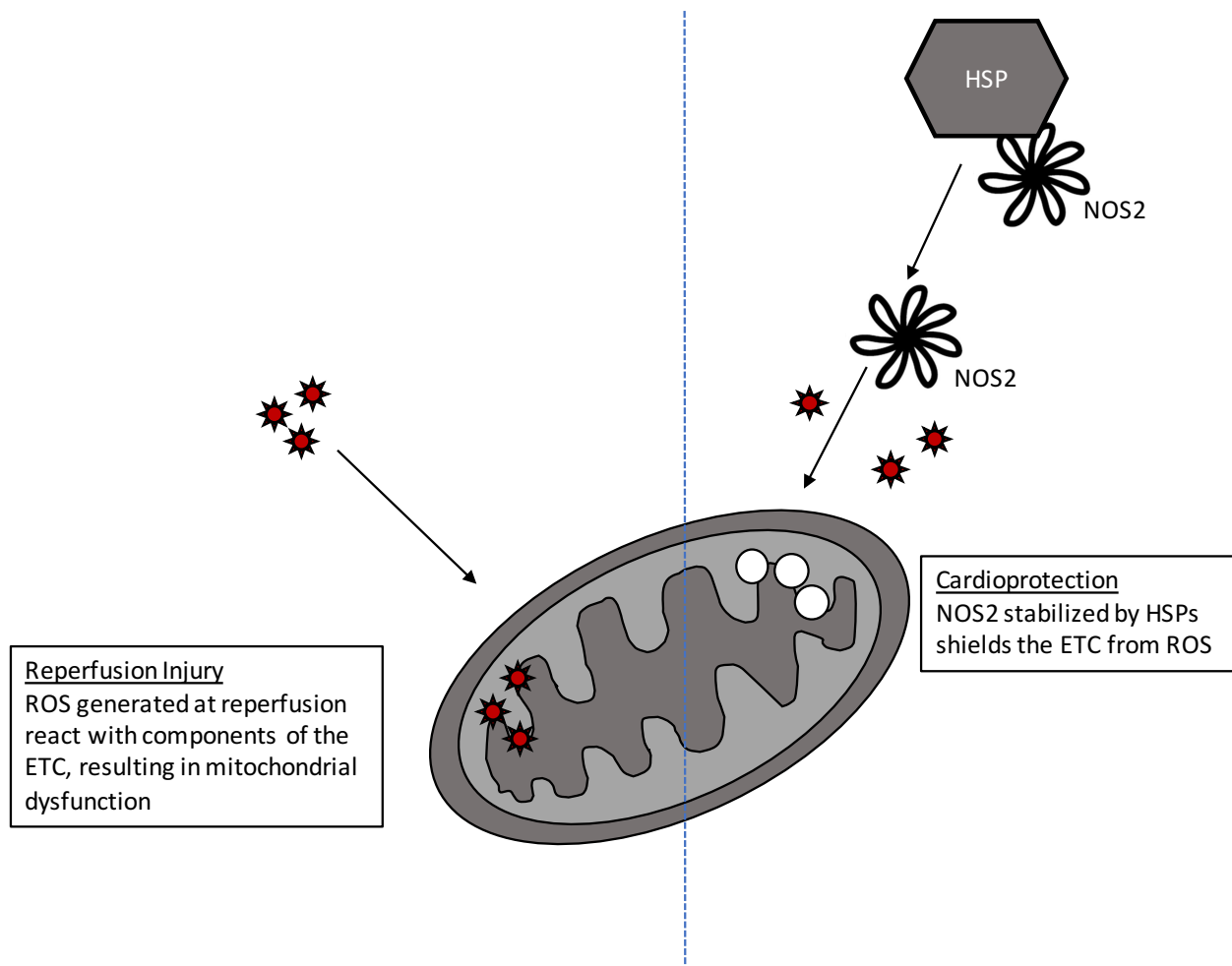


Figure 32: Summary Schematic. In the abrupt transition from ischemia to reperfusion, restored blood flow at reperfusion is associated the generation of ROS which can interact with and impair components of the ETC, leading to mitochondrial dysfunction and transition. In the context of cardioprotection, NOS2 can generate NO to shield components of the ETC from ROS and prevent reperfusion injury. NOS2 is stabilized in the cytoplasm by endogenous HSPs.

One explanation is that variation makes some expression changes difficult to resolve with small

sample sizes. Samples were also collected and prepared at different times and facilities for each assay, which are potentially confounding variables. We also employed the 3M mice to determine the NF- κ B-dependent genes after ES, as was done with IPC (Tranter, Ren et al. 2010). There were only 10 NF- κ B-dependent genes changed in expression levels after ES, and a search for each on PubMed did not reveal any literature on cardioprotection or neuroprotection. Again, we speculate that the robust induction of genes by IPC, which is a 6-fold repetitive stimulus, makes it much easier to measure transcriptomic changes. Perhaps the milder stimulus relative to IPC does not induce large increases in protein levels, or endogenous levels suffice, making detection of these mediators after their induction challenging. This underlines the importance of validation by other methods following sequencing, which we were careful to employ in all of our studies.

microRNA Next-Generation Sequencing and Validations

In a final sequencing experiment, we looked at differentially expressed microRNA after electrically-induced cardioprotection. After applying corrections for multiple comparisons to the statistics, only one microRNA was considered statistically significant: miR-10b-5p. Its downregulation (0.46-fold) was validated by PCR. When expanded to include microRNA that were differentially expressed without applying corrections for multiple comparisons, we identified members of the let-7 family among the top 3 differentially expressed microRNA. This family is well-studied in the cardioprotection field, where let-7 family inhibition protects against I/R injury in diabetic rat hearts (Li, Ren et al. 2016), augments the recruitment of epicardial cells to the infarcted area which is thought to be potentially regenerative, and improves cardiac function after MI (Seeger, Xu et al. 2016). The let-7 family has also been evaluated in the

context of neuroprotection, where knockdown protects against cerebral I/R injury (Wang, Liu et al. 2016). Data from our own lab using a combination of array data and sequencing data in mouse hearts and HL-1 cells determined that let-7a, b and c are downregulated after hypoxic preconditioning and each target at least 3 transcripts involved in the heat shock response, including HSP70.1, DNAJa1, DNAJb1 and DNAJb4 (Luther 2016). We did RT-qPCR assays for the let-7 family members and saw no significant changes following ES (Chapter 5, Figure 31).

A literature search revealed that several of our candidate microRNAs differentially expressed after ES via the sequencing data had potential epigenetic regulation over NOS2. In mouse serum, miR-10b-5p is one of the top circulating microRNAs expressed, and when RAW 264.7 murine macrophages were treated with serum or serum exosomes, levels of NOS2 were reduced (Zhou, Jiao et al. 2017). Perhaps this circulating microRNA could, in part, mediate the humoral hypothesis of cardioprotection by derepressing NOS2 post-transcriptional control. It would be enlightening to survey the serum microRNA and exosomes to address the changes occurring after electrically-induced cardioprotection. Whether these microRNAs bind directly to NOS2 or influence NOS2 through an intermediate factor remains to be determined. To investigate this, one could transfect cells with a NOS2 3'UTR GFP/luciferase reporter transcript and quantify the changes in reporter readout with the addition of microRNA mimics for those of interest. DIANA, TargetScan (Agarwal, Bell et al. 2015), and miRDB (Wong and Wang 2015) and the miRWalk comprehensive database of predicted and validated target algorithms do not predict miR10b-5p targeting of NOS2, KY, or c-Jun transcript throughout the complete sequence (promoter, 5' untranslated region, coding sequence, and 3' untranslated region). Mir-10b is predicted to target the nerve growth protein BDNF, the cell death-associated protein Bim, some

MAPK family members and other kinases, and a number of Hox genes which are involved in embryonic development and host the miR-10b gene. It is possible that miR-10b could have effects on NOS2 indirectly through one of its targets. DIANA-microT-CDS software predicts that miR-423-5p binds NOS2 3'UTR, but this interaction has yet to be validated experimentally (Reczko, Maragkakis et al. 2012, Paraskevopoulou, Georgakilas et al. 2013). A comprehensive analysis of miR-10b targets that are also differentially-expressed post-ES remains to be determined. Some genes, like the serine/threonine kinase 4 (*Stk4*), for example, fit both criteria, but validations must be done before further interpretations can be made. It is not known whether one microRNA alone is sufficient to downregulate targets like NOS2, or if the complete cohort is required for the effect.

Hypothesis 2 Summary

This study is novel because it is the first to identify the complete transcriptome of electrically-induced cardioprotection via the skin. A major observation is that the induction of genes after IPC, including HSPs, is robust. As mentioned previously, the increases in HSP70 mRNA after IPC were 8.53-fold by microarray, and over 20-40-fold higher by PCR followed by significant increases in levels of cognate proteins (Tranter, Ren et al. 2010). In contrast, the transcriptomic changes observed after ES-induced cardioprotection were much smaller compared to IPC, around 1.5-fold by next-generation sequencing and PCR, and we could not detect changes in levels of cognate proteins. Based on our sequencing data, we investigated NOS2 as a potential mediator of ES-induced cardioprotection. We demonstrated the requirement for NF- κ B and NOS in ES-induced cardioprotection using genetically modified mice. We also validated the upregulation of the novel protein KY, and showed that KY is NF- κ B-

dependent. We also demonstrated the downregulation of miR-10b in ES-induced cardioprotection. The lists of potentially cardioprotective genes curated within this dissertation is a major contribution to the field of nociceptor-induced cardioprotection.

Limitations and Alternatives

Throughout our *in vivo* experiments, we have set strict limits for physiological inclusion parameters, including age, weight, and ECG confirmation of ST-elevation throughout ischemia in infarct studies. Despite these criteria, after moving our lab into the Center for Translational Research and Education (Building 115) at Loyola University, we experienced a high level of variability in our surgical models (not experienced before in Building 110). This might have masked significant effects in our pilot studies with small numbers of mice. To address this, we set limitations to eliminate major stressors within our vivarium, such as minimizing interactions with research and vivarium staff, reducing noise in the holding room, and avoiding performing studies that spanned seasonal changes. In January 2018, we began placing the mice in a stress-reduction room within the vivarium and observed less variability. However, a small percentage of animals in the ES- conditions continued to present with unexpectedly small infarcts. We use pentobarbital as anesthesia since it is not cardioprotective, yet the drug interferes with homeothermic regulation in rodents (Kiyatkin and Brown 2005). To avoid cardioprotection by hypothermia, we maintained body temperature during surgery within a narrow range (33.5-36.5°C) by rectal probe connected to a heating pad. During recovery, animals were placed on a heating pad. However, we discovered stochastic variability in the room temperatures that might explain some of the variability in these data. When the room temperature strayed below 72°F, animals became hypothermic after I/R. Some did not survive, while others were

cardioprotected, perhaps reflecting a post-I/R phase of cold-induced protection. By tracking temperatures, we were able to remove affected mice from studies, but time and resources prevented us from repeating some studies, and we prioritized as best we could. The source of this cardioprotection has not been definitively identified, but we believe we have addressed all major environmental factors as best we could during the experimental period.

Detecting protein expression was a common challenge in these projects. We based our collection times on the protein kinetics of IPC, but we simply could have missed the time point of protein upregulation after ES. We would have liked to link infarct data with gene expression data, but TTC staining is incompatible with protein or mRNA collection and other downstream applications. Extensive time points would have to be done to determine this more completely, which we propose as a future direction.

For both our microRNA and mRNA sequencing experiments, our N was small. The monetary investment restricted the sample size we could submit for our sequencing studies. Sequencing techniques are still limited in their ability to detect low-abundance proteins with small numbers of animals. It stands to reason that variation at low levels of expression makes it more difficult to resolve modest changes in expression with such a small sample size. We chose to use the sequencing as an initial screening, then validate the results with RT-qPCR assays.

Future Directions

This dissertation project has determined that a genetic deletion of NOS2 abolishes ES-induced cardioprotection. We were unable to detect protein changes in NOS2. It is possible that we may have missed the time point of upregulation in our investigations. To determine this, we would need to perform a comprehensive time course to identify when NOS2 protein was

upregulated following ES, perhaps collecting samples at 6, 8, and 12 hours after ES. After identifying the time point at which NOS2 protein is upregulated, we would need to establish whether NOS2 was localized to the cardiomyocytes or the neurons by immunohistochemistry or *in situ* hybridization. If the NOS2 was indeed localized to the neurons and dependent on neuronal NF- κ B, the cardiomyocyte-specific 3M mice would not block induction. To discriminate between a role for NF- κ B in neurons, neuronal cell-type specific KO models would need to be employed to clarify the issue (Zhang, Potrovita et al. 2005).

Because free NO is a transient molecule that has a short half-life (only a few seconds) and diffuses between tissues *in vivo*, future directions would have to investigate events downstream of NO activity. Methods to detect and accurately quantify NO and its metabolites in biological samples like heart tissue have inherent limitations due to the rapid lability of the SNO bonds (Bryan & Grisham, 2007). It is common to use the biotin switch assay to detect SNO modifications, either on individual proteins of interest or total levels in the cell (Jaffrey and Snyder 2001). However, the time point of NOS2 protein induction would need to be established before proceeding. Low-abundance proteins, as is the case of many proteins discovered in our deep sequencing experiments, would not be well represented in the biotin-switch assay. Any follow up experiment to identify, measure, and localize S-nitrosylated proteins would require significant time and energy investment into range-finding. We might also need to investigate the NO/cGMP/PKG or PKC pathway and downstream phosphorylation targets to probe its involvement.

In addition to identifying the candidates mediating the cardioprotection, it would be useful to know whether these candidates are expressed in the cardiomyocytes themselves,

which we think is most likely, or in the nerves synapsing on the neuro-muscular junction. Nerve terminals do contain a limited amount of mRNA, but most transcripts are located in the cell body, distal from the synapse. Immunohistochemistry or *in situ* hybridization could pinpoint localization in future pursuits. Tissue-specific KO animal models could be utilized in future directions to query the functional role of KY, c-Jun, and other genes in either the cardiomyocytes or the nerves. Similarly, the complete neurobiology of ES remains a major gap in the field of electroceuticals. We've considered using retrograde and anterograde labeled viruses, injecting each into the nerves of the skin and the heart, and evaluating the overlap of signals. However, these viruses cross a limited number of synapses, so tracing the entire pathway would require the strenuous exercise of repeated injections and imaging. Optogenetic approaches to activate or inhibit specific neural systems, such as the sympathetic nerves, could be utilized to determine the functional involvement in electrically-induced cardioprotection. Our lab has considered employing both strategies, which ultimately fell beyond the scope of this project.

In this project, we compared sequencing data from IPC and ES. Ongoing projects in our lab study cardioprotection by different non-ischemic interventions, such as the application of stem cell-derived exosomes and protective microRNAs. In future studies, the transcriptomic data from this dissertation work might be combined with sequencing datasets from these other pursuits to create a more complete transcriptomic profile of cardioprotection. We envision that additional cardioprotective mediators will be revealed by this approach and will need to be validated in turn.

We believe that electrically-induced cardioprotection is a highly translatable therapy,

but wonder whether it would be effective in patient populations with comorbidities and pre-existing conditions such as diabetes, obesity, and old age. We also considered if ES therapy would be effective over the standard of care, especially β -blockers, which we did not pursue. Whether ES is effective or enhanced after multiple applications also remains to be determined. We considered these investigations, but thought the transcriptomic studies would have a greater impact based on the time and resources available.

Clinical Significance

Ischemic therapies have faced challenges in their translation to the clinic, and there are no cardioprotective therapies approved for this indication. One of the major challenges with ischemic-based cardioprotection is that these therapies cannot be used in all patient populations, such as those with atherosclerotic plaques at risk of rupture. Furthermore, cardioprotective interventions that would prolong operative time for any reason are risky. Pharmacological techniques and surgical interventions of NIC that are not ischemic and cardioprotective in animal models have their own set of challenges to translation, including invasiveness, side effects, and adverse complications. Electrically-based cardioprotection offers an alternative to such strategies of NIC. Electrically-induced protection may potentially be beneficial in other clinical situations characterized by hypoxic injury, such as ischemic stroke (Candilio, Malik et al. 2013). If possible, we would like to investigate whether NIC can reduce infarct size after middle cerebral artery occlusion *in vivo*. If ES is indeed neuroprotective, this would extend its clinical significance into other therapeutic areas.

We think the late phase of cardioprotection holds great potential and could have a large clinical impact. This electrically-based therapy is highly effective, low-cost, and easy to apply.

Since it is non-ischemic, electrically-based cardioprotection is safer than IPC, less invasive than surgery, and avoids the complications of pharmacological interventions. The long-lasting late phase of cardioprotection could be useful to maintain at-risk patients in a cardioprotected state. The timing, duration, location, and efficacy of repeated applications should be evaluated in ES-induced cardioprotection to determine the safety and optimal parameters of application. In addition to its application in ST-elevated MI, ES would be valuable as a prophylactic measure in clinical scenarios where hypoxic damage can be reliably predicted, such as elective PCI (Hoole, Heck et al. 2009), coronary artery bypass graft surgery (Theroux, Chaitman et al. 2000, Hausenloy, Mwamure et al. 2007, Venugopal, Hausenloy et al. 2009, Li, Luo et al. 2010, Wagner, Piler et al. 2010), or organ transplantation (Selzner, Boehnert et al. 2012). As a postconditioning stimulus, this therapy could be used in conjunction with PCI to improve outcomes after MI, especially in cases where time to PCI is delayed, in areas distant from the nearest PCI-capable hospital, and whenever cardioprotection could be initiated in transit.

CHAPTER VII

CONCLUSIONS

In conclusion, the data presented here demonstrate that electrically-induced NIC is effective as both an early and late phase cardioprotective stimulus. At 5 V, 4 Hz, 100 μ seconds for 15 minutes, cutaneous electrical stimulation at the abdomen reduces the size of the infarct and reduces cell death. Furthermore, electrically-induced NIC may be sufficient as a postconditioning stimulus when initiated at reperfusion. The induction of mRNA and protein levels of HSPs after electrically-induced NIC is small and mostly nonsignificant, suggesting that transcriptomic induction of a heat shock response is not involved in the effect. This is in contrast with IPC, which requires a robust induction of HSP70 and specifically, HSP70.3, for the cardioprotective effect. A deep-sequencing of the transcriptomic changes after electrically-induced cardioprotection revealed over 500 candidate genes that were differentially expressed after electrical stimulation, which could be sorted in gene ontologies of biological processes and cellular components that reflected a neural influence. None of these are HSPs. Nitric oxide synthase 2 was identified as a lead mediator of cardioprotection and upregulation of the gene was validated by RT-qPCR. Cardioprotection was lost in mice with a genetic deletion of NOS2. The NOS2 gene is known to be NF- κ B-dependent, and in a mouse model utilizing dominant negative I κ B α , we recognized that cardiomyocyte NF- κ B was also required for the infarct-sparing effect of electrically-induced cardioprotection. However, we were unable to determine that NOS2 transcriptional induction was NF- κ B-dependent using the 3M transgenic mice. This

could mean that the induction occurs in cells other than cardiomyocytes, or that expression levels in the C57 strain are too low to be resolved using the techniques that were employed. We were also able to validate the upregulation of KY and c-Jun and establish that KY is NF- κ B-dependent in cardiomyocytes and therefore must be upregulated in the cardiomyocyte. We also validated that miR-10b-5p is downregulated following ES. This study was the first to identify the transcriptomic changes associated with electrically-induced cardioprotection by utilizing a novel cutaneous patch.

Future efforts in our lab will continue to investigate these mRNA sequencing results to identify and validate additional mediators of cardioprotection, as well as investigate the timepoints and cell-specific localization of NOS2 upregulation in NIC. Further, we will continue to assess the microRNA differentially expressed after ES-induced cardioprotection and validate potential targets. Finally, we can combine the validated transcriptomic data from this dissertation work with sequencing datasets from other ongoing projects in the laboratory to assemble a more comprehensive and experimentally validated profile of cardioprotection. We envision that additional cardioprotective mediators will be revealed by combining transcriptomic data from multiple strategies of cardioprotection.

Furthermore, electrically-induced protection is highly translational as a late phase cardioprotective stimulus in MI and in clinical scenarios where hypoxic damage can be reliably predicted. We suggest establishing the timing, extent, and duration of ES-induced cardioprotection, and propose investigating ES as a neuroprotective stimulus as well. It is my hope that the discoveries made in this dissertation and those to follow will be translated into novel interventions that bring positive outcomes to the at-risk patient populations in the

cardiovascular disease therapeutic area and beyond.

APPENDIX A

**mRNA-SEQ DATA, GENES WITH DIFFERENTIAL EXPRESSION BETWEEN ES+/-
IN B6/129 MOUSE HEART TISSUE**

UPREGULATED (VS. ES-)						
Gene	Base Mean	log2 Fold Change	LFC SE	stat	p-value	p-adj
<i>Gm6472</i>	168.74	3.11	0.21	15.03	4.69659E-51	5.94E-47
<i>Gm6969</i>	158.95	2.28	0.21	10.68	1.25664E-26	7.95E-23
<i>Bend6</i>	80.40	1.28	0.21	5.99	2.05823E-09	2.10452E-06
<i>Gm5860</i>	115.39	1.28	0.21	5.99	2.16139E-09	2.10452E-06
<i>Lgi1</i>	310.70	1.18	0.18	6.43	1.24961E-10	2.25966E-07
<i>St8sia4</i>	410.98	1.17	0.18	6.37	1.92784E-10	3.05033E-07
<i>Fv1</i>	169.47	1.15	0.20	5.78	7.69164E-09	6.49072E-06
<i>Kctd21</i>	89.00	1.13	0.21	5.30	1.17047E-07	5.92632E-05
<i>8430408G22Rik</i>	2256.40	1.13	0.15	7.49	7.03286E-14	2.22555E-10
<i>Ankrd37</i>	72.26	1.09	0.21	5.12	3.09388E-07	0.000122382
<i>Zfp366</i>	305.35	1.08	0.21	5.21	1.86112E-07	8.72523E-05
<i>Wisp1</i>	91.29	1.07	0.21	5.11	3.21264E-07	0.000123229
<i>KY</i>	414.65	1.07	0.19	5.71	1.09772E-08	7.71944E-06
<i>Tet1</i>	204.80	1.06	0.18	6.02	1.7691E-09	2.03575E-06
<i>Npas2</i>	118.89	0.96	0.21	4.56	5.0622E-06	0.001001208
<i>Cxcr4</i>	114.60	0.94	0.21	4.51	6.50228E-06	0.001210381
<i>Sybu</i>	178.26	0.92	0.19	4.87	1.12772E-06	0.000340761
<i>Mboat2</i>	328.90	0.91	0.18	5.17	2.37426E-07	0.000106067
<i>Hipk2</i>	1439.64	0.90	0.18	5.04	4.62754E-07	0.000167358
<i>Jrk</i>	97.05	0.89	0.20	4.37	1.25202E-05	0.001956557
<i>Klf2</i>	726.88	0.89	0.21	4.33	1.52105E-05	0.002265108
<i>NOS2</i>	277.88	0.88	0.19	4.70	2.54608E-06	0.000596819
<i>Pgm2l1</i>	300.22	0.88	0.16	5.66	1.52483E-08	1.01586E-05
<i>Slc8a1</i>	3924.57	0.86	0.17	4.93	8.30598E-07	0.000292048
<i>Zfp60</i>	250.01	0.85	0.19	4.42	9.90664E-06	0.001694571
<i>JUN</i>	836.93	0.83	0.18	4.62	3.84491E-06	0.000824896
<i>Tmem37</i>	92.89	0.83	0.20	4.12	3.7316E-05	0.004373575
<i>Zfp420</i>	113.31	0.82	0.19	4.33	1.50159E-05	0.002262753
<i>Zfp111</i>	101.42	0.82	0.20	4.04	5.2511E-05	0.005779866
<i>Ppp1r16b</i>	422.04	0.81	0.18	4.44	8.93914E-06	0.001593685
<i>Cmtr2</i>	69.68	0.80	0.21	3.85	0.000118456	0.010460889
<i>Inpp4b</i>	628.58	0.80	0.20	4.02	5.72609E-05	0.006194947
<i>St5</i>	970.16	0.79	0.14	5.58	2.46449E-08	1.54879E-05
<i>Ccnd2</i>	3604.51	0.78	0.15	5.38	7.58924E-08	4.00269E-05
<i>Igfals</i>	166.07	0.78	0.21	3.69	0.000228401	0.016248424

<i>Senp8</i>	144.57	0.77	0.20	3.94	8.2207E-05	0.008066478
<i>Rasgrp3</i>	1215.64	0.77	0.16	4.86	1.18451E-06	0.000340761
<i>Sox4</i>	539.56	0.76	0.20	3.76	0.000166944	0.013495854
<i>Trabd2b</i>	3702.12	0.75	0.18	4.15	3.32694E-05	0.004049264
<i>Hcn4</i>	106.10	0.75	0.21	3.61	0.000308749	0.020145054
<i>Fam65b</i>	341.11	0.74	0.17	4.31	1.66807E-05	0.002372408
<i>Tmem39b</i>	73.62	0.73	0.20	3.60	0.00032111	0.020737823
<i>Tgs1</i>	309.74	0.73	0.16	4.71	2.45494E-06	0.000586315
<i>Cdk5r1</i>	37.62	0.73	0.21	3.56	0.000366906	0.021997483
<i>Ggta1</i>	569.01	0.73	0.15	4.87	1.13305E-06	0.000340761
<i>Eda2r</i>	101.61	0.72	0.21	3.46	0.000541771	0.027833771
<i>Zfp759</i>	122.78	0.72	0.20	3.69	0.000222077	0.016063112
<i>Nabp1</i>	1079.26	0.72	0.17	4.16	3.13272E-05	0.003956906
<i>Uprt</i>	87.56	0.72	0.20	3.54	0.000401579	0.023317343
<i>Gm9581</i>	258.24	0.72	0.19	3.86	0.000113376	0.010106458
<i>Mcm5</i>	108.67	0.72	0.21	3.45	0.000551622	0.028154962
<i>Ppp1r3b</i>	644.66	0.71	0.17	4.14	3.41676E-05	0.004080127
<i>Tril</i>	252.15	0.71	0.17	4.22	2.44246E-05	0.00325438
<i>Calhm2</i>	110.43	0.71	0.19	3.63	0.000281308	0.018940435
<i>Cep97</i>	212.10	0.71	0.18	3.82	0.000135295	0.011417065
<i>Samd5</i>	72.73	0.70	0.21	3.41	0.000661389	0.032575359
<i>Zfp661</i>	73.62	0.70	0.21	3.40	0.00067707	0.033167149
<i>Kcna4</i>	50.05	0.70	0.21	3.28	0.001046598	0.043578395
<i>Prickle1</i>	729.68	0.70	0.14	5.15	2.59764E-07	0.000106067
<i>Snai3</i>	246.11	0.70	0.21	3.36	0.000771526	0.035383986
<i>Rrm2</i>	71.12	0.70	0.21	3.27	0.001063622	0.043953701
<i>Nup160</i>	301.92	0.70	0.15	4.59	4.38804E-06	0.000881648
<i>Top2a</i>	123.24	0.70	0.21	3.25	0.001136105	0.045798782
<i>Klf6</i>	2296.44	0.69	0.12	5.73	9.84948E-09	7.33381E-06
<i>Kbtbd12</i>	675.36	0.69	0.19	3.68	0.000228802	0.016248424
<i>Nt5c1a</i>	183.40	0.69	0.20	3.47	0.000521501	0.027165276
<i>Alox12</i>	145.76	0.69	0.21	3.29	0.000993506	0.041780061
<i>Knstrn</i>	37.68	0.68	0.21	3.24	0.00120186	0.047541077
<i>Sesn3</i>	103.65	0.68	0.21	3.26	0.001131027	0.045798782
<i>CN725425</i>	40.28	0.68	0.21	3.21	0.001350402	0.051331479
<i>Shroom4</i>	1067.56	0.68	0.14	4.86	1.18116E-06	0.000340761
<i>Zfp873</i>	70.85	0.68	0.21	3.18	0.001471222	0.054772724
<i>Gm7452</i>	79.15	0.67	0.21	3.26	0.001132776	0.045798782
<i>Zfp72</i>	54.78	0.67	0.21	3.15	0.001620752	0.057914055

<i>Prox1</i>	1840.62	0.67	0.18	3.74	0.000182051	0.01422472
<i>Gnai1</i>	168.98	0.67	0.18	3.75	0.000177258	0.013971429
<i>Hykk</i>	60.42	0.66	0.21	3.14	0.001699194	0.059089007
<i>Tnfsf10</i>	533.79	0.66	0.18	3.59	0.000326344	0.020862953
<i>Sgcd</i>	522.62	0.65	0.18	3.69	0.000225222	0.01619804
<i>Gja1</i>	8404.63	0.65	0.17	3.78	0.000159511	0.013133181
<i>Fam198b</i>	1063.95	0.65	0.18	3.67	0.000244866	0.016959706
<i>Zfp324</i>	102.52	0.65	0.21	3.13	0.001734486	0.059660678
<i>Akap5</i>	101.11	0.65	0.21	3.09	0.002034142	0.065516965
<i>Dusp6</i>	450.42	0.65	0.18	3.60	0.000315412	0.02047428
<i>Fancb</i>	67.01	0.65	0.21	3.08	0.002086239	0.066019027
<i>Zfp719</i>	131.02	0.64	0.18	3.52	0.000425935	0.02417705
<i>Zswim3</i>	65.49	0.64	0.21	3.06	0.002199772	0.068246845
<i>Gm7292</i>	447.87	0.64	0.16	4.08	4.45247E-05	0.005170584
<i>Gm26672</i>	77.82	0.63	0.21	2.97	0.002984576	0.084516241
<i>Zfp712</i>	51.23	0.63	0.21	2.97	0.002975346	0.084443798
<i>Csf1</i>	1302.44	0.63	0.18	3.59	0.000326189	0.020862953
<i>Cdkl5</i>	42.43	0.63	0.21	2.96	0.003076067	0.08595333
<i>Chek2</i>	115.29	0.63	0.21	3.03	0.002417766	0.073215503
<i>Phlda1</i>	298.59	0.63	0.21	3.06	0.002196873	0.068246845
<i>Meox2</i>	506.28	0.63	0.16	3.90	9.76707E-05	0.009204132
<i>Slc30a6</i>	200.64	0.63	0.17	3.63	0.000287712	0.019269125
<i>Cbx8</i>	76.88	0.63	0.20	3.11	0.001871425	0.062174548
<i>Alg2</i>	230.44	0.63	0.18	3.55	0.00038839	0.022760377
<i>Lmbrd2</i>	223.77	0.63	0.18	3.58	0.000349039	0.021498008
<i>Cybb</i>	355.43	0.63	0.16	3.87	0.000109897	0.00994019
<i>Qsox2</i>	470.99	0.63	0.16	3.81	0.000141464	0.011858635
<i>Thap2</i>	173.93	0.63	0.21	3.01	0.002581633	0.076317959
<i>Zfp329</i>	405.52	0.62	0.15	4.16	3.15727E-05	0.003956906
<i>Cd200</i>	1310.29	0.62	0.14	4.32	1.54093E-05	0.00226804
<i>Fam110b</i>	188.84	0.62	0.18	3.43	0.000609638	0.030524197
<i>B230354K17Rik</i>	262.96	0.62	0.18	3.39	0.000705315	0.033779094
<i>Mest</i>	197.11	0.62	0.20	3.05	0.002321254	0.07138544
<i>Gm572</i>	88.77	0.62	0.21	3.02	0.002504015	0.075108575
<i>Frem2</i>	344.23	0.62	0.20	3.16	0.001566317	0.056817739
<i>Pcdh12</i>	541.40	0.61	0.19	3.21	0.001327142	0.051331479
<i>Abca12</i>	155.84	0.61	0.19	3.28	0.001022583	0.042718985
<i>Calcr1</i>	758.05	0.61	0.15	4.05	5.1236E-05	0.005739337
<i>Gm5595</i>	108.80	0.61	0.19	3.14	0.001682379	0.05882748

<i>Kctd12b</i>	542.82	0.61	0.20	3.02	0.002497848	0.07510157
<i>Gm14267</i>	68.04	0.61	0.21	2.94	0.003268102	0.087880174
<i>Ccdc14</i>	126.32	0.61	0.19	3.25	0.001150996	0.046105404
<i>Bahcc1</i>	404.33	0.61	0.16	3.84	0.000121326	0.010462787
<i>Gja5</i>	163.08	0.61	0.20	3.10	0.001965134	0.063945155
<i>Cdc14a</i>	112.31	0.61	0.19	3.15	0.001610918	0.057914055
<i>Btbd3</i>	1094.08	0.60	0.15	4.05	5.07052E-05	0.005730597
<i>Angpt1</i>	787.56	0.60	0.14	4.35	1.35389E-05	0.00206476
<i>Tmem229b</i>	117.81	0.60	0.19	3.08	0.002069292	0.065863541
<i>Ctnna3</i>	909.18	0.60	0.17	3.62	0.000298508	0.019679771
<i>Ankrd26</i>	112.42	0.60	0.20	2.93	0.003344038	0.089097258
<i>Gm8730</i>	568.83	0.59	0.20	2.95	0.003211878	0.087432162
<i>Gpr22</i>	849.11	0.59	0.14	4.17	2.99719E-05	0.003871262
<i>Irx3</i>	475.30	0.58	0.16	3.57	0.000350678	0.021498008
<i>Smc2</i>	123.42	0.58	0.20	2.88	0.00391843	0.098216809
<i>2610021A01Rik</i>	167.59	0.58	0.18	3.30	0.000956299	0.040620235
<i>Slc16a7</i>	128.78	0.58	0.20	2.89	0.003913773	0.098216809
<i>Ttc30a1</i>	81.90	0.57	0.20	2.87	0.004088817	0.099551072
<i>Sema3c</i>	416.42	0.57	0.15	3.88	0.000103731	0.009584118
<i>Npr3</i>	632.30	0.57	0.17	3.34	0.000844835	0.037111375
<i>Epha4</i>	1004.85	0.57	0.17	3.37	0.000741671	0.034388536
<i>Sema6a</i>	626.13	0.57	0.15	3.70	0.000214007	0.015568374
<i>Pm20d1</i>	447.65	0.57	0.19	3.02	0.002493425	0.07510157
<i>Adrb1</i>	254.28	0.57	0.19	2.98	0.002879012	0.08282208
<i>Ing3</i>	265.43	0.57	0.16	3.46	0.00054223	0.027833771
<i>Bmpr2</i>	747.03	0.56	0.16	3.51	0.000446865	0.024808827
<i>Enc1</i>	297.12	0.56	0.19	2.90	0.003707195	0.095377396
<i>Cecr2</i>	662.36	0.56	0.15	3.84	0.000121507	0.010462787
<i>Abcg1</i>	143.68	0.56	0.19	2.98	0.002843176	0.081979317
<i>Zfp518b</i>	166.29	0.56	0.18	3.16	0.001599585	0.057850122
<i>Phldb2</i>	959.21	0.55	0.16	3.43	0.000612789	0.030538131
<i>Vcam1</i>	479.04	0.55	0.19	2.95	0.003182188	0.087304971
<i>Fam117a</i>	158.14	0.55	0.18	3.01	0.002579865	0.076317959
<i>Hmgn2</i>	772.59	0.55	0.16	3.50	0.000470693	0.025880063
<i>Zfp518a</i>	361.03	0.54	0.14	3.75	0.000177706	0.013971429
<i>Fam78a</i>	499.80	0.54	0.19	2.90	0.003739825	0.095680109
<i>Zfp12</i>	331.06	0.54	0.16	3.40	0.000678645	0.033167149
<i>Ift81</i>	2764.09	0.54	0.18	3.10	0.001949538	0.063765495
<i>G0s2</i>	716.69	0.54	0.18	2.96	0.003121208	0.086451311

<i>Tbc1d2b</i>	615.00	0.54	0.15	3.56	0.000377529	0.022330666
<i>Prob1</i>	683.95	0.54	0.12	4.31	1.61826E-05	0.00232772
<i>Mdfic</i>	472.64	0.54	0.15	3.66	0.000256841	0.017573496
<i>Rassf8</i>	1315.49	0.54	0.14	3.90	9.81638E-05	0.009204132
<i>Zfp930</i>	139.21	0.54	0.18	2.90	0.003739182	0.095680109
<i>Ptplad2</i>	225.08	0.54	0.18	2.97	0.003003596	0.08458015
<i>Zfp71-rs1</i>	188.82	0.53	0.18	3.01	0.002586539	0.076317959
<i>C030046E11Rik</i>	950.28	0.53	0.13	4.00	6.25384E-05	0.006542238
<i>Wfikkn2</i>	273.98	0.53	0.18	3.02	0.002558726	0.076207894
<i>Arid5b</i>	524.03	0.53	0.15	3.57	0.000351563	0.021498008
<i>Pm20d2</i>	448.05	0.52	0.17	3.12	0.001803739	0.061211071
<i>Mlh3</i>	387.10	0.52	0.15	3.56	0.000368322	0.021997483
<i>Slc35b4</i>	266.26	0.52	0.16	3.27	0.00108791	0.044421838
<i>Lrp4</i>	442.37	0.52	0.17	2.96	0.003093551	0.08620845
<i>Gbp5</i>	309.84	0.52	0.15	3.49	0.000486325	0.026161567
<i>Hook1</i>	568.96	0.52	0.14	3.67	0.000241201	0.016868088
<i>Asap3</i>	362.42	0.52	0.17	3.11	0.001849267	0.061762588
<i>Slc29a3</i>	151.80	0.51	0.18	2.90	0.003791429	0.096485931
<i>Als2</i>	456.60	0.51	0.14	3.66	0.000256214	0.017573496
<i>Ifi203</i>	1455.60	0.51	0.14	3.73	0.000189398	0.014442138
<i>Sema4d</i>	676.21	0.51	0.14	3.68	0.000230434	0.016248424
<i>Cnot6l</i>	1397.35	0.51	0.12	4.39	1.12028E-05	0.00183303
<i>Exoc8</i>	595.67	0.51	0.13	3.86	0.000113233	0.010106458
<i>Arrdc4</i>	358.74	0.51	0.17	2.92	0.003476949	0.091433239
<i>Trim55</i>	1727.59	0.51	0.12	4.30	1.74454E-05	0.002453597
<i>Nrep</i>	638.96	0.50	0.14	3.52	0.000430735	0.024340383
<i>Chordc1</i>	931.68	0.50	0.17	3.00	0.002693673	0.078744842
<i>Garem</i>	619.50	0.50	0.13	3.92	8.99943E-05	0.008695789
<i>Chtf8</i>	1021.85	0.50	0.16	3.21	0.001346658	0.051331479
<i>Sync</i>	467.12	0.50	0.15	3.34	0.000834342	0.037111375
<i>Zfp142</i>	553.56	0.50	0.17	2.98	0.002892033	0.08282208
<i>Amot</i>	468.47	0.50	0.17	2.92	0.003516611	0.092159971
<i>Gja3</i>	191.28	0.49	0.17	2.91	0.003585267	0.093097931
<i>Ube3a</i>	1601.70	0.49	0.14	3.50	0.000472294	0.025880063
<i>Gatad2b</i>	316.57	0.49	0.16	3.13	0.001757623	0.060292667
<i>Golph3l</i>	452.32	0.49	0.14	3.56	0.00036842	0.021997483
<i>Vwa5a</i>	1160.61	0.49	0.11	4.28	1.86653E-05	0.002596326
<i>Gm16515</i>	364.09	0.49	0.16	3.10	0.00192642	0.063501632
<i>Fam53b</i>	903.88	0.49	0.14	3.45	0.000554132	0.028169497

<i>Napepld</i>	226.17	0.48	0.17	2.87	0.004044896	0.099551072
<i>Lnpep</i>	2188.40	0.48	0.16	3.11	0.001892504	0.0625465
<i>Ccnd1</i>	1474.48	0.48	0.16	3.07	0.00211085	0.066631262
<i>Xrn1</i>	396.33	0.47	0.16	2.93	0.003350474	0.089097258
<i>Ppara</i>	922.20	0.47	0.13	3.62	0.000291175	0.019398358
<i>Sort1</i>	1498.53	0.47	0.14	3.34	0.0008461	0.037111375
<i>Xpo5</i>	667.87	0.47	0.13	3.58	0.000342242	0.02137453
<i>Spry4</i>	307.98	0.47	0.16	2.92	0.003537183	0.092507576
<i>Mlst8</i>	353.22	0.47	0.15	3.07	0.002128561	0.066933714
<i>Slc41a1</i>	2086.22	0.46	0.13	3.61	0.000303449	0.019901827
<i>Ctsc</i>	1007.54	0.46	0.14	3.21	0.001347211	0.051331479
<i>Cog5</i>	728.65	0.46	0.13	3.49	0.000489832	0.026161567
<i>Tpst1</i>	394.78	0.45	0.16	2.89	0.003880192	0.098034871
<i>Rap1gap2</i>	2666.45	0.45	0.14	3.27	0.001087908	0.044421838
<i>Stk4</i>	560.70	0.45	0.13	3.39	0.000708781	0.033779094
<i>Rap2a</i>	523.22	0.45	0.14	3.23	0.001218578	0.047902986
<i>5830418K08Rik</i>	391.02	0.44	0.15	2.94	0.003236411	0.087786222
<i>Pkdcc</i>	866.11	0.44	0.15	3.00	0.00267476	0.078372956
<i>Steap3</i>	1026.58	0.44	0.12	3.58	0.000345364	0.021429495
<i>Chrm2</i>	3257.67	0.44	0.13	3.46	0.00054313	0.027833771
<i>Acvr1</i>	343.64	0.44	0.15	3.01	0.002628405	0.077372918
<i>Zfp180</i>	451.28	0.44	0.14	3.07	0.002137248	0.066933714
<i>Senp7</i>	413.72	0.44	0.15	2.94	0.003241849	0.087786222
<i>Ap5m1</i>	332.87	0.44	0.15	2.95	0.003186514	0.087304971
<i>Rrm1</i>	472.75	0.44	0.15	2.89	0.003807376	0.096580687
<i>Edem3</i>	841.14	0.44	0.12	3.53	0.000421156	0.024013477
<i>Usp31</i>	536.57	0.43	0.13	3.27	0.0010756	0.04420438
<i>ligp1</i>	1266.38	0.43	0.13	3.37	0.000745379	0.03443433
<i>Tmem126b</i>	590.80	0.42	0.13	3.21	0.001323435	0.051331479
<i>Elk3</i>	1032.91	0.42	0.14	3.04	0.002379606	0.072623477
<i>Akap6</i>	5782.41	0.42	0.13	3.35	0.000801664	0.03637085
<i>Mtf1</i>	470.79	0.42	0.14	2.93	0.003381677	0.089550779
<i>Stk10</i>	421.94	0.42	0.14	2.97	0.002954898	0.084051896
<i>Rreb1</i>	1656.50	0.41	0.13	3.15	0.001639442	0.057966651
<i>Parm1</i>	3997.15	0.41	0.11	3.71	0.000204416	0.015220574
<i>Lrsam1</i>	480.36	0.41	0.14	2.92	0.003481658	0.091433239
<i>Pot1a</i>	364.20	0.41	0.14	2.88	0.003972958	0.098800997
<i>Mdc1</i>	511.62	0.41	0.13	3.14	0.001694899	0.059089007
<i>Syde2</i>	1212.24	0.41	0.12	3.35	0.000819872	0.036801204

<i>Pxdn</i>	2537.26	0.41	0.10	3.92	8.86817E-05	0.008634867
<i>Ptpn3</i>	2136.02	0.41	0.14	2.87	0.004089866	0.099551072
<i>Gtf3c4</i>	701.21	0.41	0.12	3.32	0.000899351	0.038916367
<i>Fcho2</i>	2021.19	0.41	0.11	3.73	0.000188925	0.014442138
<i>Klhl9</i>	1682.11	0.41	0.13	3.16	0.00156655	0.056817739
<i>Sdpr</i>	3865.15	0.41	0.14	2.87	0.004059314	0.099551072
<i>Atp6v1a</i>	705.21	0.41	0.13	3.10	0.001937154	0.063689583
<i>Palld</i>	4292.44	0.41	0.11	3.68	0.000231057	0.016248424
<i>Pdcl</i>	436.71	0.41	0.14	2.94	0.003281208	0.087994781
<i>Prelp</i>	1327.05	0.40	0.11	3.54	0.000405881	0.023376222
<i>Kdm1b</i>	512.39	0.40	0.13	2.96	0.003098819	0.08620845
<i>Mtap</i>	582.84	0.40	0.14	2.88	0.003914882	0.098216809
<i>Dars2</i>	598.41	0.39	0.13	2.97	0.003012141	0.08458015
<i>Nipal3</i>	868.68	0.39	0.13	2.88	0.003947504	0.098361225
<i>Bace1</i>	1129.57	0.39	0.12	3.15	0.001633379	0.057914055
<i>Cdc40</i>	681.17	0.39	0.13	2.87	0.00405393	0.099551072
<i>Rcbtb2</i>	638.54	0.38	0.13	2.93	0.003337707	0.089097258
<i>Plxna4</i>	590.14	0.38	0.13	2.87	0.004070994	0.099551072
<i>Aqr</i>	792.60	0.38	0.12	3.25	0.001169147	0.046537949
<i>Ak4</i>	1061.90	0.38	0.12	3.08	0.002054367	0.065863541
<i>Pcdh7</i>	2303.93	0.38	0.13	2.98	0.002837862	0.081979317
<i>Ept1</i>	561.25	0.37	0.13	2.91	0.003589176	0.093097931
<i>Erap1</i>	1020.90	0.37	0.12	2.95	0.003201077	0.087432162
<i>Socs6</i>	902.53	0.36	0.12	2.94	0.003253336	0.087805396
<i>Large</i>	1743.29	0.36	0.12	2.87	0.004107249	0.099551072
<i>D2hgdh</i>	1463.03	0.36	0.12	2.90	0.003756938	0.095877651
<i>Nfix</i>	2957.32	0.35	0.12	2.99	0.002802336	0.081714265
<i>Fyco1</i>	15524.39	0.35	0.09	3.83	0.000130533	0.011089139
<i>Mmp15</i>	2824.68	0.35	0.11	3.14	0.00171742	0.059423393
<i>Suv420h1</i>	1134.43	0.34	0.11	3.07	0.002158488	0.067295906
<i>Nrp1</i>	4290.06	0.33	0.10	3.32	0.000910056	0.039049099
<i>Nfe2l2</i>	1920.04	0.33	0.11	2.91	0.00360719	0.093373858
<i>Asxl2</i>	1159.60	0.33	0.11	2.94	0.003269992	0.087880174
<i>Marcks</i>	1254.56	0.32	0.11	2.88	0.004020037	0.09919225
<i>Stom</i>	3291.72	0.32	0.11	3.02	0.002568053	0.076306136
<i>Abcc9</i>	12940.58	0.32	0.10	3.08	0.002070919	0.065863541
<i>Ank3</i>	2003.03	0.31	0.11	2.95	0.003168485	0.087304971
<i>Plod1</i>	3019.67	0.31	0.11	2.88	0.003944035	0.098361225
<i>Nedd4</i>	16672.95	0.30	0.10	3.08	0.002062391	0.065863541

DOWNREGULATED (VS. ES-)						
Gene	Base Mean	log2 Fold Change	LFC SE	stat	p-value	p-adj
<i>Wt1</i>	258.70	-1.46	0.19	-7.72	1.21E-14	5.10E-11
<i>Gm17428</i>	298.82	-1.23	0.18	-6.89	5.44E-12	1.15E-08
<i>Thbs1</i>	273.90	-1.16	0.17	-6.99	2.81E-12	7.11E-09
<i>Ager</i>	58.94	-1.02	0.21	-4.79	1.63E-06	0.000429477
<i>Acr</i>	99.30	-0.99	0.21	-4.61	4.00E-06	0.000842947
<i>Hif3a</i>	346.59	-0.98	0.21	-4.63	3.65E-06	0.00080909
<i>Dennd3</i>	625.16	-0.97	0.17	-5.78	7.47E-09	6.49E-06
<i>mt-Tl1</i>	782.18	-0.96	0.16	-6.08	1.23E-09	1.56E-06
<i>Fgfr3</i>	902.61	-0.95	0.20	-4.81	1.50E-06	0.000404558
<i>Coro2a</i>	54.41	-0.94	0.21	-4.38	1.18E-05	0.001863869
<i>Mcf2l</i>	3587.51	-0.92	0.19	-4.73	2.28E-06	0.000554756
<i>Tmc8</i>	188.60	-0.91	0.20	-4.65	3.34E-06	0.000755812
<i>Helz2</i>	2190.88	-0.90	0.15	-6.13	8.87E-10	1.25E-06
<i>Cdhr3</i>	55.99	-0.89	0.20	-4.39	1.16E-05	0.001850761
<i>D830015G02Rik</i>	2472.38	-0.87	0.15	-5.75	8.74E-09	6.92E-06
<i>Maff</i>	338.59	-0.86	0.20	-4.22	2.41E-05	0.003251953
<i>A3galt2</i>	33.32	-0.86	0.21	-4.08	4.57E-05	0.005236127
<i>Prkcg</i>	511.91	-0.85	0.21	-4.04	5.24E-05	0.005779866
<i>Mir22hg</i>	1273.69	-0.85	0.19	-4.43	9.35E-06	0.001644234
<i>Ramp3</i>	247.03	-0.84	0.19	-4.41	1.03E-05	0.001714805
<i>Crybb3</i>	106.75	-0.83	0.19	-4.31	1.61E-05	0.00232772
<i>Hecw2</i>	1031.78	-0.83	0.17	-4.90	9.40E-07	0.000313
<i>Vsig2</i>	515.63	-0.82	0.19	-4.23	2.30E-05	0.003124815
<i>Lrrc32</i>	527.55	-0.82	0.18	-4.59	4.36E-06	0.000881648
<i>Arhgap8</i>	59.19	-0.81	0.21	-3.85	0.000119832	0.010460889
<i>Nos3</i>	1668.85	-0.81	0.16	-5.08	3.84E-07	0.000142798
<i>Sox18</i>	776.67	-0.81	0.18	-4.55	5.27E-06	0.001025965
<i>Cables1</i>	267.15	-0.81	0.19	-4.19	2.79E-05	0.003680478
<i>Il18rap</i>	35.30	-0.78	0.21	-3.67	0.000245191	0.016959706
<i>Lat2</i>	93.74	-0.78	0.20	-3.87	0.000109492	0.00994019
<i>Nova2</i>	570.53	-0.77	0.17	-4.60	4.15E-06	0.000861994
<i>Litaf</i>	576.46	-0.77	0.16	-4.74	2.17E-06	0.000539464
<i>Plxna2</i>	3129.49	-0.77	0.16	-4.89	1.01E-06	0.00032744
<i>Gnal</i>	56.62	-0.77	0.21	-3.58	0.000338516	0.021318089
<i>Pla2g6</i>	356.65	-0.76	0.16	-4.76	1.94E-06	0.0004905

<i>Il20rb</i>	149.00	-0.76	0.21	-3.57	0.000359766	0.021893855
<i>Hyi</i>	151.40	-0.76	0.21	-3.64	0.000272079	0.018416987
<i>Sorbs3</i>	1568.29	-0.75	0.15	-5.15	2.54E-07	0.000106067
<i>Tbx3</i>	644.14	-0.75	0.20	-3.74	0.000185783	0.014339261
<i>Akap12</i>	2144.62	-0.75	0.19	-4.02	5.92E-05	0.006348832
<i>Trpm2</i>	34.21	-0.74	0.21	-3.46	0.000535614	0.02778608
<i>Dnaaf3</i>	376.50	-0.74	0.15	-4.77	1.87E-06	0.000483841
<i>Trpv4</i>	271.92	-0.73	0.21	-3.48	0.000497343	0.026230676
<i>Ubxn7</i>	1869.42	-0.73	0.15	-4.82	1.46E-06	0.000401684
<i>Rin3</i>	898.16	-0.73	0.13	-5.42	5.95E-08	3.43E-05
<i>Bcl3</i>	76.15	-0.73	0.21	-3.48	0.000509241	0.026746769
<i>Irak2</i>	429.11	-0.72	0.19	-3.83	0.000126081	0.010783374
<i>Socs3</i>	97.97	-0.72	0.21	-3.38	0.000715184	0.033779094
<i>Rassf1</i>	564.70	-0.72	0.14	-5.24	1.63E-07	7.94E-05
<i>Vmn1r-ps128</i>	63.39	-0.71	0.21	-3.34	0.000847305	0.037111375
<i>Egr1</i>	332.45	-0.71	0.21	-3.37	0.000740414	0.034388536
<i>Gm14827</i>	43.42	-0.71	0.21	-3.31	0.000939228	0.040029439
<i>2810474O19Rik</i>	1235.17	-0.71	0.18	-4.00	6.21E-05	0.006542238
<i>Nynrin</i>	369.27	-0.70	0.17	-4.15	3.27E-05	0.004024549
<i>Cd74</i>	2792.65	-0.70	0.16	-4.42	9.91E-06	0.001694571
<i>mt-Tw</i>	1072.10	-0.70	0.14	-5.16	2.53E-07	0.000106067
<i>Dpm1</i>	290.29	-0.70	0.17	-4.00	6.38E-05	0.006568593
<i>Gata2</i>	728.99	-0.70	0.16	-4.47	7.99E-06	0.001465414
<i>Dnah7b</i>	40.44	-0.70	0.21	-3.33	0.000854896	0.037314727
<i>Rasgrf2</i>	493.94	-0.69	0.17	-4.13	3.65E-05	0.004322908
<i>Hypk</i>	206.33	-0.69	0.19	-3.71	0.000210001	0.015454618
<i>Parvg</i>	107.65	-0.69	0.21	-3.23	0.001217339	0.047902986
<i>Clcf1</i>	134.84	-0.68	0.20	-3.49	0.000487861	0.026161567
<i>Csdc2</i>	2136.03	-0.68	0.16	-4.36	1.30E-05	0.002012458
<i>Tcf15</i>	231.68	-0.68	0.20	-3.38	0.000734016	0.034284782
<i>Ctla2a</i>	486.84	-0.68	0.18	-3.76	0.000171852	0.013767743
<i>Nt5e</i>	1166.89	-0.68	0.20	-3.34	0.000839239	0.037111375
<i>Myh11</i>	2178.90	-0.68	0.19	-3.58	0.00034279	0.02137453
<i>Cideb</i>	76.31	-0.67	0.21	-3.15	0.001626554	0.057914055
<i>Olfr78</i>	217.19	-0.67	0.19	-3.54	0.000394313	0.023000966
<i>Nr4a2</i>	52.76	-0.66	0.21	-3.15	0.001660012	0.058206169
<i>Nostrin</i>	221.12	-0.66	0.20	-3.38	0.000730693	0.034255968
<i>Vwa3a</i>	345.10	-0.66	0.19	-3.49	0.000479139	0.026029813
<i>Lama5</i>	10329.78	-0.65	0.17	-3.75	0.000174592	0.01389927

<i>Ccdc88b</i>	89.24	-0.65	0.21	-3.12	0.001833854	0.061627386
<i>Prkch</i>	877.27	-0.65	0.16	-4.19	2.85E-05	0.003718536
<i>Mgat4a</i>	922.21	-0.65	0.17	-3.78	0.000155519	0.012951022
<i>Sh2b3</i>	1755.80	-0.65	0.14	-4.63	3.71E-06	0.00080909
<i>Zfand4</i>	308.16	-0.65	0.19	-3.38	0.000714108	0.033779094
<i>Mir208a</i>	87.22	-0.65	0.21	-3.13	0.001729063	0.059636184
<i>Pde8a</i>	908.61	-0.64	0.17	-3.70	0.000213861	0.015568374
<i>Skil</i>	816.33	-0.64	0.13	-4.82	1.46E-06	0.000401684
<i>Acer2</i>	1488.41	-0.64	0.20	-3.17	0.001509949	0.055828961
<i>Zfp445</i>	2226.51	-0.64	0.14	-4.45	8.41E-06	0.001520964
<i>Map3k6</i>	1487.99	-0.64	0.21	-3.06	0.002241367	0.069367284
<i>Tmc6</i>	445.02	-0.63	0.16	-4.00	6.33E-05	0.006568593
<i>Gmeb2</i>	644.12	-0.63	0.16	-3.97	7.05E-05	0.007141684
<i>Cldn15</i>	139.72	-0.63	0.21	-2.95	0.003208532	0.087432162
<i>Plekhg2</i>	1259.61	-0.63	0.18	-3.52	0.000437993	0.024433778
<i>H2-Eb1</i>	998.88	-0.63	0.18	-3.55	0.000381819	0.022479351
<i>Lpin3</i>	336.80	-0.62	0.21	-2.93	0.003411216	0.090144412
<i>Myh7b</i>	9829.53	-0.62	0.13	-4.87	1.14E-06	0.000340761
<i>Sema3f</i>	635.05	-0.62	0.18	-3.47	0.000518235	0.027106695
<i>Figl2</i>	121.66	-0.62	0.20	-3.15	0.001626021	0.057914055
<i>Ppp1r18</i>	647.07	-0.61	0.16	-3.90	9.72E-05	0.009204132
<i>Vmn1r65</i>	42.70	-0.61	0.21	-2.89	0.003859479	0.097706582
<i>B4galt4</i>	446.31	-0.61	0.20	-3.12	0.001839033	0.061627386
<i>Gm26532</i>	228.03	-0.61	0.19	-3.30	0.000980427	0.041367475
<i>Flt1</i>	7311.27	-0.61	0.11	-5.39	7.08E-08	3.89E-05
<i>Prr5</i>	111.05	-0.61	0.19	-3.11	0.00185622	0.06183167
<i>Sox7</i>	932.75	-0.61	0.19	-3.11	0.001888715	0.0625465
<i>Slc1a1</i>	99.05	-0.60	0.19	-3.09	0.002018322	0.065173264
<i>Kdm6b</i>	1395.76	-0.60	0.15	-4.01	6.03E-05	0.00641462
<i>Notch1</i>	2370.21	-0.60	0.11	-5.57	2.57E-08	1.55E-05
<i>Cyp2d22</i>	1020.69	-0.59	0.19	-3.09	0.00197871	0.064221821
<i>Plin4</i>	18646.08	-0.59	0.19	-3.13	0.001774175	0.060695968
<i>Arhgap25</i>	165.31	-0.59	0.19	-3.12	0.001802208	0.061211071
<i>Sema4c</i>	505.65	-0.58	0.14	-4.17	3.11E-05	0.003956906
<i>Ccnl2</i>	5258.74	-0.58	0.13	-4.39	1.13E-05	0.00183303
<i>Zfp948</i>	321.92	-0.58	0.18	-3.27	0.001066028	0.043953701
<i>Rhbdf2</i>	545.07	-0.58	0.13	-4.51	6.49E-06	0.001210381
<i>Alad</i>	1591.57	-0.57	0.18	-3.21	0.001346567	0.051331479
<i>Dlg3</i>	320.79	-0.57	0.17	-3.34	0.000836664	0.037111375

<i>Lmbr1l</i>	490.99	-0.57	0.15	-3.90	9.77E-05	0.009204132
<i>Rapgef1</i>	6018.22	-0.56	0.12	-4.70	2.65E-06	0.00061092
<i>H2-Ab1</i>	749.37	-0.56	0.17	-3.25	0.001156074	0.046162734
<i>Man2a1</i>	1752.88	-0.56	0.14	-3.98	6.82E-05	0.006963332
<i>Jdp2</i>	233.25	-0.56	0.18	-3.17	0.001511427	0.055828961
<i>mt-Rnr2</i>	229449.99	-0.56	0.16	-3.54	0.000406286	0.023376222
<i>Elf4</i>	623.67	-0.55	0.18	-3.02	0.002548098	0.076070346
<i>H2-Q4</i>	850.29	-0.55	0.15	-3.59	0.000333863	0.021130209
<i>Trp53i11</i>	908.06	-0.55	0.16	-3.34	0.000844913	0.037111375
<i>Cidea</i>	609.18	-0.55	0.14	-4.04	5.35E-05	0.00583554
<i>H2-Aa</i>	1289.12	-0.54	0.18	-2.98	0.002888415	0.08282208
<i>Itpr1</i>	1740.11	-0.54	0.16	-3.48	0.000493996	0.026163211
<i>Dot1l</i>	3118.39	-0.54	0.11	-4.90	9.38E-07	0.000313
<i>Agtpbp1</i>	5019.66	-0.54	0.15	-3.71	0.000209173	0.015454618
<i>Clip2</i>	410.89	-0.54	0.15	-3.71	0.000203647	0.015220574
<i>Arhgef28</i>	318.03	-0.54	0.16	-3.39	0.000693313	0.033624365
<i>Dgkh</i>	183.04	-0.53	0.18	-3.02	0.002520578	0.075426647
<i>Gm16586</i>	1207.00	-0.53	0.14	-3.89	9.91E-05	0.009224395
<i>Lrrc8c</i>	1315.80	-0.53	0.16	-3.39	0.000708703	0.033779094
<i>Cenpa</i>	767.57	-0.53	0.17	-3.05	0.002323495	0.07138544
<i>Lgr6</i>	570.37	-0.53	0.15	-3.48	0.000492926	0.026163211
<i>Zc3h7a</i>	1755.30	-0.53	0.13	-4.15	3.38E-05	0.004077155
<i>Gm21781</i>	355.45	-0.52	0.17	-3.17	0.001515641	0.055828961
<i>Sat1</i>	978.70	-0.52	0.13	-4.16	3.19E-05	0.003964351
<i>Krba1</i>	1955.53	-0.52	0.13	-3.96	7.65E-05	0.007627772
<i>Srrm1</i>	4716.03	-0.52	0.11	-4.54	5.54E-06	0.001061854
<i>Cyth1</i>	2421.27	-0.52	0.13	-3.96	7.56E-05	0.007597792
<i>S100a9</i>	52.43	-0.52	0.18	-2.95	0.003178484	0.087304971
<i>Id1</i>	880.86	-0.52	0.13	-3.87	0.00010994	0.00994019
<i>Mbd1</i>	1059.90	-0.52	0.16	-3.31	0.000926505	0.039620596
<i>Ppip5k2</i>	8387.75	-0.51	0.16	-3.20	0.001368417	0.051860528
<i>Rusc1</i>	544.28	-0.51	0.14	-3.76	0.000167392	0.013495854
<i>Zhx3</i>	1416.61	-0.51	0.13	-3.94	8.01E-05	0.007916435
<i>Tspyl2</i>	836.20	-0.51	0.16	-3.23	0.00125494	0.049179659
<i>Rlf</i>	888.09	-0.51	0.15	-3.39	0.000700705	0.033779094
<i>Leng8</i>	6547.85	-0.51	0.14	-3.74	0.000184242	0.014307547
<i>Jag2</i>	1536.26	-0.51	0.18	-2.89	0.003796018	0.096485931
<i>Ggnbp1</i>	1581.64	-0.51	0.15	-3.43	0.000610098	0.030524197
<i>Mlxip</i>	3087.97	-0.50	0.14	-3.56	0.000375612	0.022321563

<i>Eif2ak4</i>	513.17	-0.50	0.16	-3.18	0.001469792	0.054772724
<i>Ubiad1</i>	675.14	-0.50	0.16	-3.12	0.001823766	0.061560626
<i>Max</i>	1331.19	-0.50	0.15	-3.32	0.000900813	0.038916367
<i>Sash1</i>	1871.36	-0.49	0.13	-3.85	0.000119596	0.010460889
<i>Ell2</i>	469.89	-0.49	0.15	-3.22	0.001280499	0.050026391
<i>Retsat</i>	1475.97	-0.49	0.14	-3.52	0.000432749	0.024345495
<i>Zbtb16</i>	5306.01	-0.49	0.16	-2.99	0.002823899	0.081979317
<i>Xpo6</i>	2716.85	-0.49	0.14	-3.57	0.000363441	0.021997483
<i>Gpr56</i>	2645.13	-0.48	0.17	-2.94	0.003335146	0.089097258
<i>Ldb2</i>	217.01	-0.48	0.17	-2.92	0.003456706	0.091156224
<i>Eogt</i>	900.01	-0.48	0.16	-3.08	0.002086179	0.066019027
<i>Cd300lg</i>	3445.79	-0.48	0.15	-3.30	0.000970764	0.041096742
<i>Sf3b1</i>	8411.41	-0.48	0.15	-3.25	0.001148352	0.046105404
<i>Fbxo31</i>	4031.70	-0.48	0.16	-2.92	0.003554983	0.092781382
<i>Atp6v1g1</i>	2184.79	-0.47	0.15	-3.26	0.001133521	0.045798782
<i>Colec11</i>	413.05	-0.47	0.16	-2.94	0.003245691	0.087778622
<i>Zfp236</i>	878.56	-0.47	0.13	-3.72	0.000200861	0.015133916
<i>Klf3</i>	579.74	-0.47	0.15	-3.07	0.002141583	0.066933714
<i>Esam</i>	2425.15	-0.47	0.13	-3.53	0.000420291	0.024013477
<i>Cox19</i>	1109.40	-0.47	0.12	-4.08	4.59E-05	0.005236127
<i>Lrch1</i>	862.39	-0.47	0.14	-3.24	0.001192941	0.047336198
<i>Cblb</i>	697.55	-0.47	0.15	-3.07	0.00214093	0.066933714
<i>2610203C20Rik</i>	669.15	-0.47	0.14	-3.35	0.000810113	0.03662288
<i>H2-K1</i>	3160.73	-0.46	0.14	-3.21	0.001348763	0.051331479
<i>Echdc2</i>	1538.87	-0.46	0.11	-4.26	2.09E-05	0.00287396
<i>Gse1</i>	1084.51	-0.46	0.15	-3.11	0.00184035	0.061627386
<i>Git1</i>	2333.22	-0.46	0.10	-4.41	1.03E-05	0.001714805
<i>Gm13479</i>	479.39	-0.46	0.15	-3.03	0.002407883	0.0730911
<i>Fam105b</i>	646.63	-0.46	0.14	-3.38	0.000725371	0.034132864
<i>Atp10d</i>	1170.22	-0.46	0.15	-3.12	0.001809904	0.061256051
<i>Dennd6b</i>	792.15	-0.45	0.16	-2.90	0.003698289	0.095342035
<i>2310002L09Rik</i>	1589.90	-0.45	0.14	-3.17	0.001538515	0.056284764
<i>Nktr</i>	3446.77	-0.45	0.13	-3.50	0.000469757	0.025880063
<i>Cnn3</i>	1581.46	-0.45	0.13	-3.36	0.000779675	0.035628603
<i>Icosl</i>	471.45	-0.45	0.13	-3.37	0.000758013	0.034890634
<i>Cdk18</i>	808.88	-0.45	0.13	-3.49	0.000489541	0.026161567
<i>Cdc42ep2</i>	365.12	-0.45	0.16	-2.87	0.004135889	0.099908562
<i>Slc20a1</i>	1314.11	-0.45	0.15	-3.04	0.002381004	0.072623477
<i>Bnip1</i>	697.66	-0.45	0.14	-3.08	0.002057048	0.065863541

<i>Smg1</i>	6854.41	-0.44	0.12	-3.77	0.000161407	0.013181258
<i>Nfia</i>	2154.40	-0.44	0.12	-3.78	0.000159781	0.013133181
<i>Preb</i>	1698.27	-0.44	0.12	-3.65	0.000266592	0.018142573
<i>Capn15</i>	443.71	-0.44	0.14	-3.19	0.001444228	0.054265631
<i>6720401G13Rik</i>	767.74	-0.44	0.14	-3.21	0.001331282	0.051331479
<i>Luc7l</i>	2070.28	-0.44	0.13	-3.42	0.000618992	0.030726266
<i>Rasip1</i>	1202.13	-0.44	0.14	-3.03	0.002480253	0.074928491
<i>Gpihbp1</i>	2360.26	-0.43	0.15	-2.88	0.003929199	0.098292092
<i>Aifm2</i>	1109.37	-0.43	0.12	-3.45	0.000558979	0.028302212
<i>Plcd1</i>	880.31	-0.43	0.14	-3.04	0.002377143	0.072623477
<i>Mlycd</i>	2749.46	-0.42	0.13	-3.27	0.001064685	0.043953701
<i>Snrpa1</i>	561.30	-0.42	0.14	-2.97	0.002997842	0.08458015
<i>Kmt2b</i>	1719.03	-0.42	0.13	-3.17	0.001536709	0.056284764
<i>Pear1</i>	1343.62	-0.42	0.14	-2.97	0.00293923	0.083794526
<i>S100pbp</i>	671.13	-0.42	0.14	-3.09	0.0020109	0.065099679
<i>Luc7l2</i>	9012.99	-0.42	0.13	-3.35	0.000819769	0.036801204
<i>Rapgef2</i>	1593.69	-0.42	0.12	-3.41	0.00065735	0.032502895
<i>Pnpla2</i>	9832.19	-0.42	0.12	-3.45	0.000569431	0.028716554
<i>Son</i>	16889.40	-0.41	0.11	-3.62	0.000292733	0.01940007
<i>Smpd2</i>	1023.11	-0.41	0.14	-2.88	0.004011172	0.09919225
<i>Cdk8</i>	674.42	-0.41	0.13	-3.15	0.001629387	0.057914055
<i>Myh14</i>	3849.70	-0.41	0.13	-3.18	0.001470156	0.054772724
<i>Zcchc7</i>	943.97	-0.41	0.14	-2.91	0.003656896	0.094467317
<i>Sned1</i>	1169.61	-0.41	0.13	-3.05	0.002289922	0.070697163
<i>Srsf4</i>	1089.77	-0.40	0.12	-3.32	0.000890637	0.038741195
<i>Piezo1</i>	1590.92	-0.40	0.13	-3.04	0.00239687	0.072931693
<i>Atraid</i>	961.22	-0.40	0.11	-3.52	0.000438179	0.024433778
<i>Rhbdf1</i>	1297.05	-0.40	0.13	-3.00	0.002668566	0.07837286
<i>Stxbp5</i>	867.58	-0.40	0.12	-3.19	0.00144474	0.054265631
<i>Id3</i>	1144.51	-0.40	0.12	-3.39	0.000711414	0.033779094
<i>1700021F05Rik</i>	1446.78	-0.39	0.12	-3.40	0.000683546	0.03327819
<i>Prpf39</i>	1310.26	-0.39	0.13	-2.96	0.003047621	0.085346877
<i>Pdlim7</i>	999.60	-0.39	0.12	-3.15	0.001644225	0.057973822
<i>Plbd1</i>	981.96	-0.39	0.12	-3.35	0.000799066	0.03637085
<i>Rbm39</i>	5499.13	-0.38	0.12	-3.28	0.001021169	0.042718985
<i>Metap1d</i>	1794.00	-0.38	0.12	-3.10	0.001963725	0.063945155
<i>Pcp4l1</i>	4514.44	-0.38	0.11	-3.49	0.000474754	0.025902735
<i>Ubr2</i>	6059.83	-0.38	0.11	-3.59	0.000329196	0.020939533
<i>Dock9</i>	2678.13	-0.38	0.10	-3.72	0.000200717	0.015133916

<i>Paxbp1</i>	1328.91	-0.38	0.13	-2.96	0.00311445	0.086451311
<i>Nus1</i>	2331.12	-0.38	0.12	-3.19	0.001409978	0.053276115
<i>Safb</i>	2514.00	-0.38	0.12	-3.21	0.00133453	0.051331479
<i>Srrm2</i>	14049.22	-0.37	0.11	-3.32	0.000906731	0.039038784
<i>Flt4</i>	847.53	-0.37	0.13	-2.87	0.004100594	0.099551072
<i>mt-Nd1</i>	1036154.25	-0.37	0.12	-2.99	0.002808161	0.081714265
<i>Atxn7</i>	1027.60	-0.37	0.12	-2.95	0.003156816	0.087246662
<i>Ilkap</i>	1055.65	-0.37	0.12	-2.93	0.00337066	0.089446151
<i>Iscu</i>	1732.67	-0.36	0.11	-3.15	0.00161238	0.057914055
<i>Phf1</i>	904.76	-0.36	0.11	-3.17	0.001543172	0.056292436
<i>Sbds</i>	1247.73	-0.36	0.11	-3.15	0.001653838	0.05815079
<i>Dicer1</i>	1705.57	-0.36	0.11	-3.12	0.001782459	0.060815
<i>Cxxc1</i>	1153.73	-0.36	0.12	-2.91	0.003581339	0.093097931
<i>Phc2</i>	1108.07	-0.36	0.12	-2.88	0.004018696	0.09919225
<i>Obscn</i>	53618.53	-0.36	0.11	-3.10	0.00194283	0.063710735
<i>Arglu1</i>	1398.28	-0.35	0.12	-2.90	0.003741638	0.095680109
<i>Adamtsl4</i>	2725.94	-0.35	0.12	-2.88	0.003914926	0.098216809
<i>Cirbp</i>	2182.28	-0.33	0.10	-3.17	0.001517235	0.055828961
<i>Qsox1</i>	1606.25	-0.33	0.10	-3.14	0.001718199	0.059423393
<i>Ncoa3</i>	2168.12	-0.33	0.11	-2.98	0.002840033	0.081979317
<i>Coq10a</i>	7453.95	-0.32	0.11	-2.87	0.004107025	0.099551072
<i>Eif5b</i>	4381.77	-0.31	0.10	-2.98	0.002901691	0.08291107
<i>Tnnt2</i>	223828.37	-0.30	0.10	-2.97	0.00301356	0.08458015
<i>Ddx50</i>	1751.35	-0.29	0.10	-2.88	0.00399073	0.099048354
<i>Aff1</i>	2974.06	-0.28	0.10	-2.87	0.004113226	0.099551072

4X4 DESIGN, UPREGULATED (VS. ES-)						
Gene	Base Mean	log2 Fold Change	LFC SE	stat	p-value	p-adj
<i>Gm14267</i>	62.89	2.66	0.53	5.07	3.95E-07	0.001986964
<i>Bend6</i>	59.20	2.46	0.49	5.03	4.90E-07	0.001986964
<i>Clspn</i>	17.71	2.41	0.57	4.23	2.34E-05	0.031600024
<i>Kntc1</i>	19.61	2.34	0.43	5.50	3.81E-08	0.000309468
<i>Cacng6</i>	42.82	2.33	0.54	4.32	1.57E-05	0.024300552
<i>Top2a</i>	105.19	1.79	0.39	4.61	3.96E-06	0.012852781
<i>Mki67</i>	193.90	1.59	0.38	4.15	3.34E-05	0.038764139
<i>Brca1</i>	20.19	1.57	0.39	4.04	5.41E-05	0.049851989
<i>Rrm2</i>	72.25	1.21	0.29	4.19	2.81E-05	0.035129102
<i>Mcm5</i>	106.56	0.97	0.22	4.47	7.67E-06	0.016098641

4X4 DESIGN, DOWNREGULATED (VS. ES-)						
Gene	Base Mean	log2 Fold Change	LFC SE	stat	p-value	p-adj
<i>Gm17428</i>	301.55	-1.11	0.26	-4.31	1.65E-05	0.024300552

3X3 DESIGN, UPREGULATED (VS. ES-)						
Gene	Base Mean	log2 Fold Change	LFC SE	stat	p-value	p-adj
<i>Adipoq</i>	33.44	3.68	0.93	3.95	7.74E-05	0.027545686
<i>Cidec</i>	37.89	3.21	0.86	3.74	0.000182646	0.045925968
<i>Bend6</i>	72.88	2.76	0.41	6.67	2.59E-11	3.78E-07
<i>Gm14267</i>	59.54	2.19	0.55	3.96	7.61E-05	0.027545686
<i>Kntc1</i>	18.58	2.07	0.55	3.75	0.000175814	0.045837818
<i>Top2a</i>	114.14	1.54	0.37	4.21	2.55E-05	0.016907492
<i>Zfp111</i>	98.88	1.11	0.27	4.12	3.76E-05	0.021083213
<i>Hipk2</i>	1400.54	1.06	0.20	5.32	1.05E-07	0.000510908
<i>8430408G22Rik</i>	2279.86	1.00	0.23	4.41	1.04E-05	0.008654143
<i>Enc1</i>	277.50	0.96	0.25	3.77	0.000160359	0.043308757
<i>Slc8a1</i>	3964.08	0.85	0.22	3.81	0.00013835	0.03806986

3X3 DESIGN, DOWNREGULATED (VS. ES-)						
Gene	Base Mean	log2 Fold Change	LFC SE	stat	p-value	p-adj
<i>Wt1</i>	246.80	-1.61	0.38	-4.27	1.93E-05	0.014083824
<i>Gm17428</i>	297.74	-1.33	0.28	-4.69	2.80E-06	0.004082264
<i>Tmc8</i>	191.05	-1.07	0.28	-3.85	0.000119603	0.036339233
<i>Tcf15</i>	262.25	-1.06	0.24	-4.39	1.15E-05	0.008858741
<i>Dennd3</i>	619.86	-0.94	0.25	-3.74	0.00018115	0.045925968
<i>Vwa3a</i>	385.46	-0.94	0.21	-4.49	7.15E-06	0.007452371
<i>Sox18</i>	817.16	-0.93	0.20	-4.70	2.65E-06	0.004082264
<i>Lrrc32</i>	543.67	-0.90	0.22	-4.19	2.79E-05	0.017065072
<i>D830015G02Rik</i>	2521.82	-0.85	0.19	-4.47	7.96E-06	0.007737076
<i>Lama5</i>	11241.92	-0.83	0.18	-4.54	5.70E-06	0.006933009
<i>Nova2</i>	586.41	-0.81	0.20	-4.04	5.38E-05	0.023255103

APPENDIX B

**TRANSCRIPTOMIC ANALYSIS OF GENE ONTOLOGY FOR BIOLOGICAL
PROCESSES AND CELLULAR COMPONENTS**

Biological Processes

Annotation Cluster	Enrichment Score	Term	Count	FDR
1	7.38	GO:0019438~aromatic compound biosynthetic process	150	4.12E-05
		GO:0018130~heterocycle biosynthetic process	149	5.71E-05
		GO:1901362~organic cyclic compound biosynthetic process	150	2.25E-04
2	5.29	GO:0006355~regulation of transcription, DNA-templated	124	0.009322252
		GO:1903506~regulation of nucleic acid-templated transcription	124	0.009845196
		GO:2001141~regulation of RNA biosynthetic process	124	0.010723354
3	3.54	GO:0010631~epithelial cell migration	17	0.461948317
		GO:0090132~epithelium migration	17	0.535003306
		GO:0090130~tissue migration	17	0.704350162
4	3.35	GO:0050768~negative regulation of neurogenesis	20	0.293857287
		GO:0051961~negative regulation of nervous system development	20	0.722978002
		GO:0010721~negative regulation of cell development	20	3.00662103
5	3.33	GO:0030516~regulation of axon extension	11	0.460079618
		GO:0061387~regulation of extent of cell growth	11	1.181816001
		GO:0048675~axon extension	11	1.348868357
6	3.06	GO:0045892~negative regulation of transcription, DNA-templated	49	1.27738135
		GO:1903507~negative regulation of nucleic acid-templated transcription	49	1.63903664
		GO:1902679~negative regulation of RNA biosynthetic process	49	2.118397343
7	2.53	GO:0021785~branchiomotor neuron axon guidance	4	3.948291323
		GO:1902287~semaphorin-plexin signaling pathway involved in axon guidance	4	6.514767341
		GO:1902285~semaphorin-plexin signaling pathway involved in neuron	4	6.514767341

		projection guidance		
8	2.39	GO:0045893~positive regulation of transcription, DNA-templated	50	6.132635449
		GO:1903508~positive regulation of nucleic acid-templated transcription	50	6.132635449
		GO:1902680~positive regulation of RNA biosynthetic process	50	6.488679468
		GO:0051254~positive regulation of RNA metabolic process	50	13.19305885
9	2.37	GO:0003174~mitral valve development	5	0.412262417
		GO:0003171~atrioventricular valve development	5	7.449537765
		GO:0003179~heart valve morphogenesis	5	25.15759726
		GO:0003170~heart valve development	5	39.71527908
10	2.28	GO:0030802~regulation of cyclic nucleotide biosynthetic process	10	5.30547849
		GO:1900371~regulation of purine nucleotide biosynthetic process	10	8.04360705
		GO:0030808~regulation of nucleotide biosynthetic process	10	8.447285206
		GO:0052652~cyclic purine nucleotide metabolic process	10	14.47608974
		GO:0009190~cyclic nucleotide biosynthetic process	10	15.70383606
11	1.94	GO:0030804~positive regulation of cyclic nucleotide biosynthetic process	8	9.551715268
		GO:0030810~positive regulation of nucleotide biosynthetic process	8	13.47009648
		GO:1900373~positive regulation of purine nucleotide biosynthetic process	8	13.47009648
		GO:0030801~positive regulation of cyclic nucleotide metabolic process	8	15.76970825
		GO:1900544~positive regulation of purine nucleotide metabolic process	8	44.03606339
		GO:0045981~positive regulation of nucleotide metabolic process	8	44.03606339
12	1.85	GO:0001946~lymphangiogenesis	4	18.56762729
		GO:0036303~lymph vessel morphogenesis	4	18.56762729
		GO:0001945~lymph vessel development	4	38.69998027

13	1.70	GO:0030817~regulation of cAMP biosynthetic process	8	24.01849961
		GO:0006171~cAMP biosynthetic process	8	32.87515674
		GO:0030814~regulation of cAMP metabolic process	8	41.48375142
14	1.70	GO:0010743~regulation of macrophage derived foam cell differentiation	4	23.843344
		GO:0010742~macrophage derived foam cell differentiation	4	35.60932061
		GO:0090077~foam cell differentiation	4	38.69998027
15	1.70	GO:0006486~protein glycosylation	13	30.61216924
		GO:0043413~macromolecule glycosylation	13	30.61216924
		GO:0070085~glycosylation	13	35.89070734
16	1.56	GO:0060923~cardiac muscle cell fate commitment	3	25.59321025
		GO:0060911~cardiac cell fate commitment	3	48.28127084
		GO:0042693~muscle cell fate commitment	3	53.65104186
17	1.38	GO:0021636~trigeminal nerve morphogenesis	3	15.04498761
		GO:0021637~trigeminal nerve structural organization	3	15.04498761
		GO:0021559~trigeminal nerve development	3	36.99397393
		GO:0021612~facial nerve structural organization	3	36.99397393
		GO:0021561~facial nerve development	3	42.70240489
		GO:0021610~facial nerve morphogenesis	3	42.70240489
		GO:0021604~cranial nerve structural organization	3	53.65104186
		GO:0021783~preganglionic parasympathetic fiber development	3	72.03253246
		GO:0048486~parasympathetic nervous system development	3	82.03277774
		GO:0048532~anatomical structure arrangement	3	86.98307552
		GO:0021602~cranial nerve	3	93.56199482

		morphogenesis		
		GO:0021545~cranial nerve development	3	99.94184676

Cellular Component

Annotation Cluster	Enrichment Score	Term	Count	FDR
1	1.80	GO:0071004~U2-type prespliceosome	4	7.81
		GO:0071010~prespliceosome	4	16.29
		GO:0005684~U2-type spliceosomal complex	4	60.37
2	1.55	GO:0014069~postsynaptic density	12	29.89
		GO:0099572~postsynaptic specialization	12	29.89
		GO:0060076~excitatory synapse	12	45.52
3	1.39	GO:0005923~bicellular tight junction	8	38.81
		GO:0070160~occluding junction	8	42.10
		GO:0043296~apical junction complex	8	57.68
4	1.37	GO:0005925~focal adhesion	16	44.70
		GO:0005924~cell-substrate adherens junction	16	47.41
		GO:0030055~cell-substrate junction	16	51.11
5	1.09	GO:0097517~contractile actin filament bundle	5	65.39
		GO:0001725~stress fiber	5	65.39
		GO:0032432~actin filament bundle	5	75.99
		GO:0042641~actomyosin	5	78.62
6	0.35	GO:1902554~serine/threonine protein kinase complex	4	99.25
		GO:1902911~protein kinase complex	4	99.83
		GO:0061695~transferase complex, transferring phosphorus-containing groups	4	100.00
7	0.05	GO:0034702~ion channel complex	5	100.00
		GO:1902495~transmembrane transporter complex	5	100.00
		GO:1990351~transporter complex	5	100.00

APPENDIX C

**mRNA-SEQ DATA, GENES WITH DIFFERENTIAL EXPRESSION BETWEEN ES+/- IN 3M AND
NONTRANSGENIC MOUSE HEART TISSUE**

UPREGULATED (COMPARED TO ES-)							
	Base Mean	log2 Fold Change	Fold Change	LFC SE	stat	p-value	p-adj
<i>Mrps24</i>	513.21	0.45	1.36	0.09	4.97	6.80729E-07	0.002
<i>Nr2f6</i>	271.98	0.41	1.33	0.10	4.15	3.32984E-05	0.020
<i>1810043H04Rik</i>	203.11	0.40	1.32	0.10	4.04	5.333E-05	0.025
<i>2310036022Rik</i>	321.57	0.40	1.32	0.10	4.02	5.85615E-05	0.025
<i>Pgp</i>	165.88	0.38	1.30	0.10	3.75	0.000177684	0.039
<i>0610012G03Rik</i>	162.51	0.38	1.30	0.10	3.74	0.000185658	0.039
<i>H2afj</i>	100.93	0.37	1.30	0.10	3.65	0.000258419	0.042
<i>Chchd10</i>	5069.14	0.35	1.28	0.08	4.47	7.77457E-06	0.010
<i>Cox5b</i>	3794.96	0.34	1.27	0.09	3.66	0.000251441	0.042
<i>Atp5d</i>	5382.00	0.34	1.27	0.07	4.82	1.43708E-06	0.003
<i>Fdx1</i>	428.88	0.34	1.27	0.09	3.95	7.82789E-05	0.028
<i>Nkx2-5</i>	336.37	0.34	1.26	0.10	3.38	0.000717289	0.072
<i>Coa6</i>	187.73	0.34	1.26	0.09	3.57	0.000357334	0.050
<i>Gadd45gip1</i>	359.01	0.34	1.26	0.08	4.15	3.35312E-05	0.020
<i>Irx3</i>	236.18	0.33	1.26	0.10	3.26	0.001125823	0.090
<i>Gadd45b</i>	115.53	0.33	1.26	0.10	3.28	0.001053913	0.090
<i>Mrpl34</i>	395.22	0.33	1.26	0.09	3.53	0.000410713	0.054
<i>Ndufab1</i>	2897.10	0.33	1.25	0.07	4.94	7.96564E-07	0.002
<i>Malsu1</i>	193.37	0.33	1.25	0.09	3.60	0.000323429	0.050
<i>Ssbp4</i>	184.96	0.32	1.25	0.10	3.22	0.001261489	0.091
<i>Uqcrcq</i>	5111.25	0.32	1.25	0.08	4.03	5.67306E-05	0.025
<i>Prob1</i>	348.04	0.31	1.24	0.09	3.45	0.000553282	0.065
<i>Endog</i>	312.16	0.31	1.24	0.10	3.26	0.001101759	0.090
<i>Ptpla</i>	379.35	0.31	1.24	0.08	3.96	7.4714E-05	0.028
<i>Spint2</i>	199.36	0.31	1.24	0.08	3.81	0.000138358	0.035
<i>Kcng2</i>	754.88	0.31	1.24	0.09	3.52	0.000433722	0.056
<i>Bola3</i>	1347.29	0.30	1.23	0.07	4.23	2.3051E-05	0.018
<i>Fth1</i>	19755.98	0.30	1.23	0.08	3.68	0.000228813	0.042
<i>Mpc2</i>	3438.32	0.30	1.23	0.08	3.91	9.16823E-05	0.032
<i>Fbxl22</i>	511.97	0.30	1.23	0.10	3.16	0.001594546	0.100
<i>Rps2</i>	4005.23	0.30	1.23	0.08	3.81	0.000138308	0.035
<i>Cox5a</i>	9512.73	0.30	1.23	0.08	3.82	0.000134421	0.035
<i>Emc6</i>	525.06	0.29	1.23	0.08	3.58	0.00034464	0.050
<i>Ankrd9</i>	368.55	0.29	1.23	0.09	3.36	0.000791161	0.076
<i>N6amt1</i>	290.48	0.29	1.22	0.08	3.74	0.000183729	0.039

<i>1500011K16Rik</i>	308.97	0.29	1.22	0.08	3.53	0.000418669	0.054
<i>Lsm4</i>	340.61	0.29	1.22	0.09	3.23	0.001246318	0.091
<i>Grb14</i>	1824.42	0.29	1.22	0.08	3.82	0.000131624	0.035
<i>Chchd7</i>	573.04	0.29	1.22	0.08	3.67	0.000245514	0.042
<i>Rabac1</i>	1059.49	0.29	1.22	0.08	3.66	0.000255963	0.042
<i>Spryd7</i>	604.44	0.29	1.22	0.06	4.58	4.71074E-06	0.007
<i>1810022K09Rik</i>	156.91	0.29	1.22	0.09	3.16	0.001597061	0.100
<i>Alkbh7</i>	302.60	0.29	1.22	0.09	3.15	0.001612798	0.100
<i>Tma7</i>	350.80	0.28	1.22	0.08	3.71	0.00020996	0.040
<i>Pgls</i>	323.68	0.28	1.22	0.09	3.16	0.001581365	0.100
<i>Fam195a</i>	915.20	0.28	1.22	0.08	3.57	0.000352839	0.050
<i>Fxn</i>	221.03	0.28	1.21	0.09	3.15	0.001617219	0.100
<i>Cacybp</i>	850.79	0.28	1.21	0.07	4.28	1.90692E-05	0.016
<i>Yeats4</i>	251.75	0.28	1.21	0.09	3.21	0.001322471	0.093
<i>Gng5</i>	456.74	0.28	1.21	0.07	3.90	9.5844E-05	0.032
<i>Fam174a</i>	534.50	0.28	1.21	0.08	3.38	0.000721302	0.072
Hopx	3170.77	0.27	1.21	0.05	5.42	5.8051E-08	0.001
<i>Tesc</i>	955.23	0.27	1.21	0.08	3.34	0.000844477	0.078
<i>Cisd1</i>	1944.38	0.27	1.21	0.07	4.15	3.36687E-05	0.020
2310002L09Rik	657.63	0.27	1.21	0.08	3.44	0.000586951	0.067
<i>Uqcc2</i>	927.24	0.27	1.21	0.07	3.72	0.000202215	0.039
<i>Ppp1r14c</i>	2019.16	0.27	1.20	0.06	4.36	1.32608E-05	0.013
<i>Hspb2</i>	596.51	0.26	1.20	0.08	3.38	0.000721673	0.072
<i>Pdcd5</i>	756.57	0.26	1.20	0.08	3.29	0.000985675	0.090
<i>Ola1</i>	509.27	0.26	1.20	0.06	4.08	4.46097E-05	0.025
<i>Cox14</i>	847.28	0.26	1.20	0.07	3.63	0.000280756	0.045
<i>Tarsl2</i>	512.81	0.26	1.19	0.08	3.36	0.000774941	0.076
<i>C1d</i>	583.54	0.25	1.19	0.07	3.81	0.000141633	0.035
<i>Ndufv2</i>	5750.79	0.25	1.19	0.06	4.19	2.84454E-05	0.020
<i>mt-Nd1</i>	613948.83	0.25	1.19	0.07	3.49	0.000484953	0.059
<i>Rbm24</i>	2246.53	0.25	1.19	0.06	4.34	1.40872E-05	0.013
<i>Mrpl54</i>	419.84	0.25	1.19	0.07	3.54	0.000397672	0.054
<i>Zcrb1</i>	872.42	0.25	1.19	0.07	3.70	0.000218974	0.041
<i>Slc25a3</i>	16515.97	0.25	1.19	0.07	3.45	0.000557793	0.065
<i>Pcbp4</i>	481.77	0.24	1.18	0.08	3.26	0.001102461	0.090
<i>Mrpl55</i>	643.31	0.24	1.18	0.07	3.35	0.000817364	0.078
<i>Snapin</i>	828.94	0.24	1.18	0.06	3.72	0.000197217	0.039
<i>Ndufa12</i>	1766.33	0.24	1.18	0.07	3.41	0.000649185	0.070
<i>Ube2m</i>	1137.98	0.23	1.18	0.06	3.80	0.000142783	0.035

<i>Ckm</i>	21160.09	0.23	1.17	0.07	3.27	0.001092351	0.090
<i>Uqcrfs1</i>	9131.38	0.23	1.17	0.06	3.59	0.000334051	0.050
<i>Ndufa6</i>	2794.21	0.23	1.17	0.07	3.34	0.000825672	0.078
<i>Atp5g3</i>	15755.88	0.23	1.17	0.07	3.24	0.001178847	0.091
<i>Atp5c1</i>	15857.68	0.22	1.17	0.07	3.27	0.001077887	0.090
<i>Stau2</i>	793.08	0.22	1.17	0.07	3.34	0.00084474	0.078
<i>Ndfip1</i>	966.22	0.22	1.16	0.06	3.89	0.000101288	0.033
<i>Timm23</i>	885.06	0.22	1.16	0.07	3.26	0.001128781	0.090
<i>Ndufb8</i>	4432.65	0.22	1.16	0.07	3.20	0.001351516	0.093
<i>Pkig</i>	1659.83	0.21	1.16	0.06	3.43	0.000593081	0.067
<i>Vbp1</i>	651.75	0.21	1.16	0.06	3.38	0.000721402	0.072
<i>Nudt19</i>	668.90	0.21	1.16	0.07	3.19	0.001422157	0.094
<i>Dym</i>	905.58	0.21	1.16	0.06	3.82	0.00013513	0.035
<i>Pebp1</i>	2360.39	0.21	1.16	0.07	3.21	0.00134624	0.093
<i>Gcsh</i>	684.08	0.21	1.16	0.06	3.38	0.000723186	0.072
<i>Serbp1</i>	2889.68	0.21	1.16	0.05	4.03	5.6694E-05	0.025
<i>Ifngr2</i>	2092.40	0.21	1.15	0.06	3.42	0.000621321	0.069
<i>Psmb4</i>	1237.46	0.21	1.15	0.06	3.28	0.001050272	0.090
<i>Gbas</i>	9755.37	0.21	1.15	0.04	4.74	2.14132E-06	0.004
<i>Eci1</i>	2428.95	0.21	1.15	0.06	3.51	0.00045388	0.057
<i>Acyp2</i>	1019.12	0.20	1.15	0.06	3.16	0.001581866	0.100
<i>Tmem70</i>	1161.63	0.20	1.15	0.06	3.21	0.001341295	0.093
<i>Fam96a</i>	612.90	0.20	1.15	0.06	3.20	0.001366234	0.093
<i>Set</i>	677.23	0.20	1.15	0.06	3.25	0.00115368	0.090
<i>Mrps9</i>	800.64	0.20	1.15	0.06	3.65	0.000260645	0.042
<i>Rheb</i>	1044.21	0.20	1.15	0.05	3.74	0.000184791	0.039
<i>Mrpl33</i>	856.31	0.20	1.15	0.06	3.25	0.001161157	0.090
<i>Sod2</i>	7082.57	0.19	1.14	0.05	3.79	0.000150072	0.036
<i>Sub1</i>	625.79	0.19	1.14	0.06	3.28	0.001053952	0.090
<i>Sod1</i>	1900.37	0.19	1.14	0.06	3.23	0.001224736	0.091
<i>mt-Nd4</i>	697675.37	0.19	1.14	0.05	3.81	0.000139131	0.035
<i>Poldip2</i>	1429.26	0.18	1.13	0.05	3.41	0.000641797	0.070
Tsc22d4	1612.19	0.18	1.13	0.06	3.28	0.001043619	0.090
<i>Tcea3</i>	1265.23	0.18	1.13	0.05	3.38	0.00072711	0.072
<i>Cfl2</i>	4866.92	0.18	1.13	0.05	3.78	0.000159188	0.037
<i>Tspan3</i>	2011.20	0.17	1.13	0.05	3.41	0.000649999	0.070
<i>Dmpk</i>	4671.57	0.16	1.12	0.05	3.17	0.001509759	0.097
<i>Nudt3</i>	1712.97	0.15	1.11	0.05	3.22	0.001268174	0.091

DOWNREGULATED (COMPARED TO ES-)							
	Base Mean	log2 Fold Change	Fold Change	Lfc SE	stat	p-value	p-adj
<i>Cyth4</i>	143.40	-0.36	0.78	0.09	-3.99	6.64792E-05	0.027
<i>4632428N05Rik</i>	561.36	-0.35	0.78	0.09	-3.86	0.000115107	0.035
<i>Ggta1</i>	518.15	-0.35	0.79	0.10	-3.49	0.000479124	0.059
<i>Aoc3</i>	277.64	-0.34	0.79	0.08	-4.04	5.38141E-05	0.025
<i>Vwa3a</i>	202.39	-0.34	0.79	0.09	-3.65	0.000261035	0.042
<i>Slc9a9</i>	105.29	-0.33	0.79	0.10	-3.45	0.000551036	0.065
<i>Gbp6</i>	369.33	-0.33	0.80	0.09	-3.55	0.000383651	0.053
<i>Bcl6b</i>	438.54	-0.32	0.80	0.10	-3.26	0.001109537	0.090
<i>Emr1</i>	312.38	-0.31	0.80	0.09	-3.45	0.000561022	0.065
<i>Adcy7</i>	290.22	-0.31	0.81	0.09	-3.60	0.000313273	0.049
<i>Baz1a</i>	145.73	-0.31	0.81	0.09	-3.40	0.000676964	0.072
<i>Atp2b4</i>	751.77	-0.30	0.81	0.07	-4.36	1.30033E-05	0.013
<i>Fcgr3</i>	288.36	-0.29	0.82	0.09	-3.24	0.001207923	0.091
<i>Rasa4</i>	147.12	-0.29	0.82	0.09	-3.19	0.001421496	0.094
<i>Col5a2</i>	774.09	-0.28	0.82	0.08	-3.50	0.000463807	0.058
<i>Zfp646</i>	346.45	-0.28	0.82	0.09	-3.25	0.001142196	0.090
<i>Peg3</i>	269.70	-0.28	0.83	0.09	-3.18	0.00147959	0.097
<i>Fcgr2b</i>	219.02	-0.28	0.83	0.09	-3.22	0.001282436	0.092
<i>Slco2b1</i>	522.23	-0.27	0.83	0.07	-3.75	0.000177107	0.039
<i>Tmem140</i>	665.07	-0.27	0.83	0.08	-3.21	0.001311655	0.093
<i>Arap1</i>	430.27	-0.26	0.83	0.07	-3.97	7.08327E-05	0.028
<i>Cd38</i>	327.24	-0.25	0.84	0.08	-3.23	0.001255577	0.091
<i>C1qtnf1</i>	324.00	-0.24	0.84	0.07	-3.26	0.001096399	0.090
<i>F830016B08Rik</i>	175.18	-0.24	0.85	0.07	-3.25	0.001153399	0.090
<i>Sp100</i>	571.96	-0.24	0.85	0.08	-3.18	0.001449835	0.096
<i>Ctso</i>	347.12	-0.24	0.85	0.07	-3.27	0.001075614	0.090
<i>Fn1</i>	1263.45	-0.23	0.85	0.07	-3.54	0.000407344	0.054
<i>Pros1</i>	588.49	-0.23	0.85	0.07	-3.59	0.000333144	0.050
<i>Thbd</i>	1196.31	-0.23	0.85	0.07	-3.31	0.000933647	0.086
<i>Laptm5</i>	454.57	-0.23	0.85	0.07	-3.37	0.000738502	0.073
<i>Ly6e</i>	2852.97	-0.23	0.85	0.06	-3.72	0.000199242	0.039
<i>Map3k3</i>	714.84	-0.22	0.86	0.07	-3.18	0.001496819	0.097
<i>Kmt2e</i>	1116.50	-0.22	0.86	0.06	-3.67	0.000242295	0.042
<i>Nfatc3</i>	521.12	-0.22	0.86	0.07	-3.23	0.001234348	0.091
<i>Arrb1</i>	674.75	-0.22	0.86	0.07	-3.27	0.001059927	0.090

<i>Lrp1</i>	2771.12	-0.21	0.87	0.06	-3.20	0.001382734	0.093
<i>Marf1</i>	941.68	-0.20	0.87	0.06	-3.58	0.000340202	0.050
<i>Lyz2</i>	2963.67	-0.20	0.87	0.06	-3.17	0.001509569	0.097
<i>Col1a2</i>	2179.60	-0.19	0.88	0.06	-3.23	0.001247863	0.091
<i>Eef1a1</i>	10679.17	-0.18	0.88	0.06	-3.20	0.001377545	0.093

UPREGULATED (COMPARED TO NONTRANSGENIC)							
	Base Mean	log2 Fold Change	Fold Change	LFC SE	stat	p-value	p-adj
<i>Nfkbia</i>	2513.91	1.51	2.84	0.10	14.75	2.89E-49	3.84E-45
<i>Slc17a7</i>	282.61	0.75	1.68	0.09	8.42	3.68E-17	1.63E-13
<i>Slc16a6</i>	172.49	0.63	1.55	0.10	6.37	1.94E-10	6.46E-07
<i>Lad1</i>	45.35	0.41	1.33	0.10	4.00	6.33E-05	0.030
<i>Snai3</i>	52.30	0.40	1.32	0.10	3.96	7.55E-05	0.033
<i>Scgb1c1</i>	133.80	0.40	1.32	0.10	3.93	8.34E-05	0.034
<i>Dixdc1</i>	205.20	0.38	1.30	0.10	3.84	0.000125199	0.046
<i>Ano10</i>	978.90	0.38	1.30	0.08	4.55	5.47E-06	0.007
<i>Sh3rf2</i>	334.30	0.36	1.29	0.10	3.75	0.000177082	0.056
<i>Gnb3</i>	112.41	0.36	1.29	0.10	3.59	0.000331175	0.080
<i>Itgb6</i>	179.53	0.36	1.28	0.10	3.51	0.000444196	0.092
<i>Rasd2</i>	79.17	0.36	1.28	0.10	3.50	0.000465678	0.092
<i>Gm26795</i>	85.62	0.35	1.27	0.10	3.47	0.000529893	0.098
<i>Sema6a</i>	353.02	0.34	1.27	0.10	3.48	0.00050404	0.097
<i>Kcnv2</i>	257.63	0.34	1.26	0.08	4.03	5.63E-05	0.028
<i>AW209491</i>	174.68	0.34	1.26	0.09	3.89	9.83E-05	0.038
<i>Hebp1</i>	111.83	0.33	1.26	0.09	3.48	0.000496312	0.097
<i>Cers4</i>	452.41	0.31	1.24	0.07	4.32	1.55E-05	0.013
<i>Adcy5</i>	1034.51	0.29	1.22	0.06	4.51	6.63E-06	0.007
<i>Hsbp1</i>	1426.58	0.28	1.22	0.06	4.42	9.79E-06	0.009
<i>Asb11</i>	1817.60	0.26	1.20	0.07	3.60	0.000320257	0.079
<i>Eya3</i>	492.99	0.25	1.19	0.07	3.47	0.000528819	0.098
<i>Intu</i>	523.27	0.25	1.19	0.07	3.54	0.000400539	0.089
<i>Ipo13</i>	810.91	0.24	1.18	0.07	3.54	0.00039394	0.089
<i>Pde4dip</i>	25464.20	0.20	1.15	0.06	3.47	0.000525388	0.098
<i>Tmem109</i>	1547.61	0.19	1.14	0.05	3.81	0.000141491	0.050

DOWNREGULATED (COMPARED TO NONTRANSGENIC)							
	Base Mean	log2 Fold Change	Fold Change	LFC SE	stat	p-value	p-adj
<i>Cdh13</i>	1929.93	-0.56	0.68	0.06	-8.99	2.53E-19	1.68E-15
<i>Nfkb2</i>	232.89	-0.52	0.70	0.08	-6.30	2.95E-10	7.83E-07
<i>Nfkbib</i>	164.00	-0.48	0.72	0.09	-5.29	1.21E-07	0.0002
<i>Adamtsl4</i>	435.23	-0.46	0.72	0.08	-6.03	1.68E-09	3.72E-06
<i>Myl1</i>	292.67	-0.43	0.74	0.10	-4.43	9.35E-06	0.009
2310036O22Rik	321.57	-0.42	0.75	0.10	-4.22	2.46E-05	0.016
<i>Crlf2</i>	58.83	-0.40	0.76	0.10	-4.16	3.20E-05	0.019
1810043H04Rik	203.11	-0.40	0.76	0.10	-3.99	6.69E-05	0.031
<i>Vac14</i>	225.62	-0.39	0.76	0.09	-4.57	4.88E-06	0.007
<i>Fam81a</i>	100.42	-0.38	0.77	0.10	-3.78	0.000157455	0.052
<i>Lrrc4b</i>	86.25	-0.38	0.77	0.10	-3.71	0.000206321	0.062
<i>Traf3</i>	305.49	-0.38	0.77	0.08	-4.58	4.76E-06	0.007
<i>Fscn1</i>	453.65	-0.37	0.77	0.09	-4.07	4.71E-05	0.024
<i>Sox18</i>	518.47	-0.37	0.77	0.10	-3.79	0.000152775	0.052
0610012G03Rik	162.51	-0.37	0.78	0.10	-3.60	0.000313695	0.079
Nkx2-5	336.37	-0.37	0.78	0.10	-3.64	0.000269931	0.071
<i>Scarf2</i>	103.15	-0.36	0.78	0.10	-3.51	0.000451827	0.092
Gadd45gip1	359.01	-0.36	0.78	0.08	-4.42	1.01E-05	0.009
<i>mt-Tl1</i>	412.43	-0.36	0.78	0.10	-3.70	0.000216602	0.063
<i>Tnip1</i>	335.34	-0.35	0.78	0.08	-4.29	1.82E-05	0.013
<i>Lrp11</i>	33.86	-0.35	0.78	0.10	-3.50	0.00045836	0.092
<i>Gas1</i>	350.76	-0.35	0.78	0.09	-3.84	0.00012293	0.046
Nr2f6	271.98	-0.35	0.78	0.10	-3.54	0.000396599	0.089
<i>Jund</i>	480.93	-0.35	0.79	0.09	-3.70	0.000214464	0.063
<i>Nfic</i>	1584.99	-0.34	0.79	0.08	-4.24	2.24E-05	0.015
<i>Ier5l</i>	34.12	-0.34	0.79	0.09	-3.94	8.09E-05	0.034
<i>Hnrnpa0</i>	720.76	-0.34	0.79	0.09	-3.64	0.000268257	0.071
<i>Ckb</i>	381.57	-0.33	0.80	0.08	-4.09	4.37E-05	0.023
<i>Grk5</i>	516.91	-0.33	0.80	0.08	-4.13	3.65E-05	0.020
<i>mt-Ta</i>	20.50	-0.32	0.80	0.08	-3.73	0.000187942	0.058
<i>Edf1</i>	869.29	-0.31	0.81	0.08	-3.93	8.53E-05	0.034
<i>Mvp</i>	560.23	-0.29	0.82	0.07	-4.15	3.28E-05	0.019
2310002L09Rik	657.63	-0.29	0.82	0.08	-3.68	0.000230356	0.064
<i>Ccnd1</i>	1149.72	-0.29	0.82	0.08	-3.77	0.000160252	0.052
Chchd10	5069.14	-0.28	0.82	0.08	-3.58	0.000344632	0.082

<i>Gltscr2</i>	1020.22	-0.26	0.83	0.08	-3.51	0.000442672	0.092
<i>Slc30a1</i>	529.03	-0.26	0.83	0.07	-3.51	0.000446578	0.092
<i>Parp3</i>	491.38	-0.26	0.83	0.07	-3.69	0.000221202	0.063
<i>Pfn1</i>	1438.12	-0.25	0.84	0.07	-3.62	0.000292562	0.075
<i>Tsc22d4</i>	1612.19	-0.25	0.84	0.06	-4.52	6.13E-06	0.007
<i>Rasip1</i>	510.29	-0.25	0.84	0.07	-3.52	0.000439225	0.092
<i>Tnxb</i>	1355.19	-0.24	0.85	0.05	-4.31	1.62E-05	0.013
<i>mt-Tt</i>	17.46	-0.23	0.85	0.06	-3.82	0.000131884	0.047
<i>Plec</i>	3143.84	-0.22	0.86	0.06	-3.54	0.000393872	0.089
<i>Hopx</i>	3170.77	-0.22	0.86	0.05	-4.29	1.81E-05	0.013
<i>Rhoa</i>	2648.59	-0.16	0.89	0.04	-3.64	0.000272161	0.071

APPENDIX D

miRNA-SEQ DATA, miRs WITH DIFFERENTIAL EXPRESSION BETWEEN ES+/- AND DIANA

ANALYSIS OF miRNA KEGG PATHWAYS

microRNA	Base Mean	Log2 Fold Change	LFC SE	stat	p-value	p-adj
mmu-miR-10b-5p	1007.1389	-1.1099	0.2414	-4.5985	4.25E-06	0.0032
mmu-let-7b-5p	2496.0362	-0.7927	0.2251	-3.5209	0.0004	0.1623
mmu-let-7c-5p	10023.3897	-0.6618	0.2208	-2.9972	0.0027	0.6857
mmu-miR-379-5p	80.3620	-0.5750	0.2804	-2.0510	0.0403	0.9848
mmu-miR-10a-5p	1517.0956	-0.5664	0.2397	-2.3631	0.0181	0.9848
mmu-miR-218-5p	90.8091	-0.5646	0.2693	-2.0967	0.0360	0.9848
mmu-miR-450b-3p	18.4509	-0.5387	0.3023	-1.7822	0.0747	0.9848
mmu-miR-423-5p	195.4879	-0.5361	0.2465	-2.1743	0.0297	0.9848
mmu-let-7e-5p	612.6481	-0.5239	0.2309	-2.2695	0.0232	0.9848
mmu-let-7a-5p	13927.0711	-0.4614	0.2229	-2.0701	0.0384	0.9848
mmu-miR-28a-5p	310.5846	-0.4487	0.2141	-2.0957	0.0361	0.9848
mmu-miR-674-3p	147.5102	-0.4154	0.2280	-1.8222	0.0684	0.9848
mmu-let-7d-5p	3833.4293	-0.3526	0.2054	-1.7165	0.0861	0.9848
mmu-miR-191-5p	3460.8977	-0.3179	0.1836	-1.7313	0.0834	0.9848
mmu-let-7g-5p	11159.4148	-0.3170	0.1901	-1.6676	0.0954	0.9848
mmu-miR-149-5p	1787.2760	0.3444	0.1851	1.8605	0.0628	0.9848
mmu-miR-133a-3p	22708.7427	0.3877	0.2242	1.7290	0.0838	0.9848
mmu-miR-6240	91.2381	0.4625	0.2651	1.7447	0.0810	0.9848
mmu-miR-133b-3p	52.6102	0.4681	0.2754	1.6994	0.0892	0.9848
mmu-miR-378c	538.0776	0.4792	0.2444	1.9610	0.0499	0.9848
mmu-miR-1a-1-5p	8.1698	0.5092	0.2931	1.7369	0.0824	0.9848
mmu-miR-135a-5p	24.5628	0.5347	0.3027	1.7663	0.0773	0.9848
mmu-miR-1291	13.4219	0.5960	0.3015	1.9771	0.0480	0.9848
mmu-miR-6236	5.9465	0.7187	0.2768	2.5965	0.0094	0.9848

KEGG PATHWAYS			
KEGG pathway	p-value	#genes	#miRNAs
Prion diseases	1.65E-16	9	5
Proteoglycans in cancer	9.90E-10	64	6
Thyroid hormone signaling pathway	6.20E-08	42	6
Lysine degradation	5.92E-07	18	6
MAPK signaling pathway	2.74E-05	68	6
Adherens junction	2.74E-05	30	6
Renal cell carcinoma	2.74E-05	25	6
Hippo signaling pathway	5.80E-05	35	6
Glioma	0.000561414	21	6
Pathways in cancer	0.000657582	90	6
Chronic myeloid leukemia	0.000750154	25	6
FoxO signaling pathway	0.002125304	41	6
Hepatitis B	0.002125304	39	7
Endocytosis	0.002561583	57	6
Colorectal cancer	0.002561583	19	6
Prostate cancer	0.002742581	30	6
ErbB signaling pathway	0.002752875	30	6
HTLV-I infection	0.002752875	66	6
Regulation of actin cytoskeleton	0.003667509	55	6
Galactose metabolism	0.004161906	9	6
Neurotrophin signaling pathway	0.004785759	35	6
mTOR signaling pathway	0.004912992	21	6
Bacterial invasion of epithelial cells	0.005348264	23	6
Steroid biosynthesis	0.006192337	4	4
Focal adhesion	0.006316667	54	6
HIF-1 signaling pathway	0.007083436	34	7
Viral carcinogenesis	0.007083436	48	7
Axon guidance	0.008714459	34	6
Ubiquitin mediated proteolysis	0.015798595	37	6
Insulin signaling pathway	0.020135289	38	7
AMPK signaling pathway	0.022247638	36	6
Acute myeloid leukemia	0.02289926	17	6
PI3K-Akt signaling pathway	0.024234929	76	7
Cell cycle	0.025892359	32	6
Small cell lung cancer	0.025892359	24	6
Phosphatidylinositol signaling system	0.027813964	20	6
Pancreatic cancer	0.031480848	20	6

Transcriptional misregulation in cancer	0.03986119	42	6
NF- κ B signaling pathway	0.041920997	23	6
Circadian rhythm	0.048872539	10	6

GO CATEGORY			
GO Category	p-value	#genes	#miRNAs
Homeostatic process	0.0000E+00	174	5
Molecular function	0.0000E+00	2850	6
Cellular component	0.0000E+00	2778	6
Cytoplasm	0.0000E+00	1633	6
Cellular protein modification process	0.0000E+00	477	6
Biological process	0.0000E+00	2918	6
Biosynthetic process	0.0000E+00	668	6
Embryo development	0.0000E+00	222	6
Ion binding	0.0000E+00	1107	6
Anatomical structure formation involved in morphogenesis	0.0000E+00	160	6
Anatomical structure development	0.0000E+00	726	6
Cell differentiation	0.0000E+00	525	7
Cellular nitrogen compound metabolic process	0.0000E+00	733	7
Chromosome organization	0.0000E+00	141	7
Intracellular	0.0000E+00	2059	8
Cell	0.0000E+00	2296	8
Organelle	0.0000E+00	1744	8
Cell morphogenesis	1.63647E-13	139	5
Cell cycle	6.93282E-11	179	5
In utero embryonic development	2.28241E-09	84	5
Growth	1.09568E-08	93	6
Cytoskeletal protein binding	2.56402E-07	143	4
Response to stress	1.54633E-06	240	4
Cell motility	1.94553E-06	114	4
Cytoskeleton organization	7.6214E-06	141	4
Protein complex	1.60116E-05	581	4
Cell division	2.08409E-05	93	5
Cell death	3.12212E-05	149	6
Nucleic acid binding transcription factor activity	4.63057E-05	90	2
Nuclear chromosome	8.2365E-05	44	6
Cytoskeleton	9.12065E-05	246	3
Enzyme binding	0.000853471	138	4
Catabolic process	0.001717074	194	4
Nucleoplasm	0.002873149	143	4
Protein binding transcription factor activity	0.005400327	45	1
Chromosome	0.009440752	100	4

Immune system process	0.02042566	125	2
-----------------------	------------	-----	---

REFERENCE LIST

1. Agarwal, R., E. Mokelke, S. B. Ruble and C. M. Stolen (2016). "Vagal Nerve Stimulation Evoked Heart Rate Changes and Protection from Cardiac Remodeling." J Cardiovasc Transl Res **9**(1): 67-76.
2. Agarwal, V., G. W. Bell, J. W. Nam and D. P. Bartel (2015). "Predicting effective microRNA target sites in mammalian mRNAs." Elife **4**.
3. Alderton, W. K., C. E. Cooper and R. G. Knowles (2001). "Nitric oxide synthases: structure, function and inhibition." Biochem J **357**(Pt 3): 593-615.
4. Amsterdam, E. A., N. K. Wenger, R. G. Brindis, D. E. Casey, Jr., T. G. Ganiats, D. R. Holmes, Jr., A. S. Jaffe, H. Jneid, R. F. Kelly, M. C. Kontos, G. N. Levine, P. R. Liebson, D. Mukherjee, E. D. Peterson, M. S. Sabatine, R. W. Smalling and S. J. Zieman (2014). "2014 AHA/ACC guideline for the management of patients with non-ST-elevation acute coronary syndromes: executive summary: a report of the American College of Cardiology/American Heart Association Task Force on Practice Guidelines." Circulation **130**(25): 2354-2394.
5. Anckar, J. and L. Sistonen (2007). "Heat shock factor 1 as a coordinator of stress and developmental pathways." Adv Exp Med Biol **594**: 78-88.
6. Anders, S., P. T. Pyl and W. Huber (2015). "HTSeq--a Python framework to work with high-throughput sequencing data." Bioinformatics (Oxford, England) **31**(2): 166-169.
7. Angel, P., K. Hattori, T. Smeal and M. Karin (1988). "The jun proto-oncogene is positively autoregulated by its product, Jun/AP-1." Cell **55**(5): 875-885.
8. Arias-Salvatierra, D., E. K. Silbergeld, L. C. Acosta-Saavedra and E. S. Calderon-Aranda (2011). "Role of nitric oxide produced by iNOS through NF- κ B pathway in migration of cerebellar granule neurons induced by Lipopolysaccharide." Cellular Signalling **23**(2): 425-435.
9. Arnaud, C., A. Laubriet, M. Joyeux, D. Godin-Ribuot, L. Rochette, P. Demenge and C. Ribuot (2001). "Role of nitric oxide synthases in the infarct size-reducing effect conferred by heat stress in isolated rat hearts." Br J Pharmacol **132**(8): 1845-1851.
10. Baars, T., A. Skyschally, L. Klein-Hitpass, E. Cario, R. Erbel, G. Heusch and P. Kleinbongard (2014). "microRNA expression and its potential role in cardioprotection by ischemic postconditioning in pigs." Pflugers Arch **466**(10): 1953-1961.

11. Baek, K. H., H. Zhang, B. R. Lee, Y. G. Kwon, S. J. Ha and I. Shin (2015). "A small molecule inhibitor for ATPase activity of Hsp70 and Hsc70 enhances the immune response to protein antigens." Sci Rep **5**: 17642.
12. Baker, J., G. Riley, M. R. Romero, A. R. Haynes, H. Hilton, M. Simon, J. Hancock, H. Tateossian, V. M. Ripoll and G. Blanco (2010). "Identification of a Z-band associated protein complex involving KY, FLNC and IGFN1." Exp Cell Res **316**(11): 1856-1870.
13. Banerjee, I., J. W. Fuseler, R. L. Price, T. K. Borg and T. A. Baudino (2007). "Determination of cell types and numbers during cardiac development in the neonatal and adult rat and mouse." Am J Physiol Heart Circ Physiol **293**(3): H1883-1891.
14. Bankwala, Z., S. L. Hale and R. A. Kloner (1994). "Alpha-adrenoceptor stimulation with exogenous norepinephrine or release of endogenous catecholamines mimics ischemic preconditioning." Circulation **90**(2): 1023-1028.
15. Barile, L., G. Milano and G. Vassalli (2017). "Beneficial effects of exosomes secreted by cardiac-derived progenitor cells and other cell types in myocardial ischemia." Stem Cell Investig **4**: 93.
16. Barile, L., T. Moccetti, E. Marban and G. Vassalli (2017). "Roles of exosomes in cardioprotection." Eur Heart J **38**(18): 1372-1379.
17. Basalay, M., V. Barsukevich, A. Mrochek, A. V. Gourine and A. Gourine (2013). "Right vs left vagus and cardioprotection conferred by remote ischaemic pre- and perconditioning." European Heart Journal **34**(suppl_1): 3697-3697.
18. Basalay, M. V., S. M. Davidson, A. V. Gourine and D. M. Yellon (2018). "Neural mechanisms in remote ischaemic conditioning in the heart and brain: mechanistic and translational aspects." Basic Res Cardiol **113**(4): 25.
19. Bayoumi, A. S., J. P. Teoh, T. Aonuma, Z. Yuan, X. Ruan, Y. Tang, H. Su, N. L. Weintraub and I. M. Kim (2017). "MicroRNA-532 protects the heart in acute myocardial infarction, and represses prss23, a positive regulator of endothelial-to-mesenchymal transition." Cardiovasc Res **113**(13): 1603-1614.
20. Behringer, R., M. Gertsenstein, K. Nagy and A. Nagy Manipulating the mouse embryo: a laboratory manual.
21. Bell, S. P., M. N. Sack, A. Patel, L. H. Opie and D. M. Yellon (2000). "Delta opioid receptor stimulation mimics ischemic preconditioning in human heart muscle." J Am Coll Cardiol **36**(7): 2296-2302.
22. Bencsik, P., K. Kupai, Z. Giricz, A. Gorbe, J. Pipis, Z. Murlasits, G. F. Kocsis, Z. Varga-Orvos, L. G. Puskas, C. Csonka, T. Csont and P. Ferdinandy (2010). "Role of iNOS and

- peroxynitrite-matrix metalloproteinase-2 signaling in myocardial late preconditioning in rats." *Am J Physiol Heart Circ Physiol* **299**(2): H512-518.
23. Benjamin, E. J., S. S. Virani, C. W. Callaway, A. M. Chamberlain, A. R. Chang, S. Cheng, S. E. Chiuve, M. Cushman, F. N. Delling, R. Deo, S. D. de Ferranti, J. F. Ferguson, M. Fornage, C. Gillespie, C. R. Isasi, M. C. Jimenez, L. C. Jordan, S. E. Judd, D. Lackland, J. H. Lichtman, L. Lisabeth, S. Liu, C. T. Longenecker, P. L. Lutsey, J. S. Mackey, D. B. Matchar, K. Matsushita, M. E. Mussolino, K. Nasir, M. O'Flaherty, L. P. Palaniappan, A. Pandey, D. K. Pandey, M. J. Reeves, M. D. Ritchey, C. J. Rodriguez, G. A. Roth, W. D. Rosamond, U. K. A. Sampson, G. M. Satou, S. H. Shah, N. L. Spartano, D. L. Tirschwell, C. W. Tsao, J. H. Voeks, J. Z. Willey, J. T. Wilkins, J. H. Wu, H. M. Alger, S. S. Wong and P. Muntner (2018). "Heart Disease and Stroke Statistics-2018 Update: A Report From the American Heart Association." *Circulation* **137**(12): e67-e492.
 24. Bennett, B. L., D. T. Sasaki, B. W. Murray, E. C. O'Leary, S. T. Sakata, W. Xu, J. C. Leisten, A. Motiwala, S. Pierce, Y. Satoh, S. S. Bhagwat, A. M. Manning and D. W. Anderson (2001). "SP600125, an anthrapyrazolone inhibitor of Jun N-terminal kinase." *Proc Natl Acad Sci U S A* **98**(24): 13681-13686.
 25. Berthonneche, C., B. Peter, F. Schupfer, P. Hayoz, Z. Kutalik, H. Abriel, T. Pedrazzini, J. S. Beckmann, S. Bergmann and F. Maurer (2009). "Cardiovascular response to beta-adrenergic blockade or activation in 23 inbred mouse strains." *PLoS One* **4**(8): e6610.
 26. Bhar-Amato, J., W. Davies and S. Agarwal (2017). "Ventricular Arrhythmia after Acute Myocardial Infarction: 'The Perfect Storm'." *Arrhythm Electrophysiol Rev* **6**(3): 134-139.
 27. Bian, D., H. Tian, Y. Sui, Y. Liu, R. Cao, C. Li and B. Li (2016). "[Effects of electroacupuncture at 'Neiguan' (PC 6) on sodium channel-related proteins in rats with ischemic myocardial injury]." *Zhongguo Zhen Jiu* **36**(1): 64-68.
 28. Birnbaum, Y., S. L. Hale and R. A. Kloner (1997). "Ischemic preconditioning at a distance: reduction of myocardial infarct size by partial reduction of blood supply combined with rapid stimulation of the gastrocnemius muscle in the rabbit." *Circulation* **96**(5): 1641-1646.
 29. Bishopric, N. H., P. Andreka, T. Slepak and K. A. Webster (2001). "Molecular mechanisms of apoptosis in the cardiac myocyte." *Curr Opin Pharmacol* **1**(2): 141-150.
 30. Blanco, G., G. R. Coulton, A. Biggin, C. Grainge, J. Moss, M. Barrett, A. Berquin, G. Marechal, M. Skynner, P. van Mier, A. Nikitopoulou, M. Kraus, C. P. Ponting, R. M. Mason and S. D. Brown (2001). "The kyphoscoliosis (ky) mouse is deficient in hypertrophic responses and is caused by a mutation in a novel muscle-specific

- protein." Hum Mol Genet **10**(1): 9-16.
31. Bogнар, Z., T. Kalai, A. Palfi, K. Hanto, B. Bogнар, L. Mark, Z. Szabo, A. Tapodi, B. Radnai, Z. Sarszegi, A. Szanto, F. Gallyas, Jr., K. Hideg, B. Sumegi and G. Varbiro (2006). "A novel SOD-mimetic permeability transition inhibitor agent protects ischemic heart by inhibiting both apoptotic and necrotic cell death." Free Radic Biol Med **41**(5): 835-848.
 32. Bolli, R. (2001). "Cardioprotective function of inducible nitric oxide synthase and role of nitric oxide in myocardial ischemia and preconditioning: an overview of a decade of research." J Mol Cell Cardiol **33**(11): 1897-1918.
 33. Bolli, R., Z. A. Bhatti, X. L. Tang, Y. Qiu, Q. Zhang, Y. Guo and A. K. Jadoon (1997). "Evidence that late preconditioning against myocardial stunning in conscious rabbits is triggered by the generation of nitric oxide." Circ Res **81**(1): 42-52.
 34. Bolli, R., B. Dawn, X. L. Tang, Y. Qiu, P. Ping, Y. T. Xuan, W. K. Jones, H. Takano, Y. Guo and J. Zhang (1998). "The nitric oxide hypothesis of late preconditioning." Basic Res Cardiol **93**(5): 325-338.
 35. Bopassa, J. C., R. Ferrera, O. Gateau-Roesch, E. Couture-Lepetit and M. Ovize (2006). "PI 3-kinase regulates the mitochondrial transition pore in controlled reperfusion and postconditioning." Cardiovasc Res **69**(1): 178-185.
 36. Bopassa, J. C., P. Michel, O. Gateau-Roesch, M. Ovize and R. Ferrera (2005). "Low-pressure reperfusion alters mitochondrial permeability transition." Am J Physiol Heart Circ Physiol **288**(6): H2750-2755.
 37. Botker, H. E., R. Kharbanda, M. R. Schmidt, M. Bottcher, A. K. Kaltoft, C. J. Terkelsen, K. Munk, N. H. Andersen, T. M. Hansen, S. Trautner, J. F. Lassen, E. H. Christiansen, L. R. Krusell, S. D. Kristensen, L. Thuesen, S. S. Nielsen, M. Rehling, H. T. Sorensen, A. N. Redington and T. T. Nielsen (2010). "Remote ischaemic conditioning before hospital admission, as a complement to angioplasty, and effect on myocardial salvage in patients with acute myocardial infarction: a randomised trial." Lancet **375**(9716): 727-734.
 38. Brand, T., H. S. Sharma, K. E. Fleischmann, D. J. Duncker, E. O. McFalls, P. D. Verdouw and W. Schaper (1992). "Proto-oncogene expression in porcine myocardium subjected to ischemia and reperfusion." Circ Res **71**(6): 1351-1360.
 39. Brandenburger, T., H. Grievink, N. Heinen, F. Barthel, R. Huhn, F. Stachuletz, M. Kohns, B. Pannen and I. Bauer (2014). "Effects of remote ischemic preconditioning and myocardial ischemia on microRNA-1 expression in the rat heart in vivo." Shock **42**(3): 234-238.
 40. Braunwald, E. and R. A. Kloner (1982). "The stunned myocardium: prolonged,

- postischemic ventricular dysfunction." Circulation **66**(6): 1146-1149.
41. Bridges, L. R., G. R. Coulton, G. Howard, J. Moss and R. M. Mason (1992). "The neuromuscular basis of hereditary kyphoscoliosis in the mouse." Muscle Nerve **15**(2): 172-179.
 42. Brown, M., M. McGuinness, T. Wright, X. Ren, Y. Wang, G. P. Boivin, H. Hahn, A. M. Feldman and W. K. Jones (2005). "Cardiac-specific blockade of NF-kappaB in cardiac pathophysiology: differences between acute and chronic stimuli in vivo." Am J Physiol Heart Circ Physiol **289**(1): H466-476.
 43. Bryan, N. S. and M. B. Grisham (2007). "Methods to detect nitric oxide and its metabolites in biological samples." Free Radic Biol Med **43**(5): 645-657.
 44. Buchholz, B., J. Kelly, M. Munoz, E. A. Bernatene, N. Mendez Diodati, D. H. Gonzalez Maglio, F. P. Dominici and R. J. Gelpi (2018). "Vagal stimulation mimics preconditioning and postconditioning of ischemic myocardium in mice by activating different protection mechanisms." Am J Physiol Heart Circ Physiol **314**(6): H1289-h1297.
 45. Budina-Kolomets, A., G. M. Balaburski, A. Bondar, N. Beeharry, T. Yen and M. E. Murphy (2014). "Comparison of the activity of three different HSP70 inhibitors on apoptosis, cell cycle arrest, autophagy inhibition, and HSP90 inhibition." Cancer Biol Ther **15**(2): 194-199.
 46. Bult, C. J., D. M. Krupke, D. A. Begley, J. E. Richardson, S. B. Neuhauser, J. P. Sundberg and J. T. Eppig (2015). "Mouse Tumor Biology (MTB): a database of mouse models for human cancer." Nucleic Acids Res **43**(Database issue): D818-824.
 47. Cahill, T. J. and R. K. Kharbanda (2017). "Heart failure after myocardial infarction in the era of primary percutaneous coronary intervention: Mechanisms, incidence and identification of patients at risk." World J Cardiol **9**(5): 407-415.
 48. Calvillo, L., E. Vanoli, E. Andreoli, A. Besana, E. Omodeo, M. Gnechi, P. Zerbi, G. Vago, G. Busca and P. J. Schwartz (2011). "Vagal stimulation, through its nicotinic action, limits infarct size and the inflammatory response to myocardial ischemia and reperfusion." J Cardiovasc Pharmacol **58**(5): 500-507.
 49. Candilio, L., A. Malik and D. J. Hausenloy (2013). "Protection of organs other than the heart by remote ischemic conditioning." J Cardiovasc Med (Hagerstown) **14**(3): 193-205.
 50. Cao, Q., J. Liu, S. Chen and Z. Han (1998). "Effects of electroacupuncture at neiguan on myocardial microcirculation in rabbits with acute myocardial ischemia." J Tradit Chin Med **18**(2): 134-139.

51. Carry, M. M., R. E. Mrak, M. L. Murphy, C. F. Peng, K. D. Straub and E. P. Fody (1989). "Reperfusion injury in ischemic myocardium: protective effects of ruthenium red and of nitroprusside." Am J Cardiovasc Pathol **2**(4): 335-344.
52. Carter, D. A. (1997). "Modulation of cellular AP-1 DNA binding activity by heat shock proteins." FEBS Lett **416**(1): 81-85.
53. Chai, Q., J. Liu and Y. Hu (2015). "Cardioprotective effect of remote preconditioning of trauma and remote ischemia preconditioning in a rat model of myocardial ischemia/reperfusion injury." Exp Ther Med **9**(5): 1745-1750.
54. Chandrasekar, B. and G. L. Freeman (1997). "Induction of nuclear factor kappaB and activation protein 1 in postischemic myocardium." FEBS Lett **401**(1): 30-34.
55. Chandrashekhar, Y., S. Sen, R. Anway, A. Shuros and I. Anand (2004). "Long-term caspase inhibition ameliorates apoptosis, reduces myocardial troponin-I cleavage, protects left ventricular function, and attenuates remodeling in rats with myocardial infarction." J Am Coll Cardiol **43**(2): 295-301.
56. Chapman, J. G., W. P. Magee, H. A. Stukenbrok, G. E. Beckius, A. J. Milici and W. R. Tracey (2002). "A novel nonpeptidic caspase-3/7 inhibitor, (S)-(+)-5-[1-(2-methoxymethylpyrrolidinyl)sulfonyl]isatin reduces myocardial ischemic injury." Eur J Pharmacol **456**(1-3): 59-68.
57. Chen, F. E., D. B. Huang, Y. Q. Chen and G. Ghosh (1998). "Crystal structure of p50/p65 heterodimer of transcription factor NF-kappaB bound to DNA." Nature **391**(6665): 410-413.
58. Chen, Q., A. K. Camara, D. F. Stowe, C. L. Hoppel and E. J. Lesnefsky (2007). "Modulation of electron transport protects cardiac mitochondria and decreases myocardial injury during ischemia and reperfusion." Am J Physiol Cell Physiol **292**(1): C137-147.
59. Chen, Q., Y. Zhou, A. M. Richards and P. Wang (2016). "Up-regulation of miRNA-221 inhibits hypoxia/reoxygenation-induced autophagy through the DDIT4/mTORC1 and Tp53inp1/p62 pathways." Biochem Biophys Res Commun **474**(1): 168-174.
60. Chen, Z., J. Liu, H. K. T. Ng, S. Nadarajah, H. L. Kaufman, J. Y. Yang and Y. Deng (2011). "Statistical methods on detecting differentially expressed genes for RNA-seq data." BMC systems biology **5 Suppl 3**(Suppl 3): S1-S1.
61. Chen-Scarabelli, C. and T. M. Scarabelli (2016). "Cyclosporine A Prior to Primary PCI in STEMI Patients: The Coup de Grace to Post-Conditioning?" J Am Coll Cardiol **67**(4): 375-378.
62. Cheng, Y. F. and C. C. Chen (2018). "Chronic Neuropathic Pain Protects the Heart

- from Ischemia-Reperfusion Injury." Adv Exp Med Biol **1099**: 101-114.
63. Cohen, M. V. and J. M. Downey (2007). "Cardioprotection: spotlight on PKG." British journal of pharmacology **152**(6): 833-834.
 64. Collaborators, G. M. a. C. o. D. (2016). "Global, regional, and national life expectancy, all-cause mortality, and cause-specific mortality for 249 causes of death, 1980-2015: a systematic analysis for the Global Burden of Disease Study 2015." Lancet **388**(10053): 1459-1544.
 65. Conde, R., Z. R. Belak, M. Nair, R. F. O'Carroll and N. Ovsenek (2009). "Modulation of Hsf1 activity by novobiocin and geldanamycin." Biochem Cell Biol **87**(6): 845-851.
 66. Cornelussen, R. N., A. V. Garnier, G. J. van der Vusse, R. S. Reneman and L. Snoeckx (1998). "Biphasic effect of heat stress pretreatment on ischemic tolerance of isolated rat hearts." J Mol Cell Cardiol **30**(2): 365-372.
 67. Council, N. R. (2010). Guide for the care and use of laboratory animals, National Academies Press.
 68. Cuculi, F., C. C. Lim and A. P. Banning (2010). "Periprocedural myocardial injury during elective percutaneous coronary intervention: is it important and how can it be prevented?" Heart **96**(10): 736-740.
 69. Cummings, K. L. and R. L. Tarleton (2004). "Inducible nitric oxide synthase is not essential for control of Trypanosoma cruzi infection in mice." Infect Immun **72**(7): 4081-4089.
 70. Cung, T. T., O. Morel, G. Cayla, G. Rioufol, D. Garcia-Dorado, D. Angoulvant, E. Bonnefoy-Cudraz, P. Guerin, M. Elbaz, N. Delarche, P. Coste, G. Vanzetto, M. Metge, J. F. Aupetit, B. Jouve, P. Motreff, C. Tron, J. N. Labeque, P. G. Steg, Y. Cottin, G. Range, J. Clerc, M. J. Claeys, P. Coussement, F. Prunier, F. Moulin, O. Roth, L. Belle, P. Dubois, P. Barragan, M. Gilard, C. Piot, P. Colin, F. De Poli, M. C. Morice, O. Ider, J. L. Dubois-Rande, T. Untersee, H. Le Breton, T. Beard, D. Blanchard, G. Grollier, V. Malquarti, P. Staat, A. Sudre, E. Elmer, M. J. Hansson, C. Bergerot, I. Boussaha, C. Jossan, G. Derumeaux, N. Mewton and M. Ovize (2015). "Cyclosporine before PCI in Patients with Acute Myocardial Infarction." N Engl J Med **373**(11): 1021-1031.
 71. Date, T., S. Mochizuki, A. J. Belanger, M. Yamakawa, Z. Luo, K. A. Vincent, S. H. Cheng, R. J. Gregory and C. Jiang (2005). "Expression of constitutively stable hybrid hypoxia-inducible factor-1alpha protects cultured rat cardiomyocytes against simulated ischemia-reperfusion injury." Am J Physiol Cell Physiol **288**(2): C314-320.
 72. Davidson, S. M., D. Hausenloy, M. R. Duchon and D. M. Yellon (2006). "Signalling via the reperfusion injury signalling kinase (RISK) pathway links closure of the mitochondrial permeability transition pore to cardioprotection." Int J Biochem Cell

Biol **38**(3): 414-419.

73. Dawn, B., Y. Guo, A. Rezazadeh, O. L. Wang, A. B. Stein, G. Hunt, J. Varma, Y. T. Xuan, W. J. Wu, W. Tan, X. Zhu and R. Bolli (2004). "Tumor necrosis factor-alpha does not modulate ischemia/reperfusion injury in naive myocardium but is essential for the development of late preconditioning." J Mol Cell Cardiol **37**(1): 51-61.
74. Dawn, B., Y. T. Xuan, Y. Guo, A. Rezazadeh, A. B. Stein, G. Hunt, W. J. Wu, W. Tan and R. Bolli (2004). "IL-6 plays an obligatory role in late preconditioning via JAK-STAT signaling and upregulation of iNOS and COX-2." Cardiovasc Res **64**(1): 61-71.
75. de Couto, G., R. Gallet, L. Cambier, E. Jaghatspanyan, N. Makkar, J. F. Dawkins, B. P. Berman and E. Marban (2017). "Exosomal MicroRNA Transfer Into Macrophages Mediates Cellular Postconditioning." Circulation **136**(2): 200-214.
76. De Ferrari, G. M., H. J. Crijns, M. Borggrefe, G. Milasinovic, J. Smid, M. Zabel, A. Gavazzi, A. Sanzo, R. Dennert, J. Kuschyk, S. Raspopovic, H. Klein, K. Swedberg and P. J. Schwartz (2011). "Chronic vagus nerve stimulation: a new and promising therapeutic approach for chronic heart failure." Eur Heart J **32**(7): 847-855.
77. De Ferrari, G. M., C. Stolen, A. E. Tuinenburg, D. J. Wright, J. Brugada, C. Butter, H. Klein, P. Neuzil, C. Botman, M. A. Castel, A. D'Onofrio, G. J. de Borst, S. Solomon, K. M. Stein, B. Schubert, K. Stalsberg, N. Wold, S. Ruble and F. Zannad (2017). "Long-term vagal stimulation for heart failure: Eighteen month results from the NEural Cardiac TherApy foR Heart Failure (NECTAR-HF) trial." Int J Cardiol **244**: 229-234.
78. de Marqui, A. B., A. Vidotto, G. M. Polachini, M. Bellato Cde, H. Cabral, A. M. Leopoldino, J. F. de Gois Filho, E. E. Fukuyama, F. A. Settanni, P. M. Cury, G. O. Bonilla-Rodriguez, M. S. Palma and E. H. Tajara (2006). "Solubilization of proteins from human lymph node tissue and two-dimensional gel storage." J Biochem Mol Biol **39**(2): 216-222.
79. de Torbal, A., E. Boersma, J. A. Kors, G. van Herpen, J. W. Deckers, D. A. van der Kuip, B. H. Stricker, A. Hofman and J. C. Witteman (2006). "Incidence of recognized and unrecognized myocardial infarction in men and women aged 55 and older: the Rotterdam Study." Eur Heart J **27**(6): 729-736.
80. Deer, T. R., N. Mekhail, D. Provenzano, J. Pope, E. Krames, M. Leong, R. M. Levy, D. Abejon, E. Buchser, A. Burton, A. Buvanendran, K. Candido, D. Caraway, M. Cousins, M. DeJongste, S. Diwan, S. Eldabe, K. Gatzinsky, R. D. Foreman, S. Hayek, P. Kim, T. Kinfe, D. Kloth, K. Kumar, S. Rizvi, S. P. Lad, L. Liem, B. Linderorth, S. Mackey, G. McDowell, P. McRoberts, L. Poree, J. Prager, L. Raso, R. Rauck, M. Russo, B. Simpson, K. Slavin, P. Staats, M. Stanton-Hicks, P. Verrills, J. Wellington, K. Williams and R. North (2014). "The appropriate use of neurostimulation of the spinal cord and peripheral nervous system for the treatment of chronic pain and ischemic diseases:

- the Neuromodulation Appropriateness Consensus Committee." Neuromodulation **17**(6): 515-550; discussion 550.
81. Dehmer, G. J. and K. J. Smith (2009). "Drug-eluting coronary artery stents." Am Fam Physician **80**(11): 1245-1251.
 82. Dickinson, A. G. and V. M. Meikle (1973). "Genetic kyphoscoliosis in mice." Lancet **1**(7813): 1186.
 83. Dickson, E. W., M. Lorbar, W. A. Porcaro, R. A. Fenton, C. P. Reinhardt, A. Gysembergh and K. Przyklenk (1999). "Rabbit heart can be "preconditioned" via transfer of coronary effluent." Am J Physiol **277**(6): H2451-2457.
 84. Ding, Y. F., M. M. Zhang and R. R. He (2001). "Role of renal nerve in cardioprotection provided by renal ischemic preconditioning in anesthetized rabbits." Sheng Li Xue Bao **53**(1): 7-12.
 85. Dokladny, K., O. B. Myers and P. L. Moseley (2015). "Heat shock response and autophagy--cooperation and control." Autophagy **11**(2): 200-213.
 86. Donato, M., B. Buchholz, M. Rodriguez, V. Perez, J. Inserte, D. Garcia-Dorado and R. J. Gelpi (2013). "Role of the parasympathetic nervous system in cardioprotection by remote hindlimb ischaemic preconditioning." Exp Physiol **98**(2): 425-434.
 87. Dong, B., C. Li, X. Zhang, S. Wang, Z. Cheng and P. Rong (2014). "Electroacupuncture of neiguan (PC 6) inhibits enhanced voltage-gated sodium currents in ischemic ventricular myocytes." J Tradit Chin Med **34**(6): 710-715.
 88. Dong, J. H., Y. X. Liu, J. Zhao, H. J. Ma, S. M. Guo and R. R. He (2004). "High-frequency electrical stimulation of femoral nerve reduces infarct size following myocardial ischemia-reperfusion in rats." Sheng Li Xue Bao **56**(5): 620-624.
 89. Dos Santos, M. C. T., M. A. Barreto-Sanz, B. R. S. Correia, R. Bell, C. Widnall, L. T. Perez, C. Berteau, C. Schulte, D. Scheller, D. Berg, W. Maetzler, P. A. F. Galante and A. Nogueira da Costa (2018). "miRNA-based signatures in cerebrospinal fluid as potential diagnostic tools for early stage Parkinson's disease." Oncotarget **9**(25): 17455-17465.
 90. Dos Santos, P., A. J. Kowaltowski, M. N. Laclau, S. Seetharaman, P. Paucek, S. Boudina, J. B. Thambo, L. Tariosse and K. D. Garlid (2002). "Mechanisms by which opening the mitochondrial ATP- sensitive K(+) channel protects the ischemic heart." Am J Physiol Heart Circ Physiol **283**(1): H284-295.
 91. Dougherty, C. J., L. A. Kubasiak, H. Prentice, P. Andreka, N. H. Bishopric and K. A. Webster (2002). "Activation of c-Jun N-terminal kinase promotes survival of cardiac myocytes after oxidative stress." Biochem J **362**(Pt 3): 561-571.

92. Eitel, I., T. Stiermaier, K. P. Rommel, G. Fuernau, M. Sandri, N. Mangner, A. Linke, S. Erbs, P. Lurz, E. Boudriot, M. Mende, S. Desch, G. Schuler and H. Thiele (2015). "Cardioprotection by combined intrahospital remote ischaemic preconditioning and postconditioning in ST-elevation myocardial infarction: the randomized LIPSIA CONDITIONING trial." Eur Heart J **36**(44): 3049-3057.
93. Elliott, R. E., A. Morsi, O. Tanweer, B. Grobelny, E. Geller, C. Carlson, O. Devinsky and W. K. Doyle (2011). "Efficacy of vagus nerve stimulation over time: review of 65 consecutive patients with treatment-resistant epilepsy treated with VNS > 10 years." Epilepsy Behav **20**(3): 478-483.
94. Ersahin, C., D. E. Euler and W. H. Simmons (1999). "Cardioprotective effects of the aminopeptidase P inhibitor apstatin: studies on ischemia/reperfusion injury in the isolated rat heart." J Cardiovasc Pharmacol **34**(4): 604-611.
95. Eschenhagen, T., R. Bolli, T. Braun, L. J. Field, B. K. Fleischmann, J. Frisen, M. Giacca, J. M. Hare, S. Houser, R. T. Lee, E. Marban, J. F. Martin, J. D. Molkentin, C. E. Murry, P. R. Riley, P. Ruiz-Lozano, H. A. Sadek, M. A. Sussman and J. A. Hill (2017). "Cardiomyocyte Regeneration: A Consensus Statement." Circulation **136**(7): 680-686.
96. Famm, K., B. Litt, K. J. Tracey, E. S. Boyden and M. Slaoui (2013). "Drug discovery: a jump-start for electroceuticals." Nature **496**(7444): 159-161.
97. Fan, G. C., X. Ren, J. Qian, Q. Yuan, P. Nicolaou, Y. Wang, W. K. Jones, G. Chu and E. G. Kraniias (2005). "Novel cardioprotective role of a small heat-shock protein, Hsp20, against ischemia/reperfusion injury." Circulation **111**(14): 1792-1799.
98. Fang, L., A. H. Ellims, X. L. Moore, D. A. White, A. J. Taylor, J. Chin-Dusting and A. M. Dart (2015). "Circulating microRNAs as biomarkers for diffuse myocardial fibrosis in patients with hypertrophic cardiomyopathy." J Transl Med **13**: 314.
99. Fang, Z., Y. Zhou and Y. Wang (2002). "The effects of electroacupuncture at the heart meridian on myocardial contractile function in rabbits with myocardial ischemia." J Tradit Chin Med **22**(1): 47-50.
100. Finger, J. H., C. M. Smith, T. F. Hayamizu, I. J. McCright, J. Xu, M. Law, D. R. Shaw, R. M. Baldarelli, J. S. Beal, O. Blodgett, J. W. Campbell, L. E. Corbani, J. R. Lewis, K. L. Forthofer, P. J. Frost, S. C. Giannatto, L. N. Hutchins, D. B. Miers, H. Motenko, K. R. Stone, J. T. Eppig, J. A. Kadin, J. E. Richardson and M. Ringwald (2017). "The mouse Gene Expression Database (GXD): 2017 update." Nucleic Acids Res **45**(D1): D730-d736.
101. Fishbein, M. C., S. Meerbaum, J. Rit, U. Lando, K. Kanmatsuse, J. C. Mercier, E. Corday and W. Ganz (1981). "Early phase acute myocardial infarct size

- quantification: validation of the triphenyl tetrazolium chloride tissue enzyme staining technique." Am Heart J **101**(5): 593-600.
102. Frances, C., P. Nazeyrollas, A. Prevost, F. Moreau, J. Pisani, S. Davani, J. P. Kantelip and H. Millart (2003). "Role of beta 1- and beta 2-adrenoceptor subtypes in preconditioning against myocardial dysfunction after ischemia and reperfusion." J Cardiovasc Pharmacol **41**(3): 396-405.
 103. Fu, S. P., S. Y. He, B. Xu, C. J. Hu, S. F. Lu, W. X. Shen, Y. Huang, H. Hong, Q. Li, N. Wang, X. L. Liu, F. Liang and B. M. Zhu (2014). "Acupuncture promotes angiogenesis after myocardial ischemia through H3K9 acetylation regulation at VEGF gene." PLoS One **9**(4): e94604.
 104. Gao, J., W. Fu, Z. Jin and X. Yu (2006). "A preliminary study on the cardioprotection of acupuncture pretreatment in rats with ischemia and reperfusion: involvement of cardiac beta-adrenoceptors." J Physiol Sci **56**(4): 275-279.
 105. Gao, J., W. Fu, Z. Jin and X. Yu (2007). "Acupuncture pretreatment protects heart from injury in rats with myocardial ischemia and reperfusion via inhibition of the beta(1)-adrenoceptor signaling pathway." Life Sci **80**(16): 1484-1489.
 106. Gao, J., L. Zhang, Y. Wang, B. Lu, H. Cui, W. Fu, H. Wang, Y. Yu and X. Yu (2008). "Antiarrhythmic effect of acupuncture pretreatment in rats subjected to simulative global ischemia and reperfusion--involvement of adenylate cyclase, protein kinase A, and L-type Ca²⁺ channel." J Physiol Sci **58**(6): 389-396.
 107. Gao, Y., A. P. Signore, W. Yin, G. Cao, X. M. Yin, F. Sun, Y. Luo, S. H. Graham and J. Chen (2005). "Neuroprotection against focal ischemic brain injury by inhibition of c-Jun N-terminal kinase and attenuation of the mitochondrial apoptosis-signaling pathway." J Cereb Blood Flow Metab **25**(6): 694-712.
 108. Gaspar, A., A. P. Lourenco, M. A. Pereira, P. Azevedo, R. Roncon-Albuquerque, Jr., J. Marques and A. F. Leite-Moreira (2018). "Randomized controlled trial of remote ischaemic conditioning in ST-elevation myocardial infarction as adjuvant to primary angioplasty (RIC-STEMI)." Basic Res Cardiol **113**(3): 14.
 109. Gerber, Y., S. A. Weston, C. Berardi, S. M. McNallan, R. Jiang, M. M. Redfield and V. L. Roger (2013). "Contemporary trends in heart failure with reduced and preserved ejection fraction after myocardial infarction: a community study." Am J Epidemiol **178**(8): 1272-1280.
 110. Gho, B. C., R. G. Schoemaker, M. A. van den Doel, D. J. Duncker and P. D. Verdouw (1996). "Myocardial protection by brief ischemia in noncardiac tissue." Circulation **94**(9): 2193-2200.
 111. Gill, R., R. Kuriakose, Z. M. Gertz, F. N. Salloum, L. Xi and R. C. Kukreja (2015).

- "Remote ischemic preconditioning for myocardial protection: update on mechanisms and clinical relevance." Mol Cell Biochem **402**(1-2): 41-49.
112. Giricz, Z., Z. V. Varga, T. Baranyai, P. Sipos, K. Paloczi, A. Kittel, E. I. Buzas and P. Ferdinandy (2014). "Cardioprotection by remote ischemic preconditioning of the rat heart is mediated by extracellular vesicles." J Mol Cell Cardiol **68**: 75-78.
 113. Gomez, L., N. Chavanis, L. Argaud, L. Chalabreysse, O. Gateau-Roesch, J. Ninet and M. Ovize (2005). "Fas-independent mitochondrial damage triggers cardiomyocyte death after ischemia-reperfusion." Am J Physiol Heart Circ Physiol **289**(5): H2153-2158.
 114. Goto, M., Y. Liu, X. M. Yang, J. L. Ardell, M. V. Cohen and J. M. Downey (1995). "Role of bradykinin in protection of ischemic preconditioning in rabbit hearts." Circ Res **77**(3): 611-621.
 115. Gourine, A. and A. V. Gourine (2014). "Neural mechanisms of cardioprotection." Physiology (Bethesda) **29**(2): 133-140.
 116. Gray, M. O., J. S. Karliner and D. Mochly-Rosen (1997). "A selective epsilon-protein kinase C antagonist inhibits protection of cardiac myocytes from hypoxia-induced cell death." J Biol Chem **272**(49): 30945-30951.
 117. Griffith, O. W. and D. J. Stuehr (1995). "Nitric oxide synthases: properties and catalytic mechanism." Annu Rev Physiol **57**: 707-736.
 118. Griffiths-Jones, S., Saini, H. K., van Dongen, S., & Enright, A. J. (2008). miRBase: tools for microRNA genomics. *Nucleic Acids Res*, **36**(Database issue), D154-158. doi:10.1093/nar/gkm952
 119. Gross, E. R., A. K. Hsu, T. J. Urban, D. Mochly-Rosen and G. J. Gross (2013). "Nociceptive-induced myocardial remote conditioning is mediated by neuronal gamma protein kinase C." Basic Res Cardiol **108**(5): 381.
 120. Gross, G. J., J. E. Baker, J. Moore, J. R. Falck and K. Nithipatikom (2011). "Abdominal surgical incision induces remote preconditioning of trauma (RPCT) via activation of bradykinin receptors (BK2R) and the cytochrome P450 epoxygenase pathway in canine hearts." Cardiovasc Drugs Ther **25**(6): 517-522.
 121. Gross, G. J., A. Hsu, E. R. Gross, J. R. Falck and K. Nithipatikom (2013). "Factors mediating remote preconditioning of trauma in the rat heart: central role of the cytochrome p450 epoxygenase pathway in mediating infarct size reduction." Journal of cardiovascular pharmacology and therapeutics **18**(1): 38-45.
 122. Guisasola, M. C., M. Desco Mdel, F. S. Gonzalez, F. Asensio, E. Dulin, A. Suarez and P. Garcia Barreno (2006). "Heat shock proteins, end effectors of myocardium ischemic

- preconditioning?" Cell Stress Chaperones **11**(3): 250-258.
123. Gumina, R. J., E. Buerger, C. Eickmeier, J. Moore, J. Daemmgen and G. J. Gross (1999). "Inhibition of the Na(+)/H(+) exchanger confers greater cardioprotection against 90 minutes of myocardial ischemia than ischemic preconditioning in dogs." Circulation **100**(25): 2519-2526; discussion 2469-2572.
 124. Guo, G. and N. R. Bhat (2006). "Hypoxia/reoxygenation differentially modulates NF-kappaB activation and iNOS expression in astrocytes and microglia." Antioxid Redox Signal **8**(5-6): 911-918.
 125. Guo, Y., M. P. Flaherty, W. J. Wu, W. Tan, X. Zhu, Q. Li and R. Bolli (2012). "Genetic background, gender, age, body temperature, and arterial blood pH have a major impact on myocardial infarct size in the mouse and need to be carefully measured and/or taken into account: results of a comprehensive analysis of determinants of infarct size in 1,074 mice." Basic Res Cardiol **107**(5): 288.
 126. Guo, Y., W. K. Jones, Y. T. Xuan, X. L. Tang, W. Bao, W. J. Wu, H. Han, V. E. Laubach, P. Ping, Z. Yang, Y. Qiu and R. Bolli (1999). "The late phase of ischemic preconditioning is abrogated by targeted disruption of the inducible NO synthase gene." Proc Natl Acad Sci U S A **96**(20): 11507-11512.
 127. Guo, Y., W. J. Wu, Y. Qiu, X. L. Tang, Z. Yang and R. Bolli (1998). "Demonstration of an early and a late phase of ischemic preconditioning in mice." The American journal of physiology **275**(4 Pt 2): H1375-H1387.
 128. Guzhova, I. V., Z. A. Darieva, A. R. Melo and B. A. Margulis (1997). "Major stress protein Hsp70 interacts with NF-kB regulatory complex in human T-lymphoma cells." Cell Stress Chaperones **2**(2): 132-139.
 129. Hachamovitch, R., D. S. Berman, L. J. Shaw, H. Kiat, I. Cohen, J. A. Cabico, J. Friedman and G. A. Diamond (1998). "Incremental prognostic value of myocardial perfusion single photon emission computed tomography for the prediction of cardiac death: differential stratification for risk of cardiac death and myocardial infarction." Circulation **97**(6): 535-543.
 130. Hagar, J. M., S. L. Hale and R. A. Kloner (1991). "Effect of preconditioning ischemia on reperfusion arrhythmias after coronary artery occlusion and reperfusion in the rat." Circ Res **68**(1): 61-68.
 131. Hahn, J. Y., Y. B. Song, E. K. Kim, C. W. Yu, J. W. Bae, W. Y. Chung, S. H. Choi, J. H. Choi, J. H. Bae, K. J. An, J. S. Park, J. H. Oh, S. W. Kim, J. Y. Hwang, J. K. Ryu, H. S. Park, D. S. Lim and H. C. Gwon (2013). "Ischemic postconditioning during primary percutaneous coronary intervention: the effects of postconditioning on myocardial reperfusion in patients with ST-segment elevation myocardial infarction (POST)

- randomized trial." Circulation **128**(17): 1889-1896.
132. Hamann, J. J., S. B. Ruble, C. Stolen, M. Wang, R. C. Gupta, S. Rastogi and H. N. Sabbah (2013). "Vagus nerve stimulation improves left ventricular function in a canine model of chronic heart failure." Eur J Heart Fail **15**(12): 1319-1326.
 133. Hampton, C. R., A. Shimamoto, C. L. Rothnie, J. Griscavage-Ennis, A. Chong, D. J. Dix, E. D. Verrier and T. H. Pohlman (2003). "HSP70.1 and -70.3 are required for late-phase protection induced by ischemic preconditioning of mouse hearts." Am J Physiol Heart Circ Physiol **285**(2): H866-874.
 134. Handforth, A., C. M. DeGiorgio, S. C. Schachter, B. M. Uthman, D. K. Naritoku, E. S. Tecoma, T. R. Henry, S. D. Collins, B. V. Vaughn, R. C. Gilmartin, D. R. Labar, G. L. Morris, 3rd, M. C. Salinsky, I. Osorio, R. K. Ristanovic, D. M. Labiner, J. C. Jones, J. V. Murphy, G. C. Ney and J. W. Wheless (1998). "Vagus nerve stimulation therapy for partial-onset seizures: a randomized active-control trial." Neurology **51**(1): 48-55.
 135. Hanna, E. B. and T. A. Hennebry (2010). "Periprocedural myocardial infarction: review and classification." Clin Cardiol **33**(8): 476-483.
 136. Hausenloy, D. J., L. Candilio, R. Evans, C. Ariti, D. P. Jenkins, S. Kolvekar, R. Knight, G. Kunst, C. Laing, J. Nicholas, J. Pepper, S. Robertson, M. Xenou, T. Clayton and D. M. Yellon (2015). "Remote Ischemic Preconditioning and Outcomes of Cardiac Surgery." N Engl J Med **373**(15): 1408-1417.
 137. Hausenloy, D. J., H. L. Maddock, G. F. Baxter and D. M. Yellon (2002). "Inhibiting mitochondrial permeability transition pore opening: a new paradigm for myocardial preconditioning?" Cardiovasc Res **55**(3): 534-543.
 138. Hausenloy, D. J., P. K. Mwamure, V. Venugopal, J. Harris, M. Barnard, E. Grundy, E. Ashley, S. Vichare, C. Di Salvo, S. Kolvekar, M. Hayward, B. Keogh, R. J. MacAllister and D. M. Yellon (2007). "Effect of remote ischaemic preconditioning on myocardial injury in patients undergoing coronary artery bypass graft surgery: a randomised controlled trial." Lancet **370**(9587): 575-579.
 139. Hausenloy, D. J., A. Tsang, M. M. Mocanu and D. M. Yellon (2005). "Ischemic preconditioning protects by activating prosurvival kinases at reperfusion." Am J Physiol Heart Circ Physiol **288**(2): H971-976.
 140. Hausenloy, D. J. and D. M. Yellon (2013). "Myocardial ischemia-reperfusion injury: a neglected therapeutic target." J Clin Invest **123**(1): 92-100.
 141. Hayashizaki, Y. (2003). "The Riken mouse genome encyclopedia project." C R Biol **326**(10-11): 923-929.
 142. He, Q., F. Wang, T. Honda, J. James, J. Li and A. Redington (2018). "Loss of miR-144

- signaling interrupts extracellular matrix remodeling after myocardial infarction leading to worsened cardiac function." *Sci Rep* **8**(1): 16886.
143. Hearse, D. J., S. M. Humphrey and E. B. Chain (1973). "Abrupt reoxygenation of the anoxic potassium-arrested perfused rat heart: a study of myocardial enzyme release." *J Mol Cell Cardiol* **5**(4): 395-407.
 144. Hedberg-Oldfors, C., N. Darin, M. Olsson Engman, Z. Orfanos, C. Thomsen, P. F. van der Ven and A. Oldfors (2016). "A new early-onset neuromuscular disorder associated with kyphoscoliosis peptidase (KY) deficiency." *Eur J Hum Genet* **24**(12): 1771-1777.
 145. Heinen, A., F. Behmenburg, A. Aytulun, M. Dierkes, L. Zerbin, W. Kaisers, M. Schaefer, T. Meyer-Treschan, S. Feit, I. Bauer, M. W. Hollmann and R. Huhn (2018). "The release of cardioprotective humoral factors after remote ischemic preconditioning in humans is age- and sex-dependent." *J Transl Med* **16**(1): 112.
 146. Hendgen-Cotta, U. B., D. Messiha, S. Esfeld, R. Deenen, T. Rassaf and M. Totzeck (2017). "Inorganic nitrite modulates miRNA signatures in acute myocardial in vivo ischemia/reperfusion." *Free Radic Res* **51**(1): 91-102.
 147. Henkel, D. M., B. J. Witt, B. J. Gersh, S. J. Jacobsen, S. A. Weston, R. A. Meverden and V. L. Roger (2006). "Ventricular arrhythmias after acute myocardial infarction: a 20-year community study." *Am Heart J* **151**(4): 806-812.
 148. Heusch, G. (2013). "Cardioprotection: chances and challenges of its translation to the clinic." *Lancet* **381**(9861): 166-175.
 149. Heusch, G. (2015). "CIRCUS: a kiss of death for cardioprotection?" *Cardiovasc Res* **108**(2): 215-216.
 150. Heusch, G. (2017). "Vagal Cardioprotection in Reperfused Acute Myocardial Infarction." *JACC Cardiovasc Interv* **10**(15): 1521-1522.
 151. Heusch, G. (2018). "25 years of remote ischemic conditioning: from laboratory curiosity to clinical outcome." *Basic Res Cardiol* **113**(3): 15.
 152. Heusch, G. and T. Rassaf (2016). "Time to Give Up on Cardioprotection? A Critical Appraisal of Clinical Studies on Ischemic Pre-, Post-, and Remote Conditioning." *Circ Res* **119**(5): 676-695.
 153. Hillis, L. D., P. K. Smith, J. L. Anderson, J. A. Bittl, C. R. Bridges, J. G. Byrne, J. E. Cigarroa, V. J. DiSesa, L. F. Hiratzka, A. M. Hutter, Jr., M. E. Jessen, E. C. Keeley, S. J. Lahey, R. A. Lange, M. J. London, M. J. Mack, M. R. Patel, J. D. Puskas, J. F. Sabik, O. Selnes, D. M. Shahian, J. C. Trost, M. D. Winniford, A. K. Jacobs, J. L. Anderson, N. Albert, M. A. Creager, S. M. Ettinger, R. A. Guyton, J. L. Halperin, J. S. Hochman, F. G.

- Kushner, E. M. Ohman, W. Stevenson and C. W. Yancy (2012). "2011 ACCF/AHA guideline for coronary artery bypass graft surgery: executive summary: a report of the American College of Cardiology Foundation/American Heart Association Task Force on Practice Guidelines." J Thorac Cardiovasc Surg **143**(1): 4-34.
154. Hinkel, R., D. Penzkofer, S. Zuhlke, A. Fischer, W. Husada, Q. F. Xu, E. Baloch, E. van Rooij, A. M. Zeiher, C. Kupatt and S. Dimmeler (2013). "Inhibition of microRNA-92a protects against ischemia/reperfusion injury in a large-animal model." Circulation **128**(10): 1066-1075.
 155. Hirai, T., M. Fujita, H. Nakajima, H. Asanoi, K. Yamanishi, A. Ohno and S. Sasayama (1989). "Importance of collateral circulation for prevention of left ventricular aneurysm formation in acute myocardial infarction." Circulation **79**(4): 791-796.
 156. Hochhauser, E., Y. Cheporko, N. Yasovich, L. Pinchas, D. Offen, Y. Barhum, H. Pannet, A. Tobar, B. A. Vidne and E. Birk (2007). "Bax deficiency reduces infarct size and improves long-term function after myocardial infarction." Cell Biochem Biophys **47**(1): 11-20.
 157. Hocht-Zeisberg, E., H. Kahnert, K. Guan, G. Wulf, B. Hemmerlein, T. Schlott, G. Tenderich, R. Korfer, U. Raute-Kreinsen and G. Hasenfuss (2004). "Cellular repopulation of myocardial infarction in patients with sex-mismatched heart transplantation." Eur Heart J **25**(9): 749-758.
 158. Hockenbery, D. M., M. Zutter, W. Hickey, M. Nahm and S. J. Korsmeyer (1991). "BCL2 protein is topographically restricted in tissues characterized by apoptotic cell death." Proc Natl Acad Sci U S A **88**(16): 6961-6965.
 159. Hoffmann, J., J. Haendeler, A. M. Zeiher and S. Dimmeler (2001). "TNFalpha and oxLDL reduce protein S-nitrosylation in endothelial cells." J Biol Chem **276**(44): 41383-41387.
 160. Holly, T. A., A. Drincic, Y. Byun, S. Nakamura, K. Harris, F. J. Klocke and V. L. Cryns (1999). "Caspase inhibition reduces myocyte cell death induced by myocardial ischemia and reperfusion in vivo." J Mol Cell Cardiol **31**(9): 1709-1715.
 161. Hoole, S. P., P. M. Heck, L. Sharples, S. N. Khan, R. Duehmke, C. G. Densem, S. C. Clarke, L. M. Shapiro, P. M. Schofield, M. O'Sullivan and D. P. Dutka (2009). "Cardiac Remote Ischemic Preconditioning in Coronary Stenting (CRISP Stent) Study: a prospective, randomized control trial." Circulation **119**(6): 820-827.
 162. Hoshida, S., N. Yamashita, K. Otsu and M. Hori (2002). "The importance of manganese superoxide dismutase in delayed preconditioning: Involvement of reactive oxygen species and cytokines." Cardiovascular Research **55**(3): 495-505.
 163. Hoss, A. G., A. Labadorf, J. C. Latourelle, V. K. Kartha, T. C. Hadzi, J. F. Gusella, M. E.

- MacDonald, J. F. Chen, S. Akbarian, Z. Weng, J. P. Vonsattel and R. H. Myers (2015). "miR-10b-5p expression in Huntington's disease brain relates to age of onset and the extent of striatal involvement." BMC Med Genomics **8**: 10.
164. Huang da, W., B. T. Sherman and R. A. Lempicki (2009). "Bioinformatics enrichment tools: paths toward the comprehensive functional analysis of large gene lists." Nucleic Acids Res **37**(1): 1-13.
 165. Huang da, W., B. T. Sherman and R. A. Lempicki (2009). "Systematic and integrative analysis of large gene lists using DAVID bioinformatics resources." Nat Protoc **4**(1): 44-57.
 166. Hughes, J. E., S. Srinivasan, K. R. Lynch, R. L. Proia, P. Ferdek and C. C. Hedrick (2008). "Sphingosine-1-phosphate induces an antiinflammatory phenotype in macrophages." Circ Res **102**(8): 950-958.
 167. Ibanez, B., C. Macaya, V. Sanchez-Brunete, G. Pizarro, L. Fernandez-Friera, A. Mateos, A. Fernandez-Ortiz, J. M. Garcia-Ruiz, A. Garcia-Alvarez, A. Iniguez, J. Jimenez-Borreguero, P. Lopez-Romero, R. Fernandez-Jimenez, J. Goicolea, B. Ruiz-Mateos, T. Bastante, M. Arias, J. A. Iglesias-Vazquez, M. D. Rodriguez, N. Escalera, C. Acebal, J. A. Cabrera, J. Valenciano, A. Perez de Prado, M. J. Fernandez-Campos, I. Casado, J. C. Garcia-Rubira, J. Garcia-Prieto, D. Sanz-Rosa, C. Cuellas, R. Hernandez-Antolin, A. Albarran, F. Fernandez-Vazquez, J. M. de la Torre-Hernandez, S. Pocock, G. Sanz and V. Fuster (2013). "Effect of early metoprolol on infarct size in ST-segment-elevation myocardial infarction patients undergoing primary percutaneous coronary intervention: the Effect of Metoprolol in Cardioprotection During an Acute Myocardial Infarction (METOCARD-CNIC) trial." Circulation **128**(14): 1495-1503.
 168. Ibrahim, A. G., K. Cheng and E. Marban (2014). "Exosomes as critical agents of cardiac regeneration triggered by cell therapy." Stem Cell Reports **2**(5): 606-619.
 169. Ilangovan, G., S. Osinbowale, A. Bratasz, M. Bonar, A. J. Cardounel, J. L. Zweier and P. Kuppusamy (2004). "Heat shock regulates the respiration of cardiac H9c2 cells through upregulation of nitric oxide synthase." Am J Physiol Cell Physiol **287**(5): C1472-1481.
 170. Ishii, M., Y. Suzuki, K. Takeshita, N. Miyao, H. Kudo, R. Hiraoka, K. Nishio, N. Sato, K. Naoki, T. Aoki and K. Yamaguchi (2004). "Inhibition of c-Jun NH2-terminal kinase activity improves ischemia/reperfusion injury in rat lungs." J Immunol **172**(4): 2569-2577.
 171. Iwatsu, K., S. Yamada, Y. Iida, H. Sampei, K. Kobayashi, M. Kainuma and A. Usui (2015). "Feasibility of neuromuscular electrical stimulation immediately after cardiovascular surgery." Arch Phys Med Rehabil **96**(1): 63-68.

172. Jaffrey, S. R. and S. H. Snyder (2001). "The biotin switch method for the detection of S-nitrosylated proteins." Sci STKE **2001**(86): pl1.
173. Jancso, G., B. Cserepes, B. Gasz, L. Benko, B. Borsiczky, A. Ferenc, M. Kurthy, B. Racz, J. Lantos, J. Gal, E. Arato, L. Sinayc, G. Weber and E. Roth (2007). "Expression and protective role of heme oxygenase-1 in delayed myocardial preconditioning." Ann N Y Acad Sci **1095**: 251-261.
174. Jayakumar, J., K. Suzuki, M. Khan, R. T. Smolenski, A. Farrell, N. Latif, O. Raisky, H. Abunasra, I. A. Sammut, B. Murtuza, M. Amrani and M. H. Yacoub (2000). "Gene therapy for myocardial protection: transfection of donor hearts with heat shock protein 70 gene protects cardiac function against ischemia-reperfusion injury." Circulation **102**(19 Suppl 3): Iii302-306.
175. Jayakumar, J., K. Suzuki, I. A. Sammut, R. T. Smolenski, M. Khan, N. Latif, H. Abunasra, B. Murtuza, M. Amrani and M. H. Yacoub (2001). "Heat shock protein 70 gene transfection protects mitochondrial and ventricular function against ischemia-reperfusion injury." Circulation **104**(12 Suppl 1): I303-307.
176. Jennings, R. B. (2013). "Historical perspective on the pathology of myocardial ischemia/reperfusion injury." Circ Res **113**(4): 428-438.
177. Jennings, R. B., H. M. Sommers, G. A. Smyth, H. A. Flack and H. Linn (1960). "Myocardial necrosis induced by temporary occlusion of a coronary artery in the dog." Arch Pathol **70**: 68-78.
178. Jones, S. P. and R. Bolli (2006). "The ubiquitous role of nitric oxide in cardioprotection." J Mol Cell Cardiol **40**(1): 16-23.
179. Jones, W. K., M. Brown, X. Ren, S. He and M. McGuinness (2003). "NF-kappaB as an integrator of diverse signaling pathways: the heart of myocardial signaling?" Cardiovasc Toxicol **3**(3): 229-254.
180. Jones, W. K., M. Brown, M. Wilhide, S. He and X. Ren (2005). "NF-kappaB in cardiovascular disease: diverse and specific effects of a "general" transcription factor?" Cardiovasc Toxicol **5**(2): 183-202.
181. Jones, W. K., G. C. Fan, S. Liao, J. M. Zhang, Y. Wang, N. L. Weintraub, E. G. Kranias, J. E. Schultz, J. Lorenz and X. Ren (2009). "Peripheral nociception associated with surgical incision elicits remote nonischemic cardioprotection via neurogenic activation of protein kinase C signaling." Circulation **120**(11 Suppl): S1-9.
182. Joseph, P., D. Leong, M. McKee, S. S. Anand, J. D. Schwalm, K. Teo, A. Mente and S. Yusuf (2017). "Reducing the Global Burden of Cardiovascular Disease, Part 1: The Epidemiology and Risk Factors." Circ Res **121**(6): 677-694.

183. Joy, E. R., J. Kurian and C. P. Gale (2016). "Comparative effectiveness of primary PCI versus fibrinolytic therapy for ST elevation myocardial infarction: a review of the literature." J Comp Eff Res **5**(2): 217-226.
184. Joyeux, M., D. Godin-Ribuot, A. Patel, P. Demenge, D. M. Yellon and C. Ribuot (1998). "Infarct size-reducing effect of heat stress and alpha1 adrenoceptors in rats." Br J Pharmacol **125**(4): 645-650.
185. Kaiser, R. A., Q. Liang, O. Bueno, Y. Huang, T. Lackey, R. Klevitsky, T. E. Hewett and J. D. Molkentin (2005). "Genetic inhibition or activation of JNK1/2 protects the myocardium from ischemia-reperfusion-induced cell death in vivo." J Biol Chem **280**(38): 32602-32608.
186. Kajstura, J., W. Cheng, K. Reiss, W. A. Clark, E. H. Sonnenblick, S. Krajewski, J. C. Reed, G. Olivetti and P. Anversa (1996). "Apoptotic and necrotic myocyte cell deaths are independent contributing variables of infarct size in rats." Lab Invest **74**(1): 86-107.
187. Kalogeris, T., C. P. Baines, M. Krenz and R. J. Korthuis (2012). "Cell Biology of Ischemia/Reperfusion Injury." International review of cell and molecular biology **298**: 229-317.
188. Kaptchuk, T. J. (2002). Acupuncture: theory, efficacy, and practice. *Ann Intern Med*, **136**(5), 374-383.
189. Katare, R. G., M. Ando, Y. Kakinuma, M. Arikawa, T. Handa, F. Yamasaki and T. Sato (2009). "Vagal nerve stimulation prevents reperfusion injury through inhibition of opening of mitochondrial permeability transition pore independent of the bradycardiac effect." J Thorac Cardiovasc Surg **137**(1): 223-231.
190. Katare, R. G., M. Ando, Y. Kakinuma, M. Arikawa, F. Yamasaki and T. Sato (2010). "Differential regulation of TNF receptors by vagal nerve stimulation protects heart against acute ischemic injury." J Mol Cell Cardiol **49**(2): 234-244.
191. Kawada, T., T. Yamazaki, T. Akiyama, H. Kitagawa, S. Shimizu, M. Mizuno, M. Li and M. Sugimachi (2008). "Vagal stimulation suppresses ischemia-induced myocardial interstitial myoglobin release." Life Sci **83**(13-14): 490-495.
192. Kawaguchi, M., M. Takahashi, T. Hata, Y. Kashima, F. Usui, H. Morimoto, A. Izawa, Y. Takahashi, J. Masumoto, J. Koyama, M. Hongo, T. Noda, J. Nakayama, J. Sagara, S. Taniguchi and U. Ikeda (2011). "Inflammasome activation of cardiac fibroblasts is essential for myocardial ischemia/reperfusion injury." Circulation **123**(6): 594-604.
193. Kerendi, F., H. Kin, M. E. Halkos, R. Jiang, A. J. Zatta, Z. Q. Zhao, R. A. Guyton and J. Vinten-Johansen (2005). "Remote postconditioning. Brief renal ischemia and reperfusion applied before coronary artery reperfusion reduces myocardial infarct

- size via endogenous activation of adenosine receptors." Basic Res Cardiol **100**(5): 404-412.
194. Kharbanda, R. K., U. M. Mortensen, P. A. White, S. B. Kristiansen, M. R. Schmidt, J. A. Hoschitzky, M. Vogel, K. Sorensen, A. N. Redington and R. MacAllister (2002). "Transient limb ischemia induces remote ischemic preconditioning in vivo." Circulation **106**(23): 2881-2883.
 195. Kim, D., G. Pertea, C. Trapnell, H. Pimentel, R. Kelley and S. L. Salzberg (2013). "TopHat2: accurate alignment of transcriptomes in the presence of insertions, deletions and gene fusions." Genome biology **14**(4): R36-R36.
 196. Kim, Y. C., J. H. Park and M. R. Prausnitz (2012). "Microneedles for drug and vaccine delivery." Adv Drug Deliv Rev **64**(14): 1547-1568.
 197. Kin, H., A. J. Zatta, M. T. Lofye, B. S. Amerson, M. E. Halkos, F. Kerendi, Z. Q. Zhao, R. A. Guyton, J. P. Headrick and J. Vinten-Johansen (2005). "Postconditioning reduces infarct size via adenosine receptor activation by endogenous adenosine." Cardiovasc Res **67**(1): 124-133.
 198. Kin, H., Z. Q. Zhao, H. Y. Sun, N. P. Wang, J. S. Corvera, M. E. Halkos, F. Kerendi, R. A. Guyton and J. Vinten-Johansen (2004). "Postconditioning attenuates myocardial ischemia-reperfusion injury by inhibiting events in the early minutes of reperfusion." Cardiovasc Res **62**(1): 74-85.
 199. Kingma, J. G., Jr. (1999). "Cardiac adaptation to ischemia-reperfusion injury." Ann N Y Acad Sci **874**: 83-99.
 200. Kiyatkin, E. A. and P. L. Brown (2005). "Brain and body temperature homeostasis during sodium pentobarbital anesthesia with and without body warming in rats." Physiol Behav **84**(4): 563-570.
 201. Klein, H. H., S. Pich, S. Lindert, K. Nebendahl, G. Warneke and H. Kreuzer (1989). "Treatment of reperfusion injury with intracoronary calcium channel antagonists and reduced coronary free calcium concentration in regionally ischemic, reperfused porcine hearts." Journal of the American College of Cardiology **13**(6): 1395-1401.
 202. Kleinbongard, P., M. Neuhauser, M. Thielmann, E. Kottenberg, J. Peters, H. Jakob and G. Heusch (2016). "Confounders of Cardioprotection by Remote Ischemic Preconditioning in Patients Undergoing Coronary Artery Bypass Grafting." Cardiology **133**(2): 128-133.
 203. Kloner, R. A., C. E. Ganote and R. B. Jennings (1974). "The "no-reflow" phenomenon after temporary coronary occlusion in the dog." J Clin Invest **54**(6): 1496-1508.
 204. Kloner, R. A., C. E. Ganote, R. B. Jennings and K. A. Reimer (1975). "Demonstration of

- the "no-reflow" phenomenon in the dog heart after temporary ischemia." Recent Adv Stud Cardiac Struct Metab **10**: 463-474.
205. Ko, S. K., J. Kim, D. C. Na, S. Park, S. H. Park, J. Y. Hyun, K. H. Baek, N. D. Kim, N. K. Kim, Y. N. Park, K. Song and I. Shin (2015). "A small molecule inhibitor of ATPase activity of HSP70 induces apoptosis and has antitumor activities." Chem Biol **22**(3): 391-403.
 206. Kochar, A., A. Y. Chen, P. P. Sharma, N. J. Pagidipati, G. C. Fonarow, P. A. Cowper, M. T. Roe, E. D. Peterson and T. Y. Wang (2018). "Long-Term Mortality of Older Patients With Acute Myocardial Infarction Treated in US Clinical Practice." J Am Heart Assoc **7**(13).
 207. Kohr, M. J., J. Sun, A. Aponte, G. Wang, M. Gucek, E. Murphy and C. Steenbergen (2011). "Simultaneous measurement of protein oxidation and S-nitrosylation during preconditioning and ischemia/reperfusion injury with resin-assisted capture." Circ Res **108**(4): 418-426.
 208. Konstantinov, I. E., S. Arab, J. Li, J. G. Coles, C. Boscarino, A. Mori, E. Cukerman, F. Dawood, M. M. Cheung, M. Shimizu, P. P. Liu and A. N. Redington (2005). "The remote ischemic preconditioning stimulus modifies gene expression in mouse myocardium." J Thorac Cardiovasc Surg **130**(5): 1326-1332.
 209. Konstantinov, I. E., J. Li, M. M. Cheung, M. Shimizu, J. Stokoe, R. K. Kharbanda and A. N. Redington (2005). "Remote ischemic preconditioning of the recipient reduces myocardial ischemia-reperfusion injury of the denervated donor heart via a Katp channel-dependent mechanism." Transplantation **79**(12): 1691-1695.
 210. Kottenberg, E., Thielmann, M., Bergmann, L., Heine, T., Jakob, H., Heusch, G., & Peters, J. (2012). Protection by remote ischemic preconditioning during coronary artery bypass graft surgery with isoflurane but not propofol - a clinical trial. *Acta Anaesthesiol Scand*, 56(1), 30-38. doi:10.1111/j.1399-6576.2011.02585.x
 211. Kraynik, S. M., A. Gabanic, S. R. Anthony, M. Kelley, W. R. Paulding, A. Roessler, M. McGuinness and M. Tranter (2015). "The stress-induced heat shock protein 70.3 expression is regulated by a dual-component mechanism involving alternative polyadenylation and HuR." Biochim Biophys Acta **1849**(6): 688-696.
 212. Kubasiak, L. A., O. M. Hernandez, N. H. Bishopric and K. A. Webster (2002). "Hypoxia and acidosis activate cardiac myocyte death through the Bcl-2 family protein BNIP3." Proc Natl Acad Sci U S A **99**(20): 12825-12830.
 213. Kudej, R. K., Y. T. Shen, A. P. Peppas, C. H. Huang, W. Chen, L. Yan, D. E. Vatner and S. F. Vatner (2006). "Obligatory role of cardiac nerves and alpha1-adrenergic receptors

- for the second window of ischemic preconditioning in conscious pigs." Circ Res **99**(11): 1270-1276.
214. Kung, G., K. Konstantinidis and R. N. Kitsis (2011). "Programmed necrosis, not apoptosis, in the heart." Circ Res **108**(8): 1017-1036.
 215. Lacerda, L., S. Somers, L. H. Opie and S. Lecour (2009). "Ischaemic postconditioning protects against reperfusion injury via the SAFE pathway." Cardiovasc Res **84**(2): 201-208.
 216. Lameris, T. W., S. de Zeeuw, G. Alberts, F. Boomsma, D. J. Duncker, P. D. Verdouw, A. J. Veld and A. H. van Den Meiracker (2000). "Time course and mechanism of myocardial catecholamine release during transient ischemia in vivo." Circulation **101**(22): 2645-2650.
 217. Langmead, B. and S. L. Salzberg (2012). "Fast gapped-read alignment with Bowtie 2." Nature Methods **9**: 357.
 218. Lansky, A. J. and G. W. Stone (2010). "Periprocedural myocardial infarction: prevalence, prognosis, and prevention." Circ Cardiovasc Interv **3**(6): 602-610.
 219. Laskey, W. K. (2005). "Brief repetitive balloon occlusions enhance reperfusion during percutaneous coronary intervention for acute myocardial infarction: a pilot study." Catheter Cardiovasc Interv **65**(3): 361-367.
 220. Lecour, S. (2009). "Activation of the protective Survivor Activating Factor Enhancement (SAFE) pathway against reperfusion injury: Does it go beyond the RISK pathway?" J Mol Cell Cardiol **47**(1): 32-40.
 221. Lecour, S. (2009). "Multiple protective pathways against reperfusion injury: A SAFE path without Aktion?" Journal of Molecular and Cellular Cardiology **46**(5): 607-609.
 222. Lecour, S., N. Suleman, G. A. Deuchar, S. Somers, L. Lacerda, B. Huisamen and L. H. Opie (2005). "Pharmacological preconditioning with tumor necrosis factor- α activates signal transducer and activator of transcription-3 at reperfusion without involving classic prosurvival kinases (Akt and extracellular signal-regulated kinase)." Circulation **112**(25): 3911-3918.
 223. Leist, M., B. Single, H. Naumann, E. Fava, B. Simon, S. Kuhnle and P. Nicotera (1999). "Inhibition of mitochondrial ATP generation by nitric oxide switches apoptosis to necrosis." Exp Cell Res **249**(2): 396-403.
 224. Lemasters, J. J., J. M. Bond, E. Chacon, I. S. Harper, S. H. Kaplan, H. Ohata, D. R. Trollinger, B. Herman and W. E. Cascio (1996). "The pH paradox in ischemia-reperfusion injury to cardiac myocytes." Exs **76**: 99-114.

225. Lepore, D. A., K. R. Knight, R. L. Anderson and W. A. Morrison (2001). "Role of priming stresses and Hsp70 in protection from ischemia-reperfusion injury in cardiac and skeletal muscle." Cell Stress Chaperones **6**(2): 93-96.
226. Levine, G. N., E. R. Bates, J. C. Blankenship, S. R. Bailey, J. A. Bittl, B. Cercek, C. E. Chambers, S. G. Ellis, R. A. Guyton, S. M. Hollenberg, U. N. Khot, R. A. Lange, L. Mauri, R. Mehran, I. D. Moussa, D. Mukherjee, H. H. Ting, P. T. O'Gara, F. G. Kushner, D. D. Ascheim, R. G. Brindis, D. E. Casey, Jr., M. K. Chung, J. A. de Lemos, D. B. Diercks, J. C. Fang, B. A. Franklin, C. B. Granger, H. M. Krumholz, J. A. Linderbaum, D. A. Morrow, L. K. Newby, J. P. Ornato, N. Ou, M. J. Radford, J. E. Tamis-Holland, C. L. Tommaso, C. M. Tracy, Y. J. Woo and D. X. Zhao (2016). "2015 ACC/AHA/SCAI Focused Update on Primary Percutaneous Coronary Intervention for Patients With ST-Elevation Myocardial Infarction: An Update of the 2011 ACCF/AHA/SCAI Guideline for Percutaneous Coronary Intervention and the 2013 ACCF/AHA Guideline for the Management of ST-Elevation Myocardial Infarction." J Am Coll Cardiol **67**(10): 1235-1250.
227. Li, C., W. Browder and R. L. Kao (1999). "Early activation of transcription factor NF-kappaB during ischemia in perfused rat heart." Am J Physiol **276**(2 Pt 2): H543-552.
228. Li, G., F. Labruto, A. Sirsjo, F. Chen, J. Vaage and G. Valen (2004). "Myocardial protection by remote preconditioning: the role of nuclear factor kappa-B p105 and inducible nitric oxide synthase." Eur J Cardiothorac Surg **26**(5): 968-973.
229. Li, J., S. X. Cai, Q. He, H. Zhang, D. Friedberg, F. Wang and A. N. Redington (2018). "Intravenous miR-144 reduces left ventricular remodeling after myocardial infarction." Basic Res Cardiol **113**(5): 36.
230. Li, J., Y. Ren, E. Shi, Z. Tan, J. Xiong, L. Yan and X. Jiang (2016). "Inhibition of the Let-7 Family MicroRNAs Induces Cardioprotection Against Ischemia-Reperfusion Injury in Diabetic Rats." Ann Thorac Surg **102**(3): 829-835.
231. Li, J., S. Rohailla, N. Gelber, J. Rutka, N. Sabah, R. A. Gladstone, C. Wei, P. Hu, R. K. Kharbada and A. N. Redington (2014). "MicroRNA-144 is a circulating effector of remote ischemic preconditioning." Basic Res Cardiol **109**(5): 423.
232. Li, L., W. Luo, L. Huang, W. Zhang, Y. Gao, H. Jiang, C. Zhang, L. Long and S. Chen (2010). "Remote preconditioning reduces myocardial injury in adult valve replacement: a randomized controlled trial." J Surg Res **164**(1): e21-26.
233. Li, M., C. Zheng, T. Sato, T. Kawada, M. Sugimachi and K. Sunagawa (2004). "Vagal nerve stimulation markedly improves long-term survival after chronic heart failure in rats." Circulation **109**(1): 120-124.
234. Li, Q., Y. Guo, Q. Ou, C. Cui, W. J. Wu, W. Tan, X. Zhu, L. B. Lanceta, S. K.

- Sanganalmath, B. Dawn, K. Shinmura, G. D. Rokosh, S. Wang and R. Bolli (2009). "Gene transfer of inducible nitric oxide synthase affords cardioprotection by upregulating heme oxygenase-1 via a nuclear factor- κ B-dependent pathway." Circulation **120**(13): 1222-1230.
235. Li, Q., Y. Guo, Q. Ou, W. J. Wu, N. Chen, X. Zhu, W. Tan, F. Yuan, B. Dawn, L. Luo, G. N. Hunt and R. Bolli (2011). "Gene transfer as a strategy to achieve permanent cardioprotection II: rAAV-mediated gene therapy with heme oxygenase-1 limits infarct size 1 year later without adverse functional consequences." Basic Res Cardiol **106**(6): 1367-1377.
 236. Li, Q., Y. Guo, W. Tan, Q. Ou, W. J. Wu, D. Sturza, B. Dawn, G. Hunt, C. Cui and R. Bolli (2007). "Cardioprotection afforded by inducible nitric oxide synthase gene therapy is mediated by cyclooxygenase-2 via a nuclear factor- κ B dependent pathway." Circulation **116**(14): 1577-1584.
 237. Li, Q., Y. Guo, W. Tan, A. B. Stein, B. Dawn, W. J. Wu, X. Zhu, X. Lu, X. Xu, T. Siddiqui, S. Tiwari and R. Bolli (2006). "Gene therapy with iNOS provides long-term protection against myocardial infarction without adverse functional consequences." Am J Physiol Heart Circ Physiol **290**(2): H584-589.
 238. Li, Q., Y. Guo, W. J. Wu, Q. Ou, X. Zhu, W. Tan, F. Yuan, N. Chen, B. Dawn, L. Luo, E. O'Brien and R. Bolli (2011). "Gene transfer as a strategy to achieve permanent cardioprotection I: rAAV-mediated gene therapy with inducible nitric oxide synthase limits infarct size 1 year later without adverse functional consequences." Basic Res Cardiol **106**(6): 1355-1366.
 239. Li, Q., Y. Guo, Y. T. Xuan, C. J. Lowenstein, S. C. Stevenson, S. D. Prabhu, W. J. Wu, Y. Zhu and R. Bolli (2003). "Gene therapy with inducible nitric oxide synthase protects against myocardial infarction via a cyclooxygenase-2-dependent mechanism." Circ Res **92**(7): 741-748.
 240. Li, R. C., P. Ping, J. Zhang, W. B. Wead, X. Cao, J. Gao, Y. Zheng, S. Huang, J. Han and R. Bolli (2000). "PKCepsilon modulates NF- κ B and AP-1 via mitogen-activated protein kinases in adult rabbit cardiomyocytes." Am J Physiol Heart Circ Physiol **279**(4): H1679-1689.
 241. Li, S., B. J. Scherlag, L. Yu, X. Sheng, Y. Zhang, R. Ali, Y. Dong, M. Ghias and S. S. Po (2009). "Low-level vagosympathetic stimulation: a paradox and potential new modality for the treatment of focal atrial fibrillation." Circ Arrhythm Electrophysiol **2**(6): 645-651.
 242. Li, W. S., M. Zhong, J. H. Yang and W. X. Zhao (2011). "[Effects of electroacupuncture preconditioning at "Neiguan" (PC 6) on gene expression of myocardial opioid receptors in rats with myocardial ischemia-reperfusion injury]." Zhongguo Zhen Jiu

- 31(5): 441-445.**
243. Li, X., P. Luo, Q. Wang and L. Xiong (2012). "Electroacupuncture Pretreatment as a Novel Avenue to Protect Brain against Ischemia and Reperfusion Injury." Evid Based Complement Alternat Med **2012**: 195397.
 244. Liem, D. A., P. D. Verdouw, H. Ploeg, S. Kazim and D. J. Duncker (2002). "Sites of action of adenosine in interorgan preconditioning of the heart." Am J Physiol Heart Circ Physiol **283**(1): H29-37.
 245. Lim, S. Y., D. M. Yellon and D. J. Hausenloy (2010). "The neural and humoral pathways in remote limb ischemic preconditioning." Basic Res Cardiol **105**(5): 651-655.
 246. Lima, B., M. T. Forrester, D. T. Hess and J. S. Stamler (2010). "S-nitrosylation in cardiovascular signaling." Circ Res **106**(4): 633-646.
 247. Limalanathan, S., G. O. Andersen, N. E. Klow, M. Abdelnoor, P. Hoffmann and J. Eritsland (2014). "Effect of ischemic postconditioning on infarct size in patients with ST-elevation myocardial infarction treated by primary PCI results of the POSTEMI (POstconditioning in ST-Elevation Myocardial Infarction) randomized trial." J Am Heart Assoc **3**(2): e000679.
 248. Lin, J., C. Steenbergen, E. Murphy and J. Sun (2009). "Estrogen receptor-beta activation results in S-nitrosylation of proteins involved in cardioprotection." Circulation **120**(3): 245-254.
 249. Liu, G. S., M. V. Cohen, D. Mochly-Rosen and J. M. Downey (1999). "Protein kinase C-epsilon is responsible for the protection of preconditioning in rabbit cardiomyocytes." J Mol Cell Cardiol **31**(10): 1937-1948.
 250. Liu, G. S., J. Thornton, D. M. Van Winkle, A. W. Stanley, R. A. Olsson and J. M. Downey (1991). "Protection against infarction afforded by preconditioning is mediated by A1 adenosine receptors in rabbit heart." Circulation **84**(1): 350-356.
 251. Liu, J., K. W. Kam, G. H. Borchert, G. M. Kravtsov, H. J. Ballard and T. M. Wong (2006). "Further study on the role of HSP70 on Ca²⁺ homeostasis in rat ventricular myocytes subjected to simulated ischemia." Am J Physiol Cell Physiol **290**(2): C583-591.
 252. Liu, J., K. W. Kam, J. J. Zhou, W. Y. Yan, M. Chen, S. Wu and T. M. Wong (2004). "Effects of heat shock protein 70 activation by metabolic inhibition preconditioning or kappa-opioid receptor stimulation on Ca²⁺ homeostasis in rat ventricular myocytes subjected to ischemic insults." J Pharmacol Exp Ther **310**(2): 606-613.
 253. Liu, P. Y., Y. Tian and S. Y. Xu (2014). "Mediated protective effect of

- electroacupuncture pretreatment by miR-214 on myocardial ischemia/reperfusion injury." J Geriatr Cardiol **11**(4): 303-310.
254. Livak, K. J. and T. D. Schmittgen (2001). "Analysis of relative gene expression data using real-time quantitative PCR and the 2(-Delta Delta C(T)) Method." Methods **25**(4): 402-408.
 255. Lochner, A., E. Marais, S. Genade and J. A. Moolman (2000). "Nitric oxide: a trigger for classic preconditioning?" American Journal of Physiology-Heart and Circulatory Physiology **279**(6): H2752-H2765.
 256. Lochner, A., E. Marais, E. D. Toit and J. Moolman (2002). "Nitric Oxide Triggers Classic Ischemic Preconditioning." Annals of the New York Academy of Sciences **962**(1): 402-414.
 257. Lott, F. D., P. Guo and C. F. Toombs (1996). "Reduction in infarct size by ischemic preconditioning persists in a chronic rat model of myocardial ischemia-reperfusion injury." Pharmacology **52**(2): 113-118.
 258. Loukogeorgakis, S. P., A. T. Panagiotidou, M. W. Broadhead, A. Donald, J. E. Deanfield and R. J. MacAllister (2005). "Remote ischemic preconditioning provides early and late protection against endothelial ischemia-reperfusion injury in humans: role of the autonomic nervous system." J Am Coll Cardiol **46**(3): 450-456.
 259. Love, M. I., S. Anders and W. Huber (2017). "Analyzing RNA-seq data with DESeq2." R package reference manual.
 260. Love, M. I., W. Huber and S. Anders (2014). "Moderated estimation of fold change and dispersion for RNA-seq data with DESeq2." Genome biology **15**(12): 550-550.
 261. Lu, S., Y. Tang, Y. Ding, M. Yu, S. Fu and B. Zhu (2018). "[Effects of electroacupuncture on the expression of adenosine receptors in the heart tissue of myocardial ischemia rats]." Zhongguo Zhen Jiu **38**(2): 173-179.
 262. Lu, S. F., Y. Huang, N. Wang, W. X. Shen, S. P. Fu, Q. Li, M. L. Yu, W. X. Liu, X. Chen, X. Y. Jing and B. M. Zhu (2016). "Cardioprotective Effect of Electroacupuncture Pretreatment on Myocardial Ischemia/Reperfusion Injury via Antiapoptotic Signaling." Evid Based Complement Alternat Med **2016**: 4609784.
 263. Lu, X., T. Costantini, N. E. Lopez, P. L. Wolf, A. M. Hageny, J. Putnam, B. Eliceiri and R. Coimbra (2013). "Vagal nerve stimulation protects cardiac injury by attenuating mitochondrial dysfunction in a murine burn injury model." J Cell Mol Med **17**(5): 664-671.
 264. Luther, K. (2016). The role of microRNA in cardioprotection: Ischemic preconditioning and mesenchymal stem cell paracrine effects, Loyola University

Chicago.

265. Luther, K. M., L. Haar, M. McGuinness, Y. Wang, T. L. Lynch Iv, A. Phan, Y. Song, Z. Shen, G. Gardner, G. Kuffel, X. Ren, M. J. Zilliox and W. K. Jones (2018). "Exosomal miR-21a-5p mediates cardioprotection by mesenchymal stem cells." J Mol Cell Cardiol **119**: 125-137.
266. Ma, L., B. Cui, Y. Shao, B. Ni, W. Zhang, Y. Luo and S. Zhang (2014). "Electroacupuncture improves cardiac function and remodeling by inhibition of sympathoexcitation in chronic heart failure rats." Am J Physiol Heart Circ Physiol **306**(10): H1464-1471.
267. Ma, X., X. Zhang, C. Li and M. Luo (2006). "Effect of postconditioning on coronary blood flow velocity and endothelial function and LV recovery after myocardial infarction." J Interv Cardiol **19**(5): 367-375.
268. Maciel, L., D. F. de Oliveira, G. C. Verissimo da Costa, P. M. Bisch and J. H. M. Nascimento (2017). "Cardioprotection by the transfer of coronary effluent from ischaemic preconditioned rat hearts: identification of cardioprotective humoral factors." Basic Res Cardiol **112**(5): 52.
269. Maejima, Y., S. Adachi, K. Morikawa, H. Ito and M. Isobe (2005). "Nitric oxide inhibits myocardial apoptosis by preventing caspase-3 activity via S-nitrosylation." J Mol Cell Cardiol **38**(1): 163-174.
270. Marber, M. S., D. S. Latchman, J. M. Walker and D. M. Yellon (1993). "Cardiac stress protein elevation 24 hours after brief ischemia or heat stress is associated with resistance to myocardial infarction." Circulation **88**(3): 1264-1272.
271. Marber, M. S., R. Mestril, S. H. Chi, M. R. Sayen, D. M. Yellon and W. H. Dillmann (1995). "Overexpression of the rat inducible 70-kD heat stress protein in a transgenic mouse increases the resistance of the heart to ischemic injury." J Clin Invest **95**(4): 1446-1456.
272. Marderstein, E. L., B. Bucher, Z. Guo, X. Feng, K. Reid and D. A. Geller (2003). "Protection of rat hepatocytes from apoptosis by inhibition of c-Jun N-terminal kinase." Surgery **134**(2): 280-284.
273. Martin, M. (2011). "Cutadapt removes adapter sequences from high-throughput sequencing reads." 2011 **17**(1): 3.
274. Mason, R. M. and A. J. Palfrey (1984). "Intervertebral disc degeneration in adult mice with hereditary kyphoscoliosis." J Orthop Res **2**(4): 333-338.
275. Mastitskaya, S., M. Basalay, P. S. Hosford, A. G. Ramage, A. Gourine and A. V. Gourine (2016). "Identifying the Source of a Humoral Factor of Remote

- (Pre)Conditioning Cardioprotection." PLOS ONE **11**(2): e0150108.
276. Mastitskaya, S., N. Marina, A. Gourine, M. P. Gilbey, K. M. Spyer, A. G. Teschemacher, S. Kasparov, S. Trapp, G. L. Ackland and A. V. Gourine (2012). "Cardioprotection evoked by remote ischaemic preconditioning is critically dependent on the activity of vagal pre-ganglionic neurones." Cardiovasc Res **95**(4): 487-494.
 277. Mattson, M. P. and G. Kroemer (2003). "Mitochondria in cell death: novel targets for neuroprotection and cardioprotection." Trends Mol Med **9**(5): 196-205.
 278. Maulik, N., R. M. Engelman, J. A. Rousou, J. E. Flack, 3rd, D. Deaton and D. K. Das (1999). "Ischemic preconditioning reduces apoptosis by upregulating anti-death gene Bcl-2." Circulation **100**(19 Suppl): li369-375.
 279. McCall, M. N., O. A. Kent, J. Yu, K. Fox-Talbot, A. L. Zaiman and M. K. Halushka (2011). "MicroRNA profiling of diverse endothelial cell types." BMC Med Genomics **4**: 78.
 280. McManus, D. D., M. Chinali, J. S. Saczynski, J. M. Gore, J. Yarzebski, F. A. Spencer, D. Lessard and R. J. Goldberg (2011). "30-year trends in heart failure in patients hospitalized with acute myocardial infarction." Am J Cardiol **107**(3): 353-359.
 281. Meng, X., J. M. Brown, L. Ao, A. Banerjee and A. H. Harken (1996). "Norepinephrine induces cardiac heat shock protein 70 and delayed cardioprotection in the rat through alpha 1 adrenoceptors." Cardiovasc Res **32**(2): 374-383.
 282. Meng, X., B. D. Shames, E. J. Pulido, D. R. Meldrum, L. Ao, K. S. Joo, A. H. Harken and A. Banerjee (1999). "Adrenergic induction of bimodal myocardial protection: signal transduction and cardiac gene reprogramming." Am J Physiol **276**(5 Pt 2): R1525-1533.
 283. Merlocco, A. C., K. L. Redington, T. Disenhouse, S. C. Strantzas, R. Gladstone, C. Wei, M. B. Tropak, C. Manliot, J. Li and A. N. Redington (2014). "Transcutaneous electrical nerve stimulation as a novel method of remote preconditioning: in vitro validation in an animal model and first human observations." Basic Res Cardiol **109**(3): 406.
 284. Meybohm, P., B. Bein, O. Brosteanu, J. Cremer, M. Gruenewald, C. Stoppe, M. Coburn, G. Schaelte, A. Boning, B. Niemann, J. Roesner, F. Kletzin, U. Strouhal, C. Reyher, R. Laufenberg-Feldmann, M. Ferner, I. F. Brandes, M. Bauer, S. N. Stehr, A. Kortgen, M. Wittmann, G. Baumgarten, T. Meyer-Treschan, P. Kienbaum, M. Heringlake, J. Schon, M. Sander, S. Treskatsch, T. Smul, E. Wolwender, T. Schilling, G. Fuernau, D. Hasenclever and K. Zacharowski (2015). "A Multicenter Trial of Remote Ischemic Preconditioning for Heart Surgery." N Engl J Med **373**(15): 1397-1407.

285. Mi, H., X. Huang, A. Muruganujan, H. Tang, C. Mills, D. Kang and P. D. Thomas (2017). "PANTHER version 11: expanded annotation data from Gene Ontology and Reactome pathways, and data analysis tool enhancements." Nucleic Acids Research **45**(D1): D183-D189.
286. Mi, H., A. Muruganujan, J. T. Casagrande and P. D. Thomas (2013). "Large-scale gene function analysis with the PANTHER classification system." Nature Protocols **8**: 1551.
287. Minatoguchi, S., Y. Uno, T. Kariya, M. Arai, N. Wang, K. Hashimoto, Y. Nishida, R. Maruyama, G. Takemura, T. Fujiwara and H. Fujiwara (2003). "Cross-talk among noradrenaline, adenosine and protein kinase C in the mechanisms of ischemic preconditioning in rabbits." J Cardiovasc Pharmacol **41 Suppl 1**: S39-47.
288. Mishra, S. (2017). "Electroceuticals in medicine - The brave new future." Indian Heart J **69**(5): 685-686.
289. Mitchell, M. B., X. Meng, L. Ao, J. M. Brown, A. H. Harken and A. Banerjee (1995). "Preconditioning of isolated rat heart is mediated by protein kinase C." Circ Res **76**(1): 73-81.
290. Morishita, R., T. Sugimoto, M. Aoki, I. Kida, N. Tomita, A. Moriguchi, K. Maeda, Y. Sawa, Y. Kaneda, J. Higaki and T. Ogihara (1997). "In vivo transfection of cis element "decoy" against nuclear factor-kappaB binding site prevents myocardial infarction." Nat Med **3**(8): 894-899.
291. Morita, H., G. Suzuki, W. Haddad, Y. Mika, E. J. Tanhehco, V. G. Sharov, S. Goldstein, S. Ben-Haim and H. N. Sabbah (2003). "Cardiac contractility modulation with nonexcitatory electric signals improves left ventricular function in dogs with chronic heart failure." J Card Fail **9**(1): 69-75.
292. Morris, K. R., R. D. Lutz, H. S. Choi, T. Kamitani, K. Chmura and E. D. Chan (2003). "Role of the NF-kappaB signaling pathway and kappaB cis-regulatory elements on the IRF-1 and iNOS promoter regions in mycobacterial lipoarabinomannan induction of nitric oxide." Infect Immun **71**(3): 1442-1452.
293. Mozaffarian, D., E. J. Benjamin, A. S. Go, D. K. Arnett, M. J. Blaha, M. Cushman, S. de Ferranti, J. P. Despres, H. J. Fullerton, V. J. Howard, M. D. Huffman, S. E. Judd, B. M. Kissela, D. T. Lackland, J. H. Lichtman, L. D. Lisabeth, S. Liu, R. H. Mackey, D. B. Matchar, D. K. McGuire, E. R. Mohler, 3rd, C. S. Moy, P. Muntner, M. E. Mussolino, K. Nasir, R. W. Neumar, G. Nichol, L. Palaniappan, D. K. Pandey, M. J. Reeves, C. J. Rodriguez, P. D. Sorlie, J. Stein, A. Towfighi, T. N. Turan, S. S. Virani, J. Z. Willey, D. Woo, R. W. Yeh, M. B. Turner, C. American Heart Association Statistics and S. Stroke Statistics (2015). "Heart disease and stroke statistics--2015 update: a report from the American Heart Association." Circulation **131**(4): e29-322.

294. Muller, S. (2014). "In silico analysis of regulatory networks underlines the role of miR-10b-5p and its target BDNF in huntington's disease." Transl Neurodegener **3**: 17.
295. Munk, K., N. H. Andersen, M. R. Schmidt, S. S. Nielsen, C. J. Terkelsen, E. Sloth, H. E. Botker, T. T. Nielsen and S. H. Poulsen (2010). "Remote Ischemic Conditioning in Patients With Myocardial Infarction Treated With Primary Angioplasty: Impact on Left Ventricular Function Assessed by Comprehensive Echocardiography and Gated Single-Photon Emission CT." Circ Cardiovasc Imaging **3**(6): 656-662.
296. Murphy, E., M. Kohr, S. Menazza, T. Nguyen, A. Evangelista, J. Sun and C. Steenbergen (2014). "Signaling by S-nitrosylation in the heart." J Mol Cell Cardiol **73**: 18-25.
297. Murray, C. I., L. A. Kane, H. Uhrigshardt, S. B. Wang and J. E. Van Eyk (2011). "Site-mapping of in vitro S-nitrosation in cardiac mitochondria: implications for cardioprotection." Mol Cell Proteomics **10**(3): M110.004721.
298. Murry, C. E., R. B. Jennings and K. A. Reimer (1986). "Preconditioning with ischemia: a delay of lethal cell injury in ischemic myocardium." Circulation **74**(5): 1124-1136.
299. Na, B. J., G. H. Jahng, S. U. Park, W. S. Jung, S. K. Moon, J. M. Park and H. S. Bae (2009). "An fMRI study of neuronal specificity of an acupoint: electroacupuncture stimulation of Yanglingquan (GB34) and its sham point." Neurosci Lett **464**(1): 1-5.
300. Nag, A. C. (1980). "Study of non-muscle cells of the adult mammalian heart: a fine structural analysis and distribution." Cytobios **28**(109): 41-61.
301. Nallamothu, B. K. and E. R. Bates (2003). "Percutaneous coronary intervention versus fibrinolytic therapy in acute myocardial infarction: is timing (almost) everything?" Am J Cardiol **92**(7): 824-826.
302. Nian, M., P. Lee, N. Khaper and P. Liu (2004). "Inflammatory cytokines and postmyocardial infarction remodeling." Circ Res **94**(12): 1543-1553.
303. Nishizawa, J., A. Nakai, T. Higashi, M. Tanabe, S. Nomoto, K. Matsuda, T. Ban and K. Nagata (1996). "Reperfusion causes significant activation of heat shock transcription factor 1 in ischemic rat heart." Circulation **94**(9): 2185-2192.
304. Nishizawa, J., A. Nakai, K. Matsuda, M. Komeda, T. Ban and K. Nagata (1999). "Reactive oxygen species play an important role in the activation of heat shock factor 1 in ischemic-reperfused heart." Circulation **99**(7): 934-941.
305. Node, K., M. Kitakaze, H. Sato, T. Minamino, K. Komamura, Y. Shinozaki, H. Mori and M. Hori (1997). "Role of intracellular Ca²⁺ in activation of protein kinase C during ischemic preconditioning." Circulation **96**(4): 1257-1265.

306. O'Connell, T. D., B. C. Jensen, A. J. Baker and P. C. Simpson (2014). "Cardiac alpha1-adrenergic receptors: novel aspects of expression, signaling mechanisms, physiologic function, and clinical importance." Pharmacol Rev **66**(1): 308-333.
307. Ong, S. B., K. Katwadi, X. Y. Kwek, N. I. Ismail, K. Chinda, S. G. Ong and D. J. Hausenloy (2018). "Non-coding RNAs as therapeutic targets for preventing myocardial ischemia-reperfusion injury." Expert Opin Ther Targets **22**(3): 247-261.
308. Onody, A., A. Zvara, L. Hackler, Jr., L. Vigh, P. Ferdinandy and L. G. Puskas (2003). "Effect of classic preconditioning on the gene expression pattern of rat hearts: a DNA microarray study." FEBS Lett **536**(1-3): 35-40.
309. Opie, L. H. and M. N. Sack (2002). "Metabolic plasticity and the promotion of cardiac protection in ischemia and ischemic preconditioning." J Mol Cell Cardiol **34**(9): 1077-1089.
310. Ottani, F., R. Latini, L. Staszewsky, L. La Vecchia, N. Locuratolo, M. Sicuro, S. Masson, S. Barlera, V. Milani, M. Lombardi, A. Costalunga, N. Mollicelli, A. Santarelli, N. De Cesare, P. Sganzerla, A. Boi, A. P. Maggioni and U. Limbruno (2016). "Cyclosporine A in Reperfused Myocardial Infarction: The Multicenter, Controlled, Open-Label CYCLE Trial." J Am Coll Cardiol **67**(4): 365-374.
311. Packer, M. (1992). "The neurohormonal hypothesis: a theory to explain the mechanism of disease progression in heart failure." J Am Coll Cardiol **20**(1): 248-254.
312. Pan, Y. L., Z. Y. Han, S. F. He, W. Yang, J. Cheng, Y. Zhang and Z. W. Chen (2018). "miR133b5p contributes to hypoxic preconditioning mediated cardioprotection by inhibiting the activation of caspase8 and caspase-3 in cardiomyocytes." Mol Med Rep **17**(5): 7097-7104.
313. Pan, Z., Y. Guo, H. Qi, K. Fan, S. Wang, H. Zhao, Y. Fan, J. Xie, F. Guo, Y. Hou, N. Wang, R. Huo, Y. Zhang, Y. Liu and Z. Du (2012). "M3 subtype of muscarinic acetylcholine receptor promotes cardioprotection via the suppression of miR-376b-5p." PLoS One **7**(3): e32571.
314. Papa, S., F. Zazzeroni, C. G. Pham, C. Bubici and G. Franzoso (2004). "Linking JNK signaling to NF-kappaB: a key to survival." J Cell Sci **117**(Pt 22): 5197-5208.
315. Paraskevopoulou, M. D., G. Georgakilas, N. Kostoulas, I. S. Vlachos, T. Vergoulis, M. Reczko, C. Filippidis, T. Dalamagas and A. G. Hatzigeorgiou (2013). "DIANA-microT web server v5.0: service integration into miRNA functional analysis workflows." Nucleic Acids Res **41**(Web Server issue): W169-173.
316. Parmley, W. W., L. Chuck, C. Kivowitz, J. M. Matloff and H. J. Swan (1973). "In vitro length-tension relations of human ventricular aneurysms. Relation of stiffness to mechanical disadvantage." Am J Cardiol **32**(7): 889-894.

317. Patel, H. H., A. Hsu and G. J. Gross (2001). "Cardioprotection is strain dependent in rat in response to whole body hyperthermia." Am J Physiol Heart Circ Physiol **280**(3): H1208-1214.
318. Pavo, N., D. Lukovic, K. Zlabinger, A. Zimba, D. Lorant, G. Goliasch, J. Winkler, D. Pils, K. Auer, H. Jan Ankersmit, Z. Giricz, T. Baranyai, M. Sarkozy, A. Jakab, R. Garamvolgyi, M. Y. Emmert, S. P. Hoerstrup, D. J. Hausenloy, P. Ferdinandy, G. Maurer and M. Gyongyosi (2017). "Sequential activation of different pathway networks in ischemia-affected and non-affected myocardium, inducing intrinsic remote conditioning to prevent left ventricular remodeling." Sci Rep **7**: 43958.
319. Penna, C., M. G. Perrelli, F. Tullio, C. Angotti, A. Camporeale, V. Poli and P. Pagliaro (2013). "Diazoxide postconditioning induces mitochondrial protein S-nitrosylation and a redox-sensitive mitochondrial phosphorylation/translocation of RISK elements: no role for SAFE." Basic Res Cardiol **108**(5): 371.
320. Persson, H., E. Linder-Klingsell, S. V. Eriksson and L. Erhardt (1995). "Heart failure after myocardial infarction: the importance of diastolic dysfunction. A prospective clinical and echocardiographic study." Eur Heart J **16**(4): 496-505.
321. Ping, P., J. Zhang, Y. Qiu, X. L. Tang, S. Manchikalapudi, X. Cao and R. Bolli (1997). "Ischemic preconditioning induces selective translocation of protein kinase C isoforms epsilon and eta in the heart of conscious rabbits without subcellular redistribution of total protein kinase C activity." Circ Res **81**(3): 404-414.
322. Pinto, A. R., A. Illykh, M. J. Ivey, J. T. Kuwabara, M. L. D'Antoni, R. Debuque, A. Chandran, L. Wang, K. Arora, N. A. Rosenthal and M. D. Tallquist (2016). "Revisiting Cardiac Cellular Composition." Circ Res **118**(3): 400-409.
323. Plumier, J. C., B. M. Ross, R. W. Currie, C. E. Angelidis, H. Kazlaris, G. Kollias and G. N. Pagoulatos (1995). "Transgenic mice expressing the human heat shock protein 70 have improved post-ischemic myocardial recovery." J Clin Invest **95**(4): 1854-1860.
324. Prasad, A., B. J. Gersh, M. E. Bertrand, A. M. Lincoff, J. W. Moses, E. M. Ohman, H. D. White, S. J. Pocock, B. T. McLaurin, D. A. Cox, A. J. Lansky, R. Mehran and G. W. Stone (2009). "Prognostic significance of periprocedural versus spontaneously occurring myocardial infarction after percutaneous coronary intervention in patients with acute coronary syndromes: an analysis from the ACUTY (Acute Catheterization and Urgent Intervention Triage Strategy) trial." J Am Coll Cardiol **54**(5): 477-486.
325. Prime, T. A., F. H. Blaikie, C. Evans, S. M. Nadtochiy, A. M. James, C. C. Dahm, D. A. Vitturi, R. P. Patel, C. R. Hiley, I. Abakumova, R. Requejo, E. T. Chouchani, T. R. Hurd, J. F. Garvey, C. T. Taylor, P. S. Brookes, R. A. Smith and M. P. Murphy (2009). "A mitochondria-targeted S-nitrosothiol modulates respiration, nitrosates thiols, and protects against ischemia-reperfusion injury." Proc Natl Acad Sci U S A **106**(26):

10764-10769.

326. Przyklenk, K., B. Bauer, M. Ovize, R. A. Kloner and P. Whittaker (1993). "Regional ischemic 'preconditioning' protects remote virgin myocardium from subsequent sustained coronary occlusion." Circulation **87**(3): 893-899. R Core Team (2018).
327. R Core Team (2014). R: A language and environment for statistical computing. R Foundation for Statistical Computing, Vienna, Austria. Available online at <https://www.R-project.org/>.
328. Reczko, M., M. Maragkakis, P. Alexiou, I. Grosse and A. G. Hatzigeorgiou (2012). "Functional microRNA targets in protein coding sequences." Bioinformatics **28**(6): 771-776.
329. Redgrave, J., D. Day, H. Leung, P. J. Laud, A. Ali, R. Lindert and A. Majid (2018). "Safety and tolerability of Transcutaneous Vagus Nerve stimulation in humans; a systematic review." Brain Stimul **11**(6): 1225-1238.
330. Redington, K. L., T. Disenhouse, J. Li, C. Wei, X. Dai, R. Gladstone, C. Manlihot and A. N. Redington (2013). "Electroacupuncture reduces myocardial infarct size and improves post-ischemic recovery by invoking release of humoral, dialyzable, cardioprotective factors." J Physiol Sci **63**(3): 219-223.
331. Redington, K. L., T. Disenhouse, S. C. Strantzas, R. Gladstone, C. Wei, M. B. Tropak, X. Dai, C. Manlihot, J. Li and A. N. Redington (2012). "Remote cardioprotection by direct peripheral nerve stimulation and topical capsaicin is mediated by circulating humoral factors." Basic Res Cardiol **107**(2): 241.
332. Ren, X., A. E. Roessler, T. L. t. Lynch, L. Haar, F. Mallick, Y. Liu, M. Tranter, M. Ren, W. Rui Xie, G. C. Fan, J. M. Zhang, E. Kranias, A. Anjak, S. E. Koch, M. Jiang, S. Dass, A. Cohen, J. Rubinstein, N. L. Weintraub and W. K. Jones (2018). "Cardioprotection via the skin; Nociceptor-Induced Conditioning Against Cardiac MI, in the NIC of time." Am J Physiol Heart Circ Physiol.
333. Ren, X., Y. Wang and W. K. Jones (2004). "TNF-alpha is required for late ischemic preconditioning but not for remote preconditioning of trauma." J Surg Res **121**(1): 120-129.
334. Rizvi, A., X. L. Tang, Y. Qiu, Y. T. Xuan, H. Takano, A. K. Jadoon and R. Bolli (1999). "Increased protein synthesis is necessary for the development of late preconditioning against myocardial stunning." Am J Physiol **277**(3): H874-884.
335. Rorabaugh, B. R., S. A. Ross, R. J. Gaivin, R. S. Papay, D. F. McCune, P. C. Simpson and D. M. Perez (2005). "alpha1A- but not alpha1B-adrenergic receptors precondition the ischemic heart by a staurosporine-sensitive, chelerythrine-insensitive mechanism." Cardiovasc Res **65**(2): 436-445.

336. Ross, J., Jr. and W. H. McCullagh (1972). "Nature of enhanced performance of the dilated left ventricle in the dog during chronic volume overloading." Circ Res **30**(5): 549-556.
337. Rysevaite, K., I. Saburkina, N. Pauziene, R. Vaitkevicius, S. F. Noujaim, J. Jalife and D. H. Pauza (2011). "Immunohistochemical characterization of the intrinsic cardiac neural plexus in whole-mount mouse heart preparations." Heart Rhythm **8**(5): 731-738.
338. Ryvlin, P., F. G. Gilliam, D. K. Nguyen, G. Colicchio, A. Iudice, P. Tinuper, N. Zamponi, U. Aguglia, L. Wagner, L. Minotti, H. Stefan, P. Boon, M. Sadler, P. Benna, P. Raman and E. Perucca (2014). "The long-term effect of vagus nerve stimulation on quality of life in patients with pharmaco-resistant focal epilepsy: the PuLSE (Open Prospective Randomized Long-term Effectiveness) trial." Epilepsia **55**(6): 893-900.
339. Sabbah, H. N., I. Ilisar, A. Zaretsky, S. Rastogi, M. Wang and R. C. Gupta (2011). "Vagus nerve stimulation in experimental heart failure." Heart Fail Rev **16**(2): 171-178.
340. Sadoshima, J., O. Montagne, Q. Wang, G. Yang, J. Warden, J. Liu, G. Takagi, V. Karoor, C. Hong, G. L. Johnson, D. E. Vatner and S. F. Vatner (2002). "The MEKK1-JNK pathway plays a protective role in pressure overload but does not mediate cardiac hypertrophy." J Clin Invest **110**(2): 271-279.
341. Salloum, F. N., C. Yin and R. C. Kukreja (2010). "Role of microRNAs in cardiac preconditioning." J Cardiovasc Pharmacol **56**(6): 581-588.
342. Sam, F., D. B. Sawyer, D. L. Chang, F. R. Eberli, S. Ngoy, M. Jain, J. Amin, C. S. Apstein and W. S. Colucci (2000). "Progressive left ventricular remodeling and apoptosis late after myocardial infarction in mouse heart." Am J Physiol Heart Circ Physiol **279**(1): H422-428.
343. Saraste, A., K. Pulkki, M. Kallajoki, K. Henriksen, M. Parvinen and L. M. Voipio-Pulkki (1997). "Apoptosis in human acute myocardial infarction." Circulation **95**(2): 320-323.
344. Schmidt, M. R., M. Smerup, I. E. Konstantinov, M. Shimizu, J. Li, M. Cheung, P. A. White, S. B. Kristiansen, K. Sorensen, V. Dzavik, A. N. Redington and R. K. Kharbanda (2007). "Intermittent peripheral tissue ischemia during coronary ischemia reduces myocardial infarction through a KATP-dependent mechanism: first demonstration of remote ischemic preconditioning." Am J Physiol Heart Circ Physiol **292**(4): H1883-1890.
345. Schoemaker, R. G. and C. L. van Heijningen (2000). "Bradykinin mediates cardiac preconditioning at a distance." Am J Physiol Heart Circ Physiol **278**(5): H1571-1576.

346. Schulz, R., H. Post, C. Vahlhaus and G. Heusch (1998). "Ischemic preconditioning in pigs: a graded phenomenon: its relation to adenosine and bradykinin." Circulation **98**(10): 1022-1029.
347. Schurch, N. J., P. Schofield, M. Gierlinski, C. Cole, A. Sherstnev, V. Singh, N. Wrobel, K. Gharbi, G. G. Simpson, T. Owen-Hughes, M. Blaxter and G. J. Barton (2016). "How many biological replicates are needed in an RNA-seq experiment and which differential expression tool should you use?" Rna **22**(6): 839-851.
348. Seeger, T., Q. F. Xu, M. Muhly-Reinholz, A. Fischer, E. M. Kremp, A. M. Zeiher and S. Dimmeler (2016). "Inhibition of let-7 augments the recruitment of epicardial cells and improves cardiac function after myocardial infarction." J Mol Cell Cardiol **94**: 145-152.
349. Selzner, N., M. Boehnert and M. Selzner (2012). "Preconditioning, postconditioning, and remote conditioning in solid organ transplantation: basic mechanisms and translational applications." Transplant Rev (Orlando) **26**(2): 115-124.
350. Serejo, F. C., L. F. Rodrigues, Jr., K. C. da Silva Tavares, A. C. de Carvalho and J. H. Nascimento (2007). "Cardioprotective properties of humoral factors released from rat hearts subject to ischemic preconditioning." J Cardiovasc Pharmacol **49**(4): 214-220.
351. Shaffer, F., R. McCraty and C. L. Zerr (2014). "A healthy heart is not a metronome: an integrative review of the heart's anatomy and heart rate variability." Front Psychol **5**: 1040.
352. Shen, M. J., T. Shinohara, H. W. Park, K. Frick, D. S. Ice, E. K. Choi, S. Han, M. Maruyama, R. Sharma, C. Shen, M. C. Fishbein, L. S. Chen, J. C. Lopshire, D. P. Zipes, S. F. Lin and P. S. Chen (2011). "Continuous low-level vagus nerve stimulation reduces stellate ganglion nerve activity and paroxysmal atrial tachyarrhythmias in ambulatory canines." Circulation **123**(20): 2204-2212.
353. Shi, H., L. Chen, H. Wang, S. Zhu, C. Dong, K. A. Webster and J. Wei (2013). "Synergistic induction of miR-126 by hypoxia and HDAC inhibitors in cardiac myocytes." Biochem Biophys Res Commun **430**(2): 827-832.
354. Shim, E.-H., J.-I. Kim, E.-S. Bang, J.-S. Heo, J.-S. Lee, E.-Y. Kim, J.-E. Lee, W.-Y. Park, S.-H. Kim, H.-S. Kim, O. Smithies, J.-J. Jang, D.-I. Jin and J.-S. Seo (2002). "Targeted disruption of hsp70.1 sensitizes to osmotic stress." EMBO reports **3**(9): 857-861.
355. Shimizu, M., M. Tropak, R. J. Diaz, F. Suto, H. Surendra, E. Kuzmin, J. Li, G. Gross, G. J. Wilson, J. Callahan and A. N. Redington (2009). "Transient limb ischaemia remotely preconditions through a humoral mechanism acting directly on the myocardium: evidence suggesting cross-species protection." Clin Sci (Lond) **117**(5): 191-200.

356. Shinlapawittayatorn, K., K. Chinda, S. Palee, S. Surinkaew, S. Kumfu, S. Kumphune, S. Chattipakorn, B. H. KenKnight and N. Chattipakorn (2014). "Vagus nerve stimulation initiated late during ischemia, but not reperfusion, exerts cardioprotection via amelioration of cardiac mitochondrial dysfunction." Heart Rhythm **11**(12): 2278-2287.
357. Shinlapawittayatorn, K., K. Chinda, S. Palee, S. Surinkaew, K. Thunsiri, P. Weerateerangkul, S. Chattipakorn, B. H. KenKnight and N. Chattipakorn (2013). "Low-amplitude, left vagus nerve stimulation significantly attenuates ventricular dysfunction and infarct size through prevention of mitochondrial dysfunction during acute ischemia-reperfusion injury." Heart Rhythm **10**(11): 1700-1707.
358. Shinmura, K., X. L. Tang, Y. Wang, Y. T. Xuan, S. Q. Liu, H. Takano, A. Bhatnagar and R. Bolli (2000). "Cyclooxygenase-2 mediates the cardioprotective effects of the late phase of ischemic preconditioning in conscious rabbits." Proc Natl Acad Sci U S A **97**(18): 10197-10202.
359. Shinmura, K., Y.-T. Xuan, X.-L. Tang, E. Kodani, H. Han, Y. Zhu and R. Bolli (2002). "Inducible Nitric Oxide Synthase Modulates Cyclooxygenase-2 Activity in the Heart of Conscious Rabbits During the Late Phase of Ischemic Preconditioning." Circulation Research **90**(5): 602-608.
360. Shivkumar, K., O. A. Ajijola, I. Anand, J. A. Armour, P. S. Chen, M. Esler, G. M. De Ferrari, M. C. Fishbein, J. J. Goldberger, R. M. Harper, M. J. Joyner, S. S. Khalsa, R. Kumar, R. Lane, A. Mahajan, S. Po, P. J. Schwartz, V. K. Somers, M. Valderrabano, M. Vaseghi and D. P. Zipes (2016). "Clinical neurocardiology defining the value of neuroscience-based cardiovascular therapeutics." J Physiol **594**(14): 3911-3954.
361. Skynner, M. J., U. Gangadharan, G. R. Coulton, R. M. Mason, A. Nikitopoulou, S. D. Brown and G. Blanco (1995). "Genetic mapping of the mouse neuromuscular mutation kyphoscoliosis." Genomics **25**(1): 207-213.
362. Slagsvold, K. H., O. Rognmo, M. Hoydal, U. Wisloff and A. Wahba (2014). "Remote ischemic preconditioning preserves mitochondrial function and influences myocardial microRNA expression in atrial myocardium during coronary bypass surgery." Circ Res **114**(5): 851-859.
363. Sloth, A. D., M. R. Schmidt, K. Munk, R. K. Kharbanda, A. N. Redington, M. Schmidt, L. Pedersen, H. T. Sorensen and H. E. Botker (2014). "Improved long-term clinical outcomes in patients with ST-elevation myocardial infarction undergoing remote ischaemic conditioning as an adjunct to primary percutaneous coronary intervention." Eur Heart J **35**(3): 168-175.
364. Smith, C. L., J. A. Blake, J. A. Kadin, J. E. Richardson and C. J. Bult (2018). "Mouse Genome Database (MGD)-2018: knowledgebase for the laboratory mouse." Nucleic

Acids Res **46**(D1): D836-d842.

365. Smith, R. M., N. Suleman, J. McCarthy and M. N. Sack (2002). "Classic ischemic but not pharmacologic preconditioning is abrogated following genetic ablation of the TNFalpha gene." Cardiovasc Res **55**(3): 553-560.
366. Sobel, B. E., G. F. Bresnahan, W. E. Shell and R. D. Yoder (1972). "Estimation of infarct size in man and its relation to prognosis." Circulation **46**(4): 640-648.
367. Song, Y., Y. J. Ye, P. W. Li, Y. L. Zhao, Q. Miao, D. Y. Hou and X. P. Ren (2015). "The Cardioprotective Effects of Late-Phase Remote Preconditioning of Trauma Depends on Neurogenic Pathways and the Activation of PKC and NF-kappaB (But Not iNOS) in Mice." J Cardiovasc Pharmacol Ther.
368. Song, Y., Y. J. Ye, P. W. Li, Y. L. Zhao, Q. Miao, D. Y. Hou and X. P. Ren (2016). "The Cardioprotective Effects of Late-Phase Remote Preconditioning of Trauma Depends on Neurogenic Pathways and the Activation of PKC and NF-kappaB (But Not iNOS) in Mice." J Cardiovasc Pharmacol Ther **21**(3): 310-319.
369. Song, Y. J., C. B. Zhong and X. B. Wang (2018). "Heat shock protein 70: A promising therapeutic target for myocardial ischemia-reperfusion injury." J Cell Physiol.
370. Southerland, E. M., D. M. Milhorn, R. D. Foreman, B. Linderorth, M. J. DeJongste, J. A. Armour, V. Subramanian, M. Singh, K. Singh and J. L. Ardell (2007). "Preemptive, but not reactive, spinal cord stimulation mitigates transient ischemia-induced myocardial infarction via cardiac adrenergic neurons." Am J Physiol Heart Circ Physiol **292**(1): H311-317.
371. Staat, P., G. Rioufol, C. Piot, Y. Cottin, T. T. Cung, I. L'Huillier, J. F. Aupetit, E. Bonnefoy, G. Finet, X. Andre-Fouet and M. Ovize (2005). "Postconditioning the human heart." Circulation **112**(14): 2143-2148.
372. Stavrakis, S., M. B. Humphrey, B. J. Scherlag, Y. Hu, W. M. Jackman, H. Nakagawa, D. Lockwood, R. Lazzara and S. S. Po (2015). "Low-level transcutaneous electrical vagus nerve stimulation suppresses atrial fibrillation." J Am Coll Cardiol **65**(9): 867-875.
373. Straussberg, R., G. Schottmann, M. Sadeh, E. Gill, F. Seifert, A. Halevy, K. Qassem, J. Rendu, P. F. van der Ven, W. Stenzel and M. Schuelke (2016). "Kyphoscoliosis peptidase (KY) mutation causes a novel congenital myopathy with core targetoid defects." Acta Neuropathol **132**(3): 475-478.
374. Summers, D. W., P. M. Douglas, C. H. Ramos and D. M. Cyr (2009). "Polypeptide transfer from Hsp40 to Hsp70 molecular chaperones." Trends Biochem Sci **34**(5): 230-233.
375. Sun, J., M. Morgan, R. F. Shen, C. Steenbergen and E. Murphy (2007).

- "Preconditioning results in S-nitrosylation of proteins involved in regulation of mitochondrial energetics and calcium transport." Circ Res **101**(11): 1155-1163.
376. Sun, J. and E. Murphy (2010). "Protein S-nitrosylation and cardioprotection." Circ Res **106**(2): 285-296.
 377. Sun, J. Z., X. L. Tang, S. W. Park, Y. Qiu, J. F. Turrens and R. Bolli (1996). "Evidence for an essential role of reactive oxygen species in the genesis of late preconditioning against myocardial stunning in conscious pigs." J Clin Invest **97**(2): 562-576.
 378. Surendra, H., R. J. Diaz, K. Harvey, M. Tropak, J. Callahan, A. Hinek, T. Hossain, A. Redington and G. J. Wilson (2013). "Interaction of delta and kappa opioid receptors with adenosine A1 receptors mediates cardioprotection by remote ischemic preconditioning." J Mol Cell Cardiol **60**: 142-150.
 379. Takano, H., S. Manchikalapudi, X. L. Tang, Y. Qiu, A. Rizvi, A. K. Jadoon, Q. Zhang and R. Bolli (1998). "Nitric oxide synthase is the mediator of late preconditioning against myocardial infarction in conscious rabbits." Circulation **98**(5): 441-449.
 380. Tang, G., Y. Minemoto, B. Dibling, N. H. Purcell, Z. Li, M. Karin and A. Lin (2001). "Inhibition of JNK activation through NF-kappaB target genes." Nature **414**(6861): 313-317.
 381. Tang, Y., Y. Wang, K. M. Park, Q. Hu, J. P. Teoh, Z. Broskova, P. Ranganathan, C. Jayakumar, J. Li, H. Su, Y. Tang, G. Ramesh and I. M. Kim (2015). "MicroRNA-150 protects the mouse heart from ischaemic injury by regulating cell death." Cardiovasc Res **106**(3): 387-397.
 382. Tanonaka, K., W. Toga, H. Yoshida and S. Takeo (2003). "Myocardial heat shock protein changes in the failing heart following coronary artery ligation." Heart Lung Circ **12**(1): 60-65.
 383. Tennant, R. and C. J. Wiggers (1935). "THE EFFECT OF CORONARY OCCLUSION ON MYOCARDIAL CONTRACTION." American Journal of Physiology-Legacy Content **112**(2): 351-361.
 384. Theroux, P., B. R. Chaitman, N. Danchin, L. Erhardt, T. Meinertz, J. S. Schroeder, G. Tognoni, H. D. White, J. T. Willerson and A. Jessel (2000). "Inhibition of the sodium-hydrogen exchanger with cariporide to prevent myocardial infarction in high-risk ischemic situations. Main results of the GUARDIAN trial. Guard during ischemia against necrosis (GUARDIAN) Investigators." Circulation **102**(25): 3032-3038.
 385. Theroux, P., J. Ross, Jr., D. Franklin, J. W. Covell, C. M. Bloor and S. Sasayama (1977). "Regional myocardial function and dimensions early and late after myocardial infarction in the unanesthetized dog." Circ Res **40**(2): 158-165.

386. Thygesen, K., J. S. Alpert, A. S. Jaffe, M. L. Simoons, B. R. Chaitman, H. D. White, K. Thygesen, J. S. Alpert, H. D. White, A. S. Jaffe, H. A. Katus, F. S. Apple, B. Lindahl, D. A. Morrow, B. A. Chaitman, P. M. Clemmensen, P. Johanson, H. Hod, R. Underwood, J. J. Bax, R. O. Bonow, F. Pinto, R. J. Gibbons, K. A. Fox, D. Atar, L. K. Newby, M. Galvani, C. W. Hamm, B. F. Uretsky, P. G. Steg, W. Wijns, J. P. Bassand, P. Menasche, J. Ravkilde, E. M. Ohman, E. M. Antman, L. C. Wallentin, P. W. Armstrong, M. L. Simoons, J. L. Januzzi, M. S. Nieminen, M. Gheorghiade, G. Filippatos, R. V. Luepker, S. P. Fortmann, W. D. Rosamond, D. Levy, D. Wood, S. C. Smith, D. Hu, J. L. Lopez-Sendon, R. M. Robertson, D. Weaver, M. Tendera, A. A. Bove, A. N. Parkhomenko, E. J. Vasilieva and S. Mendis (2012). "Third universal definition of myocardial infarction." Eur Heart J **33**(20): 2551-2567.
387. Tipney, H. and L. Hunter (2010). "An introduction to effective use of enrichment analysis software." Hum Genomics **4**(3): 202-206.
388. Tran, T. H., P. Andreka, C. O. Rodrigues, K. A. Webster and N. H. Bishopric (2007). "Jun kinase delays caspase-9 activation by interaction with the apoptosome." J Biol Chem **282**(28): 20340-20350.
389. Tranter, M., R. N. Helsley, W. R. Paulding, M. McGuinness, C. Brokamp, L. Haar, Y. Liu, X. Ren and W. K. Jones (2011). "Coordinated post-transcriptional regulation of Hsp70.3 gene expression by microRNA and alternative polyadenylation." J Biol Chem **286**(34): 29828-29837.
390. Tranter, M., X. Ren, T. Forde, M. E. Wilhide, J. Chen, M. A. Sartor, M. Medvedovic and W. K. Jones (2010). "NF-kappaB driven cardioprotective gene programs; Hsp70.3 and cardioprotection after late ischemic preconditioning." J Mol Cell Cardiol **49**(4): 664-672.
391. Triposkiadis, F., G. Karayannis, G. Giamouzis, J. Skoularigis, G. Louridas and J. Butler (2009). "The sympathetic nervous system in heart failure physiology, pathophysiology, and clinical implications." J Am Coll Cardiol **54**(19): 1747-1762.
392. Trost, S. U., J. H. Omens, W. J. Karlon, M. Meyer, R. Mestril, J. W. Covell and W. H. Dillmann (1998). "Protection against myocardial dysfunction after a brief ischemic period in transgenic mice expressing inducible heat shock protein 70." J Clin Invest **101**(4): 855-862.
393. Tsai, H. J., S. S. Huang, M. T. Tsou, H. T. Wang and J. H. Chiu (2015). "Role of Opioid Receptors Signaling in Remote Electrostimulation--Induced Protection against Ischemia/Reperfusion Injury in Rat Hearts." PLoS One **10**(10): e0138108.
394. Tsang, A., D. J. Hausenloy, M. M. Mocanu and D. M. Yellon (2004). "Postconditioning: a form of "modified reperfusion" protects the myocardium by activating the phosphatidylinositol 3-kinase-Akt pathway." Circ Res **95**(3): 230-232.

395. Tsou, M. T., C. H. Huang and J. H. Chiu (2004). "Electroacupuncture on PC6 (Neiguan) attenuates ischemia/reperfusion injury in rat hearts." Am J Chin Med **32**(6): 951-965.
396. Tsuchida, A., Y. Liu, G. S. Liu, M. V. Cohen and J. M. Downey (1994). "alpha 1-adrenergic agonists precondition rabbit ischemic myocardium independent of adenosine by direct activation of protein kinase C." Circ Res **75**(3): 576-585.
397. Tsutsumi, T., T. Ide, M. Yamato, W. Kudou, M. Andou, Y. Hirooka, H. Utsumi, H. Tsutsui and K. Sunagawa (2008). "Modulation of the myocardial redox state by vagal nerve stimulation after experimental myocardial infarction." Cardiovasc Res **77**(4): 713-721.
398. Tu, Y., L. Wan, Y. Fan, K. Wang, L. Bu, T. Huang, Z. Cheng and B. Shen (2013). "Ischemic postconditioning-mediated miRNA-21 protects against cardiac ischemia/reperfusion injury via PTEN/Akt pathway." PLoS One **8**(10): e75872.
399. Uitterdijk, A., T. Yetgin, M. te Lintel Hekkert, S. Sneep, I. Krabbendam-Peters, H. M. van Beusekom, T. M. Fischer, R. N. Cornelussen, O. C. Manintveld, D. Merkus and D. J. Duncker (2015). "Vagal nerve stimulation started just prior to reperfusion limits infarct size and no-reflow." Basic Res Cardiol **110**(5): 508.
400. Ursell, P. C. and M. Mayes (1995). "Anatomic distribution of nitric oxide synthase in the heart." Int J Cardiol **50**(3): 217-223.
401. Valen, G., G. K. Hansson, A. Dumitrescu and J. Vaage (2000). "Unstable angina activates myocardial heat shock protein 72, endothelial nitric oxide synthase, and transcription factors NFkappaB and AP-1." Cardiovasc Res **47**(1): 49-56.
402. Vanoli, E., G. M. De Ferrari, M. Stramba-Badiale, S. S. Hull, Jr., R. D. Foreman and P. J. Schwartz (1991). "Vagal stimulation and prevention of sudden death in conscious dogs with a healed myocardial infarction." Circ Res **68**(5): 1471-1481.
403. Varga, Z. V., A. Zvara, N. Farago, G. F. Kocsis, M. Pipicz, R. Gaspar, P. Bencsik, A. Gorbe, C. Csonka, L. G. Puskas, T. Thum, T. Csont and P. Ferdinandy (2014). "MicroRNAs associated with ischemia-reperfusion injury and cardioprotection by ischemic pre- and postconditioning: protectomiRs." Am J Physiol Heart Circ Physiol **307**(2): H216-227.
404. Venugopal, V., D. J. Hausenloy, A. Ludman, C. Di Salvo, S. Kolvekar, J. Yap, D. Lawrence, J. Bognolo and D. M. Yellon (2009). "Remote ischaemic preconditioning reduces myocardial injury in patients undergoing cardiac surgery with cold-blood cardioplegia: a randomised controlled trial." Heart **95**(19): 1567-1571.
405. Vicencio, J. M., D. M. Yellon, V. Sivaraman, D. Das, C. Boi-Doku, S. Arjun, Y. Zheng, J. A. Riquelme, J. Kearney, V. Sharma, G. Multhoff, A. R. Hall and S. M. Davidson (2015). "Plasma exosomes protect the myocardium from ischemia-reperfusion

- injury." J Am Coll Cardiol **65**(15): 1525-1536.
406. Vlachos, I. S., K. Zagganas, M. D. Paraskevopoulou, G. Georgakilas, D. Karagkouni, T. Vergoulis, T. Dalamagas and A. G. Hatzigeorgiou (2015). "DIANA-miRPath v3.0: deciphering microRNA function with experimental support." Nucleic Acids Res **43**(W1): W460-466.
 407. Wagner, R., P. Piler, H. Bedanova, P. Adamek, L. Grodecka and T. Freiburger (2010). "Myocardial injury is decreased by late remote ischaemic preconditioning and aggravated by tramadol in patients undergoing cardiac surgery: a randomised controlled trial." Interact Cardiovasc Thorac Surg **11**(6): 758-762.
 408. Walsh, S. R., T. Y. Tang, P. Kullar, D. P. Jenkins, D. P. Dutka and M. E. Gaunt (2008). "Ischaemic preconditioning during cardiac surgery: systematic review and meta-analysis of perioperative outcomes in randomised clinical trials." Eur J Cardiothorac Surg **34**(5): 985-994.
 409. Wang, G., X. Li, H. Wang, Y. Wang, L. Zhang, L. Zhang, B. Liu and M. Zhang (2015). "Later phase cardioprotection of ischemic post-conditioning against ischemia/reperfusion injury depends on iNOS and PI3K-Akt pathway." Am J Transl Res **7**(12): 2603-2611.
 410. Wang, J., J. Yuan, Y. Cai, S. Fu, M. Li, H. Hong, S. Lu and B. Zhu (2018). "[Effects of electroacupuncture on inflammatory response of cardiac muscle tissue in mice with acute myocardial ischemia]." Zhongguo Zhen Jiu **38**(5): 5133-5138.
 411. Wang, K., Z. Jiang, K. A. Webster, J. Chen, H. Hu, Y. Zhou, J. Zhao, L. Wang, Y. Wang, Z. Zhong, C. Ni, Q. Li, C. Xiang, L. Zhang, R. Wu, W. Zhu, H. Yu, X. Hu and J. Wang (2017). "Enhanced Cardioprotection by Human Endometrium Mesenchymal Stem Cells Driven by Exosomal MicroRNA-21." Stem Cells Transl Med **6**(1): 209-222.
 412. Wang, Q., Y. Cheng, F. S. Xue, Y. J. Yuan, J. Xiong, R. P. Li, X. Liao and J. H. Liu (2012). "Postconditioning with vagal stimulation attenuates local and systemic inflammatory responses to myocardial ischemia reperfusion injury in rats." Inflamm Res **61**(11): 1273-1282.
 413. Wang, Q., R. P. Li, F. S. Xue, S. Y. Wang, X. L. Cui, Y. Cheng, G. P. Liu and X. Liao (2014). "Optimal intervention time of vagal stimulation attenuating myocardial ischemia/reperfusion injury in rats." Inflamm Res **63**(12): 987-999.
 414. Wang, Q., D. Liang, F. Wang, W. Li, Y. Han, W. Zhang, Y. Xie, W. Xin, B. Zhou, D. Sun, F. Cao and L. Xiong (2015). "Efficacy of electroacupuncture pretreatment for myocardial injury in patients undergoing percutaneous coronary intervention: A randomized clinical trial with a 2-year follow-up." Int J Cardiol **194**: 28-35.
 415. Wang, Q., G. P. Liu, F. S. Xue, S. Y. Wang, X. L. Cui, R. P. Li, G. Z. Yang, C. Sun and X.

- Liao (2015). "Combined Vagal Stimulation and Limb Remote Ischemic Perconditioning Enhances Cardioprotection via an Anti-inflammatory Pathway." Inflammation **38**(5): 1748-1760.
416. Wang, S. B., S. P. Chen, Y. H. Gao, M. F. Luo and J. L. Liu (2008). "Effects of electroacupuncture on cardiac and gastric activities in acute myocardial ischemia rats." World J Gastroenterol **14**(42): 6496-6502.
 417. Wang, T. Y., B. K. Nallamothu, H. M. Krumholz, S. Li, M. T. Roe, J. G. Jollis, A. K. Jacobs, D. R. Holmes, E. D. Peterson and H. H. Ting (2011). "Association of door-in to door-out time with reperfusion delays and outcomes among patients transferred for primary percutaneous coronary intervention." Jama **305**(24): 2540-2547.
 418. Wang, X., H. Zhu, X. Zhang, Y. Liu, J. Chen, M. Medvedovic, H. Li, M. J. Weiss, X. Ren and G. C. Fan (2012). "Loss of the miR-144/451 cluster impairs ischaemic preconditioning-mediated cardioprotection by targeting Rac-1." Cardiovasc Res **94**(2): 379-390.
 419. Wang, X. R., J. Xiao and D. J. Sun (2003). "Myocardial protective effects of electroacupuncture and hypothermia on porcine heart after ischemia/reperfusion." Acupunct Electrother Res **28**(3-4): 193-200.
 420. Wang, Y. and M. Ashraf (1998). "Activation of α 1-Adrenergic Receptor during Ca^{2+} Pre-conditioning Elicits Strong Protection against Ca^{2+} Overload Injury via Protein Kinase C Signaling Pathway." Journal of Molecular and Cellular Cardiology **30**(11): 2423-2435.
 421. Wang, Y., Y. Guo, S. X. Zhang, W. J. Wu, J. Wang, W. Bao and R. Bolli (2002). "Ischemic preconditioning upregulates inducible nitric oxide synthase in cardiac myocyte." J Mol Cell Cardiol **34**(1): 5-15.
 422. Wang, Y., H. X. Ji, S. H. Xing, D. S. Pei and Q. H. Guan (2007). "SP600125, a selective JNK inhibitor, protects ischemic renal injury via suppressing the extrinsic pathways of apoptosis." Life Sci **80**(22): 2067-2075.
 423. Wang, Y. and P. A. Marsden (1995). "Nitric oxide synthases: gene structure and regulation." Adv Pharmacol **34**: 71-90.
 424. Wang, Y., W. Wang, D. Li, J. Li, J. Dai, Y. Liu, C. Li, X. Zhang, P. Rong and Y. Chen (2014). "The beneficial effect of electro-acupuncture given at PC6 (Neiguan-point) by the increase in cardiac transient outward K^{+} current channel which depends on the gene and protein expressions in artificially induced myocardial ischemia rats." Acupunct Electrother Res **39**(3-4): 259-273.
 425. Wang, Z., L. Yu, M. Chen, S. Wang and H. Jiang (2014). "Transcutaneous electrical stimulation of auricular branch of vagus nerve: a noninvasive therapeutic approach

- for post-ischemic heart failure." Int J Cardiol **177**(2): 676-677.
426. Wang, Z., L. Yu, B. Huang, S. Wang, K. Liao, G. Saren, X. Zhou and H. Jiang (2015). "Low-level transcutaneous electrical stimulation of the auricular branch of vagus nerve ameliorates left ventricular remodeling and dysfunction by downregulation of matrix metalloproteinase 9 and transforming growth factor beta1." J Cardiovasc Pharmacol **65**(4): 342-348.
 427. Wang, Z. K., F. F. Liu, Y. Wang, X. M. Jiang and X. F. Yu (2016). "Let-7a gene knockdown protects against cerebral ischemia/reperfusion injury." Neural Regen Res **11**(2): 262-269.
 428. Wei, J., W. Wang, I. Chopra, H. F. Li, C. J. Dougherty, J. Adi, N. Adi, H. Wang and K. A. Webster (2011). "c-Jun N-terminal kinase (JNK-1) confers protection against brief but not extended ischemia during acute myocardial infarction." J Biol Chem **286**(16): 13995-14006.
 429. West, M. B., G. Rokosh, D. Obal, M. Velayutham, Y. T. Xuan, B. G. Hill, R. J. Keith, J. Schrader, Y. Guo, D. J. Conklin, S. D. Prabhu, J. L. Zweier, R. Bolli and A. Bhatnagar (2008). "Cardiac myocyte-specific expression of inducible nitric oxide synthase protects against ischemia/reperfusion injury by preventing mitochondrial permeability transition." Circulation **118**(19): 1970-1978.
 430. Wijns, W., P. Kolh, N. Danchin, C. Di Mario, V. Falk, T. Folliguet, S. Garg, K. Huber, S. James, J. Knuuti, J. Lopez-Sendon, J. Marco, L. Menicanti, M. Ostojic, M. F. Piepoli, C. Pirlet, J. L. Pomar, N. Reifart, F. L. Ribichini, M. J. Schalij, P. Sergeant, P. W. Serruys, S. Silber, M. Sousa Uva and D. Taggart (2010). "Guidelines on myocardial revascularization." Eur Heart J **31**(20): 2501-2555.
 431. Wilhide, M. E., M. Tranter, X. Ren, J. Chen, M. A. Sartor, M. Medvedovic and W. K. Jones (2011). "Identification of a NF-kappaB cardioprotective gene program: NF-kappaB regulation of Hsp70.1 contributes to cardioprotection after permanent coronary occlusion." J Mol Cell Cardiol **51**(1): 82-89.
 432. Windak, R., J. Muller, A. Felley, A. Akhmedov, E. F. Wagner, T. Pedrazzini, G. Sumara and R. Ricci (2013). "The AP-1 transcription factor c-Jun prevents stress-imposed maladaptive remodeling of the heart." PLoS One **8**(9): e73294.
 433. Wolfrum, S., K. Schneider, M. Heidbreder, J. Nienstedt, P. Dominiak and A. Dendorfer (2002). "Remote preconditioning protects the heart by activating myocardial PKCepsilon-isoform." Cardiovasc Res **55**(3): 583-589.
 434. Wong, N. and X. Wang (2015). "miRDB: an online resource for microRNA target prediction and functional annotations." Nucleic Acids Res **43**(Database issue): D146-152.

435. Wu, M. T., J. M. Sheen, K. H. Chuang, P. Yang, S. L. Chin, C. Y. Tsai, C. J. Chen, J. R. Liao, P. H. Lai, K. A. Chu, H. B. Pan and C. F. Yang (2002). "Neuronal specificity of acupuncture response: a fMRI study with electroacupuncture." Neuroimage **16**(4): 1028-1037.
436. Wu, S., J. Cao, T. Zhang, Y. Zhou, K. Wang, G. Zhu and M. Zhou (2015). "Electroacupuncture Ameliorates the Coronary Occlusion Related Tachycardia and Hypotension in Acute Rat Myocardial Ischemia Model: Potential Role of Hippocampus." Evid Based Complement Alternat Med **2015**: 925987.
437. Xie, Q. W., Y. Kashiwabara and C. Nathan (1994). "Role of transcription factor NF-kappa B/Rel in induction of nitric oxide synthase." J Biol Chem **269**(7): 4705-4708.
438. Xin, P., W. Zhu, J. Li, S. Ma, L. Wang, M. Liu, J. Li, M. Wei and A. N. Redington (2010). "Combined local ischemic postconditioning and remote preconditioning recapitulate cardioprotective effects of local ischemic preconditioning." Am J Physiol Heart Circ Physiol **298**(6): H1819-1831.
439. Xu, L., J. P. Eu, G. Meissner and J. S. Stamler (1998). "Activation of the cardiac calcium release channel (ryanodine receptor) by poly-S-nitrosylation." Science **279**(5348): 234-237.
440. Xu, W., Y. Liu, S. Wang, T. McDonald, J. E. Van Eyk, A. Sidor and B. O'Rourke (2002). "Cytoprotective role of Ca²⁺-activated K⁺ channels in the cardiac inner mitochondrial membrane." Science **298**(5595): 1029-1033.
441. Xuan, Y.-T., Y. Guo, Y. Zhu, O.-L. Wang, G. Rokosh and R. Bolli (2007). "Endothelial Nitric Oxide Synthase Plays an Obligatory Role in the Late Phase of Ischemic Preconditioning by Activating the Protein Kinase C β 4/42 Mitogen-Activated Protein Kinase β 1/3 Pathway." Circulation **116**(5): 535-544.
442. Xuan, Y.-T., X.-L. Tang, Y. Qiu, S. Banerjee, H. Takano, H. Han and R. Bolli (2000). "Biphasic response of cardiac NO synthase isoforms to ischemic preconditioning in conscious rabbits." American Journal of Physiology-Heart and Circulatory Physiology **279**(5): H2360-H2371.
443. Xuan, Y. T., Y. Guo, Y. Zhu, H. Han, R. Langenbach, B. Dawn and R. Bolli (2003). "Mechanism of cyclooxygenase-2 upregulation in late preconditioning." J Mol Cell Cardiol **35**(5): 525-537.
444. Xuan, Y. T., X. L. Tang, S. Banerjee, H. Takano, R. C. Li, H. Han, Y. Qiu, J. J. Li and R. Bolli (1999). "Nuclear factor-kappaB plays an essential role in the late phase of ischemic preconditioning in conscious rabbits." Circ Res **84**(9): 1095-1109.
445. Yamashita, N., S. Hoshida, K. Otsu, N. Taniguchi, T. Kuzuya and M. Hori (2000). "The

- involvement of cytokines in the second window of ischaemic preconditioning." Br J Pharmacol **131**(3): 415-422.
446. Yancy, C. W., M. Jessup, B. Bozkurt, J. Butler, D. E. Casey, Jr., M. H. Drazner, G. C. Fonarow, S. A. Geraci, T. Horwich, J. L. Januzzi, M. R. Johnson, E. K. Kasper, W. C. Levy, F. A. Masoudi, P. E. McBride, J. J. McMurray, J. E. Mitchell, P. N. Peterson, B. Riegel, F. Sam, L. W. Stevenson, W. H. Tang, E. J. Tsai and B. L. Wilkoff (2013). "2013 ACCF/AHA guideline for the management of heart failure: a report of the American College of Cardiology Foundation/American Heart Association Task Force on Practice Guidelines." J Am Coll Cardiol **62**(16): e147-239.
 447. Yang, L., J. Yang, Q. Wang, M. Chen, Z. Lu, S. Chen and L. Xiong (2010). "Cardioprotective effects of electroacupuncture pretreatment on patients undergoing heart valve replacement surgery: a randomized controlled trial." Ann Thorac Surg **89**(3): 781-786.
 448. Yellon, D. M., A. M. Alkhulaifi and W. B. Pugsley (1993). "Preconditioning the human myocardium." Lancet **342**(8866): 276-277.
 449. Yellon, D. M. and J. M. Downey (2003). "Preconditioning the myocardium: from cellular physiology to clinical cardiology." Physiol Rev **83**(4): 1113-1151.
 450. Yellon, D. M. and D. J. Hausenloy (2007). "Myocardial reperfusion injury." N Engl J Med **357**(11): 1121-1135.
 451. Yi, C., C. Zhang, X. Hu, Y. Li, H. Jiang, W. Xu, J. Lu, Y. Liao, R. Ma, X. Li and J. Wang (2016). "Vagus nerve stimulation attenuates myocardial ischemia/reperfusion injury by inhibiting the expression of interleukin-17A." Exp Ther Med **11**(1): 171-176.
 452. Yin, C., F. N. Salloum and R. C. Kukreja (2009). "A novel role of microRNA in late preconditioning: upregulation of endothelial nitric oxide synthase and heat shock protein 70." Circ Res **104**(5): 572-575.
 453. Yin, C., X. Wang and R. C. Kukreja (2008). "Endogenous microRNAs induced by heat-shock reduce myocardial infarction following ischemia-reperfusion in mice." FEBS Lett **582**(30): 4137-4142.
 454. Yin, C., L. Xi, X. Wang, M. Eapen and R. C. Kukreja (2005). "Silencing heat shock factor 1 by small interfering RNA abrogates heat shock-induced cardioprotection against ischemia-reperfusion injury in mice." J Mol Cell Cardiol **39**(4): 681-689.
 455. Ytrehus, K., Y. Liu and J. M. Downey (1994). "Preconditioning protects ischemic rabbit heart by protein kinase C activation." Am J Physiol **266**(3 Pt 2): H1145-1152.
 456. Yu, L., B. Huang, S. S. Po, T. Tan, M. Wang, L. Zhou, G. Meng, S. Yuan, X. Zhou, X. Li, Z. Wang, S. Wang and H. Jiang (2017). "Low-Level Tragus Stimulation for the Treatment

- of Ischemia and Reperfusion Injury in Patients With ST-Segment Elevation Myocardial Infarction: A Proof-of-Concept Study." JACC Cardiovasc Interv **10**(15): 1511-1520.
457. Yuan, X. M., H. Lei, Q. Liu, Y. Xia and K. H. Ma (2011). "[Effects of hot shock protein 70 inhibitor PFTmicro on inflammatory response in lipopolysaccharide-stimulated RAW264.7 cells and mice underwent myocardial ischemia-reperfusion injury]." Zhonghua Xin Xue Guan Bing Za Zhi **39**(6): 522-525.
 458. Zhang, F., X. Yu and H. Xiao (2017). "Cardioprotection of Electroacupuncture for Enhanced Recovery after Surgery on Patients Undergoing Heart Valve Replacement with Cardiopulmonary Bypass: A Randomized Control Clinical Trial." Evid Based Complement Alternat Med **2017**: 6243630.
 459. Zhang, J., X. H. Jia, Z. W. Xu, F. P. Ding, X. Zhou, H. Fu, Y. Liu, L. L. Ou, Z. J. Li and D. L. Kong (2013). "Improved mesenchymal stem cell survival in ischemic heart through electroacupuncture." Chin J Integr Med **19**(8): 573-581.
 460. Zhang, J., Y. Yong, X. Li, Y. Hu, J. Wang, Y. Q. Wang, W. Song, W. T. Chen, J. Xie, X. M. Chen, X. Lv, L. L. Hou, K. Wang, J. Zhou, X. R. Wang and J. G. Song (2015). "Vagal modulation of high mobility group box-1 protein mediates electroacupuncture-induced cardioprotection in ischemia-reperfusion injury." Sci Rep **5**: 15503.
 461. Zhang, R. X., L. Lao, X. Wang, A. Fan, L. Wang, K. Ren and B. M. Berman (2005). "Electroacupuncture attenuates inflammation in a rat model." J Altern Complement Med **11**(1): 135-142.
 462. Zhang, W., I. Potrovita, V. Tarabin, O. Herrmann, V. Beer, F. Weih, A. Schneider and M. Schwaninger (2005). "Neuronal Activation of NF- κ B Contributes to Cell Death in Cerebral Ischemia." Journal of Cerebral Blood Flow & Metabolism **25**(1): 30-40.
 463. Zhang, Y., Z. B. Popovic, S. Bibevski, I. Fakhry, D. A. Sica, D. R. Van Wagoner and T. N. Mazgalev (2009). "Chronic vagus nerve stimulation improves autonomic control and attenuates systemic inflammation and heart failure progression in a canine high-rate pacing model." Circ Heart Fail **2**(6): 692-699.
 464. Zhao, H. X., X. L. Wang, Y. H. Wang, Y. Wu, X. Y. Li, X. P. Lv, Z. Q. Zhao, R. R. Zhao and H. R. Liu (2010). "Attenuation of myocardial injury by postconditioning: role of hypoxia inducible factor-1 α ." Basic Res Cardiol **105**(1): 109-118.
 465. Zhao, J., O. Renner, L. Wightman, P. H. Sugden, L. Stewart, A. D. Miller, D. S. Latchman and M. S. Marber (1998). "The expression of constitutively active isoforms of protein kinase C to investigate preconditioning." J Biol Chem **273**(36): 23072-23079.
 466. Zhao, X., J. Park, D. Ho, S. Gao, L. Yan, H. Ge, S. Iismaa, L. Lin, B. Tian, D. E. Vatner, R.

- M. Graham and S. F. Vatner (2012). "Cardiomyocyte overexpression of the alpha1A-adrenergic receptor in the rat phenocopies second but not first window preconditioning." Am J Physiol Heart Circ Physiol **302**(8): H1614-1624.
467. Zhao, Z. Q., J. S. Corvera, M. E. Halkos, F. Kerendi, N. P. Wang, R. A. Guyton and J. Vinten-Johansen (2003). "Inhibition of myocardial injury by ischemic postconditioning during reperfusion: comparison with ischemic preconditioning." Am J Physiol Heart Circ Physiol **285**(2): H579-588.
 468. Zheng, D., Y. Yu, M. Li, G. Wang, R. Chen, G. C. Fan, C. Martin, S. Xiong and T. Peng (2016). "Inhibition of MicroRNA 195 Prevents Apoptosis and Multiple-Organ Injury in Mouse Models of Sepsis." J Infect Dis **213**(10): 1661-1670.
 469. Zhou, C., Y. Liu, Y. Yao, S. Zhou, N. Fang, W. Wang and L. Li (2013). "beta-blockers and volatile anesthetics may attenuate cardioprotection by remote preconditioning in adult cardiac surgery: a meta-analysis of 15 randomized trials." J Cardiothorac Vasc Anesth **27**(2): 305-311.
 470. Zhou, W., Y. Ko, P. Benharash, K. Yamakawa, S. Patel, O. A. Ajijola and A. Mahajan (2012). "Cardioprotection of electroacupuncture against myocardial ischemia-reperfusion injury by modulation of cardiac norepinephrine release." Am J Physiol Heart Circ Physiol **302**(9): H1818-1825.
 471. Zhou, X., Z. Jiao, J. Ji, S. Li, X. Huang, X. Lu, H. Zhao, J. Peng, X. Chen, Q. Ji and Y. Ji (2017). "Characterization of mouse serum exosomal small RNA content: The origins and their roles in modulating inflammatory response." Oncotarget **8**(26): 42712-42727.
 472. Zhou, Y., Q. Chen, K. S. Lew, A. M. Richards and P. Wang (2016). "Discovery of Potential Therapeutic miRNA Targets in Cardiac Ischemia-Reperfusion Injury." J Cardiovasc Pharmacol Ther **21**(3): 296-309.
 473. Zhu, Q. F., F. B. Zhang, K. M. Wang and Y. P. Zhou (2007). "[CGRP may take part in the effect of electroacupuncture in resisting acute myocardial ischemic injury]." Zhen Ci Yan Jiu **32**(1): 20-23.
 474. Ziolo, M. T. and D. M. Bers (2003). "The real estate of NOS signaling: location, location, location." Circ Res **92**(12): 1279-1281.
 475. Zou, Y., W. Zhu, M. Sakamoto, Y. Qin, H. Akazawa, H. Toko, M. Mizukami, N. Takeda, T. Minamino, H. Takano, T. Nagai, A. Nakai and I. Komuro (2003). "Heat shock transcription factor 1 protects cardiomyocytes from ischemia/reperfusion injury." Circulation **108**(24): 3024-3030.
 476. Zwacka, R. M., Y. Zhang, W. Zhou, J. Halldorson and J. F. Engelhardt (1998). "Ischemia/reperfusion injury in the liver of BALB/c mice activates AP-1 and nuclear

factor kappaB independently of IkappaB degradation." Hepatology **28**(4): 1022-1030.

477. Zweier, J. L. (1988). "Measurement of superoxide-derived free radicals in the reperfused heart. Evidence for a free radical mechanism of reperfusion injury." J Biol Chem **263**(3): 1353-1357.

VITA

Anne “Annie” Elizabeth Roessler was born in Cincinnati, Ohio, to Ron and Denise Roessler. She attended Centre College in Danville, Kentucky, on a full academic scholarship as a Brown Fellow. She earned a Bachelor’s of Science in Behavioral Neuroscience and was appointed an Honorary Kentucky Colonel for her contributions to the state of Kentucky. She remains involved with Centre College and served as the President of the Brown Fellows Alumni Association for the 2018 term. In 2014, Annie joined The University of Cincinnati’s Pharmacology PhD Program in the lab of Dr. Keith Jones to study the intersection of the nervous system and the cardiovascular system. Annie subsequently transferred to the Pharmacology Department at Loyola University in Chicago when Dr. Jones was appointed as chair. In her dissertation work, she pioneered the development of an affordable and translatable electrically-based cutaneous patch that confers cardioprotection against heart attacks.

At Loyola, Annie held multiple leadership positions, including cofounder of a peer-based support group for qualifying examinees, student-faculty liaison, department representative for the graduate student council, and tutor for first year students. She is a member of the American Heart Association, the American Society for Pharmacology and Experimental Therapeutics, Women in Bio, and the Jesuit honor society Alpha Sigma Nu. Beyond the bench, Annie worked at multiple biotechnology and pharmaceutical companies as a freelancer and volunteer, blogged for the American Heart Association’s “Early Career Voices” column, coordinated social

media for Executive Women in Science's "Boardroom Ready" Program, and volunteered in the Emergency Department. In addition to her academic pursuits, Annie advocates for heart health by being an avid long distance runner, finishing several full marathons and 200-mile relays during her time as a graduate student. After completion of her graduate studies, Annie will be joining Pfizer's Professional Development Program as a Scientist to help bring affordable medications to patients worldwide.

